Real Sociedad Española de Física
R.S.E.F.

GEFENOL

FisEs'14

Libro de Resúmenes

Ourense, 2 - 4 de Abril de 2014

Concello de OURENSE

Universidade Vigo

Horarios

(I) Comunicaciones orales por invitación de 50 min
(I) Comunicaciones orales por invitación de 30 min
(O) Comunicaciones orales seleccionadas

Hora	Miércoles, 2 de abril
8:00 – 9:00 h	**Inscripción**
9:00 – 9:30 h	**Inauguración**
9:30 – 10:20 h	**I-1**. S. Manrubia: Evolutionary theory evolves: from the beagle to deep sequencing
10:20 – 10:35 h	**O.1**. P. Gómez-Álvarez. A computacional study of hydrogen bonding of water confined in nanoporous materials
10:35 – 10:50 h	**O.2**. G. Franzese. Multiscale approach to bionano interactions: from water to protein corona
10:50 – 11:15 h	**Café**
11:15 – 11:45 h	**I.2**. M. Manosas. Unraveling the mechanism of molecular motors by uning micro manipulation methods
11:45 – 12:00 h	**O.3**. J. Muñoz-García. Formation and maintenance of nitrogen fixing cell patterns in filamentous cyanobacteria
12:00 – 12:15 h	**O.4**. A. Barardi. Gamma band synchronization and communications between delay-coupled neuronal populations
12:15 – 12:45 h	**I.3**. E. Corvera. Vascular structure and hemodynamics
12:45 – 15:00 h	**Comida**
15:00 – 17:00 h	**Paneles (P-1 a P-43)**
16:30 – 17:00 h	**Café**
17:00 – 17:50 h	**I.4**. A. Sánchez. Física de las interacciones estratégicas
17:50 – 18:05 h	**O-5**. F.J. Galindo-Rosales. Non-linear behavior of Ferrofluids and Magnetorheological fluids subjected to extensional flow in a magnetic field
18:05 – 18:20 h	**O-6**. M. Nicoli. Fragility and robustness of the Kardar-Parisi-Zhang universality class
18:20 – 18:35 h	**O-7**. Luis F. Seoane. Multiobjective optimization and phase transitions
18:35 – 18:50 h	**O-8**. Daniel Campos. Búsqueda aleatoria en el espacio: ¿qué papel juegan los mecanismos de detección?

Hora	Jueves, 3 de abril
9:00 – 9:50 h	**I.5**. C. Van den Broeck. Stochastic thermodynamics: a very brief introduction
9:50 – 10:05 h	**O-9.** E. Noya. Phase behavior and self-assembly of inverse patchy colloids
10:05 – 10:20 h	**O-10.** J. J. Cerdá. Phase diagram of Stockmayer polymers in bulk and near surfaces
10:20 – 10:40 h	**O.11.** E. Abad. Random walkers that die as they move
10:40 – 11:15 h	**Café**
11:15 – 11:45 h	**I.6**. I Fischer. Neuro-inspired information processing using complex systems: concept, mechanisms and performance
11:45 – 12:00 h	**O-12**. J. M. Ortiz de Zárate. Fuerzas inducidas por fluctuaciones en sistemas fuera del equilibrio
12:00 – 12:15 h	**O-13**. P. Maynar. Fluctuaciones de energía interna en el estado de flujo tangencial uniforme
12:15 – 12:30 h	**O-14**. J. Burguete. Inverse cascades sustained by the transfer rate of angular momentum in a 3D turbulent flow
12:30 – 12:45 h	**O-15**. C. Lozano. Estudio experimental de la estabilidad de los arcos en un medio granular

12:45 – 15:00 h	**Comida**
15:00 – 17:00 h	**Paneles (P-44 a P-85)**
16:30 – 17:00 h	Café
17:00 – 17:50 h	**I.7**. E. Clement. Hydrodynamics of active bacterial fluids
	Visita a las Termas de Ourense

Hora	**Viernes, 4 de abril**
9:30– 10:20 h	**I.8**. A. Ferriz. The role of entropy stratification in the storage of magnetic flux in stars.
10:20 – 10:35 h	**O-16.** E. Cabrillo. Cristalización de *para*-hidrógeno: ¿una transición (de primer orden) cuántica a temperatura finita?
10:35 – 10:50 h	**O-17**. J. Hidalgo. Smart inference and criticality
10:50 – 11:15	**Café**
11:15 – 11:45 h	**I.8** Horacio Wio. Transiciones de fase inducidas por ruido y motores brownianos acoplados: ciclos de histéresis no convencionales
11:45 – 12:00 h	**O-18.** A. Aragoneses. Characterizing the complex dynamics of a semiconductor laser with optical feedback and modulation
12:00 – 12:15 h	**O-19.** E. Montbrió. Low-dimensional dynamics of populations of pulse-coupled oscillators
12:15 – 12:30 h	**O-20**. J. Guiu. Autoorganización de estructuras de Turing en un potencial radial con periodicidad temporal
12:30 – 12:45 h	**O-21**. J. J. Lorenzo. The last survivor: a spin glass phase in an external magnetic field
12:45 – 13:00 h	**O-22**. C. López. Optimizing the search for resources by sharing information. The case of Mongolian gazelles

Comité Científico

- Claudio Cerdeiriña, Universidad de Vigo
- Rodolfo Cuerno, Universidad Carlos III de Madrid
- Jordi García Ojalvo, Universidad Politécnica de Cataluña
- Juan Manuel López, Instituto de Física de Cantabria
- Miguel Ángel Muñoz, Universidad de Granada
- Ignacio Pagonabarraga, Universidad de Barcelona
- Andrés Santos, Universidad de Extremadura
- Raúl Toral, IFISC - Universidad de las Islas Baleares
- Enrique Velasco, Universidad Autónoma de Madrid

Comité Organizador Local

- Claudio Cerdeiriña, Universidad de Vigo
- Diego González, Universidad de Vigo
- Jacobo Troncoso, Universidad de Vigo
- Luis Romaní, Universidad de Vigo

Índice general

Comunicaciones Orales por Invitación

Evolutionary theory evolves: from the beagle to deep Sequencing

Susanna Manrubia*
Centro de Astrobiología (CSIC/INTA)
Instituto Nacional de Técnica Aeroespacial
Ctra de Torrejón a Ajalvir, km 4
28850 Torrejón de Ardoz, Madrid Spain

One of the greatest unknowns at Darwin's time was the nature of the physical mechanisms responsible for the inheritance of characters. In the course of the subsequent century, Mendel's experiments were rediscovered, genes were identified, and some mechanisms causing evolutionary novelty (as certain types of mutations or recombination) were described. In the first half of the XXth century, the so-called New Synthesis developed a framework where, apparently, all relevant evolutionary forces were conceptually integrated and, consequently, cast in mathematical form. To a large extent the New Synthesis is still the dominating paradigm in evolutionary biology. However, that scenario has not yet integrated a significant and important number of new discoveries regarding, in particular, the molecular nature of evolution. The advance in techniques able to probe the molecular diversity of populations has revealed new facts that challenge prevailing ideas, such as the many-to-many relationship between genomes and organisms, the existence of vast and connected quasi-neutral networks in the space of genomes, or alternative mutational mechanisms able to produce adaptation in few generations. In this talk, we will briefly review the history of evolutionary theory and discuss how new data are disrupting the consensus on the dominant forces behind evolution. Taking genotype networks as a specific example, we will show how fitness landscapes, evolutionary innovations, or the molecular clock are affected by our journeys of discovery to the deep molecular structure of organisms.

* scmanrubia@cab.inta-csic.es

Unraveling the mechanism of molecular motors by using micro manipulation methods

María Mañosas*
Departament de Física Fonamental
Facultat de Física,
Universitat de Barcelona Diagonal 647
08028 Barcelona, Spain.

Single-molecule micromanipulation methods have shed new light on DNA protein interactions. In particular these methods have provided novel insights on the mechanisms of molecular motors that convert chemical energy (e.g. the energy released in the hydrolysis of ATP) into mechanical work. In this talk I will describe the use of magnetic traps for the investigation of DNA processing motors involved in DNA replication and DNA repair. In these assays magnetic traps are used to mechanically manipulate a DNA molecule and follow in real time the activity of different DNA molecular motors. The applied mechanical force allows either to assist or to hinder motor activities revealing the mechanisms of individual motors as well as their coordinated action when processing DNA (such as during DNA replication). Mechanical switch in molecular motor activity offers interesting applications for single-molecule DNA sequencing.

* mmanosas@gmail.com

Vascular structure and hemodynamics

Eugenia Corvera*
Edificio F, cubículo F-211.
Facultad de Química.
UNAM. Ciudad Universitaria.
México, D.F. 04510. MEXICO

We are interested in relating the visual characteristics of blood vessel networks and the amount of blood flow that they provide to a tissue. We study the effect that vascular alterations, such as obstructions and redundancy, have on flow, and relate the geometrical place in which such variations occur with the overall capacity of the vasculature to irrigate a tissue. Our results allow us to argue that, to a large extent, the hemodynamics of the network is determined locally. That is, it depends on the structure that the underlying vessel network has in a small neighborhood around the anatomical place where the alterations occur. We also provide a plausible explanation of the hemodynamic advantages of having redundancy at key places of the vascular system, despite having an equal energetic cost than flow in non-redundant networks with wider vessels. Recent progresses on high- resolution microscopy permit the visualization of the characteristics of an individual vasculature. The concurrence of image-tracking systems and mathematical models such as the one presented, provide relevant tools in the determination of blood supply to a tissue.

* eugenia.corvera@gmail.com

Física de las interacciones estratégicas

Anxo Sánchez*
Grupo Interdisciplinar de Sistemas Complejos
Departamento de Matemáticas
Universidad Carlos III de Madrid
28911 Leganés, Madrid, Spain

En los últimos años, muchos físicos de distintas procedencias, pero sobre todo de la física estadística, se han visto atraídos por el estudio de sistemas complejos socioeconómicos y sociotecnológicos. ¿Por qué ha ocurrido esto? ¿Tiene la física algo que decir sobre dichos sistemas? ¿Es la relación entre disciplinas mutuamente beneficiosa? En esta charla discutiré estas y otras cuestiones partiendo de los trabajos que he venido realizando con distintos colaboradores sobre el problema de la cooperación. Tras una rápida introducción al tema, presentaré resultados de distintos experimentos que arrojan luz sobre como interaccionan las personas enfrentadas a un dilema social, teniendo en cuenta que esa interacción es estratégica, es decir, que los involucrados anticipan las intenciones del otro. A continuación mostraré cómo sobre la base de los resultados experimentales se pueden construir modelos estilizados de las interacciones que permiten dar el paso del nivel micro al nivel macro con buen acuerdo con las observaciones. A lo largo de la charla incluiré comentarios de tipo metodológico así como otros sobre la naturaleza de la investigación interdiscplinar. Como conclusión, espero transmitir que el paradigma y el método de la física pueden ser muy útiles y aportar nuevas perspectivas en las ciencias sociales, mientras que éstas plantean cuestiones que son interesantes para los físicos.

* anxo@math.uc3m.es

Stochastic thermodynamics: a very brief introduction

Christian Van den Broeck*
Theoretical Physics Group
Campus Diepenbeek
Agoralaan Gebouw D
BE 3590
Diepenbeek, Belgium

The main purpose of statistical mechanics is to give a microscopic derivation of macroscopic laws, including in particular the celebrated second law of thermodynamics. In recent years, there have been spectacular developments in this respect, including the integral and detailed work fluctuation theorems and the theory of stochastic thermodynamics. We give a brief introduction to these developments. In the first step, we derive the first and second law of thermodynamics for a Markovian stochastic process at the ensemble level, including two major advances: 1) the theory can be applied to small-scale systems including the effect of fluctuations, 2) the theory is not restricted to near-equilibrium dynamics. As an application, we evaluate the efficiency at maximum power of a two-state quan- tum dot. We also briefly discuss the connection to information-to-work conversion (Landauer principle). In a second step we formulate stochastic thermodynamics at the trajectory level, introducing stochastic trajectory-dependent quantities such as stochastic entropy, energy, heat, and work. Both the first and the second law can be formulated at this trajectory level. Concerning the second law, the crucial observation is that the stochastic entropy production can be written as the logarithm of the ratio of path probabilities. This in turn implies a detailed and integral work and fluctuation theorem, linking the probability to observe a given stochastic entropy production to that of observing minus this entropy change in a reverse experiment. The usual second law, stipulating the increase on average of the stochastic entropy production, follows as a subsidiary consequence.

* christian.vandenbroeck@uhasselt.be

Neuro-inspired information processing using complex systems:Concept, mechanisms, and performance

Ingo Fischer*
IFISC (UIB-CSIC)
Campus Universitat de les Illes Balears
E-07122 Palma de Mallorca
Spain

To learn from the brain how to process information has been a fascinating perspective for several decades. Many advances have been made, and powerful computational schemes have been introduced. Nevertheless, even basic mechanisms and requirements of neural information processing remain unclear. Here we choose a minimal design approach,[?] allowing for the implementation of neuro-inspired computational concepts in photonics hardware. By reducing reservoir computing and related concepts to their bare essentials, we find that nonlinear transient responses of a simple nonlinear photonic system enable the processing of information with unprecedented performance and speed.[2–4] A single dynamical element with a delayed feedback loop suffices and moreover, allows us to investigate the underlying mechanisms and properties. We specifically explore the role of the initial state, consistent responses, connectivity structure of the network, particular nonlinearity, noise and quality of projection onto a high-dimensional state space. Besides the relevance for the understanding of basic mechanisms, this approach opens direct technological opportunities. The challenges and future perspectives will be discussed.

---

* ingo@ifisc.uib-csic.es.

[1] L. Appeltant, M. C. Soriano, G. Van der Sande, J. Danckaert, S. Massar, J. Dambre,and I. Fischer, Nature Comm. **2**, 468 (2011).

[2] L. Larger, M. C. Soriano, D. Brunner, L. Appeltant, J. M. Gutierrez, L. Pesquera, and I. Fischer, Optics Express **20**, 3241 (2012).

[3] D. Brunner, M. C. Soriano, C. R. Mirasso, and I. Fischer, Nature Comm., **4**, 1364 (2013).

[4] D. Brunner, M. C. Soriano and I. Fischer, IEEE Photonics Technology Letters, **25**, 1680 (2013).

Hydrodynamics of active bacterial fluids

Eric Clément*
PMMH
École Supérieure de Physique et de Chimie Industrielles (ESPCI)
10, rue Vauquelin
75231 Paris Cedex 05
France

From the hydrodynamics point of view, assemblies of microscopic swimmers dispersed in a fluid, at very low Reynolds number, display emergent properties differing strongly from those of passive suspensions. Balances of momentum and energy as well the constitutive transport properties, are deeply modified by the active momentum sources distributed in the bulk. In the laboratory, we use E-Coli suspensions to address several of these fundamental problems around the statistical mechanics and the hydrodynamics of active fluids. We studied the enhanced Brownian diffusivity, the active shear viscosity and the anomalous dispersion of bacteria in confined environments. In this presentation, I will present some recent results and address in particular, the question of bacterial organization under flow and its impact on transport hydrodynamic properties.

* eric.clement@upmc.fr

The role of entropy stratification in the storage of magnetic flux in stars

Antonio Ferriz-Mas*
Departamento de Física Aplicada
Universidad de Vigo
E-32004 Ourense
Spain

Instituto de Astrofísica de Andalucía
IAA/CSIC
Grupo de Física Solar
E-18080 Granada
Spain

The study of the mechanical equilibrium of magnetic tubes in a stellar convection zone is of interest in the context of the storage of magnetic flux and dynamo action in the Sun and solar-like stars.

At the interface between the convection zone and the underlying stably stratified radiative interior there is a thin layer of overshooting convection ('overshoot layer') in which the temperature gradient is *subadiabatic*. Below the convection zone there also exists a shear layer known as the 'tachocline', which represents a sharp transition between two distinct rotational regimes: the differentially rotating convection zone and the almost rigidly rotating radiative interior. The relative position between these two boundary layers - one mechanical and one thermal - determines the degree of *subadiabaticity* of the tachocline. Since the decade of 1980 many astrophysicists believe that the tachocline plays a fundamental role in the generation and storage of the toroidal magnetic flux that eventually becomes unstable and buoyantly rises to emerge at the stellar surface producing sunspots.

In this talk I will discuss the role of the thermodynamic properties (and more specifically, the entropy stratification) of the overshoot layer in determining the stability of magnetic structures and, therefore, its capability to store magnetic flux. The entropy stratification is quantified by a dimensionless physical quantity called the *superadiabaticity*, δ. Tiny variations in δ (of the order of 10^{-4} or less) may determine global properties of the magnetic field at the solar surface

* ferrizantonio@gmail.com

Transiciones de fase inducidas por ruido y motores brownianos acoplados: ciclos de histéresis no convencionales

Horacio S. Wio*
Instituto de Fisica de Cantabria - Universidad de Cantabria
Statistical Physics Group
Avda. Los Castros s/n
39005 - Santander
Spain

Trabajos recientes[1–3] han mostrado la posibilidad de, mediante una ruptura de simetría inducida por ruido que da lugar a una transición de fase alejada del equilibrio, obtener un conjunto de motores Brownianos acoplados. También se mostró que,[4], en una región de parámetros tal sistema puede mostrar movilidad negativa (un movimiento opuesto a la fuerza aplicada) y un comportamiento de histéresis anómalo (en el sentido de la agujas del reloj, en oposición al más usual contrario a las agujas del reloj). Utilizando una aproximación de campo medio explícita y ruidos coloreados multiplicativos, se encontró por un lado una contracción de la fase ordenada (y reentrancia como función del acoplamiento), y por otro un cambio de comportamiento de histéresis anómala a normal.[5] Este comportamiento fue obtenido en sistemas que presentan una transición inducida por ruido originada en una inestabilidad de tiempos cortos. Aquí discutiremos un sistema similar, pero en el cual la transición inducida por ruido se origina en un mecanismo entrópico.[6] Estudios preliminares en los cuales se explotó este mecanismo indican la posibilidad de obtener ciclos de histéresis no standard mostrando una estructura escalonada. Dependiendo de la región de parámetros, el diagrama de histéresis puede mostrar uno o más bloques, los que pueden ser explorados/recorridos como un todo o paso a paso, ofreciendo la posibilidad de explotarlos como compuertas lógicas multipropósito controladas por ruido.[7]

---

* wio@ifca.unican.es

[1] Sagués et al., Rev. Mod. Phys. **79**, 829 (2007).
[2] van den Broeck et al, Phys. Rev. E **79**, 4084 (1997).
[3] Mangioni et al., Phys. Rev. E **61**, 223 (2000).
[4] Reimann et al, Europhys. Lett. **45**, 545 (1999).
[5] Mangioni et al., Phys. Rev. E **66**, 051106 (2002).
[6] Carrillo et al., Phys. Rev. E **67**, 04611 (2003).
[7] H. Wio, 22th ICNF-IEEE Proceedings (in press).

Comunicaciones Orales

A computational study of hydrogen bonding of water confined in nanoporous materials

P. Gómez-Álvarez* and S. Calero
Departamento de Sistemas Físicos, Químicos y Naturales.
Universidad Pablo de Olavide. Ctra. Utrera km. 1, 41013, Sevilla

The hydrogen bonding[1] in associated liquids has been systematically studied for many years, either experimentally or computationally. Although several techniques such as neutron and x-ray diffraction have considerably increased our knowledge of their structural properties, no accurate and unambiguous information can be extracted from experimental data. On the other hand, Molecular Simulation (MS) represents a powerful tool to complement the experimental approaches and overcome their deficiencies. Thus, the increasing computation power available to scientists has made MS a very useful alternative to gain further insight into the details of the hydrogen-bonding structure of these systems. Of course, this great interest is obviously due to the fact that hydrogen-bonded interactions play a crucial role in a variety of fields, and are responsible of a number of peculiar properties observed in associated substances. In this respect, water[2] is unarguably the most significant case. Hence, it has been studied more extensively than any other liquid. Most of the reported works are focused on analysing bulk water. It shows a complicated tetrahedral H-bonding network, the variation of which as a function of temperature and pressure provokes a considerably singular macroscopic behaviour. On the other hand, the molecular-level characterization of its structure in confining environments is also key to understanding many chemical and biological processes of relevance, from a fundamental point of view to industrial applications such as biological membrane transport, the removal of pollutants from water or water/alcohol separations, among others. In recent years, the number of available porous materials has increased substantially, with new material classes such as Metal-Organic Frameworks joining the traditional adsorbents, which include activated carbons and zeolites.

In spite of being currently of great interest, little is known about the structure of water within the nanopore. Therefore, this work is concerned with the hydrogen bond properties at room temperature of water confined in two different types of crystalline porous materials that show high stability to water: zeolites and Zeolitic Imidazolate Frameworks (ZIFs). The reason of this choice is twofold. On one hand, while zeolites are hydrophobic in their pure siliceous form, ZIFs are hydrophilic due to the metal centers. On the other hand, the pore sizes of the latter are approximately twice as large as those of their zeolite counterparts by virtue of the longer IM linking units. Specifically, we considered five industrially important zeolites with quite different pore arrangement, and their respective Zn and imidazole-based ZIFs, namely: FAU, FER, MFI, MOR, and RHO. Adsorption of water in these structures was computed via Monte Carlo simulations in the grand-canonical ensemble using previously validated force fields. The hydrogen-bonding behaviour of confined water has been described in terms of the Radial Function Distributions (RDFs) and the HB statistics. Particularly, a specific geometric criterion of HB formation[3] was applied over the generated configurations and allowed the computation of the fraction of associated molecules as well as the fraction of which with i H-bonds, f_i, and the average number of hydrogen bonds per molecule $\langle n_{\mathrm{HB}} \rangle$.

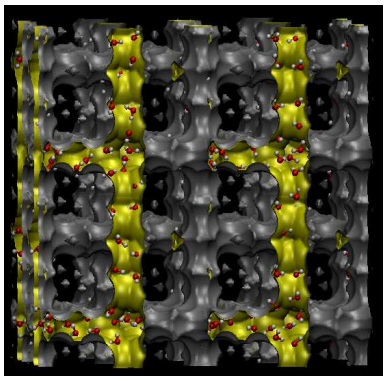

FIG. 1. Snapshot from a simulation. The interior of the energy surfaces (in yellow color) delimits the pore volume where molecules can be adsorbed.

As expected, an enhancement of hydrogen bonding with water loading within the nanopores until reaching bulk-like densities was observed. At these states, our simulations reveal that, although association is still important, the confinement prevents the tetrahedrally coordinated structure characteristic of bulk liquid water. Instead, water molecules form mainly aggregates, whose nature was found notably sensitive to the type of confining material.

* pgomalv1@upo.es

[1] E. Arunan, G. R. Desiraju, R. A. Klein, J. Sadlej, S. Scheiner, I. Alkorta, D. C. Clary, R. H. Carbtree, J. J. Dannenberg, P. Hobza, H. G. Kjaergaard, A. C. Legon, B. Mennucci, and D. J. Nesbitt, Pure Appl. Chem. **83(8)**,1619 (2011).
[2] D. Eisenberg, and W. Kauzmann, The Structure and Properties of Water (Oxford University Press, London, 1969).
[3] A. Luzar, and D. Chandler, J. Chem. Phys. **98**, 8160 (1993).

Multiscale Approach to BioNano Interactions: From Water to Protein Corona

Giancarlo Franzese, Marco Bernabei, Valentino Bianco, Oriol Vilanova
Departament de Física Fonamental (Facultat de Física) Martí i Franquès 1, ES-08028 Barcelona

The recent exploitation of nanoparticles in commercial and medical applications has increased the possibility that people could enter in direct contact with these materials. Thousands of products in the market, such as fabrics, cleaning products and cosmetics, include nanocomponents. Nanomaterials are already used in medical treatments, electronics or as food additives, generating millions of dollars in sales. Human exposure to nanomaterials, smaller than a thousandth the diameter of a hair, raises important issues about if the interactions between nanomaterials and biological systems can have adverse health effects. Therefore, it is fundamental to study the BioNano Interactions and to understand how we can control them. This is relevant both for the technological applications and for the social impact. In fact, a distorted knowledge or a superficial control of the nanoparticle effect for the health could generate a social concern. For example, in the past years these issues have generated a strong reaction to the OGM food, limiting the research and its possible benefits. The starting hypothesis of our research is that water dominates the structure and the organization of the biosystems at the molecular level. Water properties are paramount in BioNano Interactions. The presence of water in living organisms is responsible for much of the structural and physicochemical properties of biomolecules because of the unique water ability to form hydrogen bonds. In this report we will present our recent results in describing the formation of the "protein corona" around the nanoparticles when these are in aqueous solutions with biomolecules. With great simplification, chemical molecules interact directly with the biological elements, while nanoparticles are coated with proteins and lipids. These macromolecules adhere so strongly to the nanoparticle surface that the exchange times with the solution are extremely long. As a consequence, the biological identity of the particles depends largely of the protein corona, instead of the nanoparticle material.

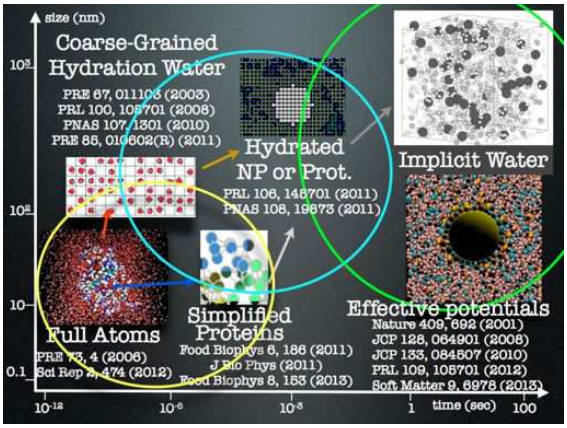

FIG. 1. Schematic representation of our multiscale approach. The horizontal axis represents the time scale and covers fourteen orders of magnitude. The vertical axis shows the length scales and covers five orders of magnitude. The circles mark the different scales that are considered here. The citations and insets refer to the works that we published in relation to each scale.

Formation and maintenance of nitrogen fixing cell patterns in filamentous cyanobacteria

Javier Muñoz-García* and Saúl Ares†
*Departamento de Matemáticas and Grupo Interdisciplinar de Sistemas Complejos (GISC), Universidad Carlos III de Madrid, 28911 Leganés, Spain
†GISC and Logic of Genomic Systems Laboratory, Centro Nacional de Biotecnología - CSIC, 28049 Madrid, Spain

In the study of the transition between unicellular and multicellular living forms, cyanobacteria forming one-dimensional filaments are important model organisms. Cyanobacteria were the first organisms to use oxygenic photosynthesis and are currently one of the most successful living groups, occupying a broad range of habitats across all latitudes and producing 20-30% of Earth's photosynthetic activity. These cyanobacteria may form colonies consisting of a one-dimensional filament composed under normal conditions only of vegetative cells. However, as a response to different environmental stresses they can differentiate into specialized cell types that perform important functions for the survival of the colony[1].

The genus *Anabaena* has received special interest because under nitrogen-limiting conditions, some cells of the filament differentiate into heterocysts, which lose the possibility to divide but are able to fix environmental nitrogen for the colony. These heterocysts form a quasi-regular pattern in the filament, representing a prototype of patterning and morphogenesis in prokaryotes. Here we will focus on the case of heterocyst differentiation. Heterocysts are specialized cells able to fix atmospheric nitrogen into a chemical form usable by vegetative cells. When external nitrogen sources are scarce heterocysts appear in regular patterns, with intervals of around 10 vegetative cells between consecutive heterocysts, representing a paradigmatic example in pattern formation of developing biological systems[2]. Since a continuous outer membrane covers the whole filament, the fixed nitrogen produced by heterocysts can diffuse through the periplasm and reach the vegetative cells. In turn, nutrients produced by photosynthesis in vegetative cells are also shared and reach the heterocysts.

The biology of this differentiation process has been the subject of several studies (for recent reviews see for example Refs. 1, 3). Most of these genetic studies have been focused on a particular species named Anabaena sp. PCC 7120 (also known as Nostoc sp. PCC 7120), which has become a prototypical organism in this field. However, theoretical models are scarce and the inclusion of recently discovered genetic regulations is still lacking.

In this study[4] we formulate a theoretical description of heterocyst pattern formation that includes the genetic regulations between the main genes identified in the process, such as hetR, patS, and hetN (see figure 1 for a diagram of the regulatory network and its interactions). This description has been coded using an object-oriented platform based on systems of stochastic reaction-diffusion differential equations for each cell, with variables representing the concentration of each molecular species. We reproduce qualitatively and quantitatively many important features of the observed differentiation process, including the appearance of heterocysts forming a quasi-regular pattern. Our results are in good agreement with experimental observations in wild type and mutants of Anabaena sp. PCC 7120, adding support for the regulatory relations proposed and allowing to make predictions on the role of recently described genes.

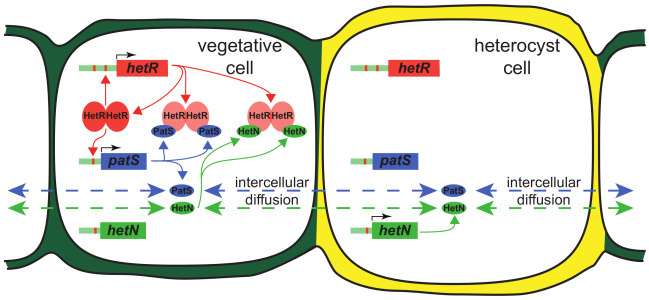

FIG. 1. Diagram of the regulatory network and its interactions. HetR dimers activate the expression of *hetR* and *patS*. *patS* is only expressed in vegetative cells, *hetN* is expressed constitutively in heterocystes. Active products of PatS and HetN can diffuse between cells in the filament and bind HetR, preventing it from binding DNA.

* javiermunozgarcia@gmail.com
http://gisc.uc3m.es/~javier

[1] E. Flores and A. Herrrero, *Nat. Rev. Microbiol.* **8**, 39 (2010).
[2] L. G. Morelli, K. Uriu, S. Ares, and A. C. Oates, *Science* **336**, 187 (2012).
[3] K. Kumar, R. A. Mella-Herrera, and J. W. Golden, *Cold Spring Harb. Perspect. Biol.* **2**, a000315 (2010).
[4] J. Muñoz-García and S. Ares, *preprint* (2014).

Gamma band synchronization and communication between delay-coupled neuronal populations

Alessandro Barardi*, Belen Sancristóbal, Jordi Garcia-Ojalvo
Departament of Experimental and Health Sciences, Universitat Pompeu Fabra, Barcelona Biomedical Research Park, Dr. Aiguader 88, Barcelona, Spain

In neuronal systems, firing synchronization is of great importance in information transmission between brain areas.

It is known that synchronized spikes increase their impact to a given target neuron[1]. Analogously, synchronized electrical oscillations emerging from the activity of thousands of neurons can increase the functional connectivity between neural assemblies by coherently coordinating their firing dynamics.

According to the communication-through-coherence hypothesis of Pascal Fries[3] synchronization between neuronal oscillations of different cortical areas might offer a mechanism for selecting the route of information. In order to communicate effectively the synaptic delay, the phase difference and the frequency of the oscillatory LFPs of the two areas should match. Neurophysiological and modeling results suggest that neuronal populations influence one another most strongly if they oscillate at zero phase lag[4]. However, zero lag synchrony between neuronal ensembles can only be achieved by mechanisms that are able to compensate for the axonal delays involved in the propagation of the spikes. Given that propagation times between different cortical regions, including interhemisferic areas[5] and not only short-range interactions within a cortical area, could be of several tens of milliseconds[6], zero lag synchronization seems implausible. Interestingly, Vicente et al.[7] showed that zero- lag synchronization can be achieved despite long axonal delays when two neuronal populations interact via a third population, which can be associated to the thalamus.

In this work, we have studied the influence of the synaptic delay on the synchronization of neural populations oscillating in the gamma range. To this aim we have modeled two neural populations using conductance-based models for both excitatory and inhibitory cells. We have reproduced particular features of cortical dynamics such as the coexistence of irregular firing at the single-neuron level with collective oscillations at the population level, emerging from the synaptic recurrent connections. The emergent rhythmicity is achieved by a balance between the excitatory and inhibitory synaptic currents[2] and can be explained by periodic changes of the excitability of the network, i.e. periodic modulation of the distance to threshold. We have both the multi-unit activity (MUA) and local field potential (LFP) to characterize the global activity.

A key requirement of the CTC hypothesis is the existence of a constant phase difference between the oscillations that reliably allows a stationary binding between networks, favoring communication. Therefore, we have first quantified phase coherence between the oscillatory activity of the two delayed coupled populations at varying mean axonal delays. In order to assess whether different synchronization scenarios boost communication, we have next used information theory to quantify the response of one population (the receiver) to a varying external input impinging on the other population (the emitter). To this purpose, we have increased the external firing rate of the background synaptic activity affecting a neuronal subpopulation of the emitter network and we have computed the LFP and MUA power spectrum of the receiver network. So we quantify how well the power spectrum of LFP and MUA conveys information about which stimulus is being applied to the receiver population.

In summary, we have performed extensive simulations with a conductance-based neuronal network model to characterize the effect of long conduction delays in the synchronization patterns of two coupled networks. Phase coherence and mutual information has been evaluated in terms of frequency in order to provide a wide analysis of the complex dynamics of neuronal networks, which are far from being harmonic oscillators.

---

* alessandro.barardi@upf.edu

[1] E. Salinas, TJ. Sejnowski. *Impact of correlated synaptic input on output firing rate and variability in simple neuronal models*. The Journal of Neuroscience, 2000, 20: 6193-6209.

[2] N. Brunel, XJ. Wang. *Effects of neuromodulation in a cortical network model of object working memory dominated by recurrent inhibition*. J Computational Neuroscience, 2001, 11: 63-85.

[3] P. Fries. *A mechanism for cognitive dynamics: neuronal communication through neuronal coherence. Trendes in Cognitive sciences*. Trendes in Cognitive sciences, 2005, 9: 474-480.Trendes in Cognitive sciences, 2005, 9: 474-480.

[4] T. Womelsdorf, P. Fries. *Gamma-band synchronization in visual cortex predicts speed of change detection*. Nature, 2006, 439: 733-736.

[5] E. Rodriguez, N. George, J. Lachaux, J. Martinerie, BRF. Varela. *Perceptions shadow: Long-distance synchronization of human brain activity*. Nature, 1999, 397: 430-433.

[6] J. Ringo, S. Demeter, P. Simard. *Time is the essence: A conjecture that hemispheric specialization arises from interhemispheric conduction delay*. Cerebral Cortex, 1994, 4: 331-343.

[7] R. Vicente, L. Gollo, I. Fischer, G. Pipa. *Dynamical relaying can yield zero time lag neuronal synchrony despite long conduction delays*. Proc Natl Acad Sci U S A, 2008, 105: 17157-17162.

Non-linear behavior of Ferrofluids and Magnetorheological fluids subjected to extensional flow in a magnetic field

F.J. Galindo-Rosales[a]*, J.P. Segovia-Gutiérrez[b], F.T. Pinho[a], M.A. Alves[a] and J. de Vicente[b]
[a] FEUP, Faculdade de Engenharia da Universidade do Porto, 4200-465 Porto (Portugal)
[b] UGR, Facultad de Ciencias de la Universidad de Granada, 18071 Granada (España).

Experiments under controlled shear and elongational flows[1] are typically performed in Rheology in order to measure material functions of non-Newtonian fluids and, subsequently, to fit to an appropriate constitutive equation. In the particular case of magnetic colloids (ferrofluids -FF- and/or magnetorheological fluids -MRF-), many rotational rheometers have been conveniently modified with fixtures to apply external magnetic fields to the sample undergoing shear deformation, either using magnetic circuits or solenoids. However, to our best knowledge, measurements of rheological material functions in uniaxial extension of FF and MRF have not been carried out, at least for low viscosity solutions.

We have developed a technique (patent pending) that, in general terms, allows the application of an external homogeneous magnetic field (AC or DC, constant or tuneable, and aligned or perpendicular to the flow direction) to the uniaxial extension flow kinematics undergone by a fluid sample in the commercial version of the Capillary Breakup Extensional Rheometer[2] (Haake^{TM} CaBER1^{TM}, Thermo Scientific). The same principle can be also adapted to FiSER-type rheometers[3] with relative ease.

Using such feature, we present data from measurements of commercial ferrofluids and magnetorheological fluids, obtained on the commercial CaBER 1 rheometer. Fig.1 plots the filament thinning with time for different ferrofluids (FF40, FF200 and FF500) having the same magnetization (M) versus field strength (H) hysteresis curve but with different shear viscosities, measured under three different configurations: (1) absence of magnetic field, (2) under the influence of a fixed DC external magnetic field by means of rod-like permanent magnets (Neodymium N42, 8mm diameter and 30mm length) perpendicular to the extensional flow and (3) under the influence of a fixed DC external magnetic field by means of rod-like permanent magnets (Neodymium N40, 8mm diameter and 77.5mm length) parallel to the extensional flow. All fluids exhibited a Newtonian-like behavior when no magnetic field was applied, i.e. the filament decreased linearly in time. Thus, the filament thinning process is determined by the balance between viscous and capillary forces. The capillary forces are determined by the Laplace pressure, which for curved filament shape is given by $\Delta P = \sigma(\frac{1}{R_1} + \frac{1}{R_2})$, with σ representing the surface tension of the fluid, R_1 the filament radius and R_2 the radius of curvature. Nevertheless, the time evolution of the filament thinning became non-linear under the effect of a magnetic field, due to the particle-particle interaction forces generated by the magnetic field. As expected, the shape of the curve depends on the demagnetization factor of the ferrofluid sample under deformation. Thus, when the field is aligned with the flow direction the breaking time is longer, as the interparticle forces are also aligned with the direction of flow. Moreover, the larger the viscosity of the ferrofluid the larger the breaking time will be. According to Niedzwiedz et al.[4], the profile of the filament thinning observed in Fig. 1, under the effect of a magnetic field, corresponds to a yield stress material.

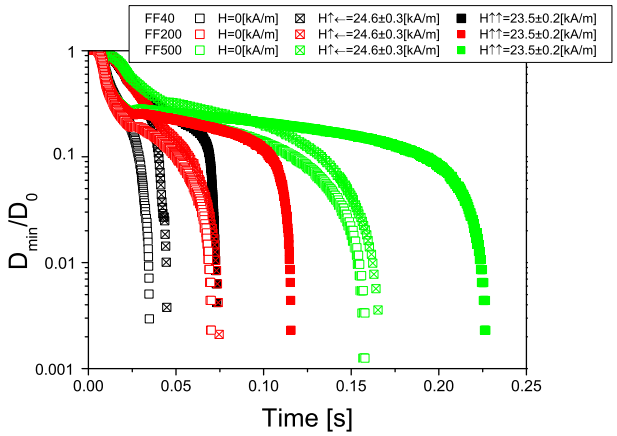

FIG. 1. Filament thinning evolution with time for different ferrofluids (FF40, FF200 and FF500) measured in the CaBER device with no magnetic field supplied (empty symbols) and under the influence of a constant external magnetic field perpendicular (crossed symbols) and parallel (filled symbols) to the extensional flow at 25±1°C.

Authors would like to acknowledge funding from Fundação para a Ciência e a Tecnologia (FCT), COMPETE, QREN and European Union (FEDER) through project PTDC/EQU-FTT/113811/2009 and FCT Investigator grant IF/00190/2013; CEFT/FEUP via CCO VCEFT1; MINECO through project MAT2010-15101; Junta de Andalucìa through projects P10-RNM-6630 and P11-FQM-7074; and the Spanish Ministry of Science and Innovation (FPU program) through the pre-doctoral fellowship AP2008-02138.

* galindo@fe.up.pt

[1] F.A. Morrison, Oxford University Press (2001).
[2] G.J.C. Braithwaite et al., US Patent 006711941B2.
[3] S.L. Anna et al., J. Rheol., 45 (2001).
[4] K. Niedzwiedz et al., Appl. Rheol., 19 (2009).

Fragility and robustness of the Kardar-Parisi-Zhang universality class

Matteo Nicoli*, Rodolfo Cuerno†, and Mario Castro‡
Department of Physics and Center for Interdisciplinary Research on Complex Systems
Northeastern University, 02115 – Boston, USA

One of the most powerful concepts in contemporary Statistical Mechanics is the idea of universality, by which microscopically dissimilar systems show the same large scale behavior, provided they are controlled by interactions that share dimensionality, symmetries, and conservation laws. In complex systems it becomes enormously simplifying, as significant descriptions can be put forward on the basis of the general principles just mentioned.

Celebrated non-equilibrium systems include those with generic scale invariance, displaying criticality throughout parameter space. Examples are self-organized-critical and driven-diffusive systems, or surface kinetic roughening. Indeed, the paradigmatic Kardar-Parisi-Zhang (KPZ) equation for a rough interface,

$$\partial_t h = \nu\nabla^2 h + \frac{\lambda}{2}(\nabla h)^2 + \eta(\mathbf{x},t), \qquad (1)$$

is very recently proving itself as a remarkable instance of universality. The exact asymptotic height distribution function has been very recently obtained for $d = 1$:[1] it is given by the largest-eigenvalue distribution of large random matrices in the Gaussian unitary (GUE) (orthogonal, GOE) ensemble, the Tracy-Widom (TW) distribution, for globally curved (flat) interfaces, as proposed in Ref. 2 and reviewed in Ref. 3. Beyond their fascinating connections with probabilistic and exactly solvable systems, these results are showing that, not only are the critical exponent values common to members of this universality class, but also the distribution functions and limiting processes are shared by discrete models and continuum equations,[4] and by experimental systems, from turbulent liquid crystals[5] to drying colloidal suspensions.[6]

In this work we assess the dependence on substrate dimensionality of the asymptotic scaling behavior of a whole family of nonlocal equations that feature the basic symmetries of the KPZ equation[7]

$$\partial_t h_{\mathbf{k}}(t) = (\nu k^{\mu} - \mathcal{K}k^2)h_{\mathbf{k}}(t) + \frac{\lambda}{2}\mathcal{F}[(\nabla h)^2]_{\mathbf{k}} + \eta_{\mathbf{k}}(t). \qquad (2)$$

Even for cases in which, as expected from universality arguments, these models display KPZ critical exponent values, their behavior deviates from KPZ scaling for increasing system dimensions.[8] Such a fragility of KPZ universality contradicts naive expectations, and questions straightforward application of universality principles for the continuum description of experimental systems. Still, we find that the ensuing limit distributions coincide with those of the KPZ class in one and two dimensions (see Fig. 1), demonstrating the robustness of the latter under changes of the critical exponent values.

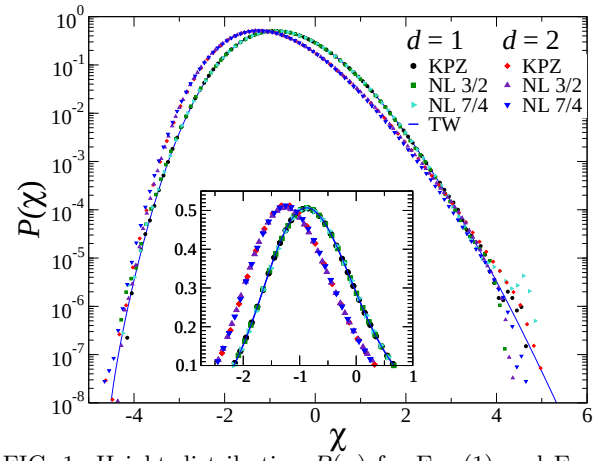

FIG. 1. Height distribution $P(\chi)$ for Eq. (1) and Eq. (2) for $\mu = 3/2,\ 7/4$ in case of one- and two-dim. substrates. The solid line is the TW-GOE distribution expected for $d = 1$.[9]

* m.nicoli@neu.edu
† Departamento de Matemáticas and Grupo Interdisciplinar de Sistemas Complejos (GISC), Universidad Carlos III de Madrid, 28911 – Leganés, Spain.
‡ GISC and Grupo de Dinámica No Lineal (DNL), Escuela Técnica Superior de Ingeniería (ICAI), Universidad Pontificia Comillas, 28015 – Madrid, Spain.

[1] T. Sasamoto and H. Spohn, Phys. Rev. Lett. **104**, 230602 (2010); G. Amir, I. Corwin, and J. Quastel, Commun. Pure Appl. Math. **64**, 466 (2011); P. Calabrese and P. Le Doussal, Phys. Rev. Lett. **106**, 250603 (2011).
[2] M. Prähofer and H. Spohn, Phys. Rev. Lett. **84**, 4882 (2000); Physica A **279**, 342 (2000).
[3] T. Kriecherbauer and J. Krug, J. Phys. A: Math. Theor. **43**, 403001 (2010); I. Corwin, Random Matrices: Theor. Appl. **1**, 1130001 (2012).
[4] S. G. Alves, T. J. Oliveira, and S. C. Ferreira, EPL **96**, 48003 (2011); T. J. Oliveira, S. C. Ferreira, and S. G. Alves, Phys. Rev. E **85**, 010601(R) (2012).
[5] K. A. Takeuchi and M. Sano, Phys. Rev. Lett. **104**, 230601 (2010); K. A. Takeuchi *et al.*, Sci. Rep. **1**, 34 (2011).
[6] P. Yunker *et al.*, Phys. Rev. Lett. **110**, 035501 (2013); *ibid.* **111**, 209602 (2013); M. Nicoli, R. Cuerno, and M. Castro, *ibid.* **111**, 209601 (2013).
[7] M. Nicoli, R. Cuerno, and M. Castro, Phys. Rev. Lett. **102**, 256102 (2009); J. Stat. Mech.: Theor. Exp. (2011) P10030.
[8] M. Nicoli, R. Cuerno, and M. Castro, J. Stat. Mech.: Theor. Exp. (2013) P11001.
[9] A. Edelman and P.-O. Persson, *Numerical Methods for Eigenvalue Distributions of Random Matrices*, arXiv:math-ph/0501068 (2005).

Multiobjective optimization and phase transitions

Luís F. Seoane[†,@], Ricard V. Solé[†,‡]
ICREA-Complex Systems Lab, Universitat Pompeu Fabra (GRIB), Dr. Aiguader 80, 08003 Barcelona, Spain.

Historically, we can fairly attribute the introduction and development of Multi-Objective Optimization (MOO) to economists and engineers. Economic setups usually imply satisfying conflicting interests and thus they pioneered the field quite naturally. Meanwhile, we owe to engineers the development of efficient algorithms to approximate the solutions to complicated MOO problems numerically. Engineering and Economy are relatively peripheral to natural sciences. A side effect of this is that MOO had little impact in areas such as ecology or molecular and systems biology. Only recently we find outstanding applications of MOO to these disciplines which put optimization and natural selection in a different, richer perspective[1,2]. Also physics did not pay much attention to MOO despite that a large literature exists linking Single Objective Optimization (SOO) algorithms–such as the Metropolis-Hastings or Genetic Algorithms–and their dynamics to statistical mechanics.

Contributions from complex systems usually dealt with MOO problems by integrating the many optimization targets into single fitness functions using arbitrary metaparameters[3,4] as in:

$$\Omega = \lambda t_1(x) + (1-\lambda)t_2(x), \qquad (1)$$

with Ω the global fitness, λ a bias (the metaparameter) that assigns different and arbitrary importance to $t_1(x)$ and $t_2(x)$. These $t_1(x)$ and $t_2(x)$ are the multiple objectives that we would wish to optimize simultaneously in an ideal scenario. Of course, equation 1 generalizes to any number K of target functions $t_k(x)$. Note that the many targets for optimization can be conflicting and thus impose a trade-off upon the MOO solutions. Systems researched using this SOO methodology usually report interesting features such as phase transitions or the existence of critical regimes[3,4].

In a recent paper[5] we provide an elegant and robust theoretical framework to study systems that involve MOO and their behavior when the different objectives are integrated into SOO problems, such as in equation 1. Our theory relies on the interplay between the Pareto front (a geometric object that encompasses all MOO optimal solutions and that defines the best trade-off possible given the MOO problem) and a hyperplane defined by the global fitness function.

We find out that phase transitions are parsimoniously and precisely explained within our framework–also for thermodynamics. We propose that our theory provides a very robust generalization of the concept of phase transition to any MOO system whose targets are collapsed into SOO by some natural or artificial means. Because the results are valid for any such a system, our generalization of phase transitions does not rely on partition functions and does not require–in principle–that systems are ergodic, although the precise implications of our theory for non-ergodic systems still requires further investigation.

Altogether, the theory allows us to safely talk about phase transitions in a series of systems ranging from biology to social dynamics knowing that a rigorous definition exists. Our framework provides very robust groundings for MOO, which were missing in the literature, and furthers our understanding about solutions to MOO problems. Finally, the novelty of our theory is revealed in that state of the art contributions[1,2] lack any references to our findings.

[†] Institut de Biologia evolutiva, CSIC-UPF, Pg. Maritim de la Barceloneta 37, 08003 Barcelona.
[@] luis.seoane@upf.edu
[‡] Santa Fe Institute, 1399 Hyde Park Road, Santa Fe NM 87501, USA.

[1] R. Schuetz, N. Zamboni, M. Zampieri, M. Heinemann, U. Sauer, Multidimensional Optimality of Microbial Metabolism *Science* **336**, 601-604 (2012).
[2] O. Shoval, H. Sheftel, G. Shinar, Y. Hart, O. Ramote, A. Mayo, E. Dekel, K. Kavanagh, U. Alon, Evolutionary Trade-Offs, Pareto Optimality, and the Geometry of Phenotype Space. *Science* **336**, 1157-1160 (2012).
[3] R. Ferrer i Cancho, R. V. Solé, Least effort and the origins of scaling in human language. *Proc. Natl. Acad. Sci.* **100**(3), 788-791 (2003).
[4] M. E. J. Newman, Networks, Oxford University Press, (2010).
[5] L. F. Seoane, R. V. Solé, A multiobjective optimization approach to statistical mechanics. http://arxiv.org/abs/1310.6372

Búsqueda aleatoria en el espacio: ¿qué papel juegan los mecanismos de detección?

Daniel Campos [1,*], Vicenç Méndez[1], Frederic Bartumeus[2]
[1] *Grupo de Física Estadística. Universidad Autónoma de Barcelona 08193 Bellaterra, Barcelona*
[2] *Centre d'Estudis Avançats de Blanes (CEAB-CSIC), Accés Cala Sant Francesc 14, 17300 Blanes, Girona*

Existen numerosos procesos en la naturaleza en los cuales una partícula (Browniana, por ejemplo) o un individuo describen una trayectoria aleatoria hasta alcanzar un determinado objetivo (un reactivo en el caso de reacciones químicas, una fuente de alimento en el caso de microorganismos o animales más complejos, etc).

Cuando las propiedades del sistema hacen que el tiempo característico necesario para alcanzar ese objetivo sea relativamente largo comparado con las escalas de tiempo de transporte (por ejemplo, el tiempo medio entre colisiones o tiempo de persistencia) podemos interpretar dichos procesos en términos de una "búsqueda aleatoria" en el espacio. En estas situaciones resulta útil el cálculo de tiempos de *primer paso*, probabilidades de supervivencia, y otras magnitudes que han sido largamente estudiadas en la literatura desde la física estadística[1,2].

Un aspecto que sin embargo ha quedado relativamente olvidado es el papel que los mecanismos de detección juegan dentro de este proceso. Por lo general la hipótesis de partida suele ser la de que la reacción o la detección se producen de forma automática cuando la partícula alcanza la posición del objetivo. Sin embargo, esta "detección perfecta" está muy lejos de ser realista para muchos problemas particulares en los cuales las restricciones externas, la capacidad de la partícula para *reconocer* su objetivo, o los mecanismos de *protección* que éste pueda emplear pueden comprometer el éxito de dicha búsqueda.

En la presente contribución presentaremos un modelo mesoscópico[3–5] que permite estudiar las propiedades estadísticas de estos procesos de búsqueda *imperfecta*, aplicable a cualquier tipo de restricción y/o mecanismo de detección. En particular, veremos que como consecuencia de esas restricciones aparecen nuevos paradigmas que nos obligan a replantear las estrategias óptimas que una partícula debería usar para minimizar su tiempo medio de búsqueda.

Finalmente, discutimos el posible interés de este tipo de problemas, así como los correspondientes retos teóricos y experimentales que se plantean, de cara a su posible aplicación en la optimización de procesos de búsqueda en organismos superiores, particularmente en humanos.

---

* daniel.campos@uab.es

[1] S. Redner, *A Guide to First-Passage Processes* (Cambridge University Press, Cambridge, 2001).
[2] R. Metzler, G. Oshanin, S. Redner (eds.) *First-passage phenomena and their applications.* (World Scientific, Singapore, 2013).
[3] D. Campos, V. Méndez, F. Bartumeus. Phys. Rev. Lett. 108, 028102 (2012).
[4] D. Campos, F. Bartumeus, V. Méndez. Phys. Rev. E 88, 022101 (2013).
[5] V. Méndez, D. Campos, F. Bartumeus. *Stochastic Foundations in Movement Ecology: anomalous diffusion, front propagation and random searches.* (Springer-Verlag, Berlin, 2013).

Phase Behaviour and Self-Assembly of Inverse Patchy Colloids

Eva G. Noya[1]*, Ismene Kolovos[2], Günther Doppelbauer[2], Emanuela Bianchi[2] and Gerhard Kahl[2]
[1] *Instituto de Química Física Rocasolano, Consejo Superior de Investigaciones Científicas (CSIC), C/ Serrano 119, 28006 Madrid, Spain*
[2] *Institut für Theoretische Physik and Center for Computational Materials Science (CMS), Technische Universität Wien, Wiedner Hauptstraße 8-10, A-1040 Vienna, Austria*

In the last few years the theoretical investigation of the phase behaviour of particles either with anisotropic shapes or interactions has been a very active field of research. Initially this work was motivated by advances in colloidal science that allowed the synthesis of those particles and that lead to the suggestion of building new materials with the desired properties using a "bottom-up" approach, i.e. by designing the particles that would self-assemble into the target structure[1,2]. However it soon became evident that the theoretical study of those particles was interesting also from a fundamental point of view. Anisotropic particles can exhibit an amazingly reach and unusal phase behaviour[3]. Here we investigate the phase behaviour of Inverse Patchy Particles (IPC), a model representative of negatively charged particles with two positively charged patches at the poles[4]. As a consequence regions with opposite charge attract each other but regions with like charge repel each other. The equilibrium phase diagram was evaluated using a combination of two well established techniques: first, an efficient optimization tool based on ideas of evolutionary algorithm is used to identify the stable structures at zero temperature and, second, the stability of those phases at finite temperature is investigated by free energy calculations[5]. We found that the competition between the attractive and repulsive interactions leads to a wealth of ordered structures, including a laminar structure that is stable over a quite broad region of the phase diagram.

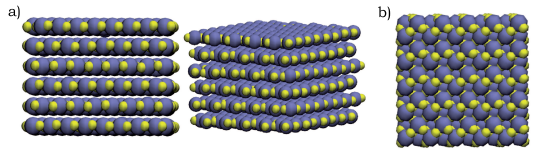

FIG. 1. Two examples of ordered structures formed by IPC particles.

* eva.noya@iqfr.csic.es

[1] A. B. Pawar and I. Kretzschmar, *Macromol. Rapid Commun.* **31**, 150 (2010).
[2] E. Bianchi, R. Blaak and C. N. Likos, *Phys. Chem. Chem. Phys.* **13**, 6397 (2011).
[3] See, for example, T. Vissers, Z. Preisler, F. Smallenburg, M. Dijkstra, and F. Sciortino *J. Chem. Phys.* **138**, 164505 (2013).
[4] E. Bianchi, G .Kahl, and C. N. Likos, *Soft Matter* **7**, 8313 (2011).
[5] G. Doppelbauer, E. G. Noya, E. Bianchi, and G .Kahl, *Soft Matter* **8**, 7768 (2012); G. Doppelbauer, E. G. Noya, E. Bianchi, and G .Kahl, *J. Phys.: Condens. Matter* **24**, 284124 (2012).

Phase diagram of Stockmayer polymers in bulk and near surfaces

Joan J. Cerdà*, Pedro A. Sánchez†, C. Holm‡, Tomàs Sintes
IFISC, Instituto de Física Interdisciplinar y Sistemas Complejos
CSIC-Universidad de las Islas Baleares 07122-Palma (Mallorca)

Artificial magnetic filaments can be obtained by mutually linking magnetic colloids to form a chain. These magnetic chains represent the equivalent to magnetic polymers but at supra-molecular scale. In difference to one-dimensional chemical magnetic polymers which only manifest their magnetic properties at $T < 100K$, magnetic filaments can retain their magnetism at room temperature and zero field.

In this contribution we present the results of our previous studies[1–3] on the equilibrium conformations of flexible and semiflexible magnetic filaments in different physical environments of relevance for forthcoming applications. In particular, we focus on the determination of the phase diagram at zero field for magnetic filaments which monomers exhibit short-range LJ attractive interactions (Stockmayer polymers, i.e. filaments in poor solvent conditions) in the limit of strong dilution, as well as filaments in good solvent conditions. We study the cases of magnetic chains in bulk (see figure 1) and near an attractive surface. We find that the phase diagrams of magnetic systems exhibit a rich variety of new phases when compared with non-magnetic chains in similar environments.

The emerging interest in this relatively novel field is due to the fact that magnetic filaments are very appealing from the technological point of view. They can be thought as improved substitutes of current ferrofluids, or as elements for magnetic memories, chemical and pressure nanosensors, micro-propellers, non-permanent photonic crystals, and generation of unique patterns able to provide watermarks to authenticate cards or other documents, to just mention a few.

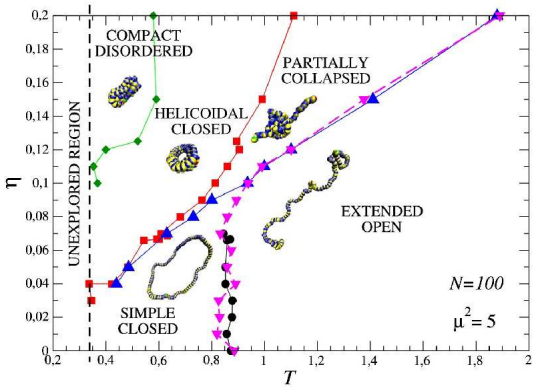

FIG. 1. A tentative phase diagram for magnetic filaments of length N=100, and a dipole moment per monomer of fixed strength $\mu^2 = 5$.

Acknowledgements: We thank the projects FISICOS (FIS2007-60327), GRID-CSIC and BwGrid founded by the Spanish MICNN and the ERDF, respectively.

* joan@ifisc.uib-csic.es
† Universität Wien, Computergestützte Physik, 1090 Wien, Boltzmanngasse 5.
‡ Institute for Computational Physics- ICP (Universtität Stuttgart), Stuttgart, Germany.

[1] J. J. Cerdà, P. A. Sánchez, C. Holm, T. Sintes, Soft Matter, *9*, 7185-7195, (2013).
[2] P. A. Sánchez, J. J.Cerdà, T. Sintes, C.Holm, J.Chem.Phys., *139*, 044904, (2013).
[3] P. A. Sánchez, K., J. J.Cerdà, V. Ballenegger, T. Sintes, C. Holm, Soft Matter, *7*, 1809, (2011).

Random walkers that die as they move

S.B. Yuste[†], E. Abad[*], and K. Lindenberg[‡]
Centro Universitario de Mérida
Departamento de Física Aplicada, Universidad de Extremadura
06800-Mérida (Badajoz)

In statistical physics, random walks are widely used to study stochastic transport in a large variety of experimental systems. Exploration and trapping properties of walkers that do not undergo reactions or transformations have been comprehensively studied by many authors. However, the corresponding properties of reactive walkers have received considerably less attention. In particular, work involving the arrival statistics of so-called mortal or evanescent walkers, that is, walkers that die in the course of their motion, is surprisingly scarce in spite of the obvious ubiquity of death and death-like processes in many real problems in physics, biology and chemistry.

As it turns out, we have found a few examples where *ad-hoc* models were developed and tailored to study particular experimental situations (e.g., photon scattering accompanied by absorption in a tissue). However, the fact that the effect of elementary death processes on the exploration properties of random walkers can be investigated using arguments and techniques similar to those used for conventional, immortal walkers has, until recently, gone largely unnoticed. As a result of this observation, we have been able to develop an overarching theoretical framework allowing one to obtain the most relevant properties of mortal walkers[1]. This achievement seems very timely to us, as the presence of death processes leads to a completely new physics in the transport behavior of diffusing particles, and it also has potential relevance for a wealth of experimental problems. These problems touch on fundamental questions as diverse as the relaxation behavior of defects in dielectric media or the extent of the region where a diffusing radioisotope remains potentially emissive.

We aim to present in a pedagogical way some results that have been published recently[1,2]. To begin with, we shall focus on exploration and trapping properties in discrete time, such as the average number S_n^* of distinct sites visited by a mortal walker on perfect lattices of arbitrary dimension after a certain number of time steps n (at each time step the walker is assumed to perform a jump). Let us denote by S_n the counterpart of S_n^* for an immortal walker, that is, a walker that lives forever. The quantity S_n is known to diverge with n in all dimensions. However, if the walker has a constant probability of dying $1-e^{-\lambda}$ in each time step, S_n^* tends to a *finite* value expressible in terms of λ and the generating function of S_n (see, e.g., Fig. 1, displaying the behavior of S_n^* in the one-dimensional case).

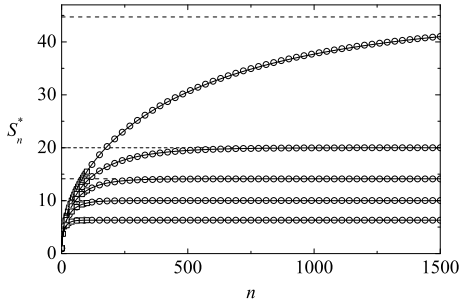

FIG. 1. Average number S_n^* of distinct sites visited by a Markovian mortal walker vs. the time step number n. The walker performs nearest neighbor jumps on an infinite $1d$ lattice as long as it survives. The curves correspond, from top to bottom, to $\lambda = 0.001, 0.005, 0.01, 0.02$ and 0.05 ($e^{-\lambda n}$ is the probability that the walker has survived after n steps). Solid lines give analytic results and broken lines give analytic asymptotic values; circles, simulation values; squares, exact values obtained from the first 100 coefficients in the ξ power expansion of the generating function $S^*(\xi)$ associated with S_n^*.

We shall also consider the continuous time limit of the above system, namely, the behavior of the Wiener sausage defined by a mortal random walker as a function of time[2], a key quantity for the computation of reaction rates in chemical kinetics. We shall also address memory effects, that is, the behavior of the average number of distinct sites visited by an evanescent continuous time random walker up to a given time[3]. The above results are expected to be relevant for problems involving diffusing particles subject to photon emission or radioactive decay, or stochastically moving prey hunted by a collection of predators, to name but a few.

---

[*] E-mail: eabad@unex.es
[†] Facultad de Ciencias, Departamento de Física, Universidad de Extremadura, Avda. de Elvas s/n, E-06071, Badajoz.
[‡] Department of Chemistry and Biochemistry, and BioCircuits Institute, University of California San Diego, 9500 Gilman Drive, La Jolla, CA 92093-0340, USA.

[1] S. B. Yuste, E. Abad, and K. Lindenberg, Phys. Rev. Lett. **110**, 220603 (2013).
[2] S. B. Yuste, E. Abad, and K. Lindenberg, *Arrival statistics and exploration properties of mortal walkers*, to appear in *First-Passage Phenomena and Their Applications*, R. Metzler, G. Oshanin, and S. Redner (Eds.) (World Scientific, Singapore, to appear in 2014).
[3] E. Abad, S. B. Yuste, and K. Lindenberg, Phys. Rev. E, **88**, 062110 (2013).

Fuerzas inducidas por fluctuaciones en sistemas fuera del equilibrio

José María Ortiz de Zárate*
Departamento de Física Aplicada I
Universidad Complutense
28040-Madrid

Fuerzas inducidas por fluctuaciones son comunes en la naturaleza[1]. Prototipo de ellas es la bien conocida fuerza de Casimir, que aparece entre placas conductoras de la electricidad debido a las fluctuaciones cuánticas del campo electromagnético[2] (EM). En este caso, la escala de energía está dada por la constante de Planck, $\hbar$, y la fuerza por unidad de área, o presión, es

$$p_{\rm EM} = -\frac{\pi^2 \hbar c}{240 L^4}, \tag{1}$$

donde L es la distancia entre placas, c la velocidad de la luz, y donde el signo menos indica que la fuerza es atractiva. Otro tipo relativamente conocido son las fuerzas inducidas por fluctuaciones térmicas, para las que la escala de energía es $k_{\rm B}T$, con $k_{\rm B}$ la constante de Boltzmann y T la temperatura[1]. Estas fuerzas de origen térmico son importantes cuando las fluctuaciones poseen correlaciones espaciales de largo alcance, lo que hace que su intensidad dependa del tamaño del sistema. El primer ejemplo de este tipo de fuerzas fue descrito por Fisher y de Gennes, al estudiar correcciones de tamaño finito a la energía libre de un fluido cerca de su punto crítico[3]. En ese caso, se encuentra una fuerza por unidad de área, a la que se suele denominar presión de Casimir crítica, $p_{\rm c}$, que viene dada por[4]

$$p_{\rm c} = \frac{k_{\rm B}T}{L^3}\Theta\left(L/\xi\right), \tag{2}$$

con $\Theta\left(x\right)$ es una función de escala y ξ la longitud de correlación. Para predicciones concretas se define una amplitud de Casimir, $\Delta = \lim_{x\to 0}\Theta\left(x\right)$, que para la clase de universalidad de Ising varía desde -0.01 hasta $+2$ dependiendo de las condiciones de contorno[5]. Nótese que para L suficientemente grande, $|p_{\rm c}| > |p_{\rm EM}|$. Asimismo, fuerzas inducidas por fluctuaciones térmicas se han predicho en sistemas en equilibrio más complejos, en los que existen modos Goldstein, como el helio superfluido o los cristales líquidos[1]. También en fluidos confinados, donde la función de correlación de las fluctuaciones de la velocidad depende del tamaño del sistema[6].

Está hoy en día bien establecido que, debido a efectos de acoplamiento entre modos, las fluctuaciones térmicas en fluidos fuera del equilibrio poseen correlaciones de largo alcance espacial, lo que hace que su intensidad dependa del tamaño del sistema. El problema más estudiado es el de un fluido en reposo sometido a un gradiente uniforme de temperaturas[7], ∇T. Los efectos de tamaño finito, cuando el gradiente se establece confinando el fluido entre dos placas a distinta temperatura separadas una distancia L, han sido tratados en detalle[8].

Recientemente[9], en colaboración con otros colegas, hemos demostrado que el largo alcance espacial de las fluctuaciones de no-equilibrio induciría presiones de tipo Casimir, que dependen del tamaño L de confinamiento. Específicamente, para el caso de condiciones de contorno *free-slip*, obtuvimos una expresión analítica para la presión media generada por las fluctuaciones de no-equilibrio, en el orden más bajo[9]

$$p_{\rm NE} = \frac{c_p k_{\rm B} T^2 \left(\gamma - 1\right)}{96\pi D_T \left(\nu + D_T\right)} L \left(\frac{\nabla T}{T}\right)^2. \tag{3}$$

Aquí c_p es el calor específico isobárico, γ el índice adiabático, α el coeficiente de expansión térmica, ν la viscosidad cinemática y D_T la difusividad térmica. Se observa que esta presión inducida aumenta proporcionalmente a L, un comportamiento anómalo debido al extremadamente largo alcance espacial de las fluctuaciones de no-equilibrio. Si se fija la diferencia de temperatura ΔT entre placas, la presión inducida disminuye como L^{-1}. En cualquier caso, para L suficientemente grande, $p_{\rm NE}$ podría ser más importante que $p_{\rm EM}$ o $p_{\rm c}$.

Najafi y Golestanian[10] han estudiado presiones inducidas de no-equilibrio, pero sólo considerando ruido inhomogéneo, no acoplamiento de modos. Wada y Sasa[11] presiones anómalas en el caso de un fluido isotermo que está fuera de equilibrio por flujo.

---

* jmortizz@fis.ucm.es

[1] M. Kardar, R. Golestanian, Rev. Mod. Phys. **71**, 1233 (1999).
[2] H.B.G. Casimir, Koninklijke Nederlandse Akad. Wetenschappen **851**, 793 (1948).
[3] M.E. Fisher and P.G. de Gennes, C.R. Acad. Sc. Paris B **287**, 207 (1978).
[4] A. Gambassi, C. Hertlein, L. Heiden, S. Dietrich, and C. Bechinger, Europhysics News **40**, 18 (2009).
[5] M. Krech, J. Phys. Condens. Matter **11**, R391 (1999).
[6] R.B. Jones, Physica **105A**, 395–146 (1981)
[7] T.R. Kirkpatrick, E.G.D. Cohen, and J.R. Dorfman, Phys. Rev. A **26**, 995 (1982). D. Ronis and I. Procaccia, Phys. Rev. A **26**, 1812 (1982).
[8] J.M. Ortiz de Zárate, R. Pérez Cordón, and J.V. Sengers, Physica A **291**, 113 (2001). J.M. Ortiz de Zárate and J.V. Sengers, Hydrodynamic Fluctuations in Fluids and Fluid Mixtures (Elsevier, Amsterdam, 2006).
[9] T.R. Kirkpatrick, J.M. Ortiz de Zárate and J.V. Sengers, Phys. Rev. Lett. **110**, 235902 (2013). See also: http://arxiv.org/abs/1401.1339
[10] A. Najafi and R. Golestanian, Europhys. Lett. **68**, 776 (2004).
[11] H. Wada and S. Sasa, Phys. Rev. E **67**, 065302(R) (2003)

Fluctuaciones de energía interna en el estado de flujo tangencial uniforme

Pablo Maynar*, M. I. García de Soria, and J. J. Brey
Física Teórica, Universidad de Sevilla, Apartado de Correos 1065, E-41080, Sevilla, Spain

En este trabajo estudiamos las fluctuaciones de energía interna en un gas granular diluido en el estado estacionario de flujo tangencial uniforme. Este estado está caracterizado por una densidad y temperatura homogéneas, y un campo de velocidades con un gradiente constante (en la dirección perpendicular al vector velocidad). El estudio teórico se realiza desde dos puntos de vista: por una parte, mediante una teoría fenomenológica basada en hidrodinámica fluctuante, y, por otra más fundamental, usando Teoría Cinética. Los resultados son comparados con simulaciones de Dinámica Molecular. Además, los límites de la primera teoría son discutidos desde el punto de vista de la segunda[1,2].

* maynar@us.es

[1] J. J. Brey, M. I. García de Soria, and P. Maynar, Phys. Rev. E **86**, 031304 (2012).
[2] J. J. Brey, P. Maynar, and M. I. García de Soria, Phys. Rev. E **86**, 061308 (2012).

Inverse cascades sustained by the transfer rate of angular momentum in a 3D turbulent flow

Miguel López-Caballero and Javier Burguete*
Departamento de Física y Matemática Aplicada, Universidad de Navarra
Irunlarrea 1, E-31008 Pamplona, Spain

The existence of energy cascades as signatures of conserved magnitudes is one of the universal characteristics of turbulent flows. In homogeneous 3D turbulence the energy conservation produces a direct cascade from large to small scales, although in 2D it produces an inverse cascade pointing towards small wavenumbers. In this work we present the first evidence of an inverse cascade in a fully developed 3D experimental turbulent flow where the conserved magnitude is the angular momentum.

We analyze the behavior of a fluid in a closed cavity where two inhomogeneous and strongly turbulent flows collide in a thin region. Depending on the spatial position different cascades have been found. Far from the collision layer a classical Kolmogorov scenario is found, but in the shear region inverse cascades appear.

The experimental volume is a closed cylinder with diameter $D = 20cm$ and $H = 20cm$. Two impellers of diameter $D_{prop} = 17.5$cm with 10 curved blades rotate in opposite directions, powered by two independent motors (maximum power of 1.5kW) regulated through a computer. The rotation frequency of the propellers can be adjusted independently between $f = 0.5 - 12.5$Hz generating a maximum torque of 15Nm. A key characteristic of this setup is the high inertia of the propeller and motor set and the high stability of the propellers, i.e. the instantaneous fluctuations of each one of the propeller's velocities are well below one part in one thousand 0.1%.

We have performed PIV (high spatial resolution) and LDA (high temporal resolution) measurements of the velocity fields. From these data, we can determine that the Reynolds number is $Re = 7 \times 10^5$, the typical turbulent intensity is 50%, the $Re_\lambda = 900$, the Taylor microscale $\lambda_T = 1.8$mm and the integral scale $L_I = 15$mm. The analysis of the data series, both in space and time, reveal that below the injection scales there are inverse cascades (-1/3 in time, -7/3 in space) that can be explained as the transfer of angular momentum between the diferent fluid layers.

With these results as an starting point, a new experiment in Helium superfluid has been run in the Superfluid Helium Facility (SHREK) in Grenoble, where a Reynolds number of 10^8 has been reached.

More information can be found in[1,2].

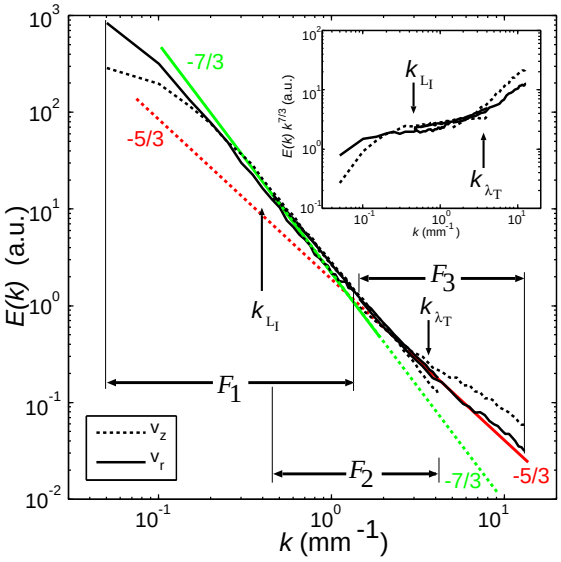

FIG. 1. Spatial spectra computed from PIV measurements. The wave number ranges covered by the different fields of view F1, F2, and F3 are presented (the full range covers from 0.05 to 13 mm^{-1}). Inset: Spectra compensated by $k^{7/3}$ where the slope change is clearly visible. k_{L_I} and k_{λ_T} correspond to the integral scale and the Taylor microscale. Each one of these spectra is the average of 1500 realizations along a diameter.

* javier@unav.es

[1] A. de la Torre, J. Burguete, Phys Rev Lett 99 (2007) 054101.
[2] M. Lopez-Caballero, J. Burguete, Phys Rev Lett 110 (2013) 124501.

Estudio experimental de la estabilidad de los arcos en un medio granular

C. Lozano*, I. Zuriguel, A. Garcimartín y G. Lumay‡
Departamento de Física y Matemática Aplicada
Facultad de Ciencias, Universidad de Navarra
31080 Pamplona

Cuando un conjunto de partículas se hace pasar por un orificio, el flujo se puede interrumpir debido a la formación de un arco (una estructura mecánicamente estable). Esto puede ocurrir tanto en medios granulares, como en suspensiones o en avalanchas humanas.

Para romper los arcos, es necesario un aporte de energía como el uso de vibraciones. Este proceso tiene gran importancia industrial. El objetivo de este trabajo es el estudio experimental de la estabilidad de los arcos que se forman a la salida de un silo frente a las vibraciones externas. En un trabajo publicado recientemente[1] se analizó cómo depende de la forma de los arcos la energía necesaria para romperlos .

En un silo con un orificio en la base el material granular puede estar atascado o no, y en distintos trabajos se ha intentado estudiar la transición entre estos dos estados[2,3]. Con el fin de arrojar luz sobre este planteamiento, hemos medido experimentalmente la distribución de los tiempos durante los cuales el silo se encuentra atascado mientras es vibrado a una frecuencia y amplitud fija. Se ha hallado que la distribución decae como una ley de potencias con un exponente que depende de la amplitud de la vibración, Γ, y del tamaño del orificio, R. Se debe tener en cuenta que si el valor del exponente de la ley de potencias es menor de 2 el primer momento de la distribución no converge. En otras palabras, la duración de los atascos puede exhibir sucesos extremos, y el tiempo medio durante el cual se ha atascado el silo dependerá del tiempo total que el experimento ha estado funcionando. En la Fig. 1, aparece representado el valor del exponente 2 con una línea continua: los datos que se encuentran por encima de esta línea tienen un exponente menor a 2, mientras si se están por debajo es mayor. Debe notarse que el exponente se hace menor de 2 para oficios pequeños e intensidades de vibración bajas. Por tanto, se pueden encontrar un estado no atascado aumentando bien el tamaño del orificio o bien Γ. Pasar de ≥ 2 a <2 puede considerarse, por tanto, una transición al atasco.

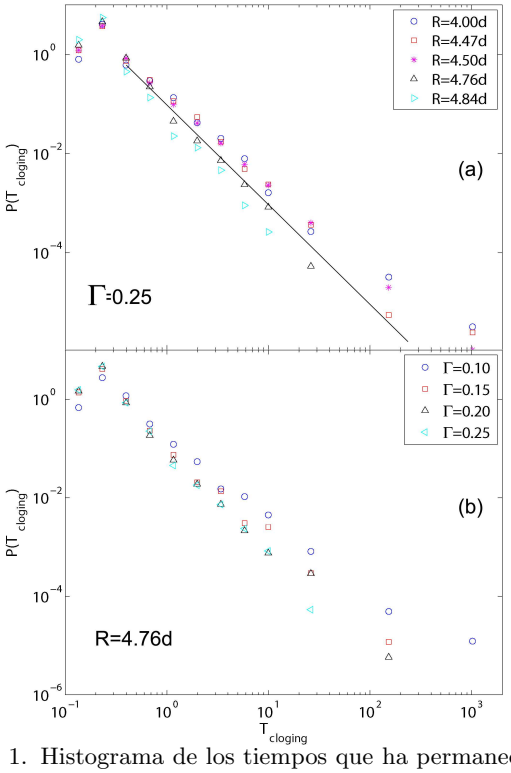

FIG. 1. Histograma de los tiempos que ha permanecido el silo atascado mientras se estaba vibrando (a) correspondiente a $\Gamma = 0.25$ para distintos tamaños de orificio, siendo d=1 *mm* el diámetro de la partícula, (b) correspondiente a R=4.76 *mm* para distintas amplitudes de vibración. La línea negra tiene una pendiente de dos.

* clozano@alumni.unav.es
http://www.unav.edu/centro/granularlab
‡ GRASP, Université de Liège, B-4000 Liège, Bélgica.

[1] C. Lozano, G. Lumay, I. Zuriguel, R. C. Hidalgo, A. Garcimartín, *Phys. Rev. Lett.* **109**, 068001 (2012).
[2] C. Mankoc, A. Garcimartín, I. Zuriguel, D. Maza, L. Pugnaloni, *Phys. Rev. E.* **80**, 011309 (2009).
[3] A. Janda, D. Maza, A. Garcimartín, E. Kolb, J. Lanuza and E. Clément, *Euro. Phys. Lett* **87**, 24002 (2009).

Cristalización de *para*-Hidrógeno: ¿una transición (de primer orden) cuántica a temperatura finita?

C. Cabrillo[1*], F. Fernández-Alonso[2], R. Fernández-Perea[1], F. J. Bermejo[3], M. A. González[4], C. Mondelli[4], E.Farhi[4]
[1] *Instituto de Estructura de la Materia, IEM-CSIC, Serrano 123, Madrid 28006, Spain.*
[2] *ISIS Facility, Rutherford Appleton Laboratory, Chilton, Didcot, Oxfordshire OX11 0QX, United Kingdom*
[3] *IEM-CSIC, Unidad Asociada de Física Aplicable, Department of Electricity and Electronics, University of the Basque Country, P.O. Box 664, 48080 Bilbao, Spain*
[4] *Institut Laue Langevin, 6 rue Jules Horowitz 38042, Grenoble Cedex 9, France*

Los sólidos cuánticos se caracterizan por grandes fluctuaciones cuánticas incluso a las mas bajas temperaturas de tal modo que la aproximación harmónica no es aplicable ni tan siquiera a temperatura cero. El ejemplo mas notable es el cristal de para-Hidrógeno (*para*-H_2). Dado su carácter molecular y su mínima masa, tanto los grados de libertad rotacionales como los traslacionales muestran un comportamiento fuertemente cuántico. De hecho la isotropía del estado rotacional fundamental $J = 0$ implica un promediado cuántico que tiende a a minimizar los efectos anisotrópicos. De ahí que el potencial intermolecular resulta adecuadamente descrito mediante un potencial efectivo completamente isotrópicol[1] de tal forma que una primera aproximación semi-cuántica útil en muchos cáculos, consiste simplemente en un una dinámica clásica bajo dicho potencial isotrópico ignorando completamente la estructura de dímero de la molécula.

El estado cristalino fundamental del *para*-H_2 es un estructura hcp con una distancia de primeros vecinos de $R_{NN} = 3.78$Å y una temperatura de fusión de 14.8 K. En esta fase el desplazamiento cuadrático medio (dcm) del centro de masas molecular debido a la energía de punto cero, esto es, a la deslocalización cuántica, es suficiente para explorar el corazón repulsivo del potencial de interacción. Como consecuencia el cristal se expande para minimizar su energía libre de tal forma que el valor de R_{NN} mencionado arriba es sustancialmente mayor que la distancia correspondiente al mínimo del potencial H_2-H_2, esto es, $R \simeq 3.41$ Å. Como consecuencia de esta notable expansión de volumen (~ 30 %), la aproximación de Born-Karman produce modos normales inestables caracterizados por frecuencias imaginariasl[1]. Esta sería la señal de identidad de un sólido cuántico. Por otro lado, dada la ligereza de la molécula la energía del primer nivel rotacional es muy alta, mas concretamente $E_{J=0\to1} = 14.6$ meV (~ 170 K) de tal forma que el carácter cuántico de las rotaciones es conspicuo mientras que la molédula rota de forma prácticamente libre incluso en la fase cristalina. El momento angular molecular permanece como un buen número cuántico pero poco se sabe de la forma de línea espectral.

Los estudios teóricos, empezando por los trabajos pioneros de Elliot y Hartmann[2] y de Van Krannendonk y colaboradores[3], han identificado como mecanismo principal de ensanchamiento de dicha línea una sutil ruptura de la degeneración inducida por el campo cristalino dependiente de la anisotropía del campo fonónico[4]. Estas cantidades son difíciles de calcular ya que son muy sensibles al delicado balance entre las fuerzas experimentadas por un molécula situada en una red periódica altamente simétrica. Desde el lado experimental, el acceso directo a la anchura de línea de la trasición $J = 0 \to 1$ (ópticamente prohibida) es todo un reto ya que las anchuras estimadas son del orden del μeV para un eneroía de transición de unos 14.6 meV.

Recientemente[5], utilizando la técnica de eco de espín neutrónico inelástico hemos tenido éxito en medir dicha anchura de línea en función de la temperatura en todo el rango de existencia del cristal. Para ello hemos hecho uso de lo que podría considerarse como el montaje experimental de dispersoón de neutrones mas completo posible de tal forma que en la misma muestra y las mismas condiciones termodinámicas se pudo medir también dispersión de Bragg, que nos da información directa sobre la expansión de la red cristalina, y el factor de forma molecular, que nos da información directa sobre el dcm molecular. Sorprendentemente ninguna de estas tres cantidades muestra una dependencia con la temperatura apreciable en todo el rango de temperaturas de existencia del cristal. Es decir, el cristal se muestra completamente expandido ya desde la temperatura de cristalización.

En la presente ponencia argumentaremos que este comportamiento termodinámico inesperado se puede entender si la transición de fase de cristalización está inducida por fluctuaciones cuánticas debidas a la deslocalización asociada al caráter ondulatorio de la dinámica no ya del cristal sino del líquido antes de cristalizar.

---

* ccabrilo@foton0.iem.csic.es

[1] I.F. Silvera, Rev. Mod. Phys. **52**, 393 (1980).
[2] R.J. Elliot and M.W. Hartmann, Proc. Phys. Soc. (London) **90**, 671 (1967).
[3] J. Van Kranendonk, *Solid Hydrogen: Theory of the Properties of Solid H_2, HD, and D_2* (Plenum Press, New York, 1983).
[4] V.G. Manzhelii and Y.A. Freiman, *Physics of Cryocrystals* (American Institute of Physics, New York, 1997).
[5] F. Fernandez-Alonso et al, Phys. Rev. B **86**, 144524 (2012).

Smart Inference and Criticality

Jorge Hidalgo*[1], Jacopo Grilli[2], Samir Suweis[2], Miguel Á. Muñoz[1], Jayanth R. Banavar[3], Amos Maritan[2]
[1] *Dpto. Electromagnetismo y Física de la Materia, Universidad de Granada, 18071 Granada (Spain)*
[2] *Dipartimento di Fisica 'G. Galilei', Universitá di Padova, 35131 Padova (Italy)*
[3] *Department of Physics, University of Maryland, College Park, MD 20742, Maryland (USA)*

There is increasing evidence that some aspects of living systems exhibit critical-like behavior[1]. One can find examples ranging from flock dynamics to regulatory genetic networks and neural avalanches in the brain. However, understanding why this happens and the mechanisms that bring individuals to exhibit criticality is still unclear.

To shed some light on such a general question, we present a different perspective to understand criticality, in the context of Information Theory[2]. Within this framework, we sketch some of the general aspects of living systems modeling them as *inferring* systems.

We implement two variants of our model, inspired by the genetic algorithm. In a nutshell, we have a community of individuals coping with an external environment, gathering the information coming from different sources. We find that the best strategy to do it efficiently is to tune their parameters in the vicinity of the critical point, provided that there is any. But even in the absence of any external sources, the same result still applies when individuals, far away from criticality, try to cope with each other. The critical point becomes a global attractor in response to this smart inference.

Mathematically, we encode a source of stimuli $\vec{s} = (s_1, ..., s_N)$ in a distribution $P_{\rm src}(\vec{s}|\vec{\alpha})$. Allowing parameters $\vec{\alpha}$ to vary, different sources can be modeled. On the other hand, each of the individuals in the community seeks to represent, with the largest possible fidelity, the essential aspects of the stimuli coming from the source in a distribution $P_{\rm map}(\vec{s}|\vec{\beta})$. Different values of the parameters $\vec{\beta}$ accounts for different maps. Finally, to measure the 'closeness' between both distributions, Information Theory provides a robust measure through the Kullback-Leibler divergence, $D_{KL}(\vec{\alpha}|\vec{\beta}) = \sum_{\vec{s}} P_{\rm src}(\vec{s}|\vec{\alpha}) \log\left(P_{\rm src}(\vec{s}|\vec{\alpha})/P_{\rm map}(\vec{s}|\vec{\beta})\right)$, which quantifies the loss of information when the map is used to approximate the source:

In the first model, we have a community of M individuals, each one characterized by its internal parameters $\vec{\beta}$. At every time step, S sources are generated at randomly from a pool $\rho_{\rm src}(\vec{\alpha})$. Then, we kill one of the individuals with a probability proportional to the mean KL divergence with respect to the environment,

$$P_{\rm kill}(i) \propto \frac{1}{S}\sum_{k=1}^{S} D_{KL}(\vec{\alpha}_k|\vec{\beta}_i), \quad i = 1, ..., M. \qquad (1)$$

The unlucky individual is replaced by another one in the community, and then we introduce a perturbation in the parameters with a small probability.

When the process is iterated, if the internal map presents a continuous phase transition, and *only* when the environment $\rho_{\rm src}$ is highly heterogeneous, parameters fall down in the vicinity of the critical point, $\vec{\beta} = \vec{\beta}_c$.

In the second model, there is no *a priori* choice for the pool of sources, and the community plays itself the role of the environment. In other words, individuals evolve trying to 'understand' each other. At every time step, S individuals are picked at randomly, and one of them is killed with a probability proportional to the mean D_{KL} respect to the other $(S-1)$ individuals. Mutations are introduced again with a small probability.

In this case, and regardless of the initial conditions, complexity emerges and individuals' parameters tune themselves in the critical point.

In summary, the observed criticality in living systems can be understood as a result from the necessity of coping with many diverse external conditions and their ability of building up accurate maps of the environment.

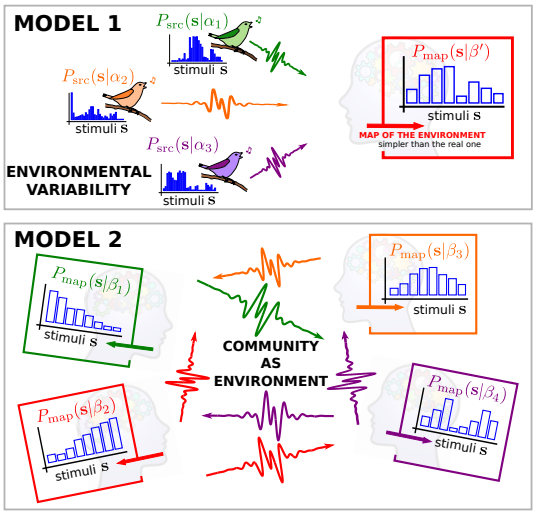

FIG. 1. Sketch of the two computational models.

* hidalgoj@ugr.es

[1] Mora, T., and Bialek, W. (2011). Are biological systems poised at criticality? *Journal of Statistical Physics*, 144(2), 268-302.

[2] Hidalgo, J., Grilli, J., Suweis S., Munoz, M.A., Banavar, J.R and Maritan, A. (2013). Emergence of criticality in living systems through adaptation and evolution: Practice Makes Critical. *arXiv preprint arXiv:1307.4325.*

Characterizing the complex dynamics of a semiconductor laser with optical feedback and modulation.

Andrés Aragoneses*[1], Sandro Perrone[1], Taciano Sorrentino[1,2], M. C. Torrent[1], Cristina Masoller[1]

[1] *Departament de Física i Enginyeria Nuclear, Universitat Politècnica de Catalunya, Colom 11, Terrassa, 08222 Barcelona, Spain*

[2] *Departamento de Ciências Exatas e Naturais, Universidade Federal Rural do Semi-Árido, 59625-900 Mossoró, Brazil*

The task of infering signatures of determinism in a complex system, by means of analyzing aperiodic, noisy time series, is recurrent in the study of nonlinear systems. Recently, methods to distinguish signatures of determinism that employ ordinal patterns analysis have received considerable attention for being computationally fast, conceptually simple, and for maintaining their usefulness even in the presence of high levels of noise[1–3].

One longstanding discussion about the roles of stochastic and deterministic processes, and where their detection and distinction are crucial, comes from semiconductor laser dynamics[4]. Semiconductor lasers subject to optical feedback and/or injection are paradigmatic nonlinear systems. They have been studied for decades and are still object of intense investigation, allowing experimental observation of a great variety of nonlinear behaviors. One of the most remarkable phenomena observed in a semiconductor laser under optical feedback are the low-frequency fluctuations (LFFs). LFFs are irregular, sudden power dropouts followed by a gradual stepwise recovery, that occur for moderate feedback levels near the laser's solitary threshold. This dynamical regime is of widespread interest in complex systems, as it involves the interplay of nonlinearity (light-matter interactions), time-delayed feedback and noise that induces this dynamics, ingredients which are ubiquitous in nature.

One particular configuration where a semiconductor laser with feedback results of special interest is when the laser is submitted to a external periodic forcing, as it is very useful in telecommunications and new phenomena manifest[5]. Also, many other dynamical systems tend to appear in nature subjected to an external modulation: electronic circuits, neuronal networks, metabolic system[6], ..., increasing the interest in characterizing the dynamics of nonlinear oscillators under an external periodic forcing.

We characterize the dynamics of a semiconductor laser subjected to optical feedback and modulation of the injection current. We measure the experimental power output of the laser in the LFF regime (see Fig. 1(a)) and compute the inter dropout intervals. We transform the time series into sequences of ordinal patterns (words of dimension 2, labelled as '01' and '10'), and compute the probability of each word, and the transition probabilities (see figure 1(b)) versus the modulation amplitude, to distinguish signatures of determinism and stochasticity in the dynamics of the system. We detect transitions in its dynamics as the amplitude of the modulation is varied, and we unveil a structure in the underlying dynamics of the IDIs, in good agreement with previous works and with the Lang-Kobayashi model[7].

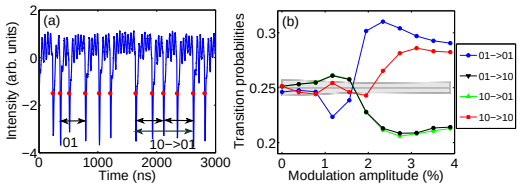

FIG. 1. (a) Experimental time series of the intensity of the laser with feedback and modulation. One word ('01') and one transition ('10− > 01') are shown as examples. (b) Transition probabilities of the different ordinal patterns are depicted versus the modulacion amplitude.

* andres.aragoneses@upc.edu

[1] C. Bandt, B. Pompe, *Phys. Rev. Lett.* **88**, 174102 (2002).

[2] L. Zunino, M. C. Soriano, O. A. Rosso, *Phys. Rev. E* **86**, 046210 (2012).

[3] Andrés Aragoneses, Nicolás Rubido, Jordi Tiana-Alsina, M. C. Torrent, Cristina Masoller, *Sci. Rep.* **3**, 1778 (2013).

[4] Miguel C. Soriano, Jordi García-Ojalvo, Claudio R. Mirasso, Ingo Fischer, Rev. Mod. Phys., **85**, 421–470 (2013).

[5] D. W. Sukow, D. J. Gauthier, *IEEE J. Quantum Electron.* **36**, 175 (2000).

[6] N. Mitarai, U. Alon, M. H. Jensen, Chaos **23**, 023125 (2013)

[7] R. Lang, K. Kobayashi, IEEE, J. Quantum Electron., **16**, 347 (1980).

Low-Dimensional Dynamics of Populations of Pulse-Coupled Oscillators

Ernest Montbrió*, Diego Pazó†
Department of Information and Communication Technologies
Universitat Pompeu Fabra 08018-Barcelona

Clapping audiences, pedestrians in the London's millennium bridge, and flashing fireflies offer spectacular examples of collective synchronization. This pervasive tendency towards synchrony also occurs at the microscopic level, where heart pacemaker cells self-organize their rhythmic activity to initiate the heartbeat. In 1967, Arthur Winfree proposed a mathematical model[1] that successfully replicated this natural phenomenon of self-organization in time, and initiated a prolific research program on collective synchronization. Only a few years after Winfree's seminal paper, Kuramoto proposed a model singularly amenable to mathematical analysis[2], which rapidly became the canonical model to mathematically investigate synchronization phenomena.

Despite their importance and generality, Kuramoto-like models —in which interactions are expressed by phase differences— are approximations of more realistic models such as the Winfree model, and typically their parameters do not have a simple mapping with biologically meaningful parameters. In contrast, the Winfree model incorporates explicit pulse-like interactions and phase response curves (PRCs) that are customarily obtained from experiments or from biologically realistic conductance-based models.

In this contribution we report on the first complete mathematical analysis of the Winfree model. Winfree considered of a large population of pulse-coupled oscillators, and the assumtion of weak coupling permited him to describe the state of each oscillator solely by its phase variable θ:

$$\dot{\theta}_i = \omega_i + Q(\theta_i)\frac{\varepsilon}{N}\sum_{j=1}^{N} P(\theta_j), \tag{1}$$

where ε controls the coupling strength, and the oscillators are labeled by $i = 1, \ldots, N \gg 1$. Heterogeneity is modeled via the natural frequencies ω_i, which are drawn from a probability distribution $g(\omega)$. The PRC function Q, measures the degree of advance or delay of the phases when the oscillators are perturbed. We adopt here a PRC with a sinusoidal shape:

$$Q(\theta) = \sin\beta - \sin(\theta + \beta) \tag{2}$$

We complete the definition of system (1) with the smooth pulse-like signal:

$$P(\theta) = a_n(1 + \cos\theta)^n \tag{3}$$

Here $n \geq 1$ allows to control the width of the pulses, and a_n is a normalization constant.

Our most important finding[3] is that the Winfree model (1) with the family of PRCs in Eq. (2) belongs to a family of systems that have asymptotic dynamics in a reduced space, called Ott-Antonsen manifold[4]. This important property allows to exactly describe the dynamics of the Winfree model with only two ODEs for Lorentzian

$$g(\omega) = \frac{\Delta/\pi}{(\omega - \omega_0)^2 + \Delta^2} \tag{4}$$

Using this low-dimensional description, we fully investigate the dynamics of the Winfree model in terms of four parameters: Δ, ε, β, and n controlling the spread of the natural frequencies, the coupling strength, the PRC, and the pulses' width, respectively.

Interestingly, as a result of our study, we find that brief pulse-like interactions generically favor synchronization, what could be conjectured as a reason for their occurrence in nature. This result is not captured using Kuramoto-like models, since these models are only valid for weak coupling and low frequency heterogeneity.

Finally, the potential of our findings is illustrated uncovering a variety of chimera states in networks of pulse-coupled oscillators, which include a new class of chimeras with chaotic dynamics. All in all, we believe our results will foster theoretical advances on the collective dynamics of oscillators' systems, upgrading the mathematical basis of macroscopic synchronization beyond Kuramoto-like models.

---

* ernest.montbrio@upf.edu
† Instituto de Física de Cantabria (CSIC-UC), Santander.

[1] A. T. Winfree, J. Theor. Biol. **16**, 15 (1967).
[2] Y. Kuramoto, in *International Symposium on Mathematical Problems in Theoretical Physics*, Vol. 39 of *Lecture Notes in Physics*, edited by H. Araki (Springer, Berlin, 1975).
[3] D. Pazó and E. Montbrió, *accepted in* Phys. Rev. X.
[4] E. Ott and T. M. Antonsen, Chaos **18**, 037113 (2008)

Autoorganización de Estructuras de Turing en un Potencial Radial con Periodicidad Temporal

Jacobo Guiu-Souto* and Alberto P. Muñuzuri
Grupo de Física No Lineal
Facultad de Física. Universidad de Santiago de Compostela 15706-Santiago de Compostela (A Coruña)

Desde el punto de vista de la Dinámica no Lineal la autoorganización puede definirse como la tendencia espontánea que presentan muchos sistemas a organizarse en estructuras complejas, a partir de componentes elementales desordenados que fluctúan en una escala inferior. Este fenómeno tiene especial importancia en el marco de los sistemas biofísicos, ya que permite explicar por qué muchos de ellos experimentan una ruptura espontánea de la simetría que da lugar a la formación de estructuras espacio-temporales macroscópicas, como por ejemplo, los patrones observados en las pieles de diferentes animales[1].

Muchos de los procesos inherentes a dicho fenómeno son fruto de la interacciń entre el sistema en cuestión y un agente externo que modifica la dinámica del transporte difusivo en el medio[2]. En el presente trabajo se elucidan los efectos de un campo de fuerzas radial de magnitud oscilante sobre un sistema quḿico concreto, esto es, la reacción de Belousov-Zhabotinsky en microemulsión de aerosol-OT, el cual a su vez es susceptible de presentar autoorganización vía bifurcación de Turing[3]. Observaciones experimentales muestran que la perturbación es capaz de modificar las principales características de los patrones de Turing, tanto en términos de su longitud de onda como en su morfología[4]. A través de un enfoque mecánico-estadístico se propone un modelo teórico-numérico que permite elucidar la existencia de diferentes acoplamientos resonantes entre la formación de la estructuras de Turing y la simetría del forzamiento.

* jacobo.guiu@usc.es

[1] D. G. Míguez, E. M. Nicola, A. P. Muñuzuri, J. Casademunt, F. Sagués, and L. Kramer, *Phys. Rev. Lett.* **93** 048303 (2004).
[2] J. Guiu-Souto, J. Carballido-Landeira, A. P. Muñuzuri and V. Pérez-Villar *Phys. Rev. E.* **82** 066209 (2010).
[3] J. Guiu-Souto, L. Michels, A. Von Kameke, J. Carballido-Landeira and A. P. Muñuzuri *Soft Matter* **9** 4509 (2013).
[4] J. Guiu-Souto, J. Carballido-Landeira and A. P. Muñuzuri. *Phys. Rev. E.* **85** 056205 (2012).

The Last Survivor: a Spin Glass Phase in an External Magnetic Field.

J. J. Ruiz-Lorenzo*
(Janus Collaboration)
Departamento de Física, Universidad de Extremadura, 06071 Badajoz

Spin glasses are a longstanding model for the sluggish dynamics that appears at the glass transition. However, spin glasses differ from structural glasses for a crucial feature: they enjoy a time reversal symmetry. This symmetry can be broken by applying an external magnetic field, but embarrassingly little is known about the critical behavior of a spin glass in a field. In this context, the space dimension is crucial.

Whether spin glasses in a magnetic field undergo a phase transition has been a long-debated and still open question. In the mean-field approximation, which is valid for dimensions greater than the upper critical dimension ($d_u = 6$), the de Almeida-Thouless line separates the high-temperature paramagnetic phase from the glassy phase. However, the droplet model predicts no phase transition at all. Finally, experimental studies are still controversial. In this abstract we will present results on four and three dimensions (both dimensions below the upper critical dimension).

We have obtained conclusive evidence for the presence of a phase transition in a four-dimensional spin glass in a field[1] using the Janus special-purpose computer[2] and employing a novel finite size study. In a complementary approach, based in the study of the one dimensional Ising spin glass model with decaying algebraic coupling (whose exponent allows us to connect with finite dimensional short range spin glasses), similar conclusions were reached[3].

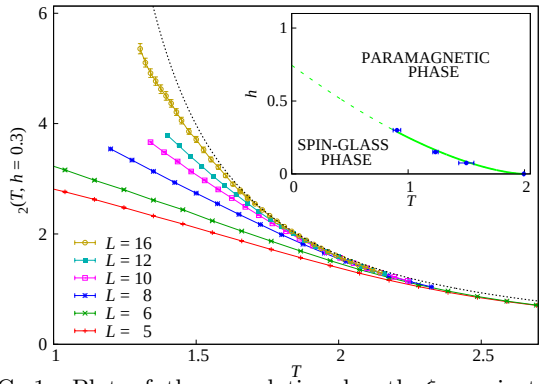

FIG. 1. Plot of the correlation length ξ_2 against temperature in an external field $h = 0.3$ in four dimensions. The dotted black line is a fit to a critical divergence as $\xi_2^\infty \propto [T - T_{c(h)}]^{-\nu}$. The inset is a sketch of the phase diagram (the de Almeida-Thouless line), including a fit to the Fisher-Sompolinsky scaling $h_c^2(T) \simeq A|T - T_c^{(0)}|^{\beta^{(0)}+\gamma^{(0)}}$. The quantities with a superindex (0) are the values for the $h = 0$ critical point, so the only free parameter is the amplitude A.

In Fig. 1 we show the behavior of the finite computed correlation length, ξ_2 (avoiding the zero mode of the system in its definition) as a function of the temperature, behavior which marks the presence of a phase transition.

The situation in three dimensions, is still not clear. To address this problem we have changed the (static) equilibrium approach, we have used in four dimensions, for a dynamical, on and off equilibrium, study[4]. We have used again the Janus special-purpose computer and we have been able to reach times equivalent to 0.01 seconds in experiments. We have studied the system relaxation both for high and for low temperatures, clearly identifying a dynamical transition point. This dynamical temperature is strictly positive and depends on the external applied magnetic field (see Fig. 2). However, it is not clear whether this dynamical phase transition corresponds or not with a thermodynamical one.

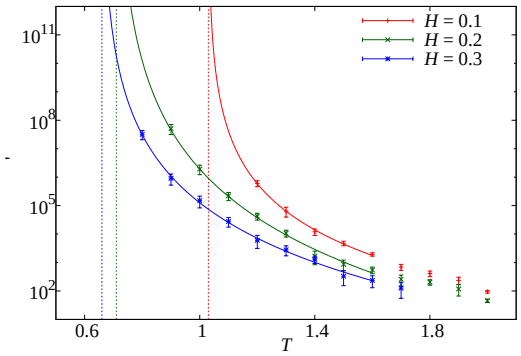

FIG. 2. Three dimensional spin glass. Behavior of the relaxation time τ' as a function of the temperature for the three magnetic fields simulated. We also plot our fits to a power-law divergence of τ' for a finite temperature: $\tau' \propto (T - T_d(h))^{-\nu z}$. z is the dynamical critical exponent.

* ruiz@unex.es.

[1] R. Alvarez Banos et al. Proceedings of the National Academy of Science of USA (PNAS) 109 (17) 6452 (2012).
[2] F. Belletti et al. Comp. Phys. Comm., 178, 208(2008).
[3] L. Leuzzi, G. Parisi, F. Ricci-Tersenghi and J.J. Ruiz-Lorenzo. Phys. Rev. Lett. 103, 267201 (2009).
[4] M. Baity-Jesi et al. http://arxiv.org/abs/1307.4998.

Optimizing the search for resources by sharing information. The case of Mongolian gazelles.

Ricardo Martínez-García, Cristóbal López, Justin M. Calabrese, Thomas Mueller, Kirk A. Olson.
IFISC, Instituto de Física Interdisciplinar y Sistemas Complejos, 07122-Palma (Mallorca)
Smithsonian Conservation Biology Institute, Front Royal VA (USA).

Many living organisms, including bacteria, insects, and mammals, communicate for a variety of reasons including facilitation of social cohesion, defense against predators, maintenance of territories, and to pool information on resource locations when no single individual is sufficiently knowledgeable[1]. However, research on foraging efficiency has focused largely on independent individuals[2], or on comparing foraging behavior across species[3]. Very few models have examined the potential effect that long-distance communication can have on movement behaviors and population distributions, and many open questions remain, particularly on the interrelation between communication in a population and optimal search efficiency in a biological context. How can communication facilitate group formation and identification of areas of high quality resources? Does a communication range exist that optimizes foraging efficiency? To what degree does search efficiency depend on the communication mechanism? Finally, how does communication affect individual space use in a heterogeneous environment?

In this work[4,5] we address these questions with a general model of random search with two main ingredients: resource gradients and long-range communication. In a first part, we propose a model of Brownian searchers which are able to perceive the quality of the environment at its location, and with a long-range pairwise interaction that provides information on the habitat in far away regions of the space. First, we study the efficiency of the search depending on the range of the communication from a temporal and a spatial point of view. To this aim, we measure the population mean searching time (Figure) and the spatial distribution of individuals in the long time limit (Figure) respectively. Using Monte Carlo simulations and density equations our results point out that the search is optimal at intermediate scales of communication, showing that both an excess and a lack of information may worsen it.

In the second part we show an application of the model to the particular case of acoustic communication among Mongolian gazelles, for which data are available, searching for good habitat areas. We couple an individual based representation of our model with remotely-sensed data on resource quality in the Eastern Steppe of Mongolia and show that at intermediate lengths of communication gazelles optimize the search. Finally, the optimal communication range and frequency obtained with our model are in good agreement with experimental results, suggesting that gazelles might have optimized their vocal tract and the frequency of their voices to communicate in the Mongolian Steppe.

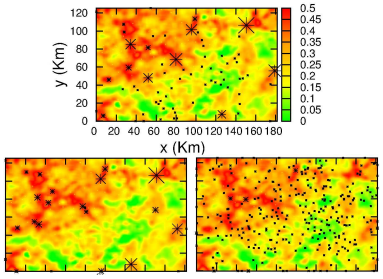

FIG. 1. Group formation in a population of 500 gazelles foraging in the Mongolian Steppe for communication at low (top), intermediate (bottom left) and high frequencies (bottom right).

Finally we compare the theoretical results obtained in the first part with the ones obtained considering Lévy flights instead of Brownian motion[6].

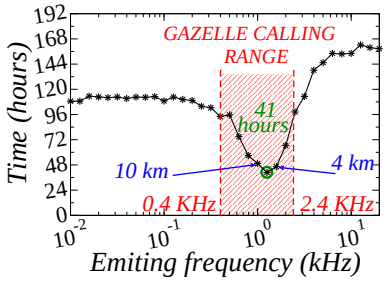

FIG. 2. The searching time is minimized at intermediate frequencies, at a value that agrees with the measurements done in Mongolian gazelles.

* clopez@ifisc.uib-csic.es

[1] A. Berdahl et al., Science **339**, 574 (2013).
[2] F. Bartumeus, et al., Phys. Rev. Lett. **88**, 097901 (2012).
[3] F. Lenz, et al., Phys. Rev. Lett. **108**, 098103 (2012).
[4] R. Martínez-García, J.M. Calabrese, T. Mueller, K.A. Olson, and C. Lopez, Phys. Rev. Lett. **110**, 248106 (2013).
[5] Highlited in Physics Focus, "Animal Communication Could Support Efficient Foraging", David Lindley, Physics APS, **68**, 6 (2013).
[6] R. Martínez-García, J.M. Calabrese, C. López, (Submitted).

Comunicaciones tipo Póster

Switching-induced phase transition in a 2D magnetic colloidal crystal

Ricard Alert*, Jaume Casademunt, Pietro Tierno
Departament d'Estructura i Constituents de la Matèria, Universitat de Barcelona, Avinguda Diagonal 647, 08028 Barcelona, Spain

Colloids are excellent model systems for condensed matter phenomena because of their experimental accessibility and the tunability of their interactions[1,2]. We study the equilibrium and nonequilibrium phases of a 2D colloidal crystal of dipolar paramagnetic colloids on a periodic substrate. In contrast to a recent work[3], our system features anisotropic interactions, giving rise to a rich phase behaviour. The substrate has a striped pattern of consecutive magnetic domains of opposite magnetization. Then, the paramagnetic colloidal particles suspended on top of it pin on the Bloch walls between the magnetic domains, acquiring magnetic dipoles corresponding to the local field. This creates a dipolar colloidal crystal where dipoles are oriented in the same direction along a given Bloch wall but in opposite directions between consecutive Bloch walls (FIG. 1a).

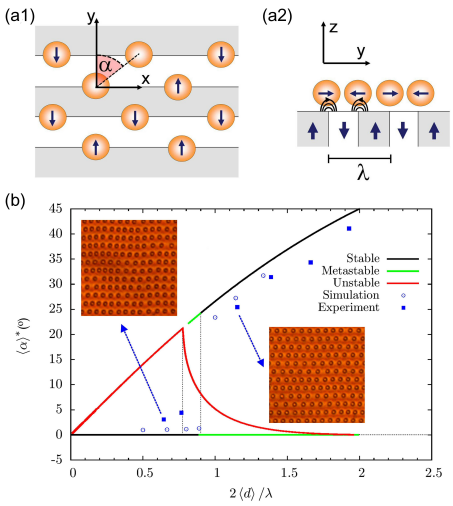

FIG. 1. (a) Schematics of the system. (a1) Top view, (a2) side view. (b) Equilibrium phase diagram displaying the orientational angle as a function of the inverse of the linear density of particles, $\langle d \rangle = 1/\rho$. Theoretical predictions are shown together with simulation and experimental results.

Tuning the density of particles in our system we find a phase transition between two structural phases. We characterize the phase diagram via a theoretical model, molecular dynamics simulations, and experiments (FIG. 1b). However, the system also presents a more interesting phase transition when an external magnetic field is applied in the plane, perpendicular to the Bloch walls. When the external field overcomes the one of the substrate the system undergoes a phase transition to the state that was previously the more unstable one. We term this phenomenon a stability inversion phase transition (FIG. 2 top).

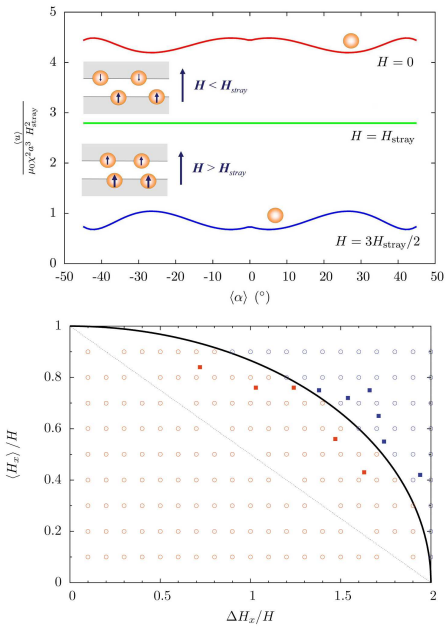

FIG. 2. (Top) Stability inversion phase transition. Mean energy landscape per particle as a function of the orientational angle for external magnetic fields below and over the threshold H_{stray}. (Bottom) Presence (blue) or absence (red) of the switching-induced phase transition as a function of the average value of the magnetic field, $\langle H_x \rangle$, always below the threshold H, and the peak-to-peak amplitude of the switching, ΔH_x. The line indicates the theoretical prediction, empty circles correspond to simulations and filled squares to experiments.

Interestingly, this phase transition can be induced by switching the magnetic field between the two inverted stability situations even when the average field is below the threshold needed in static conditions. This effect and the conditions under which it takes place have been theoretically predicted and verified in both simulations and experiments (FIG. 2 bottom). For fast enough driving frequencies, it is due to the nonlinear dependence of the mean energy per particle on the magnetic field.

* ricardaz@ecm.ub.edu

[1] A. Yethiraj and A. van Blaaderen, Nature, **421**, 513 (2003)
[2] A. Yethiraj, Soft Matter, **3**, 1099 (2007)
[3] C. Bechinger, M. Brunner, and P. Leiderer, Phys. Rev. Lett., **86**, 930 (2001)

Theory of cell membrane-cortex adhesion dynamics

Ricard Alert*, Jaume Casademunt
Departament d'Estructura i Constituents de la Matèria, Universitat de Barcelona, Avinguda Diagonal 647, 08028 Barcelona, Spain

Adhesion between cell membrane and cytoskeletal cortex is involved in several cellular functions, including apoptosis, cell spreading, cytokinesis, virus uptake or even cell motility. Membrane-cortex adhesion is carried out by molecular linkers attached both to membrane lipids or proteins and cytoskeletal proteins[1,2]. These molecular linkers are stretched or compressed by membrane and cytoskeleton movements and continuously attach and detach, so that the network they form is highly dynamic. When a large membrane patch detaches from the cortex, a bleb can form. Blebs are cell membrane protrusions arising from membrane-cortex detachment, so that they constitute one of the most prominent consequences of complex membrane-cortex interactions (FIG. 1). The formation of blebs constitues a mechanism of cell crawling on substrates with reduced adhesion, and it could be relevant for tissue invasion by cancerous cells[3,4]. The so-called bleb-based motility, then, crucially depends on how membrane-cortex detachment is controlled by the cell.

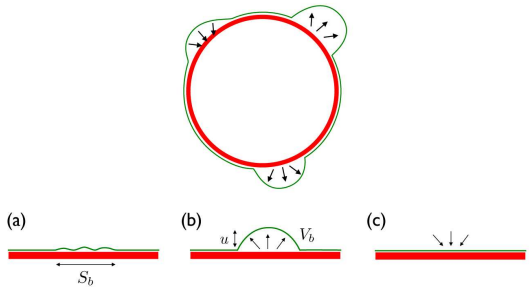

FIG. 1. (Top) Schematic illustration of a blebbing cell, with two expanding and one retracting bleb (black arrows). The cortex is shown in red and the membrane in green. (Bottom) Bleb nucleation. The detachment of a membrane patch (a) can lead to the formation of a bleb (b) or to a resealing of membrane-cortex adhesion (c). Adapted from Brugués[5].

We have extended a kinetic model for membrane-cortex adhesion (FIG. 2) to include both thermal and chemical fluctuations and spatial modulations along the membrane, which allows us to study the kinetics bleb nucleation. Numerical simulations provide information about the typical lengths and times involved in spontaneous membrane-cortex detachment and their dependence on external conditions and the internal state of the cell. We also study analytically how membrane fluctuations and spatial correlations mediated by hydrodynamics do influence membrane-cortex adhesion and, thus, how the cell can act on it. Moreover, the spatially extended model sets the range of validity of the simpler zero-dimensional model via the identification of a correlation length λ^* of membrane fluctuations (FIG. 3).

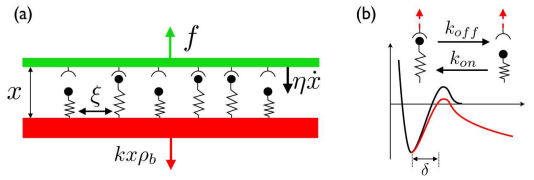

FIG. 2. Schematic illustration of the kinetic model for membrane-cortex adhesion. From Brugués[5]. (a) Rigid and flat cortex (red) and membrane (green) are dynamically linked through model springs (black). (b) Energy landscape of a linker, both in the absence (black) and in the presence of force (red).

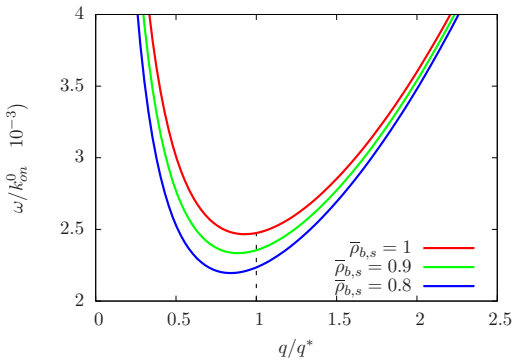

FIG. 3. Relaxation rate of a membrane fluctuation of wave-vector q for some values of the density of bound connectors. $\lambda^* = 2\pi/q^*$ is identified as a correlation length of membrane fluctuations.

* ricardaz@ecm.ub.edu

[1] M. P. Sheetz, Nat. Rev. Mol. Cell Bio. **2**, 392 (2001)
[2] G. T. Charras, J. Microsc. **231**, 466 (2008)
[3] G. T. Charras and E. Paluch, Nat. Rev. Mol. Cell Bio. **9**, 730 (2008)
[4] O. T. Fackler and R. Grosse, J. Cell Biol. **181**, 879 (2008)
[5] J. Brugués, Ph.D. thesis, Universitat de Barcelona (2008)

Unveiling the complex organization of recurrent patterns in spiking dynamical systems

Andrés Aragoneses*[1], Sandro Perrone[1], Taciano Sorrentino[1,2], M. C. Torrent[1], Cristina Masoller[1]
[1] *Departament de Física i Enginyeria Nuclear, Universitat Politècnica de Catalunya, Colom 11, Terrassa, 08222 Barcelona, Spain*
[2] *Departamento de Ciências Exatas e Naturais, Universidade Federal Rural do Semi-Árido, 59625-900 Mossoró, Brazil*

Nature presents many fascinating complex systems in which distinguishing signatures of determinism in their high-dimensional dynamics is extremely challenging, not only because of the presence of noise, but also, because of lack of information about the system: one can measure only one or few relevant variables, and with a limited spatial and/or temporal resolution. A successful approach for studying such systems is by focusing on an event-level description of their dynamics, considering, for example, intervals between events. Examples of this approach include neuronal inter-spike-intervals, heart beat-to-beat intervals, earthquake waiting times, intervals between peak communication activity in social networks, activity of variable stars, etc. For the analysis of these events, a popular symbolic method, known as ordinal analysis[1,2], considers the relative order in which the events occur.

Here we use ordinal analysis to study the spiking output of a stochastic optical system, consisting of a semiconductor laser with feedback from an external reflector. Close to the lasing threshold, moderate feedback levels induce apparently random spikes in the laser output intensity, which become more frequent as the laser pump current is increased. This spiking output (see figure) has been referred to as low-frequency-fluctuations (or dropouts) and has attracted a lot of attention in the last decades[3], not only because of potential applications of optical chaos, but also, because the mechanisms triggering the spikes involve the interplay of nonlinearity, delay and noise, which are ubiquitous in nature.

We analyze experimentally recorded sequences of spikes by transforming the time trace into a sequence of ordinal patterns, or words. We unveil a nontrivial organization of ordinal patterns underlying the sequence of optical spikes. It is shown a hierarchical and clustered organization of the ordinal patterns, with a well defined structure of the probabilities of occurrence. Simulations of the Lang and Kobayashi (LK) model[4] are in good agreement with the observations. To the best of our knowledge, in spite of the large attention that the optical spikes have attracted over the years, ours is the first demonstration of an organized structure of spike patterns.

Most importantly, we identify a minimal iterative model, a modified circle map (proposed by Neiman et al.[5] to represent spike correlations in sensory neurons) that, despite its simplicity, displays a symbolic dynamics with the same hierarchical and clustered organization of patterns as the experimental data. In order to confirm that this minimal model indeed represents the symbolic dynamics underlying the sequence of optical spikes, we consider the spiking output of the laser with periodic forcing (via a direct modulation of the pump current). We demonstrate that the symbolic dynamics underlying the spikes emitted by the forced laser is also in good qualitative agreement with the symbolic dynamics of the modified circle map.

Since the circle map is a generic model, we expect that our finding will apply also to other dynamical systems. Moreover, our results suggest that optical neurons inspired by biological ones could be built using semiconductor lasers, and could provide a controllable set up to mimic neuronal activity. Our findings could also pave the way for novel neuro-inspired optical computing devices.

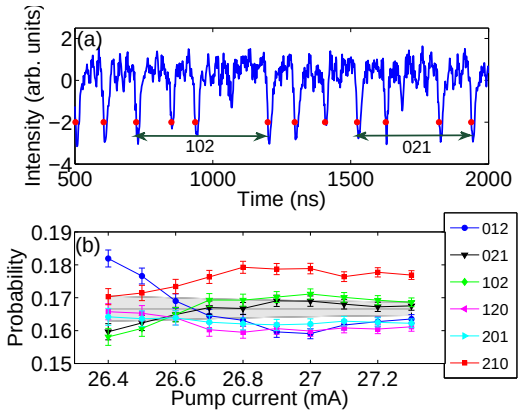

FIG. 1. (a) Experimental time trace of the laser intensity. The red dots indicate the spike times and two ordinal patterns (words) are indicated as examples. (b) Probabilities of the different patterns versus pump current.

* andres.aragoneses@upc.edu

[1] C. Bandt, B. Pompe, *Phys. Rev. Lett.* **88**, 174102 (2002).
[2] Andrés Aragoneses, Nicolás Rubido, Jordi Tiana-Alsina, M. C. Torrent, Cristina Masoller, *Sci. Rep.* **3**, 1778 (2013).
[3] Miguel C. Soriano, Jordi García-Ojalvo, Claudio R. Mirasso, Ingo Fischer, Rev. Mod. Phys., **85**, 421–470 (2013).
[4] R. Lang K. Kobayashi, *IEEE J. Quantum Electron.* **16**, 347 (1980).
[5] A. B. Neiman, D. F. Russell, *Phys. Rev. E.* **71**, 061915 (2005).

Dynamics of mobile coupled phase oscillators

Koichiro Uriu[§†‡], Saúl Ares[‡*], Andrew C. Oates[†] and Luis G. Morelli[†‡¶]
Grupo Interdisciplinar de Sistemas Complejos (GISC)
Centro Nacional de Biotecnología - CSIC, Madrid, Spain.

We study the transient synchronization dynamics of locally coupled phase oscillators moving on a one-dimensional lattice. Analysis of spatial phase correlation shows that mobility speeds up relaxation of spatial modes and leads to faster synchronization. We show that when mobility becomes sufficiently high, it does not allow spatial modes to form and the population of oscillators behaves like a mean-field system. Estimating the relaxation timescale of the longest spatial mode and comparing it with systems with long-range coupling, we reveal how mobility effectively extends the interaction range[1].

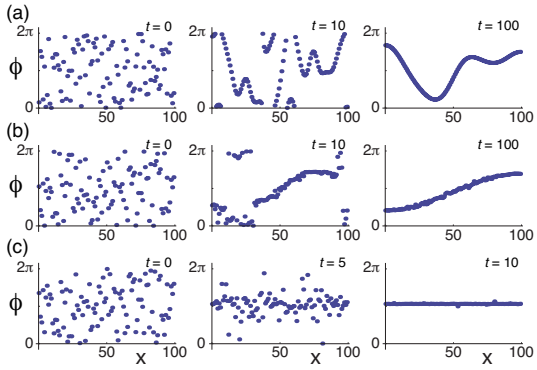

FIG. 1. Oscillator mobility speeds up synchronization. Snapshots of spatial phase profiles. Each dot represents an oscillator. (a) No oscillator mobility, (b) medium oscillator mobility, and (c) high oscillator mobility. t is time.

* saul.ares@csic.es
§ Theoretical Biology Laboratory, RIKEN Advanced Science Institute, Saitama, Japan.
† Max Planck Institute of Molecular Cell Biology and Genetics, Dresden, Germany
‡ Max Planck Institute for the Physics of Complex Systems, Dresden, Germany
¶ Departamento de Física, FCEyN, UBA, Buenos Aires, Argentina

[1] K. Uriu, S. Ares, A.C. Oates and L.G. Morelli, *Phys. Rev. E***87**, 032911 (2013).

Topology and Dynamics of the Zebrafish Segmentation Clock Core Circuit

Christian Schröter[‡†], Saúl Ares[‡*], Luis G. Morelli[†¶], Alina Isakova[♭], Korneel Hens[♭], Daniele Soroldoni[†], Martin Gajewski[§], Frank Jülicher[‡], Sebastian J. Maerkl[♯], Bart Deplancke[♭] and Andrew C. Oates[†]
Grupo Interdisciplinar de Sistemas Complejos (GISC)
Centro Nacional de Biotecnología - CSIC, Madrid, Spain.

The segmented pattern of the vertebral column, one of the defining features of the vertebrate body, is established during embryogenesis. The embryo's segments, called somites, form sequentially and rhythmically from head to tail. The periodicity of somite formation is regulated by the segmentation clock, a genetic oscillator that ticks in the posterior-most embryonic tissue: for each tick of the clock, one new bilateral pair of segments is made. The period of the clock appears to determine the number and the length of segments, but what controls this periodicity? In this contribution[1], we have investigated the interactions of three transcription factors that form the core of the clock's regulatory circuit, and have measured how the period of segmentation changes when these factors are mutated alone or in combination. We find that these three factors contribute to a "dimer cloud" that contains all possible dimeric complexes formed from monomeric protein molecules; however, only two dimers in this cloud can bind DNA, which allows them to directly regulate the oscillatory gene expression that underpins the periodicity of segment formation. Nevertheless, a mathematical model of the clock's dynamics based on our experimental findings (see Fig. 1) indicates that the non-DNA-binding dimers also influence the stability, and hence the function, of the two DNA-binding dimers controlling the segmentation clock's period. Such involvement of non-DNA-binding dimers is a novel regulatory principle for the segmentation clock, which might also be a general mechanism that operates in other biological clocks.

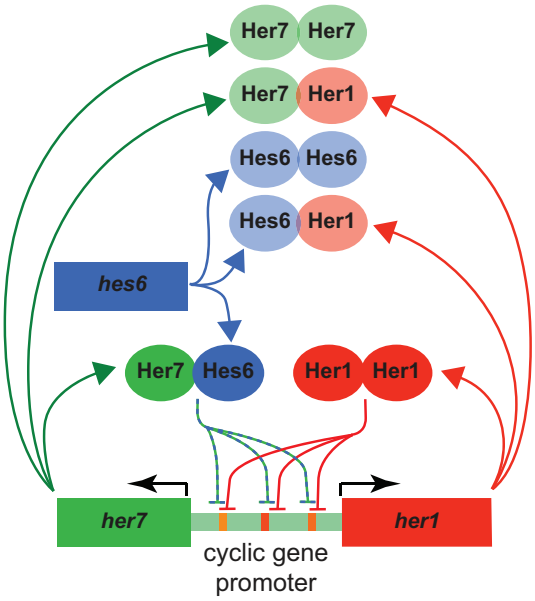

FIG. 1. Schematic representation of experimentally determined protein-protein interactions and protein-DNA interactions, neglecting weak protein-DNA interactions. Proteins are represented as ovals and genes by rectangular boxes. Blunted arrows represent repression of her1 and her7 promoters by Her1 homodimers and Her7:Hes6 heterodimers. Colored arrows represent production.

* saul.ares@csic.es
† Max Planck Institute of Molecular Cell Biology and Genetics, Dresden, Germany
‡ Max Planck Institute for the Physics of Complex Systems, Dresden, Germany
¶ Departamento de Física, FCEyN, UBA, Buenos Aires, Argentina
♭ École Polytechnique Fédérale de Lausanne, Institute of Bioengineering, School of Life Sciences, Lausanne, Switzerland
§ Institute for Genetics, University of Cologne, Cologne, Germany
♯ École Polytechnique Fédérale de Lausanne, Institute of Bioengineering, School of Engineering, Lausanne, Switzerland

[1] C. Schröter, S. Ares, L.G. Morelli, A. Isakova, K. Hens, D. Soroldoni, M. Gajewski, F. Jülicher, S.J. Maerkl, B. Deplancke and A. C. Oates, *PLoS Biol.* **10**, e1001364 (2012).

Estudio del ordenamiento de partículas cúbicas un sistema sometido a rotaciones alternantes

K. Asencio*, M. Acevedo, I. Zuriguel, D. Maza
LMG, Laboratorio de medios granulares
Departamento de Física y Matemática Aplicada, Universidad de Navarra 31008-Pamplona (Navarra)

El comportamiento colectivo de los materiales granulares es un problema de gran importancia desde el punto de vista tecnológico. Dentro de la gran variedad de fenómenos que es posible observar con este tipo de materiales se encuentra la compactación granular, la cual se entiende genéricamente como el reacomodamiento de un grupo de partículas cuando es sometido a diferentes tipos de solicitaciones externas. El más común de los mecanismos de solicitación externa es la aplicación se sacudidas o *taps* en la dirección de la gravedad, lo que ocasiona que los granos que componen el material se reacomoden disminuyendo su volumen aparente.

En medios granulares los estudios de compactación u ordenamiento de partículas con caras planas son escasos. Además de la agitación en la dirección vertical, existen otros mecanismos que pueden compactar un medio granular como la aplicación cíclica y repetida de esfuerzos de corte en direcciones distintas a la de la gravedad.

En el Laboratorio de Medios Granulares (LMG) de la Universidad de Navarra estamos desarrollando experimentos en esta línea, en particular, mediante la aplicación cíclica y repetida de esfuerzos de corte mediante rotaciones alternantes tal y como se ha esquematizado en la Figura 1.

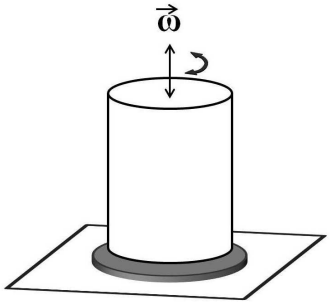

FIG. 1. Representación gráfica de la aplicación de las rotaciones alternantes en el sistema exprimental.

El dispositivo consta de un motor trifásico que controlamos mediante un ordenador y con el cual podemos hacer girar el contenedor en un sentido u otro. Como medio granular usamos partículas cúbicas. Con una cámara lineal realizamos la reconstrucción de la imagen de la superficie lateral del cilindro (Figura 2) y a partir de estas imágenes analizamos la evolución del empaquetamiento en función del número de ciclos aplicados. Bajo estas condiciones hemos verificado que la evolución de fracción de compactación es análoga a la encontrada en el caso de agitación vertical[1]y puede ajustarse mediante una ley logarítmica inversa, Figura 3.

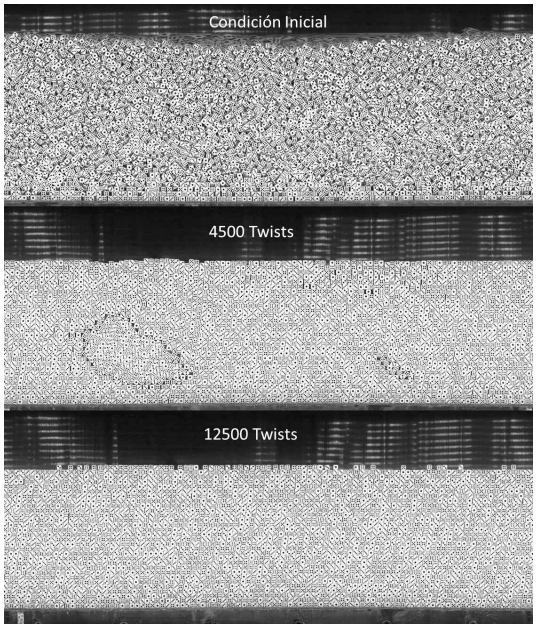

FIG. 2. Imagen de la superficie lateral del cilindro donde se observa como evoluciona el ordenamiento de la muesta tras aplicar diferente número de ciclos (twists), utilizando una muestra de 25000 cubos y un Γ=0,52.

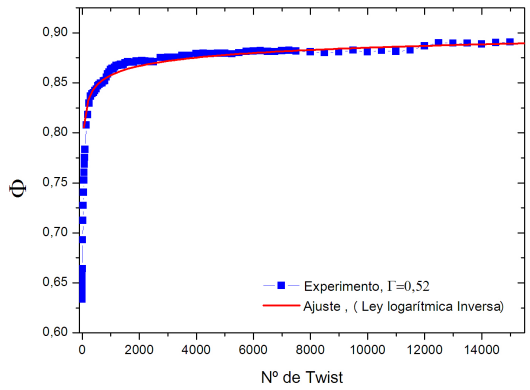

FIG. 3. Evolución del empaquetamiento Φ de los cubos en el cilindro respecto al N° de twist aplicados y su ajuste (línea continua).

* kasencio@alumni.unav.es

[1] J. Knight, C. G. Fandrich, C. N. Lau, H. Jaeger and S. Nagel, Phys. Rev. Lett. **51** 3957 (1995)

Estado homogéneo de un gas granular confinado

J. Javier Brey, M.I. García de Soria, P. Maynar, and V. Buzón*
Facultad de Física, Departamento de Física Atómica, Molecular y Nuclear. Universidad de Sevilla. 41080-Sevilla

Se desarrolla el formalismo mecánico-estadístico de no equilibrio y la teoría cinética para un modelo de gas confinado casi-bidimensional de esferas duras inelásticas. La dinámica de las partículas incluye un mecanismo efectivo para la transmisión de la energía inyectada en la dirección vertical a los grados de libertad horizontales. Se formula la aproximación de Enskog y se usa como base para investigar la temperatura y la función de distribución del estado estacionario, eventualmente alcanzado por el sistema. Se identifica un escalamiento exacto de la función de distribución del sistema que tiene implicaciones en la forma de los momentos de la velocidad. Las predicciones teóricas son comparadas con resultados numéricos obtenidos mediante simulación de la dinámica molecular, encontrándose un buen acuerdo.

* VBuzon@us.es

Shape and Size Optimization of Swimming Microbots in Viscoelastic Biofluids

Laura Campo-Deaño*
FEUP, Faculdade de Engenharia da Universidade do Porto, 4200-465 Porto (Portugal)

The use of microbots in different areas of research have increased in the last years. Microbots are mechanical or electromechanical devices whose components are at or close to the scale of micrometers. Among the wide range of applications, the most promising ones lie in the field of biomedicine in the reparation of diseased cells, performing eye surgery, detecting cerebral aneurysms, delivering drugs in the right place without collateral damages or to remove blood clots[1]. Most of the potential microbots are bio-inspired swimming microdevices based on the propulsion mechanism of microorganisms like bacteria or spermatozoa, in fact, some recent works were focused in the study of the motion of these microbots according to the different natural techniques of these kind of microorganisms. Other works dealt with other robot capabilities, as the remote control or autonomy[2]. However, the body shape and size play a very important role in the study of their flow through the main conduits of the human body. The non-linear rheological behavior of the biofluids is crucial when the characteristic length scales are of the order of micrometers since the elastic effects are enhanced even at low Reynolds numbers. In this sense, *in vitro* experiments are fundamental for their relevance to *in vivo* applications of microbots in order to understand the flow field under different flow conditions. The aim of this work is to optimize the morphology of microbots in order to achieve a most effective motion when they swim through different conducts of the human body taking into account the viscoelastic properties of the biofluids.
This work is therefore, divided in different subobjectives which are describing in detail (Fig. 1):

- Selection and rheological characterization of solutions analogues to main human biofluids, i.e. blood. The selection of the blood analogues is done based on previous work[3] with a viscoelastic behavior close to real human blood and with a refractive index suitable for the *in vitro* models made of PDMS.
- The models with the characteristics geometries of the human body like veins or arteries are designed in AutoCAD. The microchannels are fabricated in polydimethylsiloxane (PDMS) from SU-8 photoresist molds using standard soft lithography techniques[4].
- The prototype of the microbot is developed according to some designs in literature which are bio-inspired microdevices.
- Flow visualizations, pressure drop measurements and micro-PIV are carried out with the biofluids analogues, and under different flow conditions: pulsatile and stationary. In order to visualize the flow streak-line photography technique is used. Pressure drop measurements is also important in order to study the impact on the flow dynamics due to the presence of the microbot and the possible repercussions on the channel walls. Moreover, the drag forces experienced by the microbot during the flow are measured simultaneous with birefringence tests to understand the non-Newtonian flow around the microdevice.

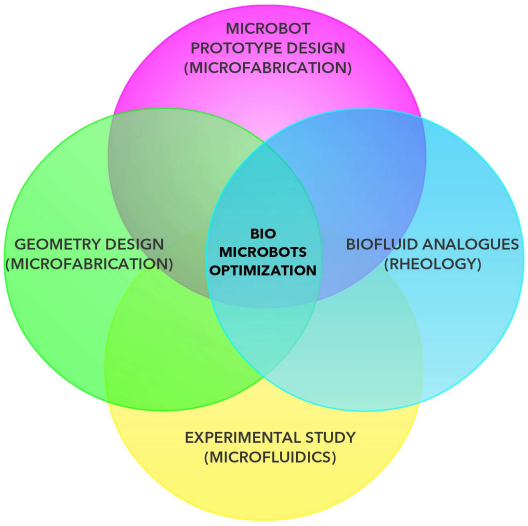

FIG. 1. Relationship between microfluidics, rheology and microfabrication in the optimization of swimming microbot's morphology.

The author acknowledges the financial support from FCT, COMPETE, QREN and European Union (FEDER) through project EXPL/EMS-TRA/2306/2013 and FCT Investigator grant IF/00148/2013.

* campo@fe.up.pt

[1] B.J. Nelson, I.K. Kaliakatsos, and J.J. Abbott, Annu. Rev. Biomed. Eng. 12, 55 (2010).
[2] K.E. Peyer, L. Zhang, and B. Nelson, Nanoscale 5, 1259 (2013).
[3] L. Campo-Deaño, R.P.A. Dullens, D.G.A.L. Aarts, F.T. Pinho, and M.S.N. Oliveira, Biomicrofluidics 7, 034102 (2013).
[4] J.C. McDonald, D.C. Duffy, and J.R. Anderson, Electrophoresis 21, 27 (2000).

Influence of the non-linear rheological properties of blood in middle cerebral aneurysms: numerical and experimental *in vitro* analysis

Laura Campo-Deaño[a*], João Carneiro[a], Mónica S.N. Oliveira[b] and Fernando T. Pinho[a]
[a] *FEUP, Faculdade de Engenharia da Universidade do Porto, 4200-465 Porto (Portugal)*
[b] *James Weir Fluids Laboratory, Department of Mechanical and Aerospace Engineering, University of Strathclyde, Glasgow G1 1XJ (United Kingdom)*

It is well known that the non-linear rheological properties of blood have a great influence in the development of cardiovascular diseases. Among these pathologies, cerebral aneurysms are one of the most common cerebrovascular accidents and are the cause of one-third of deaths worldwide[1]. This kind of accident starts with a dilatation of an artery usually occurring near arterial bifurcations in the Circle of Willis[2,3]. Despite increasing progress, the initiation, growth and rupture of aneurysms are still not well understood, and further hemodynamic studies are crucial for the diagnostic and treatment of these diseases. However, due to the difficulties associated with working with real blood (due to the economical, safety and ethical issues involved), synthetic models of blood are often used.

Recently, Campo-Deaño et al.[4] developed viscoelastic blood analogues able to mimic the complex rheological behavior of real blood and simultaneously exhibit a refractive index suitable for their use in microchannels made of PDMS (polydimethylsiloxane). In addition, the viscoelastic moduli and the steady shear viscosity data obtained experimentally were fitted using two viscoelastic multi-mode differential constitutive equations-the simplified Phan-Thien-Tanner (sPTT) and Giesekus models:

$$\tau_{ij} = \tau_{ij_s} + \tau_{ij_p} \tag{1}$$

$$\tau_{ij_s} = -2\eta_s D_{ij} \tag{2}$$

$$\tau_{ij_p} = \sum_{k=1}^{n} \tau_{ij_k} \tag{3}$$

with

$$f(\tau_{nn_k})\tau_{ij_k} + \lambda_k \overset{\nabla}{\tau}_{ij_k} - \alpha_k \frac{\lambda_k}{\eta_{pk}} \{\tau_{ij_k}.\tau_{ij_k}\} = -2\eta_{pk} D_{ij_k} \tag{4}$$

and

$$f(\tau_{nn_k}) = 1 + \frac{\lambda_k \epsilon_k \tau_{nn_k}}{\eta_{p_k}} \tag{5}$$

The deformation tensor is given by

$$D_{ij} = \frac{1}{2}\left(\frac{\partial u_j}{\partial x_i} + \frac{\partial u_i}{\partial x_j}\right) \tag{6}$$

The two multi-mode models considered have three coefficients in each mode: the relaxation time (λ_k), the viscosity contribution to the zero shear viscosity (η_{p_k}) and the extensibility coefficient (ϵ_k) or the mobility factor (α_k). α_k should be set to zero for the sPTT model and for the Giesekus model the function should be made equal to 1.

In this work we perform numerical simulations to investigate the hemodynamics in simplified geometries representative of middle cerebral aneurysms using Computational Fluid Dynamics (CFD), which is a technique that has been progressively used for modelling the flow in diseased arteries and it is a tool of great potential for the diagnostic, prediction and treatment of cerebral aneurysms[5]. We consider a Newtonian approximation and the Giesekus and sPTT models based on fitting the rheology of human blood[4]. Three geometries are considered consisting of different bifurcations with an aneurysm located at the end of the parent vessel, between two daughter vessels, in which the neck of the aneurysm and the shape of the daughter branches are varied (Fig. 1). The numerical results were afterwards compared with experimental results of the velocity profiles obtained by means of micro-Particle Image Velocimetry measurements in the different aneurysm configurations using blood analogue solutions.

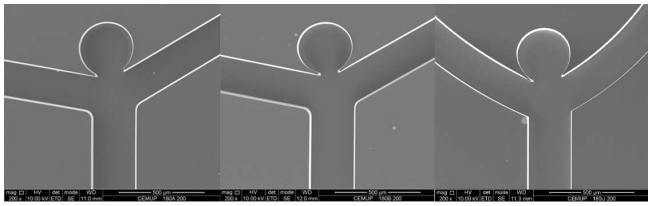

FIG. 1. SEM images of the planar microchannels fabricated in PDMS.

The authors acknowledge the financial support from FCT, COMPETE, QREN and European Union (FEDER) through projects PTDC/EME-MFE/99109/2008, EXPL/EMS-TRA/2306/2013 and FCT Investigator grant IF/00148/2013.

* campo@fe.up.pt

[1] C. Deaton, E.S. Froelicher, L.H. Wu, C. Ho, K. Shishani, and T. Jaarsma, J. Cardiovasc. Nurs. 26, S5 (2011).
[2] J.C. Lasheras, Annu. Rev. Fluid Mech. 39, 293 (2007).
[3] D.M. Sforza, C.M. Putman, and J.R. Cebral, Annu. Rev. Fluid Mech. 41, 91 (2009).
[4] L. Campo-Deaño, R.P.A. Dullens, D.G.A.L. Aarts, F.T. Pinho, and M.S.N. Oliveira, Biomicrofluidics 7, 034102 (2013).
[5] L. Campo-Deaño, M.S.N. Oliveira, and F.T. Pinho, Appl. Mech. Rev. (2014) *submitted*.

Co-evolving link states dynamics

Adrián Carro*, Raúl Toral, Maxi San Miguel
IFISC, Instituto de Física Interdisciplinar y Sistemas Complejos
CSIC-Universidad de las Islas Baleares
07122-Palma (Mallorca)

Collective properties of interacting units have traditionally been studied considering that each of these units is characterized by a property or state, and interacts with others in a network of interactions. The result of the interaction depends on the state of the interacting units and the rules of the particular dynamics implemented. The typical example would be a spin system in a lattice, where there is a spin in each node with a given state and it interacts with its lattice neighbors in a way that depends on their relative spin state. However, there is a number of possible interactions, particularly when considering social systems, in which the state variable is more properly described as a state of the interaction link than a state of the interacting individuals. Typical examples are interactions such as friendship-enmity relationships[2], trust or the use of competing languages.

Motivated by this idea, J. Fernández-Gracia *et al.*[1] have studied a prototype model for the dynamics of the states of the links in a fixed network of interacting units. In their model, each link can be in one of two equivalent states and the dynamics implemented is a simple majority rule for the links, so that in each dynamical step the state of a randomly chosen link is updated to the state of the majority of its neighboring links. The authors find a broad distribution of possible asymptotic configurations, including both frozen and dynamically trapped configurations, some of which have no counterpart under traditional node dynamics in the same topologies and whose probability of appearance is significantly increased.

The study of co-evolving dynamics and topologies has also received much attention recently, particularly in relation to a social context. The most common finding in these coupled systems is a fragmentation transition, which usually occurs for a certain relationship between the time scales of both processes: node states are updated according to their neighbors' states, links between nodes are rewired according to their states. A large number of dynamics and rewiring rules have been studied[3],[4],[5], using different methods to characterize the resulting critical point.

Taking the model studied by J. Fernández-Gracia *et al.*[1] as our starting point, we develop a co-evolving dynamics by defining a certain rewiring mechanism inspired by the case of competing languages. We find that, for any value of the probability of rewiring, frozen disordered configurations are not stable, so the system fully orders. However, this ordering may lead to a one component consensus or to a fragmentation into two components, each one with different link states. We show that the critical point of this fragmentation transition tends to zero in the thermodynamic limit. We also present evidence of the different time scales in which the ordering process takes place depending on which mechanism is responsible for the ordering: majority rule or rewiring. Finally, we present an analytical treatment explaining the behavior of the system when the rewiring process is the leading mechanism.

---

* adrian.carro@ifisc.uib-csic.es

[1] J. Fernández-Gracia, X. Castelló, V. M. Eguíluz, M. San Miguel. Dynamics of link states in complex networks: The case of a majority rule. Phys. Rev. E, 86, 2012.

[2] M. Szell, R. Lambiotte, S. Thurner. Multirelational organization of large-scale social networks in an online world. Proceedings of the National Academy of Sciences, 2010.

[3] P. Holme, M. E. J. Newman. Nonequilibrium phase transition in the coevolution of networks and opinions. Phys. Rev. E, 74, 2006.

[4] F. Vázquez, V. M. Eguíluz, and M. San Miguel. Generic absorbing transition in coevolution dynamics. Phys. Rev. Lett., 100, 2008.

[5] S. Mandrà, S. Fortunato, and C. Castellano. Coevolution of glauber-like ising dynamics and topology. Phys. Rev. E, 80, 2009.

Receptor pre-clustering and T cell responses: insights into molecular mechanisms

M. Castro[1*], H.M. van Santen[2,*], M. Férez[2], B. Alarcón[2], G. Lythe[3], and C. Molina-París[3]

[1] *Grupo de Dinámica No-Lineal and Grupo Interdisciplinar de Sistemas Complejos (GISC) and Escuela Técnica Superior de Ingeniería (ICAI), Universidad Pontificia Comillas, 28015, Madrid, Spain*

[2] *Departamento de Biología Celular e Inmunología, Centro Biología Molecular Severo Ochoa, Consejo Superior de Investigaciones Científicas, Universidad Autónoma de Madrid, 28049 Madrid, Spain*

[3] *Department of Applied Mathematics, School of Mathematics, University of Leeds, Leeds LS2 9JT, UK*

A hallmark of the adaptive immune system is the ability of T cells, making use of the T cell receptors (TCRs) on their surface, to recognise a given agonist peptide-MHC ligand complex (pMHC) with high sensitivity[4]. Some aspects of TCR-pMHC molecular interactions that are of current research interest are the frequency of encounters between T cells and the agonist pMHC, how cell-cell interactions determine the activation of lymphocytes[1], how early interactions change the state of the T cell receptor, what are the mechanisms of modulation of receptor-ligand interactions at cell-cell interfaces, and how protein organisation in the cell membrane (for instance, protein islands or lipid rafts) affect the recognition process[6].

While antigen presenting cells (APCs), such as dendritic cells or B cells, present $10^3 - 10^4$ times more self pMHC than antigenic pMHC, self pMHC ligands by themselves do not usually elicit a T cell response, even though their affinity for TCR$\alpha\beta$ is only 10 times lower than the affinity of the antigenic pMHC[3]. This illustrates how a small difference in affinity results in high specificity, when there is only a few antigenic pMHC molecules in a background of self pMHC ligands[5].

In this poster, we discuss the consequences of TCR pre-clustering in signalling and in distinguishing naive and memory T cell responses. We present some experimentally obtained distributions of TCR clusters for both types of cells (see Fig. 1), and two complementary theoretical models: (i) a simple model of receptor oligomerisation that describes cluster size distributions, and (ii) a generalisation of a novel stochastic T cell response criterion previously used for monomeric interactions[2], to accommodate the hypothesis that the minimum signalling unit is composed of a TCR receptor cluster that is bound by the same cross-linked multivalent ligand (see Fig. 2).

We find that this signalling unit is able to discriminate between agonist and antagonist pMHC ligands, (with greater sensitivity than in the monomeric case), and to explain some of the advantages that higher cluster sizes can provide to memory T cells. The model also points at the need to invoke additional cooperative mechanisms, to explain the experimentally observed role of clustering in T cell responses.

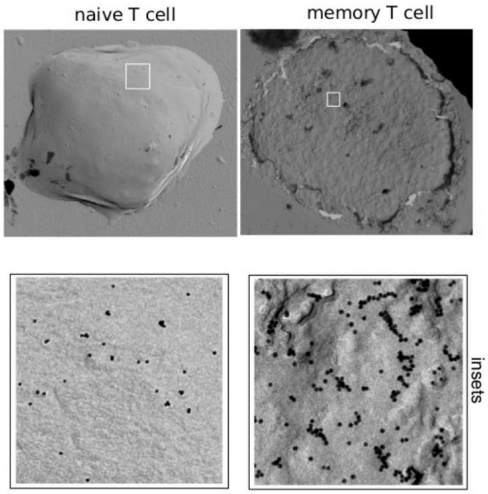

FIG. 1. TCR clusters on the surface of T-cells.

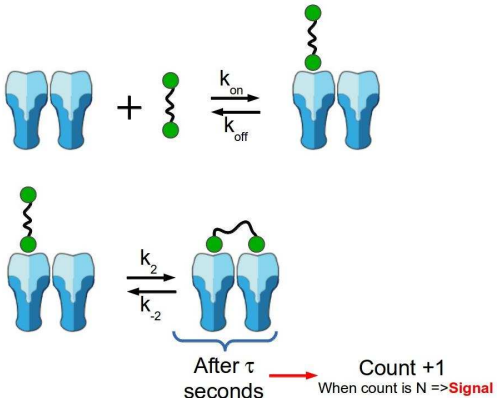

FIG. 2. Reactions involved in the stochastic activation model.

* marioc@upcomillas.es

[1] F D Batista and M L Dustin. *Immunological Reviews*, 251(1):7–12, 2013.

[2] J. Currie, M. Castro, G Lythe, E. Palmer, and C Molina-París. *Journal of The Royal Society Interface*, 9(76):2856–2870, 2012.

[3] M A Daniels, *et al.* *Nature*, 444(7120):724–729, 2006.

[4] J B Huppa and M M Davis. *Nature Reviews Immunology*, 3(12):973–83, December 2003.

[5] S. Valitutti, D. Coombs, and L. Dupré. *FEBS Letters*, 2010.

[6] V. Zarnitsyna and C. Zhu. *Physical Biology*, 9(4):045005, 2012.

toyLIFE: un universo de juguete para comprender mejor la evolución

Pablo Catalán*, Clemente Fernández-Arias y José A. Cuesta
Grupo Interdisciplinar de Sistemas Complejos (GISC)
Departamento de Matemáticas, Universidad Carlos III de Madrid 28911 Leganés (Madrid)

La existencia de mutaciones neutrales se conoce desde la mitad del siglo XX. Con el reciente acceso a secuencias genómicas, sin embargo, la relevancia de esta neutralidad se ha hecho más patente. Muchos modelos han intentado estudiar los efectos de esta neutralidad en la evolución. Normalmente, estos modelos asumen que cada organismo posee un genotipo y un fenotipo asociado. Si el organismo muta, su genotipo cambia, pero su fenotipo puede permanecer constante. Aquellos genotipos que están asociados al mismo fenotipo pertenecen a la misma *red neutra*. Si un genotipo puede sufrir muchas mutaciones sin cambiar de fenotipo, se dice que es *robusto*.

Los modelos que estudian estos fenómenos definen varias clases de "genotipos", como el RNA, las proteínas o las redes de regulación genéticas, y un "fenotipo" correspondiente: la estructura secundaria en el caso del RNA y las proteínas, y los patrones de expresión génica, en el caso de las redes de regulación. Posteriormente, se estudian varias propiedades de estas redes neutras. Sin embargo, hay muchos niveles de degeneración que contribuyen a la neutralidad y no se tienen en cuenta en estos modelos. Por ejemplo, la misma proteína puede ser codificada por diferentes secuencias de DNA, diferentes proteínas dan lugar a redes de regulación idénticas, etcétera. Además, es difícil definir la mutación en "genotipos" como las redes de genes: si las mutaciones afectan al DNA, ¿cómo se traducen estos cambios en la estructura de la red? Para resolver estos problemas, hemos desarrollado un modelo de juguete que incluye varios niveles de organización para poder estudiar el efecto de la degeneración en la robustez mutacional.

Presentamos toyLIFE, un nuevo marco diseñado para estudiar la evolución de organismos a distintos niveles de organización. toyLIFE contiene análogos de genes, proteínas y metabolitos (ver figura 1), que interaccionan mediante reglas físicas bien definidas para formar redes de regulación de juguete. Este sencillo sistema nos permite estudiar cómo una mutación al nivel del DNA de juguete se transmite a través de los distintos niveles, mejorando nuestra comprensión de la evolución de estos sistemas.

El funcionamiento de los organismos en toyLIFE se parece mucho al que observamos en células reales. Complejos patrones en regulación de la expresión de genes y en el metabolismo emergen a partir de las sencillas reglas físicas de interacción. Es posible diseñar redes de regulación con capacidad de romper metabolitos y, más aún, se pueden encontrar estas redes buscando al azar en el espacio de genotipos. Además, estas redes son robustas a cambios en sus componentes.

Con toyLIFE podemos observar cómo cambios en el DNA se traducen en cambios en la estructura de las proteínas, las interacciones entre estas o el comportamiento de la red. Se observa que la degeneración entre niveles se acumula de manera no trivial, de forma que, por ejemplo, cambios en las proteínas que forman una red de regulación pueden alterar el patrón de expresión génica, sin alterar la función metabólica.

Hemos estudiado también la abundancia de las distintas redes de regulación, que no es homogénea. Así, algunas redes son mucho más frecuentes que otras, e incluso algunas no aparecen. Es decir, hay redes de regulación que no son alcanzables, no porque el espacio de posibilidades sea muy amplio, sino porque no hay ninguna combinación de genes que dé lugar a esa topología particular. Esto introduce una importante limitación a lo que la evolución puede alcanzar, que no estaba presente en otros modelos de redes neutras.

En conclusión, para poder estudiar las propiedades de una red neutra, todos los niveles de organización deben ser tenidos en cuenta. En caso contrario, se corre el riesgo de introducir sesgos espurios en la dinámica evolutiva.

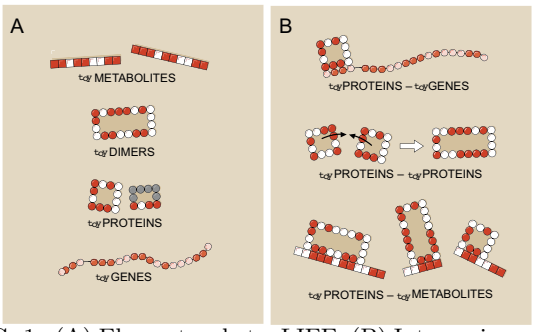

FIG. 1. (A) Elementos de toyLIFE. (B) Interacciones entre elementos de toyLIFE.

* pcatalan@math.uc3m.es

Fluctuaciones térmicas y propiedades elásticas de membranas bicapas de fosfolípidos

Enrique Chacón[1]
Instituto de Ciencia de Materiales de Madrid, CSIC, 28049, Madrid, Spain and Instituto de Ciencia de Materiales Nicolás Cabrera, Universidad Autońoma de Madrid, Madrid, 28049, Spain

Pedro Tarazona[2]
Departamento de Física Teórica de la Materia Condensada, Universidad Autónoma de Madrid, Madrid, 28049, Spain and Instituto de Ciencia de Materiales Nicolás Cabrera, Universidad Autónoma de Madrid, Madrid, 28049, Spain

Fernando Bresme[3]
Department of Chemistry, Imperial College London, SW7 2AZ, London UK and Department of Chemistry, Norwegian University of Science and Technology, Trondheim, Norway

Las membranas bicapas fosfolípidas son el principal componente estructural de las membranas biológicas. Sus propiedades elásticas juegan un papel fundamental en el anclaje , insersión y función de las proteinas. Las propiedades macroscópicas-mesoscópicas de la membrana están muy bien descritas por el hamiltoniano superficial efectivo de Helfrich. Dentro de este formalismo el módulo elástico de curvatura (bending), κ, es el parámetro más importante para describir la flexibilidad de las membranas biológicas. El problema es que los valores reportados de κ para una misma membrana, tanto experimentales como teóricos, pueden diferir de unos cálculos (medidas) a otros por un factor alrededor de 2, disparidad que lleva a comportamientos muy diferentes de la misma membrana. Por ello es importante desarrollar métodos que mejoren la precisión en la estimación de κ.

En este trabajo[4] se presenta un nuevo método para evaluar las propiedades elásticas de membranas biológicas en simulaciones numéricas. El método analiza las fluctuaciones térmicas en término del modo ondulatorio-acoplado, el cuál extiende significativamente el rango de valores del vector de onda k, hacia k más altos, que puede ser usado para estimar κ, lo que permite un cálculo mucho más preciso del mismo. Este hecho adquiere gran relevancia si se tiene en cuenta que si hacemos simulaciones con areas más grandes para ir hacia valores de k muy bajos, además del coste computacional prohibitivo, los resultados se contaminan con la aparición de fenómenos asociados a la compresibilidad de la membrana, que aunque es bastante incomprensible no los es del todo.

En los métodos anteriores es habitual describir las fluctuaciones de las membranas bicapas como la suma de tres modos; el modo ondulatorio que describe el movimiento de la posición media entre las dos capas; el modo peristáltico que describe los cambios locales en la anchura de la bicapa; y las protrusiones, movimientos desacoplados de las moléculas de cada capa. En el límite de vector de onda pequeño las ondulaciones dominan el espectro de fluctuaciones. En el caso de membranas libres la amplitud de las ondulaciones está controlada por el módulo elástico de curvatura κ , el cual, en simulaciones numéricas, puede ser evaluado a partir de la desviación cuadrática media de las amplitudes de las fluctuaciones. El problema es que el modo ondulatorio tradicional, basado en la posición media entre las dos capas, incluye contribuciones del tipo protrusión que contaminan el análisis para valores intermedios del vector de onda. Por el contrario nuestro análisis se basa en el modo ondulatorio-acoplado que describe el movimiento correlacionado de las dos capas, por lo que evita el problema anterior. Nuestro método también aporta una mejor caracterización del modo peristáltico en término de una energía elástica interna y de una contribución superficial.

---

[1] echacon@icmm.csic.es
[2] pedro.tarazona@uam.es
[3] f.bresme@imperial.ac.uk
[4] P. Tarazona, E. Chacón, and F.Bresme, J. Chem. Phys. **139**, 094902 (2013).

Non-axisymmetric Resonant Modes under Oscillating Magnetic Fields for very low Interaction Parameter Values

Iván Cortés-Domínguez*, Javier Burguete
University of Navarra, Pamplona, Spain

It is well known that the application of large external magnetic fields that evolve in time produce surface waves or instabilities in conducting fluid layers [1], [2]. This effect depends mainly on two sets of parameters, the fluid layer characteristics (electrical conductivity, layer depth, diameter) and the magnetic field (frequency and intensity). Many experimental works have been done for the large frequencies regime, where the instabilities appear due to forces localized near the surface. Plenty of industrial applications rely on high frequencies ranges. On the other hand, in the range of low frequencies, there is a lack of results close to the threshold because of its limited potential applications.

In this work we will focus on this range of frequencies, where the magnetic field may penetrate and produce a bulk force destabilizing the fluid layer. Specifically, we will study the range between 0.1Hz and 10Hz. An eutectic InGaSn alloy is placed on a Teflon® cylindrical cavity. The alloy adopts the form of a thin circularly-shaped fluid layer (a large drop of fluid) on the bottom of the container, with free surface. No external current is applied on the fluid. The force only appears through a purely vertical time dependent magnetic field perpendicular to the free surface. The field evolution is slow enough to avoid skin effects. The magnetic field is induced by modulating an electric current on an external coil. The power source that drives the coil can deliver up to 60A producing magnetic fields up to 70mT.

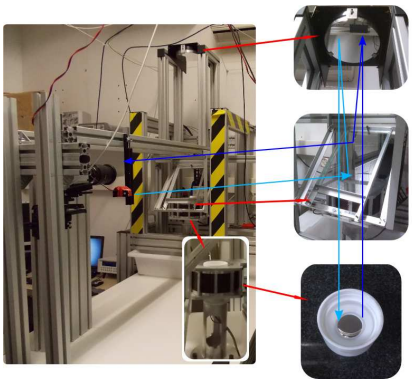

FIG. 1. Experimental setup.

This electrical current can be modulated, in a extremely low frequency range. This field generates in the fluid an azimuthal current due to Lenz's law that interacts again with the magnetic field producing a radial force (Lorenz's forces) if we assume that the system is axisymmetric. Any perturbation that deviates the system from the axisymmetry can produce an azimuthal force that can destabilize the fluid and will generate spatial patterns. So, depending on the experimental parameters, a flow is created that can be axisymmetric or not, and different resonances appear in the time domain and different spatial patterns are created associated to azimuthal wave numbers that break the symmetry of the system.

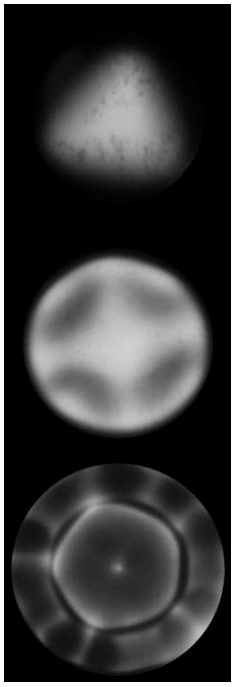

FIG. 2. m=3,4,5 azimuthal wavenumbers

Using Fourier analysis tools, we have observed patterns appearing on different regions. For the same parameter values, the azimuthal wavenumbers can even coexist and we have identified various sets of harmonics that evolve slaved. For large values of the exciting frequency we have observed that a radial wave number can be identified. These instabilities have been observed for interaction parameters as low as $N = 0.001$, and up to know these structures appear without threshold.

* icortes.1@alumni.unav.es

[1] J. Burguete, M. A. Miranda. Instabilities of conducting fluid layers in cylindrical cells under the external forcing of weak magnetic fields. *Magnetohydrodynamics. Vol.48, No.1, Pp.69-75* (2012).

[2] Y. Fautrelle, A.D. Sneyd. Surface waves created by low-frequency magnetic fields. *European Journal of Mechanics B/Fluids. Vol.24, pp.91-112* (2005).

Modelación numérica de medios granulares en arquitectura de tarjetas gráficas (GPUs).

Raúl Cruz Hidalgo
Departmento de Física y Matemática Aplicada
Edificio de los Castaños. C/Irunlarrea s/n
Universidad de Navarra, 31080 Pamplona (Navarra)

Las propiedades mecánicas y el comportamiento global de un medio granular dependen fuertemente de la forma y el tamaño de las partículas que lo componen. La modelación numérica de este tipo de sistemas mediante algoritmos de elementos discretos, comúnmente está limitado por el número de partículas y el elevado tiempo de cómputo. Hoy día la implementación de algoritmos de cómputo en unidades de procesamiento gráfico (GPU) es una alternativa muy novedosa que permite superar los inconvenientes mencionados. Recientemente hemos implementado un algoritmo hibrido CPU-GPU de dinámica molecular 3D, muy flexible y numéricamente preciso, en arquitectura de procesamiento gráfico. Esta herramienta numérica ha sido adaptada para describir sistemas de esferas polidispersas, elipsoides, esfero-cilindros y esfero-poliedros. La utilización de esta técnica ha mejorado notablemente el tiempo de ejecución respecto a resultados de otras paralizaciones tradicionales; lo cual permite acceder a escalas espacio-temporales relevantes, así como abordar fenomenologías y formación de patrones más complejos, especialmente en el caso de partículas no-esféricas. En nuestra presentación describiremos la implementación del nuevo algoritmo y mostraremos como hemos comprobado que cumple las leyes de la mecánica stadística y que sus resultados están en excelente correspondencia con teorías de campo medio para sistemas granulares diluidos. Además, expondremos resultados de algunas aplicaciones como, el estudio de flujos granulares y la estabilidad de arcos en silos, el proceso de penetración de un impactador en un medio granular a diferentes gravedades y la reología de un medio granular de partículas anisótropas. Finalmente describiremos la aplicación de una teoría de campo medio muy novedosa para el cálculo de esfuerzos dinámicos y estáticos dentro de medios granulares densos.

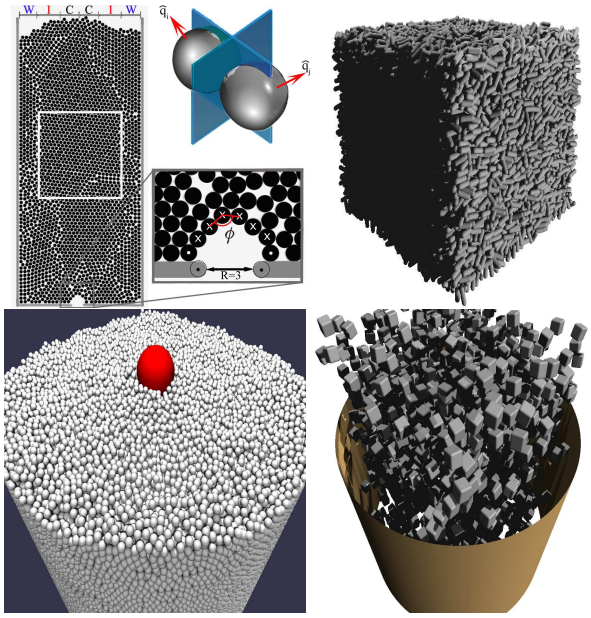

FIG. 1. Ejemplos de aplicaciones del algoritmo de elementos discretos en arquitectura de tarjetas gráficas (GPUs)

* raulcruz@unav.es

[1] Lozano, G. Lumay, I. Zuriguel, R.C. Hidalgo, and A. Garcimartín. Breaking Arches with Vibrations: The Role of Defects. *Phys. Rev. Lett.* **109** 068001 (2012)
[2] E. Altshuler, H. Torres, A. González-Pita, G. Sánchez-Colina, C. Pérez-Penichet, S. Waitukaitis, R. C. Hidalgo Extraterrestrial sink dynamics in granular matter enviado a PRL (Octubre 2013) http://arxiv.org/abs/1305.6796
[3] R. C. Hidalgo, T. Kanzaqui, F. Alonso-Marroquin and S. Luding. On the Use of Graphics Processing Units (GPUs) for Molecular Dynamics Simulation of Spherical Particles. *AIP Conf. Proc.* **1542** 169-172 (2013).
[4] R.C. Hidalgo, C. Lozano, I. Zuriguel, and A. Garcimartín. Force analysis of clogging arches in a silo. *Granular Matter* **15** 841-848 (2013)

Comparison of the transport properties in fluids of equivalent prolate and oblate mesogens in the nematic phase

Francisco Rodrigo and Alejandro Cuetos[?]
Departamento de Sistemas Físicos, Químicos y Naturales, Universidad Pablo de Olavide, 41013 Seville, Spain

Liquid crystalline phases appear in fluids of anisotropic particles with different shapes, as rod-like or disk-like particles. In this work, we establish several geometrical equivalences for prolate and oblate spherocylinders to compare their equilibrium dynamical properties, such diffusion coefficients or rotational viscosities. By means of molecular dynamics simulation, we conclude that several regimes appear for the transport behavior at similar packing fraction, from important viscosity dissimilarities to practically equal transport properties.

Piezoelectric energy harvesting from strongly colored supra Gaussian fluctuations: An electronic analogy

Julián I. Peña Rosselló, J. Ignacio Deza†, Horacio S. Wio‡ y Roberto R. Deza*
IFIMAR, Instituto de Investigaciones Físicas de Mar del Plata
CONICET-Universidad Nacional de Mar del Plata B7602AYL Mar del Plata (Bs.As.) Argentina

Recently[1,2], we have proposed a wide-spectrum piezoelectric energy-harvesting model based on a monostable oscillator obeying a Woods–Saxon[3] potential

$$U(x) := -V_0/\{1 + \exp[(|x| - r)/a]\},$$

capable of interpolating between square-well and harmonic-like behaviors. We found an increase of the output rms voltage V_{rms} for deep potential wells and low noise intensity σ, as the model external noise $\eta(t)$ became supra Gaussian (Fig. 1). We chose for $\eta(t)$ the process defined by

$$\tau\dot{\eta} = -V_q'(\eta) + \xi(t), \text{ with} \quad (1)$$
$$V_q(\eta) := \ln[1 + \tau(q-1)\eta^2/2]/[\tau(q-1)]$$

and $\xi(t)$ white, Gaussian, unit variance because it is easy to generate dynamically and depends on only two parameters (q and τ) with clear interpretation: for $q = 1$, $\eta(t)$ is Ornstein–Uhlenbeck's with correlation time τ, for $q < 1$ it is bounded, for $1 < q < 5/3$ it is supra Gaussian (finite variance but constructively contributing higher cumulants), and for $q > 5/3$ it is fat-tailed (in particular for $q = 2$, it is Cauchy's)[4]. Those results led us to conclude that a deep square-well potential acts as a selector of the large highly correlated oscillator excursions provoked by the supra Gaussian noise.

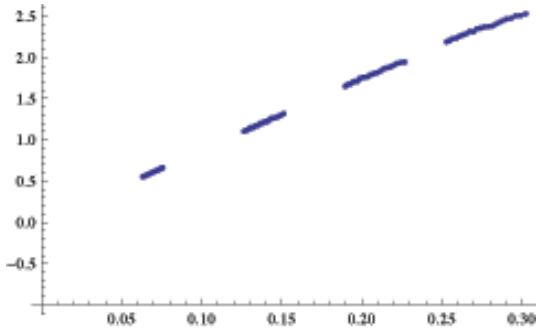

FIG. 1. V_{rms} *vs* σ_{eff} for $V_0 = 10$, $\sigma = 0.2$, and $a = 0.05$.

In order to further explore that mechanism, we performed a real experiment on an incomplete but illustrative electronic analog: $\eta(t)$ noise synthetized by means of Eq. (1) is fed to the circuit in Fig. 2 using a `MATLAB` function, through the computer's audio output. The Zener diode is a metaphor of the square-well potential and the OP AMP is required because the `MATLAB` output is limited between ± 2V. As q grows larger than 1 (and thus $\sigma_{eff} := \sigma\sqrt{2/[\tau(5-3q)]}$ increases, Fig. 3), so does the frequency of Zener current peaks (Fig. 4).

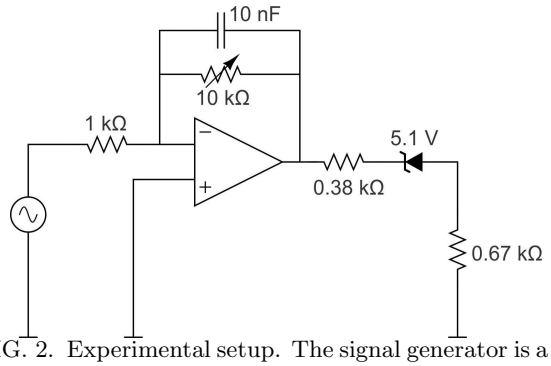

FIG. 2. Experimental setup. The signal generator is a computer.

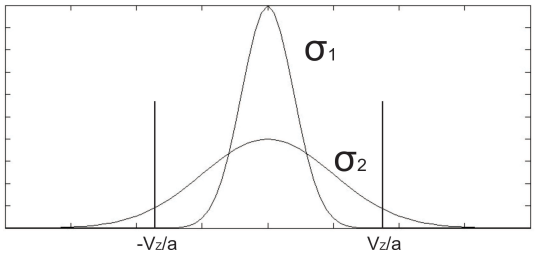

FIG. 3. V_z/a: Zener voltage over amplification factor.

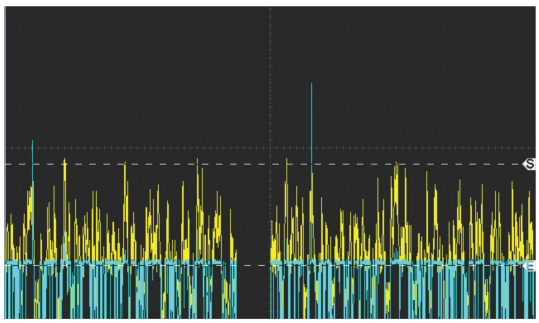

FIG. 4. $q = 1.6$, $\sigma = 0.4$.

* deza@mdp.edu.ar
† Departament de Física i Enginyeria Nuclear, Universitat Politècnica de Catalunya, 08222-Terrassa (Barcelona).
‡ IFCA, Instituto de Física de Cantabria, CSIC-Universidad de Cantabria 39005-Santander (Cantabria)

[1] J.I. Deza, R.R. Deza and H.S. Wio, Europhys. Lett. **100**, 38001 (2012).
[2] J.I. Deza, R.R. Deza and H.S. Wio, "Cosecha de energía de espectro amplio con osciladores alineales monoestables: mejora con potenciales de paredes finitas y ruidos tipo Lévy" (poster contribution at FISES 2012).
[3] A. Bohr and B.R. Mottelson, *Nuclear structure* v1 (Benjamin, New York, 1975).
[4] H.S. Wio, Europhys. News **36**, 197 (2005).

Stochastic-resonant spatiotemporal patterns in a FitzHugh–Nagumo ring with electric inhibitory coupling: A reduced gradient description

Alejandro D. Sánchez, Gonzalo G. Izús, Matías G. dell'Erba y Roberto R. Deza*
IFIMAR, Instituto de Investigaciones Físicas de Mar del Plata
CONICET-Universidad Nacional de Mar del Plata B7602AYL Mar del Plata (Bs.As.) Argentina

We study from the *nonequilibrium-potential* (NEP) viewpoint, the self-organization induced by local noises with common variance η—which includes synchronization with a global, periodic, adiabatic and subthreshold signal $S(t)$—of networks of excitable elements with FitzHugh–Nagumo (FHN) dynamics. After having coupled (chemically[1–3] or electrically[4]) their *activator* fields in *antiphase* fashion, we study electric coupling (in phase, with strength E) between nearest-neighbors' *inhibitor* fields. Excitability allows us to set a threshold u_{th} (its precise value is irrelevant as far as it lies within some interval), call cell i *active* if $u_i > u_{th}$ and define the (time-dependent) *activity* as the average number of active cells.

As in previous work[1–4], we study numerically the activity as a function of η for fixed E (Fig. 1), finding a stochastic-resonant behavior (Fig. 2), and elucidate the dynamics in terms of noise-assisted transitions between (signal-dependent) attractors. We introduce a *two-cell* model that allows the characterization of an antipahase state (besides homogeneous one). At variance with former cases[1–4], a NEP is not easily found for this system. So we project the dynamics along the *slow manifolds*. All the point-like attractors fall along this projection. This alternative is used *only* to calculate *heigths* of barriers. The resulting system is gradient, and its potential ϕ is symmetric under $u_1 \leftrightarrow u_2$.

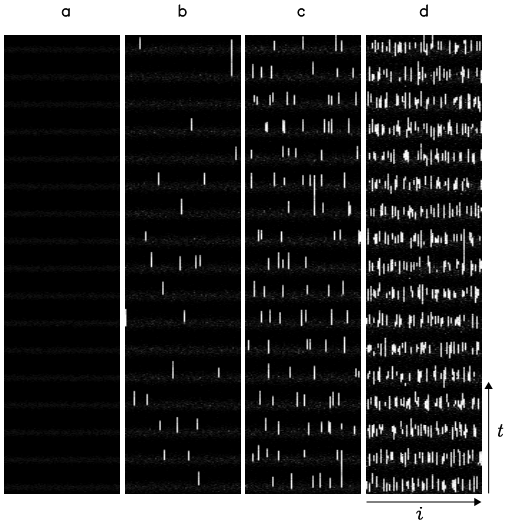

FIG. 1. Record of a set of 80 cells (white: 'activated', black: 'inhibited') with $E = 1$. a) $\eta = 2 \times 10^{-8}$ (subthreshold homogeneous oscilation), b) $\eta = 1.4 \times 10^{-7}$ (Partially synchronized state), c) $\eta = 2 \times 10^{-7}$ (partially synchronized state), and d) $\eta = 5.6 \times 10^{-7}$ (noise-sustained synchronization).

The number and relative stability of attractors changes with the signal amplitude (Fig. 3). For maximum amplitude, the difference in ϕ between the saddle and the uniform state is $\Delta\phi = 7 \times 10^{-7}$. *For a noise level of this order, the two-cell system would climb that potential barrier and transit to the antiphase state, that has a lower ϕ value.* The antiphase state can then *deterministically* return to the uniform state because the saddle-antiphase fixed points collapse. $\eta \sim \Delta\phi$ is the expected order of magnitude of noise for full synchronization, in good agreement with the numerical results.

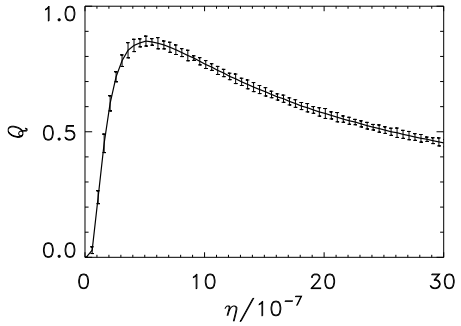

FIG. 2. $Q-$factor of the activity for $E = 0.5$ (average over 20 realizations). Q_{max} occurs at $\eta \approx 5 \times 10^{-7}$.

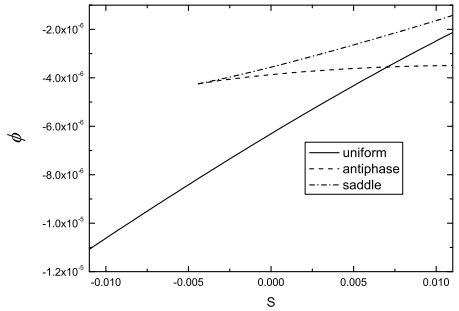

FIG. 3. ϕ values vs S for the uniform (inhibited-inhibited), the saddle and the antiphase states. Note that the last two fixed point disappear for S below $\sim -5 \times 10^{-3}$ (deterministic decay). Here $E = 0.5$

* deza@mdp.edu.ar

[1] G. G. Izús, R. R. Deza and A. D. Sánchez, AIP Conf. Proc. **887**, 89 (2007).
[2] G. G. Izús, A. D. Sánchez and R. R. Deza, Physica A **388**, 967 (2009).
[3] A. D. Sánchez and G. G. Izús, Physica A **389**, 1931 (2010).
[4] M. dell'Erba, G. Cascallares, A. Sánchez and G. Izús, Eur. Phys. J. B (submitted).

Synchronization of bursting oscillators by a common noise source

Guillermo V. Savino, Carlos M. Formigli, J. Ignacio Deza† y Roberto R. Deza*
Facultad de Ciencias y Tecnología, Universidad Nacional de Tucumán, San Miguel (Tucumán) Argentina

Neuron synchronization plays a fundamental role in many complex brain functions (memory, control, thought, etc.) Its study might help understand e.g. why (and how) do neurons use either single spikes or bursts to transmit, encode and process information. Since a single neuron typically receives random inputs from nearly 10^4 others, the neurocomputational paradigm finally arising will necessarily have noise as a central ingredient. Previous theoretical studies[1,2] have shown that—against common sense—*noise may improve neuron synchronization*. We are not aware of such paradoxical noise effect having been reported in any physical device that emulates the spiking *and bursting* neuron electrical activity.

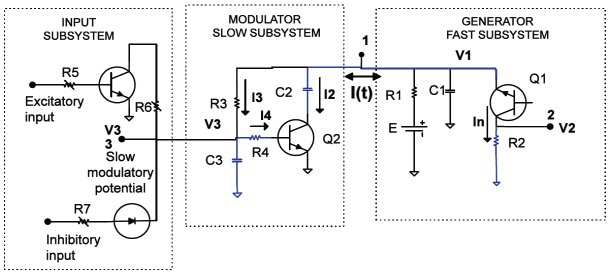

FIG. 1. Non-identical weakly coupled bursting electronic model of a neuron.

Our analog electronic circuit[3] (Fig. 1) is based on the *same operating principles* (conductance change) as neurons (analogues for potentials, currents and conductances can be easily identified) and exhibits the *same bifurcation scenarios* and essentially the same bursting behavior as the Hodgkin–Huxley model. Through a single parameter (a conductance) our circuit can be set into different self-oscillating regimes: *single spikes at nonregular interspike intervals*, and *two- and three-spike bursts interspersed with single spikes*.

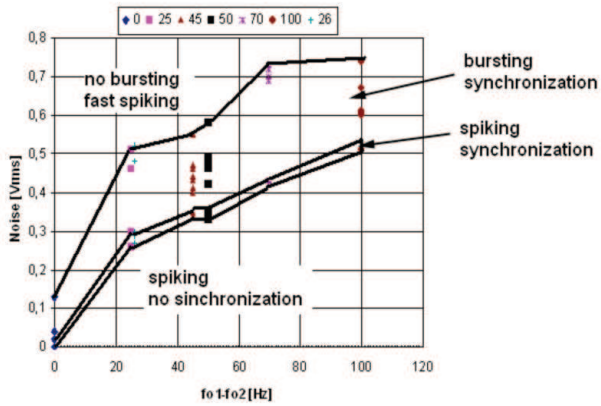

FIG. 2. Synchronization regimes.

The circuits are naturally nonidentical due to their components' value dispersion, and unavoidably coupled—even if not deliberately done—when using a common noise source. By applying to two such circuits a common noise of increasing intensity, their initially very different instantaneous frequencies increase and match, and the system's self-oscillation becomes periodic. We show that this effect is noise-mediated rather than due to the (very) weak coupling. The histograms, frequency spectra, correlation and recurrence plots show the measured activation and excursion times as the frequencies of both oscillators become equal for a definite noise intensity. Moreover, the plots for different noise intensities of the spike-sequence phase differences between the two circuits as time goes on show plateaux with different duration, indicating phase synchronization induced by the common noise. Complete synchronization has never been observed. When the circuits undergo saddle–homoclinic bifurcation, phase synchronization of spikes, spikes-bursts, and bursts occurs for definite noise intensities. The experimental results confirm the theoretical assertion that for noise mediated synchronization of two nonidentical oscillators, a stable and an unstable manifolds are necessary. When the circuits undergo a saddle–node bifurcation on invariant circle, no synchronization is detected in our experimental setup.

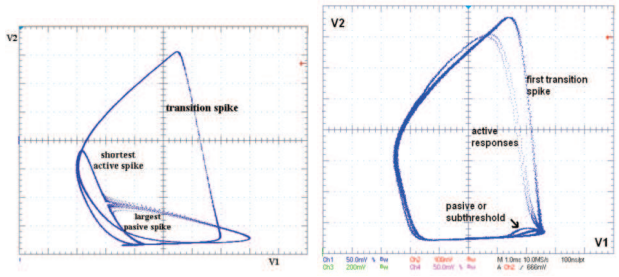

FIG. 3. a) saddle–homoclinic bifurcation; b) saddle–node bifurcation on invariant circle.

* IFIMAR (CONICET-UNMdP) B7602AYL Mar del Plata (Bs.As.) Argentina. deza@mdp.edu.ar
† Departament de Física i Enginyeria Nuclear, Universitat Politècnica de Catalunya, 08222-Terrassa (Barcelona).

[1] C.S. Zhou and J. Kurths, Phys. Rev. Lett. **88**, 230602 (2002); Chaos **13**, 401 (2003).
[2] C.S. Zhou, J. Kurths, I.Z. Kiss and J.L. Hudson, Phys. Rev. Lett. **89**, 014101 (2002).
[3] G. V. Savino and C. M. Formigli, BioSystems **97**, 9-14 (2009).

Pinning by noise

Sergio E. Mangioni and Roberto R. Deza*
IFIMAR, Instituto de Investigaciones Físicas de Mar del Plata
CONICET-Universidad Nacional de Mar del Plata B7602AYL Mar del Plata (Bs.As.) Argentina

Research on *localized patterns*—bubbles of *metastable* homogeneous states (HS), also called *pinning states* or "solitons"—has recently undergone an upsurge of interest. Especially puzzling are those arising in one-dimensional (1D) reaction–diffusion (RD) systems, since "inverse nucleation"-like arguments (invoking negative surface tension) break down. Moreover in *simple* 1D bistable RD systems, localized patterns *cannot* be stable because for equally stable HS, the solvability condition determining the time-derivative of the "soliton" width Δ can be interpreted as an "attracting force" between the kinks bounding the bubble, which make it shrink and disappear[1]. A route to stable localized patterns in 1D RD systems is to introduce a *nonlocal interaction* term[2].

Here we report another route, involving *two* essential ingredients[3]: i) an aggregating current $J_A(x,t)$ which can in certain situation (e.g. when due to an attracting potential with range $r_a \ll L_{diff}$) be assimilated to an "antidiffusive" term[4]; ii) a *multiplicative* noise of the kind leading to *entropic* noise-induced phase transition[5]. The dynamical equation of a field $0 < \phi(x,t) < 1$ is

$$\partial_t \phi = Q_\lambda(\phi) + \partial_x[D_{eff}(\phi)\partial_x \phi] \qquad (1)$$

with $Q_\lambda(\phi) := Q(\phi) - \lambda \frac{\mathrm{d}\Gamma}{\mathrm{d}\phi}$ accounting for ingredient (ii) and $D_{eff}(\phi)$ accounting for ingredient (i).

We aim to stabilize "solitons" when introducing as initial condition either

$$\phi_0^u(x) := 0.48[\tanh \rho A(x+x_f) - \tanh \rho A(x-x_f)] \text{ or}$$
$$\phi_0^d(x) := 1 - 0.48[\tanh \rho A(x+x_f) - \tanh \rho A(x-x_f)],$$

(with $\rho > 1$ and $A := L_{diff}/r_a$) according to whether we want to perturb the low-value (ϕ_d) or the high-value (ϕ_u) HS. (We take $x_f = 21,600\,\delta x$, with $\delta x = 2.510^{-4}$) Regarding the simplest multiplicative-noise factor $\Gamma^{1/2}(\phi)$ enabling the noise to destabilize only one HS, it comes out that

$$\Gamma_u := \exp[b(\phi-1)] \text{ affects } \phi_u \text{ and}$$
$$\Gamma_d := \exp[-b\phi] \text{ affects } \phi_d$$

(we use $b = 10$). These factors put the affected HS around the critical point that designates his disappearance. This idea is not expected to work for too large noise intensities, since the solution that is intended to affect would cease to exist. Figure 1 (respectively Fig. 2) shows states where ϕ_d (respectively ϕ_u) has been pinned by the multiplicative noise. This numerical result is supported by a rough calculation that appeals to the solvability condition[1,2,7].

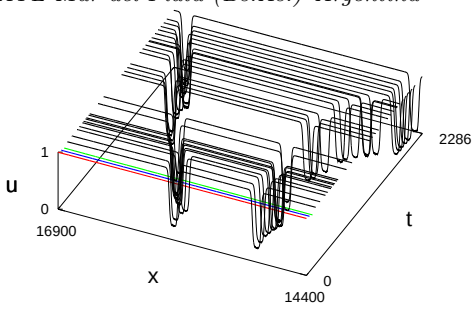

FIG. 1. System excited with $\phi_0^d(x)$. Evolution of two "solitons" with ϕ_d pinned.

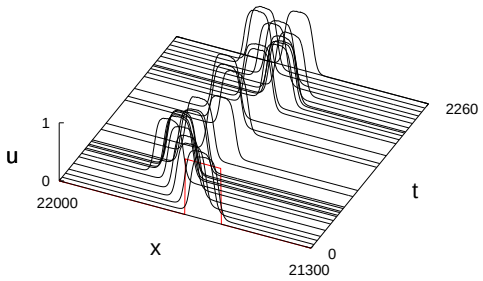

FIG. 2. System excited with $\phi_0^u(x)$. Evolution of one "soliton" with ϕ_u pinned.

We take for $Q(u)$ in Eq. (1) the normal form $Q(u) = (\beta - u^2)u + \mu$, with $u = \phi - 0.5$ and μ a small parameter, so that its stationary front solutions can be written as

$$u^s \approx u_\pm^s = \sqrt{\beta}\,\tanh\left[(\beta/2)^{1/2} A(x - x_f^\pm)\right].$$

The resulting equation for Δ shows that under certain conditions,
- with Γ_u, the only solution is stable S^+ solitons and
- with Γ_d, the only solution is stable S^- solitons.

* deza@mdp.edu.ar

[1] P. Coullet, Int. J. Bif. Chaos Appl. Sci. Eng. **12**, 2445 (2002).
[2] M.G. Clerc, D. Escaff and V.M. Kenkre, Phys. Rev. E **72**, 056217 (2005).
[3] S.E. Mangioni, Physica A **389**, 1799 (2010); S.E. Mangioni and R.R. Deza, Phys. Rev. E **82**, 042101 (2010); S.E. Mangioni and R.R. Deza, Physica A **391**, 419 (2012).
[4] M. Hildebrand and A.S. Mikhailov, J. Phys. Chem. **100**, 19089 (1996).
[5] M. Ibañes, J. García-Ojalvo, R. Toral and J.M. Sancho, Phys. Rev. Lett. **87**, 020601 (2001).
[6] O. Carrillo, M. Ibañes, J. García-Ojalvo, J. Casademunt and J.M. Sancho, Phys. Rev. E **67**, 046110 (2003).
[7] S.E. Mangioni, Eur. Phys. J. B **86**, 390 (2013).

Fragmentation Transitions in the Multilayer Coevolving Voter Model

Marina Diakonova*, Victor M. Eguíluz and Maxi San Miguel
IFISC, Instituto de Física Interdisciplinar y Sistemas Complejos
CSIC-Universidad de las Islas Baleares 07122-Palma (Mallorca)

Coevovling voter models are cornerstone frameworks for representing systems whose topology depends on the state of agents and whose simultaneous evolution of nodes and links would ordinarily lead to a fragmentation transition. We couple two such models, first proposed in[2], into a multilayer structure, and investigate effect of interlayer coupling and variation in the layer rewiring rates. The precise nature of interlayer coupling that we implemented is motivated by a number of recent works[1],[3] that consider the individual (a node) as an agent *simultaneously existing and being influenced by a number of contexts*, e.g. various relationships, or differing online platforms, etc. This accomodates the possibility of being subjected to differing processes, but requires the state of the node itself to be consistent across the layers. Specifically, we evolve the binary-state multi-layer network to mimick the process of opinion-formation in several social contexts by first, evolving layers randomly and second, synchronising the layers by potential vertical propagation of any change of state. The main parameters in our model are the rewiring probabilities p_1, p_2 of the two layers, and the fraction q of nodes existing in both layers, which we call the degree of multiplexing.

The asymptotic density of active links ρ^{asym} for the multilayer system with two identical co-evolving voter models ($p = p_1 = p_2$) is shown in figure figure (a). Whereas the trend with $q = 0$ corresponds to known results, we find that the fully-interconnected multiplex ($q = 1$) also displays an absorbing transition that is, however, offset to a higher level of rewiring. The same transition-delay effect is confirmed by averaging out the size of the largest component in a frozen state, a signature of fragmentation transition. The presence of fragmentation transition is also confirmed by the peaking of convergence times around the critical values of rewiring probabilities.

We thus see that there is a finite range of rewiring just above the critical rewiring probabilities for the monoplex, a range defined by a persistence of the absence of fragmentation. A single network with a rewiring probability in this range would fragment. Coupling two such networks together would, however, stop them from doing so. The strength of coupling needed for this offset to take place depends on the exact values of p. This means that a multiplex allows for greater topological activity before fragmentation sets in. These offset effects are confirmed by the the mean-field pair approximation for the equations governing ρ_1 and ρ_2. Our analytical approach is able to explain both the shift in the transition and the higher level of active links brought about by the increase in q.

We proceed to study how fragmentation in finite-size multilayer system varies in the parameter hypercube. A typical final configuration in the cases of extreme asymmetry ($p_1 = 1$, $p_2 = 0$) is shown in figure (b). This is exemplary of a range of rewiring probabilities for which the two layers *fail to synchronise*. In other words, the interlayer connectivity is not sufficiently strong to prevent the slower layer from freezing in one giant component, while the faster layer still fragments. The surprising side-effect of a gradual coupling between two disparate layers is the erosive nature of the fragmentation occuring on the faster, more dynamic layer. Indeed, while the difference in the sizes of the two largest components stays low, their absolute sizes decrease as well. This is accompanied by an explosion (linear with q for the extreme asymmetry) in the number of *isolated* components. We characterise this erosive fragmentation, which we consider to be a signature of a subcritical degree of multiplexing in asymmetric systems.

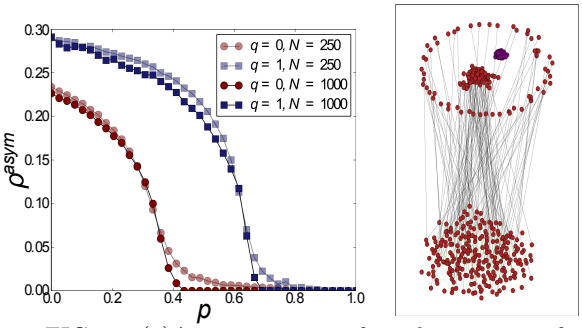

FIG. 1. (a)Asymptotic interface density as a function of layer rewiring probabilities, ensemble size 10^4. (b) Final configuration with $p_1 = 1$ (top layer), $p_2 = 0$, and $q = 0.5$, $N = 250$. Networks random regular, with $\mu = 4$.

* marina@ifisc.uib-csic.es

[1] Michael Szell, Renaud Lambiotte, and Stefan Thurner. Multirelational organization of large-scale social networks in an online world. *Proceedings of the National Academy of Sciences*, 2010.

[2] Federico Vazquez, Víctor M. Eguíluz, and Maxi San Miguel. Generic absorbing transition in coevolution dynamics. *Phys. Rev. Lett.*, 100:108702, March 2008.

[3] Rafael Vida, Javier Galeano, and Sara Cuenda. Vulnerability of multi-layer networks under malware spreading. *ArXiv*, October 2013.

Difusión anómala inducida por la interacción hidrodinámica

J. Bleibel[1], Alvaro Domínguez[2*], M. Oettel[1]
[1] *Institut für Angewandte Physik, Universität Tübingen, Auf der Morgenstelle 10, 72076 Tübingen, Germany*
[2] *Física Teórica, Universidad de Sevilla, Apdo. 1065, E–41080, Sevilla*

Es bien conocido que las interacciones hidrodinámicas (IH) juegan un papel relevante en la dinámica de los coloides. Por otra parte, en los últimos años ha surgido un interés renovado por el estudio teórico y experimental de coloides confinados por distintos mecanismos (p.ej., pinzas ópticas, atrapamiento por interfases,...). A pesar del carácter casi bidimensional (2D) o monodimensional (1D) de estos coloides confinados, las partículas se encuentran en muchas ocasiones inmersos en un fluido sin restricciones cinemáticas, de manera que experimentan una IH completamente tridimensional (3D). Puesto que una parte del sistema está confinada y otra parte no, se puede denominar a esta situación *"confinamiento parcial"*.

Considerando el modelo teórico más sencillo para la dinámica del coloide (difusión corregida por la IH al nivel del tensor de Oseen), demostramos que el coeficiente de difusión colectiva para tiempos largos del coloide en *confinamiento parcial* no existe[1,2]. Este resultado se debe al "desajuste dimensional" entre el coloide (2D/1D) y la interacción hidrodinámica (3D) y tiene un origen diferente del resultado análogo para fluidos puramente 2D y 1D (efecto de las "colas largas"). El coeficiente de difusión dependiente del número de onda, $D(k)$, exhibe una divergencia característica cuando $k \to 0$ que es independiente de las interacciones directas entre las partículas coloidales y que está determinada únicamente por las características cinemáticas del *confinamiento parcial*.

Estas conclusiones han sido validadas mediante el empleo de simulaciones numéricas que incluyen el efecto de la IH de manera más realista que el tensor de Oseen. En estas simulaciones la difusión anómala se manifiesta como una aceleración de la dinámica respecto al caso en ausencia de IH. Igualmente, el modelo teórico y los resultados deducidos proporcionan un marco conceptual para la interpretación de la divergencia del coeficiente de difusión medido en monocapas coloidales[3–5].

* dominguez@us.es

[1] G. Nägele, M. Kollmann, R. Pesché, A. Banchio, *Mol. Phys.* **100** (2002) 2921
[2] J. Bleibel, A. Domínguez, F. Günther, J. Harting, M. Oettel (2013), http://xxx.lanl.gov/abs/1305.3715
[3] B. Lin, S. A. Rice, D. A. Weitz, *Phys. Rev. E* **51** (1995) 423
[4] K. Zahn, J. M. Méndez–Alcaraz, G. Maret, *Phys. Rev. Lett.* **79** (1997) 175
[5] B. Lin, B. Cui, X. Xu, R. Zangi, H. Diamant, S. A. Rice (2013), http://xxx.lanl.gov/abs/1308.6508

Nestedness in complex networks

Virginia Domínguez García* [1], Sam Johnson [2] and Miguel A. Muñoz [1]
[1] *Departamento de Electromagnetismo y Física de la materia, and instituto carlos I de Física Teórica y Computacional, universidad de Granada,18010 Granada,Spain.*
[2] *Department of Mathematics, Imperial College, London, SW7 2AZ United Kingdom*

Understanding the causes and effects of network structural features is a key task in deciphering complex systems. In this context, the property of network nestedness has aroused a fair amount of interest as regards ecological networks. In order to make progress, systematic analyses of nestedness and nestedness indices are necessary. Indeed, Bastolla et al. introduced a simple measure of network nestedness[1] which opened the door to analytical understanding, allowing them to conclude that biodiversity is strongly enhanced in highly nested mutualistic networks.

In this work[2] we suggest a slightly refined version of such a measure of nestedness that exhibits a number of additional advantages: (i) it allows us to identify the amount of nestedness associated with each single node in a network, making it possible to define a "local nestedness"; (ii) the new index is properly normalized and provides an output equal to unity in uncorrelated random networks, allowing us in this way to discriminate contributions to nestedness beyond network heterogeneity. Having removed the direct effects of the degree distribution - which has a dominant contribution to other measures of nestedness - it is possible to move one step forward and ask how degree-degree correlations (as quantified by Pearson's coefficient) influence nestedness measurements. We aim to understand to what extent nestedness is a property inherited from imposing a given degree distribution or a certain type of degree-degree correlations on a network.

We find that most of the empirically found nestedness stems from heterogeneity in the degree distribution. Once such an influence has been discounted - as a second factor - we find that nestedness is strongly correlated with disassortativity and hence - as random networks have been recently found to be naturally disassortative - they also tend to be naturally nested just as the result of chance. In conclusion, degree heterogeneity together with the finite size of real networks suffice to justify most of the empirically observed levels of nestedness in ecological bipartite network.

---

* virginia@onsager.ugr.es

[1] Bastolla U, Fortuna M, Pascual-García A., Ferrera A, Luque B, et al. (2009) The architecture of mutualistic networks minimizes competition and increases biodiversity. Nature 458: 1018-21

[2] S.Johnson, V. Domínguez-García, M.A. Muñoz (2013) Factors Determining Nestedness in Complex Networks. PLos ONE 8:e74025

Coupled maps analysis of cardiac wave instabilities due to tissue contraction

B. Echebarria*, E. Alvarez-Lacalle, M. Radszuweit†, M. Bär†
Departament de Física Aplicada, Universitat Politècnica de Catalunya-BarcelonaTech, Av. Dr. Marañón 44-50, E-08028, Barcelona.

Several life-threateaning arrhythmias are related to electrical wave instabilities in the heart. At rest, there is a large gradient of ionic concentration across the myocytes' cell membrane. Given an external stimulus, ion channels at the membrane open, allowing the flux of ions, that results in an increase in transmembrane electrical potential - the depolarization of the cell. This front then propagates along tissue, triggering the contraction of the cardiac cells in a coordinated manner. Instabilities of propagation give rise to wavebreak, the formation of reentry (i.e., tachycardia) and, eventually, a disordered electrical wave pattern (i.e., fibrillation) in which the heart is not able to pump blood and death intervenes in a matter of minutes.

In all the former mechanism, tissue contraction is usually thought to be of no relevance, being just a consecuence of electrical depolarization. However, several studies suggest that it can play an important role in sustaining and/or inducing the instability. In this contribution we will show that a small amount of contraction can in fact give rise to a wave instability, termed alternans, followed by wave blocks and the initiation of reentry.

At a cellular level, an alternans rhythm is characterized by a beat-to-beat change in the duration of the depolarized phase, or action potential (AP). In tissue, this may result in spatially homogeneous patterns of oscillations (concordant alternans, CA), or in domains of out-of-phase oscillations (discordant alternans, DA)[1]. Remarkably, besides all the complex microscopic details neccessary to properly characterize the dynamics of the transmembrane potential, the main characteristics of this instability can be captured considering a mesoscopic approach[2]. In this, a description in terms of coupled maps, relating the action potential duration (APD) and the conduction velocity (CV) of the AP, at a given point, with the local time lapse between the end of an excitation and the beginning of the following one (diastolic interval, DI), reproduces the main characteristic observed during cardiac alternans. Furthermore, close to the transition to alternans, the small oscillations in the APD have been shown generically to obey a Ginzburg-Landau type equation with an additional nonlocal term that causes spontaneous nucleations of domains giving rise to DA[3].

We have recently used a simplified model of cardiac excitation-contraction coupling to study the effect of tissue deformation on the dynamics of alternans[4]. We showed that small stretch-activated currents produce large effects, causing a transition from in-phase to off-phase alternations (i.e. from concordant to discordant alternans) and to conduction blocks. This effect is the result of a generic change in the slope of the CV-restitution curve due to electromechanical coupling. Thus, excitation-contraction coupling plays a relevant role in the transition to reentry and fibrillation. This effect can be traced to a change in the spatial and functional dependence of the CV, that modifies the solutions of the coupled maps. In this contribution, we elaborate further on the details of this transition, analysing the solutions of the coupled maps equations close to the onset of alternans. We find a good agreement between the full ionic equations, the coupled map equations and the reduced description in terms of Ginzburg-Landau amplitude equations, therefore stressing the usefulness of studying simplified models for the undertanding of complex spatio-temporal phenomena in cardiac tissue.

---

* blas.echebarria@upc.edu
† Physikalisch-Technische Bundesanstalt, 10587 Berlin, Germany

[1] J. M. Pastore, S. D. Girouard, K. R. Laurita, F. G. Akar and D. S. Rosenbaum, Circulation **99**, 1385 (1999).
[2] M. Courtemanche, L. Glass and J. Keener, Phys. Rev. Lett. **70**, 2182–2185 (1993).
[3] B. Echebarria and A. Karma, Phys. Rev. Lett. **88**, 208101 (2002); Phys. Rev. E **76**, 051911 (2007).
[4] M. Radszuweit, E. Alvarez-Lacalle, M. Bär, B. Echebarria, preprint.

Are Atmospheric Rivers attracting Lagrangian Coherent Structures in the wind field?

Daniel Garaboa[1], Jorge Eiras[1], Florian Huhn[2] and Vicente Pérez-Muñuzuri[1*]
[1] *Group of Nonlinear Physics, Faculty of Physics, University of Santiago de Compostela. Santiago de Compostela, Spain.*
[2] *ETH Zurich, Institute for Mechanical Systems, Center of Mechanics. Zurich, Switzerland.*

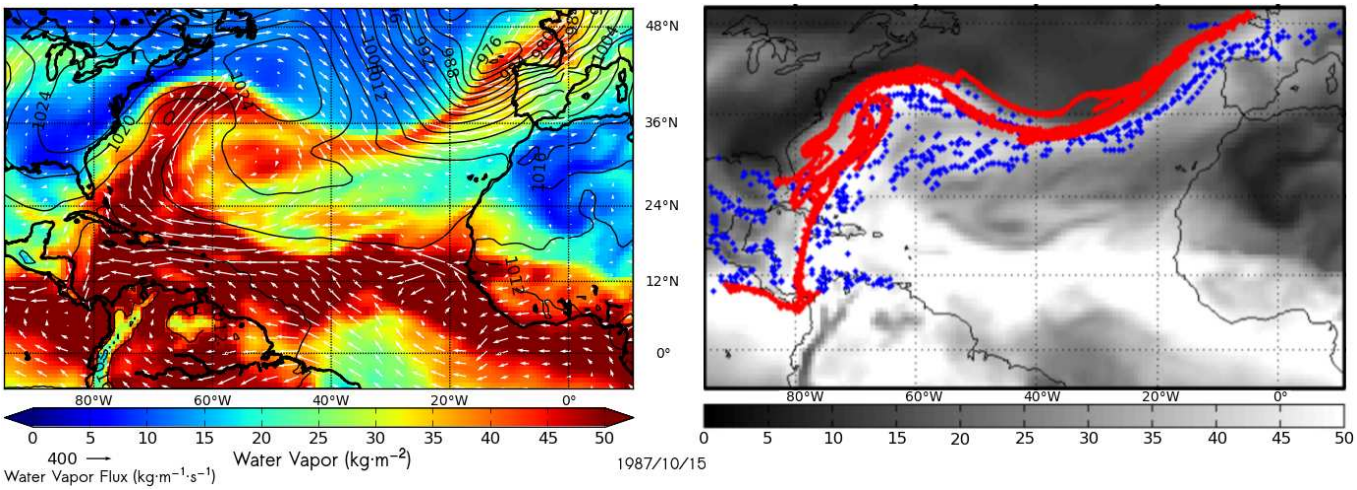

FIG. 1. Intense Atmospheric River impacting over the Iberian Peninsula (left) and the Lagrangian Coherent Structure (LCS) (ridge red points) calculated from the FTLE using the integrated column water vapor (right). Blue dots correspond to the ridge position of the Atmospheric River.

Most of the advective moisture transport from the tropics (main planetary precipitable water source) to mid-latitudes is not smooth and uniform. More than 90% of poleward water vapor transport is accomplished by narrow and elongated (longer than 2000 km and narrower than 1000 km) structures with very high water vapor content within the pre-cold frontal Warm Conveyor Belt (WCB) and Low Level Jet (LLJ) of extratropical cyclones[1] mostly associated to the polar front. These structures, labeled as Tropospheric or Atmospheric Rivers (ARs)[2], are defined as areas of Integrated Water Vapor (IWV) column over 2 cm and strong winds, transporting water vapor in the lower troposphere, close to 1 km above the sea level[3].

Due to their filamentous shape, these structures have been analyzed in terms of Lagrangian Coherent Structures (LCS), using the Finite-Time Lyapunov Exponents (FTLE)[4,5].

In order to develop such analysis, a 2D-velocity field from vector flux fields was extracted over the North Atlantic Ocean, using vertical integrals of water vapor (Q) and eastward/northward water vapor flux (Φ_λ, Φ_ϕ), retrieved from the ECMWF Reanalysis (ERA-Interim) at a $0.7° \times 0.7°$ horizontal resolution,

$$Q = \frac{1}{g}\int_0^1 q\frac{\partial p}{\partial \eta}d\eta \qquad (\Phi_\lambda, \Phi_\phi) = \frac{1}{g}\int_0^1 (u,v)q\frac{\partial p}{\partial \eta}d\eta \quad (1)$$

with η a hybrid vertical coordinate. Eastward and northward average drift velocities,

$$<\lambda>=\frac{\Phi_\lambda}{Q} \qquad <\phi>=\frac{\Phi_\phi}{Q} \quad (2)$$

were used at each grid point of the domain, so the velocity is dominated by those layers with high water vapor content.

An Atmospheric River analysis in terms of the FTLE was developed for 10 strong events over the North Atlantic Ocean. To that end, we compare the LCS extracted from the FTLE fields computed backward and forward for 5 days with the ridge extracted from the vertical integral of water vapor variable Eq. (1). We found that repelling LCS derived from the forward FTLE do not show any connection with the ARs. However, there is a strong correlation between the AR ridges and the attracting LCS and both present similar structures, Fig. 1. This opens interesting possibilities for the understanding of the general circulation of the atmosphere.

* vicente.perez@cesga.es

[1] P.J. Neiman, F.M. Ralph, G.A. Wick, J.D. Lundquist, and M.D. Dettinger, J. Hydrometeor **9**, 22–47 (2008).
[2] R.E. Newell, N.E. Newell, Y. Zhu, and C. Scott, Geophys. Res. Lett. **19**, 2401–2404 (1992).
[3] F.M. Ralph, P.J. Neiman, and G.A. Wick, Mon. Wea. Rev. **132**, 1721–1745 (2004).
[4] S.C. Shadden, F. Lekien, and J. Marsden, Physica D **212**, 271–304 (2005).
[5] F. Huhn, A. von Kameke, V. Pérez-Muñuzuri, M.J. Olascoaga, and F.J. Beron-Vera, Geophys. Res. Lett. **39**, L06602 (2012).

Electrocardiogram classification using Reservoir Computing

M. Escalona-Morán, M. C. Soriano, I. Fischer, C. R. Mirasso
IFISC, Instituto de Física Interdisciplinar y Sistemas Complejos
CSIC-Universidad de las Islas Baleares 07122-Palma (Mallorca)

An adapted state-of-the-art method of processing information known as Reservoir Computing (RC) is used to show its utility on the open and time consuming problem of heartbeat classification. RC mimics brain neural networks by processing information that generates patterns of transient neural activity as a response to a sensory signal[1] and is composed of layers for processing the information. It has been used for classification tasks, time series prediction and modeling[2,3]. We use a kind of reservoir consisting of a nonlinear dynamical element subject to delayed feedback. Nonlinear systems with delayed feedback and/or coupling, also known as delay systems, arise in a variety of real live contexts[4]. These systems can exhibit a wide range of dynamics ranging from stable operation to periodic oscillations and deterministic chaos[5]. At least three layers are needed for the classification task, an input layer to feed the information, the reservoir layer that transforms the input through the nonlinearity and an output layer collecting the results of the processing and adapting the classifier through the learning process. Our approach includes a minimum pre-processing consisting on expanding the dimmension of the input using a mask. The reservoir layer consists in a single node with a nonlinearity known as Mackey-Glass oscillator[6]. The model contains a delayed feedback term and has been extended to include an external input $I(t)$. Appeltant et al.[2] presented the extended model as:

$$\dot{X}(t) = -X(t) + \frac{\eta \cdot [X(t-\tau) + \gamma \cdot I(t)]}{1 + [X(t-\tau) + \gamma \cdot I(t)]^p}, \qquad (1)$$

with X denoting the dynamical variable, $\dot{X}$ being its derivative with respect to a dimensionless time t, and τ denoting the normalized delay in the feedback loop. Parameters η and γ represent feedback strength and input scaling, respectively. Without an external input ($\gamma = 0$) the system is chosen to operate in a stable fix point. However, under external inputs the system can exhibit complex dynamics. In particular, we are interested in a dynamical regime that produces consistent transient responses. The exponent p can be used to tune the nonlinearity. Although we have chosen the Mackey-Glass nonlinearity, it is expected that other nonlinear functions perform similarly well. For instance, a semiconductor laser has been used to perform similar tasks[3,7]. Finally, the learning process is a logistic regression method. The logistic regression (LR)[8] is a widely used learning technique in biostatistical applications in which binary responses occur quite frequently, in questions such as a condition is present or absent. LR uses logit transformation in order to give the probability that a input belongs to a particular class. We use the MIT-BIH Arrhythmia Database[9] available at Physionet which contains 48 ambulatory ECG recordings of half hour each, obtained from 47 subjects. The recordings were digitized at 360 samples per second with 11-bit resolution over a $10mV$ range. Two or more cardiologists independently annotated every heart beat in each record. We followed the guidelines of the Association for the Advancement of Medical Instrumentation (AAMI)[10] for the definition of classes and measures of performance. Comparing performance with other published results is a difficult task due to the different parameters and criteria used in this field. Our multiclass classification results indicate an average specificity of 92.24% with an average accuracy of 86.99% showing an improvement on previously reported results. Recall and precision show an average of 80.01% and 78.65%, respectively, what makes our approach significant for its use in a clinical context.

[1] M. Ravinovich, R. Huerta and G. Laurent. *Transient dynamics for neural processing*. Science 321, pp. 48-50 (2008).
[2] L. Appeltant, M. C. Soriano,G. Van der Sande, J. Danckaert, S. Massar, J. Dambre, B. Schrauwen, C. R. Mirasso, and I. Fischer. *Information processing using a single dynamical node as complex system*. Nat Comm 2, pp 468 (2011).
[3] K. Hicke, M. Escalona-Morán, D. Brunner,M. C. Soriano, I. Fischer, and C. R. Mirasso. *Information processing using transient dynamics of semiconductor lasers subject to delayed feedback*. IEEE J Sel Topics in Quan Electro, 19 pp. 4 (2013).
[4] T. Erneaux. *Applied delayed differential equations*. Springer Science and Busniess Media (2009).
[5] K. Ikeda and K. Matsumoto. *High-dimmensional chaotic behavior in systems with time-delayed feedback*. Physica D29, pp. 223-235 (1987).
[6] M. Mackey and L. Glass. *Oscillation and chaos in physiological control systems*. Science 197, pp. 287-289 (1977).
[7] D. Brunner, M. C. Soriano, C. R. Mirasso, and I. Fischer. *Parallel photonic information processing at gigabyte per second data rates using transient states*. Nat Comm 4, pp. 1364 (2013).
[8] Y. Pawitan. *In all likelihood: statistical modelling and inference using likelihood* Osford University Press (2001).
[9] R. G. Mark, P. S. Schluter, G. B. Moody, P. H. Devlin, D. Chernoff. *An annotated ECG database for evaluating arrhythmia detectors*. Front Eng Health Care, pp. 205-210 (1982).
[10] R. Mark and R. Wallen. *AAMI-recommended practice: Testing and reporting performance results of ventricular arrhythmia detection algorithm* Association for the advancement of medical instrumentation, Arrhythmia monitoring subcommittee AAMI ECAR (1987).

Firing-rate model for ensembles of quadratic integrate-and-fire neurons

Jose M. Esnaola, Alex Roxin†, Diego Pazó‡, Ernest Montbrió.
Departament de Tecnologies de la Informació i les Comunicacions
Universitat Pompeu Fabra 08003 Barcelona, Spain

When studying the collective dynamics of cortical neurons computationally, networks of large numbers of spiking neurons have naturally been the benchmark model. Network models incorporate the most fundamental physiological properties of neurons: sub-threshold voltage dynamics, spiking (via spike generation dynamics or a fixed threshold), and discontinuous synaptic interactions. For this reason, networks of spiking neurons are considered to be biologically realistic.

However, network models of spiking neurons are typically not amenable to analytical work, and thus constitute above all a computational tool. Rather, researchers use reduced or simplified models which describe some measure of the mean activity in a population of cells, oftentimes taken as the firing rate.

Firing-rate models are simple, phenomenological models of neuronal activity, generally in the form of continuous, first-order ordinary differential equations[1]. Such firing-rate models can be analyzed using standard techniques for differential equations, allowing one to understand the qualitative dependence of the dynamics on parameters.

Nonetheless, firing-rate models do not represent, in general, proper mathematical reductions of the original network dynamics but rather are heuristic. As such, there is in general no clear relationship between the parameters in the rate model and those in the full network of spiking neurons.

In this contribution we derive the firing rate description corresponding to a population of heterogeneous quadratic integrate-and-fire neurons (QIF).

An ensemble of i ($i = 1, \ldots, N$) recurrently coupled QIF writes:

$$\dot{v}_i = v_i^2 + I_{i,\text{ext}} + I_{i,\text{rec}}, \qquad (1)$$
$$\text{if } \; v = v_{\text{peak}}, \; \text{then } v \to v_{\text{reset}}$$

$$I_{i,\text{ext}} = \eta_i, \qquad (2)$$
$$I_{i,\text{rec}} = J_i r\left(t\right) - g_i r\left(t\right)\left(v_i - E\right). \qquad (3)$$

Here v_i is the deviation from the voltage at threshold. Additionally, $I_{i,\text{ext}}$ is an external current and $I_{i,\text{rec}}$ is a current due to recurrent connections. The parameters η_i, J_i and g_i are all quenched random variables. The mean field is

$$r\left(t\right) = \frac{1}{N}\sum_{i=1}^{N}\sum_{j}\delta\left(t - t_i^j\right), \qquad (4)$$

which corresponds to the sum over all N neurons.

The change of variable $v = \tan(\theta/2)$, allows to transform the QIF model into a phase model —the so-called θ-neuron model—, and to apply the recently discovered Ott-Antonsen[2,3] theory to this problem.

Using this technique, we are able to exactly reduce the ensemble of θ-neurons, to a system of two ordinary differential equations for two macroscopic variables. One of these variables is found to describe the center of the distribution of subthreshold voltages. In addition, the other variable describes the *firing rate* of the population, which corresponds to the width of the distribution of subthreshold voltages. These dynamical equations are then used to investigate the dynamics of the QIF model in full detail.

---

* fises12@gefenol.es
† Centre de Recerca Matemàtica (CRM), 08196 Bellatera, Spain
‡ Instituto de Física de Cantabria (CSIC-UC), Santander.

[1] H. R. Wilson, and J. D. Cowan, Biophys. J. **12**, 1 (1972).
[2] E. Ott and T. M. Antonsen, Chaos **18**, 037113 (2008)
[3] D. Pazó and E. Montbrió, *accepted in* Phys. Rev. X.

Reservoir Computing capabilities of Gene Regulatory Networks

Marçal Gabaldà-Sagarra, Jordi Garcia-Ojalvo*
Dynamical Systems Biology group, Department of Experimental and Health Sciences
Pompeu Fabra University (UPF), Barcelona

Single cells have the potential and the necessity to process the information they receive from their environment. The interaction of the elements of their regulatory networks allows them to integrate different inputs and, even more, process temporal information. The global logic that these networks follow to perform such calculations is not well known yet.

Our hypothesis is that regulatory networks are able to function as a Reservoir Computing (RC) system. RC is based on a central recurrent reservoir of hidden nodes, analogous to a Recurrent Neural Network (RNN), with fading memory. In contrast to standard RNN, however, the output nodes are placed one or more linear layers of nodes that read the state of the recurrent part of the network in a strictly feed-forward manner[2]. The recurrences in the network would enhance its computational potential in general, and specially allow the processing of temporal information. On the other hand, the specific RC architecture would facilitate the learning of new environmental conditioning. Since, only the connections between the reservoir and the output layer need to be trained to learn a new task, it is easier to change a given behaviour without modifying the comportment of the whole network. This is especially relevant when the training happens through an evolutionary process and thus the weights are changed randomly. All in all, the approach based on RC simplifies notably the training of the RNN and makes it more meaningful as a biological model.

We analyzed gene regulatory networks already available in the bibliography, and found that their topologies are perfectly compatible with a RC functionality. The nodes in the networks are organised in three groups: a recurrent group, a small number of nodes upstream of the recurrent part and finally a major group of nodes downstream of the recurrent structure, which follow a strictly feed-forward organisation.

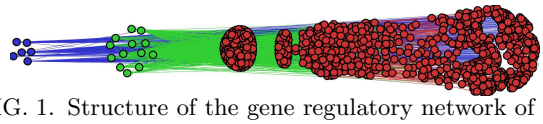

FIG. 1. Structure of the gene regulatory network of *Bacillus subtilis*. Green nodes form part of a recurrent structure or reservoir, while blue and red nodes form strictly feed-forward structures, upstream and downstream of the reservoir, respectively.

Further support of our hypothesis — i.e. that the regulatory networks adhere to a RC paradigm — was obtained confronting the systems to a prediction task. The dataset used in our prediction task benchmark was given by the *Nonlinear AutoRegressive Moving Average* (NARMA) function[1].

In general, modelling this system is difficult, due to the nonlinearity and potentially long memory.

The topologies of the recurrent parts of the of the gene regulatory networks analysed proved to be able to perform calculations comparable to other topologies that are known to perform well in RC, for a similar number of nodes.

Presumably, the differences in performance between the tested networks would be explained by the different number of nodes and cycles. A larger recurrent network would have more complex transient dynamics and a longer fading memory[2].

On the other hand, the dynamics of a gene acting as node are not as simple. In the first place, it can be activated to any degree of a continuous range of levels of expression between zero and an asymptotic maximum. Additionally, the biological processes that underlie expression —from the start of the transcription to the end of the translation— will introduce a delay in the activation of the nodes. These more complex dynamics of the genes can change the temporal dynamics of the reservoir, for example making its fading memory last longer. On top of that, it is important to note that the processing tasks of a biological network are remarkably different in nature and intensity to those addressed by non-standard computations in machine learning. Furthermore, in the former case results do not need to be as stably precise as in the latter.

These results suggest that the regulatory network core may be able to generate transient dynamics that encode the information obtained in the recent past from multiple inputs. Furthermore, plenty of nodes found downstream of the recurrent core, wich would function as output nodes, are reported to be involved in processes that are observable and meaningful as a learning layer of a RC. Some examples of those processes are biofilm formation, flagellum synthesis, protection against oxidative stresses, growth rate control, etc.

* jordi.g.ojalvo@upf.edu

[1] Atiya, A. F. & Parlos, A. G. (2000) IEEE Trans Neural Networks 11(3), 697-709
[2] Buonomano, D. V. & Maass, W. (2009) Nat Rev Neurosci 10(2), 113-25

A novel focus on population dynamics under mutualistic interactions

Javier García-Algarra, Javier Galeano, Juan Manuel Pastor, José María Iriondo[†], and José J. Ramasco[‡]
Complex System Group, Universidad Politécnica de Madrid, 20040 Madrid, Spain

Mutualistic interactions, which are beneficial for all the species involved, have an internal structure that makes them resilient to external perturbations. Actually, the relations between plants and their pollinators and seed dispersers are paradigmatic examples of mutualism. In this context, Ehrlich and Raven[1] alluded to the importance of plant-animal interactions in the generation of Earth's biodiversity. The simplest mutualistic model was proposed by May[2]. Each of May's equations for two species is a logistic model with an extra term accounting for the mutualistic benefit. It is the same idea as in the Lotka-Volterra model but interactions between species always add to the resulting population. May's equations for two species can be written as

$$\frac{dN_1}{dt} = r_1 N_1 \left(1 - \frac{N_1}{K_1}\right) + r_1 N_1 \beta_{12} \frac{N_2}{K_1}, \tag{1}$$

$$\frac{dN_2}{dt} = r_2 N_2 \left(1 - \frac{N_2}{K_2}\right) + r_2 N_2 \beta_{21} \frac{N_1}{K_2} \tag{2}$$

where $N_1\,(N_2)$ is the population of the species $1\,(2)$; $r_1\,(r_2)$ is the intrinsic growth rate of population $1\,(2)$ and $K_1\,(K_2)$ the carrying capacity. This is the maximum population that the environment can sustain indefinitely, given food, habitat, water and other supplies available in the environment. Finally, β_{12} is the coefficient that embodies the benefit for N_1 of each interaction with N_2. May's model major drawback is that it may lead to unbounded growth, but anyway it has been an inspiration for subsequent mutualistic models that incorporate terms to solve this problem.

In this work, we introduce a model for population dynamics under mutualism that preserves the original logistic formulation. It is mathematically simpler than the widely used type II models, although it shows similar complexity in terms of fixed points and stability of the dynamics. We perform an analytical stability analysis and numerical simulations to study the model behavior in more general interaction scenarios including tests of the resilience of its dynamics under external perturbations. Despite its simplicity, our results indicate that the model dynamics shows an important richness that can be used to gain further insights in the dynamics of mutualistic communities.

Our hypothesis is that mutualism is just another element that contributes to the species growth rate, that means r is a function of mutualism and not a third term added to the logistic equation. We choose a linear approach:

$$r_i^{new} = r_i^a + \sum_{k=1}^{n_p} b_{ki}^{pa} N_k^p \tag{3}$$

where the superscript p stands for *plants* and a for *animals*. Following this reasoning, the friction α must also take mutualism into account to avoid an unreallistic infinite benefit. To simplify the model, we assume that the effect is proportional to the benefit.

$$\alpha_i^{new} = \alpha_i^a + c_i^a \sum_{k=1}^{n_p} b_{ki}^{pa} N_k^p \tag{4}$$

Under these assumptions the system is described by this set of differential equations for n_p species of plants and n_a of animals:

$$\frac{1}{N_j^p}\frac{dN_j^p}{dt} = r_j^p + \sum_{l=1}^{n_a} b_{lj}^{ap} N_l^a - \left(\alpha_j^p + c_j^p \sum_{l=1}^{n_a} b_{lj}^{ap} N_l^a\right) N_j^p \tag{5}$$

The right term can be interpreted as an *effective growth rate*.

$$r_{eff_j}^p = r_j^p + \sum_{l=1}^{n_a} b_{lj}^{ap} N_l^a - \left(\alpha_j^p + c_j^p \sum_{l=1}^{n_a} b_{lj}^{ap} N_l^a\right) N_j^p \tag{6}$$

$$\frac{dN_j^p}{dt} = r_{eff_j}^p N_j^p \tag{7}$$

The *carrying capacities* are fixed points of system. It is easy to deduce that without mutualism K is the constant r/α. Under the presence of hypothetical infinite mutualism would be $1/c_i^a$. So, the coefficient we included in (4) is the inverse of the maximum population of the species i when the number of mutualistic individuals is so high that $c_i \sum_{k=1}^{m} b_{ki} N_k >> \alpha_i$.

Finally, we perform an analytical stability analysis and numerical simulations to study the model behavior in more general interaction scenarios including tests of the resilience of its dynamics under external perturbations. Despite its simplicity, our results indicate that the model dynamics shows an important richness that can be used to gain further insights in the dynamics of mutualistic communities[3]

[†] Área de Biodiversidad y Conservación, Dept. Biología y Geología, Universidad Rey Juan Carlos, 28933 Móstoles, Spain.
[‡] Instituto de Física Interdisciplinar y Sistemas Complejos IFISC (CSIC-UIB), Campus UIB, 07122 Palma de Mallorca, Spain

[1] Ehrlich, P., Raven, P., 1964. Evolution 18, 586–608.
[2] May, R., 1981. Models for two interacting populations. in theoretical ecology. Principles and applications. 2nd edn.(ed. rm may.) pp. 78–104.
[3] J. Garcia-Algarra, J. Galeano, J. M. Pastor, J. M. Iriondo, J. J. Ramasco, 2013, arXiv:1305.5411

Development of eco-friendly advanced energy absorbing composites

Francisco J. Galindo-Rosales*
FEUP, Faculdade de Engenharia da Universidade do Porto, 4200-465 Porto (Portugal)

The absorption of energy during impacts is ubiquitous in our society and there is an increasing need for advanced energy absorbing materials, especially for human protection applications. The development of advanced energy absorbing composites is an issue that has many engineering challenges. In the last decade Shear Thickening Fluids (STF's) have attracted the attention of the industry for the fabrication of passive dissipative devices, due to their viscosity increase with the applied shear stress over a critical value. Moreover, the increase in the viscosity can be tailored for the specific application by choosing properly the components of the STF[1]. All this has led to a considerable interest in incorporating STF's into other materials, like rubbers and foams (flexible porous media in general) in order to obtain energy absorbing composites possessing a combination of their best properties/characteristics[2]. The nature of the STF's can be colorful, but discontinuous STF's are particularly interesting for this work, since they transform into a material with solid-like properties at high shear rates[3]. Stabilized suspensions of cornstarch with a high loading fraction of particles are a typical example of a discontinuous and eco-friendly STF.
One of the major concerns when trying to create an effective energy-absorbing composite with these fluids is the interaction between the fluid and the geometry which confines it, as the rheological response of STF's is greatly affected by the deformation rates at which it is undergone. For these reasons, the early composites for energy absorption systems based on STF's have used porous media as scaffold, where the tortuosity of the micro-paths subjects the STF to a complex flow under confinement[4]. Thus, the addition of STF's to the porous media increases their energy absorption capabilities, due to the contribution of the viscous work done by expelling the fluid from inside the cells of the porous medium, which is added to the energy dissipated due to the elastic, plastic, and buckling modes that occur during compression. However, filled porous media by STF's bring some operational drawbacks: the filling process is not straightforward; the shape of the flow paths inside the porous media is unknown and, subsequently, it is impossible to predict the response of the composite a priori; the sealing of the filled porous media is an additional problem; by replacing the air inside the porous medium by the STF, the resulting composite is not going to be light weight anymore; etc.

An alternative way of developing energy absorbing composites able to maximize the energy dissipated under impact would be based on the combination of the mechanical properties of natural cork, shear thickening behavior of stabilized suspensions of cornstarch and microfluidics. The novelty consists of engraving a network of microchannels on a sheet of micro-agglomerated cork, filling them with a discontinuous STF and closing it with another sheet of micro-agglomerated cork. When subjected to an impact, the energy will be absorbed and dissipated by the combined effect of the elasticity of the cork and the enhanced viscous/normal forces of the STF flowing under confinement through the microchannels. So the question we want to address with this work is the following one: How can we relate the viscosity curve of a STF with the mechanical properties of the natural cork and the pattern of a network of microchannels in order to create customized composites able to maximize the dissipation of energy under impact for any application? As depicted in Fig.1, the answer will require combining experimental, theoretical and computational approaches.

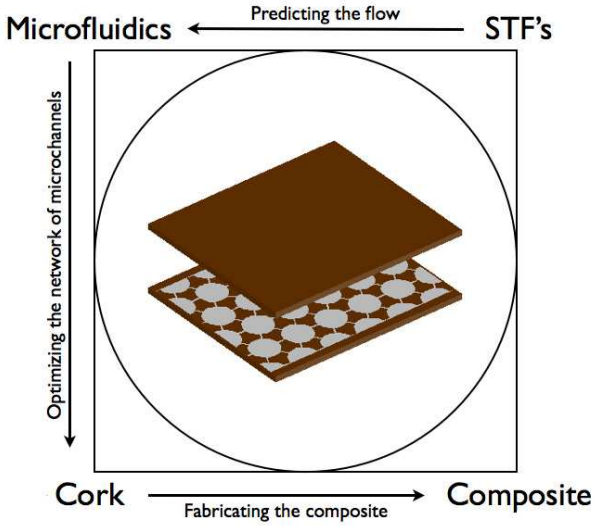

FIG. 1. Development of eco-friendly advanced energy absorbing composites: Flow chart.

Author would like to acknowledge funding from Fundação para a Ciência e a Tecnologia (FCT), COMPETE, QREN and European Union (FEDER) through FCT Investigator grant IF/00190/2013.

* galindo@fe.up.pt

[1] H.A. Barnes. J. Rheol., 33 (1998).
[2] N.J. Wagner et al. (2010) Patent Application No. US2010/0221521A1.
[3] E. Brown et al.. Nature Mater., 9 (2010).
[4] M.A. Dawson. Int. J. Impact Eng., 36 (2009)

Thermal capillary waves in colloid-polymer mixtures - static and dynamic correlation functions

Lia Verhoeff[a], Francisco J. Galindo-Rosales[b], Laura Campo-Deaño[b], Roel Dullens[a], and Dirk Aarts[a*]
[a] Physical and Theoretical Chemistry Laboratory, University of Oxford, Oxford OX1 3QZ (United Kingdom)
[b] FEUP, Faculdade de Engenharia da Universidade do Porto, 4200-465 Porto (Portugal)

At rest, the free interface between any two fluids appears to be smooth. However, due to the thermal energy k_BT, all fluid interfaces are corrugated and these fluctuations are suppressed by the interfacial tension (γ) and gravity. This leads to a mean square amplitude h_q of each Fourier mode q: $\left\langle |h_q|^2 \right\rangle = \frac{k_BT/L^2}{\gamma\left(q^2+L_c^{-2}\right)}$, with L the system size and L_c the capillary length. Furthermore, each mode is damped exponentially with a decay rate of $\omega_q = \left(qL_c + \frac{1}{qL_c}\right)\gamma/\left(2\eta L_c\right)$, where η is the sum of the viscosities of the two fluid phases.

The interface fluctuations can be observed experimentally in phase separated colloid-polymer mixtures by means of laser scanning confocal microscopy. This allows us to construct real space height-height correlation functions, either statically or dynamically, from a 1D cut through our 2D interface. From the theoretical expressions in Fourier space it is possible to obtain the theoretical correlation functions: the static correlation $g_h(x) = \langle h(x',t')\,h(x'+x,t')\rangle = \frac{k_BT}{2\pi\gamma}K_0(x/L_c)$ and the dynamic correlation $g_h(t) = \langle h(x',t')\,h(x',t'+t)\rangle = \frac{k_BT}{2\pi\gamma}K_0(t/\tau)$, with K_0 the modified Bessel function of the second kind and the capillary time $\tau = \frac{\eta L_c}{\gamma}$. With these expressions it is possible to fit the experimentally constructed correlation functions very well, using the interfacial tension and the capillary length or the capillary time as fit parameters.[1]

However, recent experiments have shown that for the capillary waves in aqueous PMMA-Xanthan mixtures there is a discrepancy between the interfacial tension obtained from the static and dynamic correlation functions. The value obtained from the dynamic correlation function is consistently higher than the one from the static correlation function (factor of ~ 1.75).[2,3] Therefore, the aim of this work is to find out the reason behind this discrepancy.

Firstly, we considered the influence of the rheological properties of the fluid phases on the interface dynamics. Especially the colloidal gas phase exhibits strong shear thinning behaviour, which we tried to incorporate by using a decay rate dependent viscosity in the derivation of the dynamic correlation function.

Another point we will discuss is the fact that both colloid and polymer are relatively large (with a hydrodynamic radius $R_h = 112$ nm and a radius of gyration $R_g = 222$ nm respectively) and therefore also relatively slowly diffusing. We took this into account by adding a diffusion term (Dq^2) to the decay of each wave mode.

Finally, we investigated whether the equilibration time that is needed to reach the mean-field depletion attraction force[4] could possibly interfere with the interface dynamics. This equilibration time strongly depends on the colloid-polymer size ratio, so we studied the capillary waves in mixtures with twice as large PMMA particles.

Authors would like to acknowledge funding from FCT, COMPETE, QREN and European Union (FEDER) through FCT Investigator grants IF/00148/2013 and IF/00190/2013. The research leading to these results has received funding from the People Programme (Marie Curie Actions) of the European Union's Seventh Framework Programme (FP7/2007-2013) under REA grant agreement n° 302798.

* dirk.aarts@chem.ox.ac.uk

[1] D.G.A.L. Aarts, M. Schmidt, H.N.W. Lekkerkerker, Science 304, 5672 (2004)
[2] E.A.G. Jamie, G.J. Davies, M.D. Howe, R.P.A. Dullens, D.G.A.L. Aarts, J. Phys.: Condens. Matter 20, 494231 (2008)
[3] E.A.G. Jamie, H.H. Wensink and D.G.A.L. Aarts, J. Stat. Mech. P11008 (2010)
[4] G.A. Vliegenthart and P. van der Schoot, Europhys. Lett. 62 (4), 600 (2003)

Sincronización y predicción por conjuntos con un modelo atmosférico de juguete

Rafael Gallego*, Diego Pazó† y Juan M. López†
Departamento de Matemáticas
Universidad de Oviedo 33203-Gijón

La predicción por conjuntos[1] (*'ensemble forecasing'*) es una técnica de uso habitual y operativo en la predicción de la atmósfera (y otros fluidos geofísicos como el océano). En esta técnica, en vez de usar una realización del modelo para predecir, se integran varias copias del modelo con distintas condiciones iniciales con la ventaja de que la media del conjunto es un buen predictor. Existen varias técnicas para generar los miembros del conjunto. En esta comunicación proponemos un acoplo como los usados en sincronización como método para generar los miembros del conjunto. Este procedimiento está inspirado por el 'nudging'[1], una técnica clásica de 'asimilación de datos'. En esta técnica un modelo (imperfecto) es acoplado con la realidad mediante las observaciones, es decir en una configuración llamada maestro-esclavo (o emisor-receptor). Con objeto de generar un *ensemble* acoplamos varias copias del modelo con la realidad. Las perturbaciones resultantes son usadas para realizar predicción por conjuntos.

En esta comunicación nos centramos en estudiar el efecto de tener un modelo que carece de grados de libertad rápidos presentes en la realidad (en analogía con la turbulencia de pequeña escala). Para la realidad tomamos el modelo de juguete de la atmósfera con *dos* capas propuesto por Lorenz[2] en 1996. El sistema consta de K variables lentas X_i cada una de ellas acoplada a J variables rápidas $Y_{j,i}$. Los dos grupos de variables X e Y forman sendos anillos y satisfacen las siguientes ecuaciones:

$$\frac{dX_i}{dt} = X_{i-1}(X_{i+1} - X_{i-2}) - X_i + F - \frac{hc}{b}\sum_{j=1}^{J} Y_{j,i},$$

$$\frac{dY_{j,i}}{dt} = cbY_{j+1,i}(Y_{j-1,i} - Y_{j+2,i}) - cY_{j,i} + \frac{hc}{b}X_i,$$

donde $i = 1, \ldots, K$, $j = 1, \ldots, J$. El parámetro h es la constante de acoplamiento entre las variables rápidas y las lentas, b y c son constantes de escala y F simula un forzamiento (solar) constante. Los parámetros se eligen de tal forma que el sistema se encuentre en un régimen de caos espacio-temporal.

Como modelo (imperfecto) consideramos un sistema de Lorenz '96 de *una* escala acoplado a la realidad

$$\frac{dZ_i}{dt} = Z_{i-1}(Z_{i+1} - Z_{i-2}) - Z_i + F_m + \kappa(X_i - Z_i),$$

en el que κ es la constante de acoplamiento entre modelo y realidad, y el forzamiento F_m es una constante que reproduce el forzamiento promedio efectivo:

$$F_m = F - \frac{hc}{b}\left\langle \sum_{j=1}^{J} Y_{j,i} \right\rangle_t ,$$

donde $\langle\cdot\rangle_t$ denota un promedio temporal.

La disimilitud entre la realidad y el modelo (para $h \neq 0$) hace que no se pueda alcanzar la sincronización perfecta ($X_i = Z_i$) para ningún valor de κ. A medida que κ aumenta X_i y Z_i convergen pero, a efectos de construir un *ensemble*, no es deseable tomar un κ demasiado grande por dos razones:

(i) La estructura espacial de los errores $\delta Z_i = Z_i - X_i$ deja de reflejar las direcciones más inestables del flujo.

(ii) Al usar un conjunto de modelos $\{Z_i^{(n)}\}_{n=1,\ldots,N}$ estos tienden a converger (como en la 'sincronización generalizada') y se pierde diversidad, lo que no es adecuado para inicializar una predicción por conjuntos.

Para determinar el acoplamiento óptimo κ_{op} medimos dos cantidades: (i) La correlación espacial W que informa la consistencia de las perturbaciones con las inestabilidades del flujo[3]; y (ii) La dimensión de ensemble D_{en} que informa del número de dimensiones efectivas que cubren los N miembros del conjunto. Finalmente comprobamos como un compromiso entre las optimizaciones de W^2 y D_{en} conduce a la mejora de la predicción considerando un conjunto se condiciones iniciales perturbadas según las direcciones definidas por los miembros del *ensemble*.

* rgallego@uniovi.es
† Instituto de Física de Cantabria (CSIC-UC), Santander.

[1] E. Kalnay, *Atmospheric Modeling, Data Assimilation and Predictability* (Cambridge University Press, Cambridge, 2003).
[2] E. N. Lorenz. Predictability, a problem partially solved. In *Proceedings of ECMWF seminar on Predictability*, pp. 1 − 19, (ECMWF, Reading, 1996).
[3] I. G. Szendro, M. A. Rodríguez y J. M. López. J. Geophys. Res. **114**, D20109 (2009).

Hydrodynamics in a driven homogeneous granular gas

María Isabel García de Soria*, Pablo Maynar, and Emmanuel Trizac
Física Teórica, Universidad de Sevilla, Apartado de Correos 1065, E-41080, Sevilla, Spain

We study the dynamics of a homogeneous granular gas heated by a stochastic thermostat, in the low density limit. It is found that, before reaching the stationary regime, the system quickly "forgets" the initial condition and then evolves through a universal state that does not only depend on the dimensionless velocity, but also on the instantaneous temperature, suitably renormalized by its steady state value. The existence of this state is exploited to derive hydrodynamic equations, obtaining explicit expressions for the transport coefficients which depend explicitely on the structure of the universal state. We find excellent agreement between the theoretical predictions and numerical simulattions[1,2].

---

* gsoria@us.es

[1] M. I. García de Soria, P. Maynar, and E. Trizac, Phys. Rev. E **85**, 051301 (2012)
[2] M. I. García de Soria, P. Maynar, and E. Trizac, Phys. Rev. E **87**, 022201 (2013)

FIS.es : *F*aster *I*s *S*lower, con *es*tudiantes

A. Garcimartín*, I. Zuriguel, J.M. Pastor, C. Martín-Gómez†, L.M. Ferrer‡, J.J. Ramos‡.
Depto. de Física y Matemática Aplicada, Facultad de Ciencias, Universidad de Navarra, 31080 Pamplona.

Un flujo de partículas discretas disipativas no sigue las leyes habituales de la mecánica de fluidos. Un caso concreto es el paso a través de un estrangulamiento: más presión puede provocar menor velocidad de salida, porque las partículas se atascan más[1].

Cuando eso tiene lugar en la materia activa (sean bacterias, animales, partículas autopropulsadas, personas, etc.) el fenómeno se denomina ***Faster Is Slower* (FIS)**, es decir: más rápido es más lento. Empujar para salir más pronto hace que se tarde más en salir.

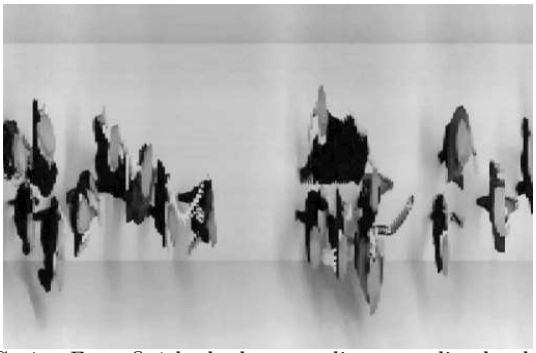

FIG. 1. *Foto finish* de los estudiantes saliendo de una puerta (se muestra sólo una porción). La puerta está a la izquierda de la imagen

Que esto es así se sospechaba desde hace tiempo, pues se había comprobado en simulaciones numéricas y en observaciones fortuitas. Aquí presentamos experimentos controlados en los que por primera vez se observa FIS: en un caso, con un rebaño de ovejas, y en otro caso, con un grupo de estudiantes.

El procedimiento consiste en medir la diferencia temporal entre individuos consecutivos, Δt. Para ello, mediante una técnica conocida, se obtiene la *foto finish* del paso por una puerta de un grupo de estudiantes voluntarios (Fig. 1). El experimento se realizó repetidas veces, y se obtuvo la función de distribución de probabilidad de Δt. El aspecto clave es la cola potencial que presenta esta distribución: $P(t) \propto t^{-\alpha}$. El exponente α se obtiene con más precisión del histograma acumulado (Fig. 2). El valor de esta pendiente, además, da una idea del peligro de atasco: si $\alpha < 2$ la media de la distribución no converge y cabe el peligro de que se produzcan catástrofes (atascos muy largos, sucesos extremos) en la evacuación.

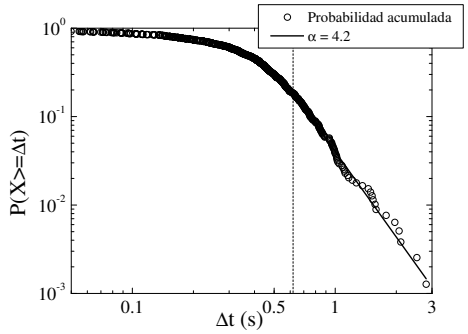

FIG. 2. Histograma acumulado de los intervalos temporales entre individuos consecutivos, Δt, en escala logarítmica. La cola potencial se ha ajustado para obtener la pendiente, que en este caso es $\alpha = 4.2$.

Agradecemos a la Mutua Montañesa y al PIUNA (Universidad de Navarra) la financiación que nos ha permitido llevar a cabo este proyecto.

---

* angel@unav.es
† Sección de Instalaciones y Energía, Escuela de Arquitectura, Universidad de Navarra, 31080 Pamplona
‡ Dpto. de Patología Animal, Facultad de Veterinaria, Universidad de Zaragoza, c/ Miguel Servet 177, 50013 Zaragoza.

[1] D. Helbing, I. Farkas and T. Vicsek, Nature **407**, 487 (2000).

Phase diagrams of Janus particles with fixed orientations

Miguel Ángel G. Maestre* and Andrés Santos**
Departamento de Física, Universidad de Extremadura, E-06071 Badajoz, Spain

A Janus fluid generally refers to a system composed of particles divided into two hemispheres, each hemisphere-hemisphere interaction being described by a different potential. The study of this class of systems has become quite relevant due to its close relation with the hydrophobic-hydrophillic behavior shown by certain colloidal systems. A simple characterization of the general Janus model with the the potential being defined as attractive in one hemisphere and non-attractive in the other hemisphere may be used to study such systems. Additionally, if the orientation of the hemispheres is constrained to two possibilities (up or down), the system becomes a binary mixture of particles of species 1 (active hemisphere pointing up) and species 2 (active hemisphere pointing down). This is sketched in Fig. 1.

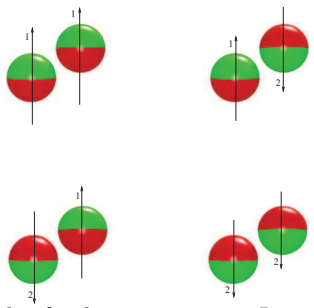

FIG. 1. Sketch of a binary-mixture Janus fluid with up–down constrained orientations.

We define the hemisphere-hemisphere interactions to be of square-well (SW) type. More explicitly, if a particle of species i is "below" a particle of species j (so that the top hemisphere of i interacts with the bottom hemisphere of j), the interaction potential is

$$\varphi_{ij}(r) = \begin{cases} \infty, & 0 \le r < \sigma, \\ -\epsilon_{ij}, & \sigma \le r < \sigma + \Delta, \\ 0, & \sigma + \Delta \le r, \end{cases} \tag{1}$$

where σ is the hard-sphere (HS) diameter, Δ is the width of the attractive well, and ϵ_{ij} is the depth of the well. By symmetry, one must have $\epsilon_{22} = \epsilon_{11}$ (see Fig. 1), so that (for given values of σ and Δ) the space parameter of the interaction potential becomes three-dimensional, as displayed in Fig. 2. We call $\epsilon = \max_{i,j}\{\epsilon_{ij}\}$ and use the three independent ratios ϵ_{ij}/ϵ as axes in Fig. 2. Next, without loss of generality, we choose $\epsilon_{12} \ge \epsilon_{21}$. With those criteria, all possible models of the class lie either inside the triangle SW-I0-B0-SW or inside the square SW-B0-A0-J0-SW.[1]

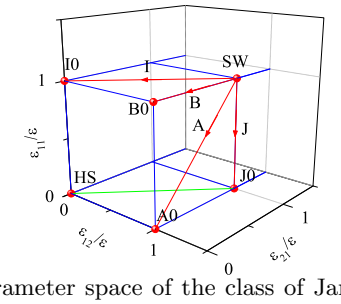

FIG. 2. Parameter space of the class of Janus models defined by Eq. (1).

This novel class of binary-mixture Janus fluids with up-down constrained orientations encompasses, as particular cases, the conventional one-component SW fluid, mixtures with isotropic attractive interactions only between like particles (model I0) or unlike particles (model J0), and genuine Janus fluids with anisotropic interactions and different patch-patch affinities (models A0 and B0).

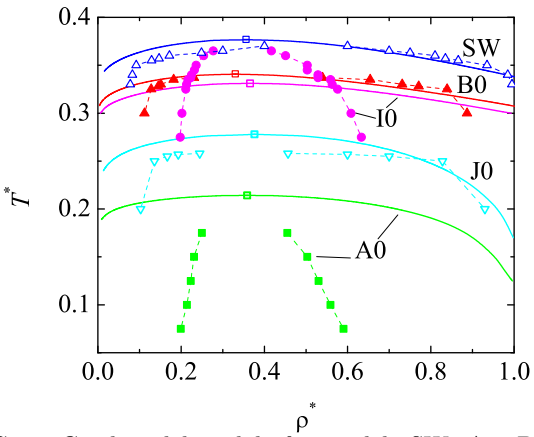

FIG. 3. Gas-liquid binodals for models SW, A0, B0, I0, and J0, as obtained from our theoretical method (solid lines) and from GEMC simulations (symbols).

In this work we focus on models SW, I0, J0, A0, and B0, and make and systematic study of the properties of the gas-liquid binodal (see Fig. 3) both from simple theoretical approaches[1,2] and from simulation results[1] obtained by means of the Gibbs ensemble Monte Carlo (GEMC) method.[3]

* maestre@unex.es
** andres@unex.es

[1] R. Fantoni, A. Giacometti, M. A. G. Maestre, and A. Santos, J. Chem. Phys. **139**, 174902 (2013).
[2] M. A. G. Maestre, A. Santos, R. Fantoni and A. Giacometti, J. Chem. Phys. **138**, 094904 (2013).
[3] A. Z. Panagiotopoulos, Mol. Phys. **61**, 813 (1987).

Liquid-crystal patterns of rectangular particles in a square nanocavity

M. González Pinto[1]*, Y. Martínez-Ratón[2] and E. Velasco[1]
[1] *Departamento de Física Teórica de la Materia Condensada, Universidad Autónoma de Madrid, 28049 Madrid*
[2] *Grupo Interdisciplinar de Sistemas Complejos (GISC), Departamento de Matemáticas, Universidad Carlos III de Madrid, 28911 Leganés, Madrid*

Using density-functional theory in the restricted-orientation approximation, we analyse[1] the liquid-crystal patterns and phase behaviour of a fluid of hard rectangular particles confined in a two-dimensional square nanocavity of side length H composed of hard inner walls. Patterning in the cavity is governed by surface-induced order, capillary and frustration effects, and depends on the relative values of particle aspect ratio $\kappa \equiv L/\sigma$, with L the length and σ the width of the rectangles ($L \geq \sigma$), and cavity size H. Ordering may be very different from bulk ($H \to \infty$) behaviour when H is a few times the particle length L (nanocavity). Bulk and confinement properties are obtained for the cases $\kappa = 1$, 3 and 6. In bulk the isotropic phase is always stable at low packing fractions $\eta = L\sigma\rho_0$ (with ρ_0 the average density), and nematic, smectic, columnar and crystal phases can be stabilised at higher η depending on κ: for increasing η the sequence isotropic $\to$ columnar is obtained for $\kappa = 1$ and 3, whereas for $\kappa = 6$ we obtain isotropic $\to$ nematic $\to$ smectic (the crystal being unstable in all three cases for the density range explored). In the confined fluid surface-induced frustration leads to four-fold symmetry breaking in all phases (which become two-fold symmetric). Since no director distorsion can arise in our model by construction, frustration in the director orientation is relaxed by the creation of domain walls (where the director changes by 90°); this configuration is necessary to stabilise periodic phases. For $\kappa = 1$ the crystal becomes stable with commensuration transitions taking place as H is varied. These transitions involve structures with different number of peaks in the local density. In the case $\kappa = 3$ the commensuration transitions involve columnar phases with different number of columns. Finally, in the case $\kappa = 6$, the high-density region of the phase diagram is dominated by commensuration transitions between smectic structures; at lower densities there is a symmetry-breaking isotropic $\to$ nematic transition exhibiting non-monotonic behaviour with cavity size. Apart from the present application in a confinement setup, our model could be used to explore the bulk region near close packing in order to elucidate the possible existence of disordered phases at close packing.

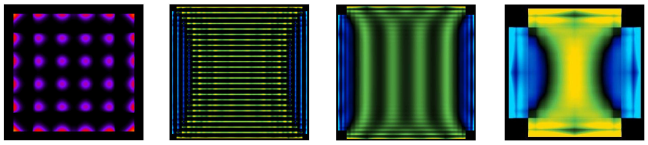

FIG. 1. Equilibrium density profiles for different conditions of rod aspect ratio, chemical potential and cavity size. From left to right they are shown crystal, columnar, smectic and nematic phases respectively. Yellow/green colors represent particles with their director paralell to x-axis and blue color means particles paralell to y-axis. The crystal phase is different because it comes from a system with aspect ratio 1 (squares) so color only represents density value.

* miguel.gonzalezp@uam.es

[1] M. González-Pinto, Y. Martínez-Ratón and E. Velasco, *Phys. Rev. E* 88 032506 (2013)

Networks of fluid transport in the ocean

Enrico Ser-Giacomi, Emilio Hernández-García*, Cristóbal López and Vincent Rossi
IFISC†, Instituto de Física Interdisciplinar y Sistemas Complejos
CSIC-Universitat de les Illes Balears
07122-Palma de Mallorca

The transport of particles or substances in fluids is a fundamental process of relevance in contexts ranging from cell biology to geophysics. In this last setting, the transport of nutrients or heat in the oceans or of pollutants and humidity in the atmosphere determine most of the biogeochemical cycles in the Earth and the related climatic phenomena.

We have analyzed transport phenomena in the ocean by using techniques from modern *network theory*. The aim is to search for connectivity patterns between sources and receptors determined by the ocean currents, and to use the power of the new techniques, for example regarding community detection, to assess questions about mixing, transport barriers, coherent regions, etc.

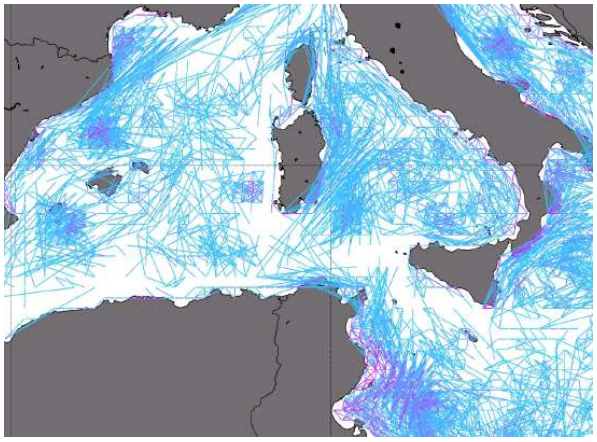

FIG. 1. A part of a weighted Lagrangian network obtained by particle advection in the Mediterranean during one month.

We have first applied this methodology to surface currents in the Mediterranean Sea obtained from a realistic ocean circulation model (NEMO[1]) with a spatial resolution of about 1/16 degrees. We simulate then the motion in this velocity field of more than 1,000,000 ideal fluid particles following their trajectories. After this first step we discretize the sea domain and construct a transport matrix that describes the strenght of transport between ideal cells in which the sea is divided. By interpreting this transport matrix as the connectivity matrix of a weighted and directed graph –the *Lagrangian Network*– we can use graph theory techniques to characterize the transport and connectivity patterns[2].

Figure 1 shows an example of Lagrangian network obtained in this way. Figure 2 shows the communities identified by the Infomap algorithm[3] in such network. The communities are interpreted as regions that remain relatively coherent after the integration time, and the boundaries between them act as barriers to transport.

Application of these ideas to larval transport in the sea and its role in the design of marine reserves will be also discussed[4].

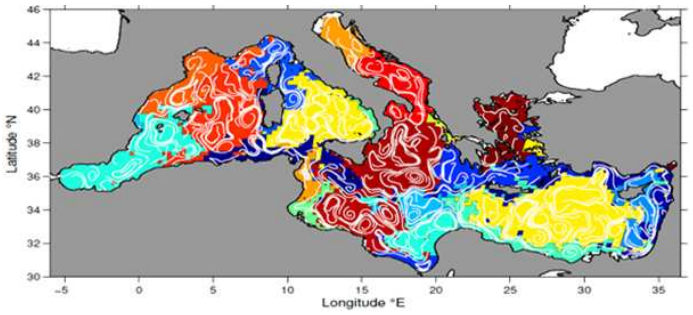

FIG. 2. Communities identified in the 1-month Lagrangian network of the Mediterranean by the *infomap* algorithm. White lines are average streamlines.

* emilio@ifisc.uib-csic.es
† http://ifisc.uib-csic.es

[1] P. Oddo, M. Adani, N. Pinardi, C. Fratianni, M. Tonani, D. Pettenuzzo, *A nested Atlantic-Mediterranean sea general circulation model for operational forecasting*, Ocean Sci. **5**, 461 (2009).
[2] E. Ser-Giacomi, E. Hernández-García, C. López and V. Rossi, in preparation (2014).
[3] M. Rosvall, M., C.T. Bergstrom, *Maps of random walks on complex networks reveal community structure*, P. Natl. Acad. Sci. USA **105**, 1118–1123 (2008).
[4] V. Rossi, E. Ser-Giacomi, C. López, E. Hernández-García, *Hydrodynamic provinces and oceanic connectivity from a transport network help designing marine reserves*, http://ifisc.uib-csic.es/publications/publication-detail.php?indice=2463, submitted (2013).

Efecto del tamaño molecular y la flexibilidad de cadenas moleculares sobre las propiedades interfaciales líquido-vapor

Felipe J. Blas*[1,2], A. Ignacio Moreno-Ventas Bravo[2,3], Jesús Algaba[1,2], Francisco José Martínez-Ruiz[1,2], Luis G. MacDowell[4], José Manuel Míguez[5] y Manuel M. Piñeiro[5]

[1] *Departamento de Física Aplicada, Facultad de Ciencias Experimentales, Universidad de Huelva, 21071 Huelva*
[2] *Centro de Investigación de Física Teórica y Matemática, Universidad de Huelva, 21071 Huelva*
[3] *Departamento de Geología, Facultad de Ciencias Experimentales, Universidad de Huelva, 21071 Huelva*
[4] *Departamento de Química-Física, Facultad de Ciencias Químicas, Universidad Complutense, 28040 Madrid*
[5] *Departamento de Física Aplicada, Facultade de Ciencias, Universidade de Vigo, 36310 Vigo*

La naturaleza de las interacciones molecular que ocurren en las interfases es clave desde el punto de vista teórico: el conocimiento de como el tamaño molecular, las interacciones dispersivas y otros tipos de fuerzas intermolecular, intramoleculares e interacciones específicas, como fuerzas debidas a enlaces de hidrógeno, la arquitectura molecular y la flexibilidad, entre otras, afecta a las propiedades interfaciales (incluyendo propiedades termodinámicas y estructurales) es esencial para comprender el delicado equilibrio entre contribuciones superficiales y *bulk* a la energía libre del sistema[1]. En particular, los sistemas formados por cadenas moleculares han atraído la atención de la comunidad del estado líquido, no sólo debido a interés teórico en sí en la predicción de sus propiedades termodinámicas y estructurales, sino también debido a la enorme importancia industrial que estos sistemas posee en el campo del modelado a nivel molecular.

Durante la última década se ha producido un intenso y cada vez mayor desarrollo de nuevos y mejorados métodos de simulación (particularmente de tipo Monte Carlo) para determinar las propiedades interfaciales de todo tipos sistemas, incluyendo sistemas complejos como cadenas moleculares. En particular, se ha prestado especial atención en el desarrollo de nuevos métodos para la determinación de la tensión interfacial fluido-fluido.

El método del virial o ruta mecánica[1] ha sido la técnica tradicional empleada para la determinación de la tensión interfacial fluido-fluido, y de hecho, hoy en día sigue siendo considerada la metodología estńdar utilizada por un gran número de simuladores en todo el mundo mediante simulación Monte Carlo y Dinámica Molecular.

En los últimos años se han propuesto nuevas metodologías, como el Test-Area[2], el Wandering Interface Method WIM)[3] o el uso del colectivo Expanded Ensemble[4], entre otros, que permiten determinar la tensión interfacial de un modo relativamente sencillo y elegante de todo tipo de sistemas de interés, incluyendo fluidos complejos como sistemas moleculares.

En este trabajo se han utilizado algunas de estas técnicas para determinar la tensión interfacial de cadenas moleculares[5–7,9], con diferentes grados de flexibilidad, que interaccionan a través del potencial de interacción intermolecular Lennard-Jones. En particular, en esta investigación nos centramos en el comportamiento de la tensión superficial, perfiles de densidad, densidad y temperatura críticas, presión de vapor y anchura interfacial, como funciones de la temperatura y de algunas características moleculares de las moléculas consideradas, como tamaño molecular y flexibilidad.

Se ha tenido especial cuidado en el tratamiento de las correcciones de largo alcance inhomogéneas[8,6,7], la determinación de la presión de vapor[6], especialmente en el caso de moléculas largas, y en el tratamiento de los errores asociados a los cálculos de integración termodinámica.

---

* felipe@uhu.es

[1] J. S. Rowlinson and B. Widom, *Molecular Theory of Capillarity*, Claredon Press (1982).
[2] G. J. Gloor, G. Jackson, F. J. Blas, y E. de Miguel, *J. Chem. Phys.* 123, 134703 (2005).
[3] L. G. MacDowell y P. Bryk, *Phys. Rev. A* 75, 061609 (2007).
[4] E. de Miguel, *J. Phys. Chem. B* 112, 4647 (2008).
[5] F. J. Blas, L. G. MacDowell, E. de Miguel y G. Jackson, *J. Chem. Phys.* 129, 144703 (2008).
[6] L. G. MacDowell y F. J. Blas, *J. Chem. Phys.* 131, 074705 (2009).
[7] F. J. Blas, F. J. Martínez-Ruiz, A. I. Moreno-Ventas Bravo y L. G. MacDowell, *J. Chem. Phys.* 137, 024702 (2012).
[8] J. Janeček, *J. Phys. Chem. B* 110, 6264 (2006).
[9] F. J. Blas, A. I. Moreno-Ventas Bravo, J. Algaba, F. J. Martínez-Ruiz y L. G. MacDowell, submitted to *J. Chem. Phys.*

Universal scaling behaviour of surface tension of molecular chains

Felipe J. Blas*[1,2], Francisco José Martínez-Ruiz[1,2], A. Ignacio Moreno-Ventas Bravo[2,3], Luis G. MacDowell[4], José Manuel Míguez[5] y Manuel M. Piñeiro[5]

[1] *Departamento de Física Aplicada, Facultad de Ciencias Experimentales, Universidad de Huelva, 21071 Huelva*
[2] *Centro de Investigación de Física Teórica y Matemática, Universidad de Huelva, 21071 Huelva*
[3] *Departamento de Geología, Facultad de Ciencias Experimentales, Universidad de Huelva, 21071 Huelva*
[4] *Departamento de Química-Física, Facultad de Ciencias Químicas, Universidad Complutense, 28040 Madrid*
[5] *Departamento de Física Aplicada, Facultade de Ciencias, Universidade de Vigo, 36310 Vigo*

We use and extend the universal relationship recently proposed by Galliero,[1] based on a combination of the corresponding-states principle of Guggenheim[2] and the parachor approach of Macleod[3], to predict the vapour-liquid surface tension of fully flexible chainlike Lennard-Jones molecules. In the original study of Galliero, the reduced surface tension of short-chain molecules formed by up to five monomers is expressed as a unique function of the difference between the liquid and vapour coexistence densities.

In this work, we extend the applicability of the recipe and demonstrate that it is also valid for predicting the surface tension of two different chainlike molecular models, namely, linear tangent chains that interact through the Lennard-Jones intermolecular potential and fully flexible chains formed by spherical segments interacting through the square-well potential. Computer simulation data for vapour-liquid surface tension of fully flexible and rigid linear Lennard-Jones, and fluid flexible square-well chains is taken from our previous works. Our results indicate that the universal scaling relationship is able to correlate short- and long-chain molecules with different degrees of flexibility and interacting through different intermolecular potentials.

G. Galliero, J. Chem. Phys. 133, 074705 (2010) E. A. Guggenheim, J. Chem. Phys. 13, 253 (1945) J. Macleod, Trans. Faraday Soc. 19, 38 (1923)

---

* felipe@uhu.es

[1] G. Galliero, *J. Chem. Phys.* 133, 074705 (2010).
[2] E. A. Guggenheim, *J. Chem. Phys.* 13, 253 (1945).
[3] J. Macleod, *Trans. Faraday Soc.* 19, 38 (1923).

Multiple time-delay effect on synchronization of chaotic systems

Manuel Jiménez-Martín*, Elka Korutcheva
Departamento de física fundamental, UNED.
Paseo del Rey 9, 28040, Madrid

Our research focuses on synchronization of chaotic systems with several time-delays. The formalism of the Master Stability Function is used to study small graphs of chaotic maps with different topologies, with both analytical and computational approaches. Special attention is paid on the corresponding phase diagrams and the conditions for the maximal stability gap.
Some general analytical results are obtained in the case of Bernoulli maps taking into account the interplay between synchronization of networks with heterogeneous delays and the greatest common divisor of loops composing the network.
On a second stage, we study the prevalence or not of the previous results replacing networks units with Integrate and Fire neurons with inhibitory delayed synapses. Finally, extention to more complicated neuronal systems with several time-delays is considered as well.

* manuel.jimenez@bec.uned.es

The role of individual neutrality in growing mutualistic networks

Manuel Jiménez-Martín*, Juan Manuel Pastor, Juan Carlos Losada, Javier Galeano
GSC, Grupo de Sistemas Complejos
ETSI Agrónomos, Universidad Politécnica de Madrid Av. Complutense 3, 28040-Madrid

Many ecosystems exhibit a complex network of mutualistic relationships among their species, such as those between plants and pollinators. The structure of mutualistic networks have been thorougly studied[2] but the processes leading to the formation of these communities are still unclear. Our research aims to describe a novel yet simple mechanism for mutualistic network formation. These weighted bipartite networks can be represented by an interaction matrix $\mathbf{W}$, where element w_{ij} represents the observed frequency of interaction between A-species i and P-species j. Mutualistic networks are significantly *nested* ($w_{ij} \geq \max(w_{i+1,j}, w_{i,j+1})$) and exhibit truncated power-law degree and strength distributions. It is known that species degree, strength and abundance (population) are correlated in mutualistic communities. Individual neutrallity hypothesizes that topological features of mutualistic networks can be explained as a consequence of species abundance considering random interactions between individuals. Thus, stronger interactions occur between species with higher population[1].
We have incorporated this information into a minimal, analitically solvable, growth model where the probability of interaction between individuals is proportional to the strength of both species. Here, species strength acts as a proxy for species abundance. Our model generates nested networks with truncated k and s-distributions. Our results support the hypothesis that exponential truncations are a finite size effect that would not be observed in infinitely large networks. We have compared the simulated networks topology with 9 empirical datasets. We have also tested the role of *forbidden links* on the growth process and found that these do not improve our previous results. On the contrary, considering a high percentage of a priori forbidden interactions severely damages network connectivity.

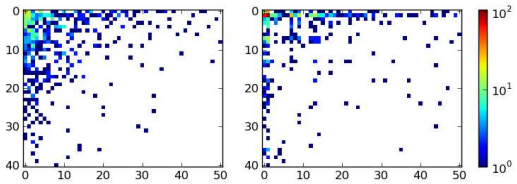

FIG. 1. Empirical and simulated interaction matrices ($N_A = 41$, $N_P = 51$, $W = 641$).

* manuel.jimenez@bec.uned.es
Facultad de ciencias, dpto. física fundamental, UNED. Paseo del Rey 9, 28040, Madrid

[1] D.P. Vázquez and M. A. Aizen, *Ecology* **84(9)**, 2493 (2003).
[2] J. M. Olesen, J. Bascompte, Y. L. Dupont, H. Elberling, C. Rasmussen and P. Jordano, *Proceedings of the National Academy of Sciences of the United States of America* **100**, 9383 (2003).

The trophic coherence of networks: Diversity and stability reconciled?

Samuel Johnson*, Virginia Domínguez-García†, and Miguel A. Muñoz†
Department of Mathematics, Imperial College London, SW7 2AZ, United Kingdom.

Will a large, complex system be stable? Robert May asked this question in 1972, and showed that the answer was, in general, no – at least if the interactions between elements were randomly placed.[1] In the case of ecosystems, as well as financial and other complex systems, both received wisdom and empirical research suggested that size and link density increased stability, so the result became known as May's Paradox. In ecology the "diversity-stability debate" rages on, and it has often be conjectured that large, complex (i.e., dense) ecosystems are stable thanks to some unidentified structural property.[2]

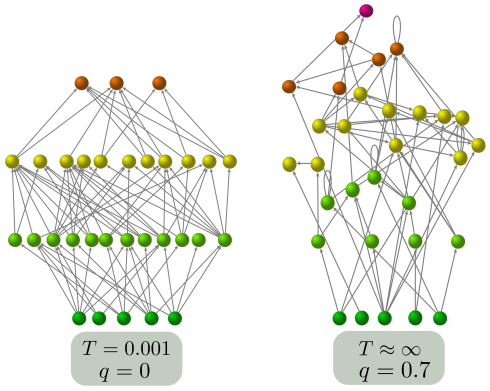

FIG. 1. Networks generated with the Preferential Preying Model (PPM), using the number of species and links of the Chesapeake Bay food web, for $T = 0.001$ (left) and $T = 10$ (right). The height of nodes represents their *trophic level*, defined for each node as the mean trophic level of its incoming nodes (e.g., prey), plus one. The network on the left has maximum trophic coherence, while the one on the right is highly incoherent; the parameter q captures this.

We show that *trophic coherence* – a hitherto ignored feature of food webs which current structural models fail to reproduce – is significantly correlated with ecosystem stability, whereas size and link density are not.[3] Together with cannibalism, trophic coherence accounts for over 80% of the variance in stability observed in a 16-food-web dataset. We propose the Preferential Preying Model (PPM), whose single free parameter, T, sets the degree of trophic coherence. For $T \simeq 0$ we obtain maximally coherent networks (left panel of Fig. 1), whereas very incoherent structures (similar to those produced by current food-web models) ensue from a high T (right panel of Fig. 1). By adjusting T to the empirical coherence of food webs, the PPM predicts their stability much more accurately than do other models, and is at least as successful as regards all other structural features analysed.

Most remarkably, the PPM shows that stability can increase with size and link density if networks are sufficiently coherent. As shown in Fig. 2, while for high T stability decreases with size and density according to the May-Wigner law, as in other food-web models, below a certain value of T the size-stability relationship is inverted. This suggests that it is trophic coherence which accounts for the high stability of large, dense ecosystems – such as rainforests or coral reefs – and may be significant for other complex dynamical systems. This result raises the concern that loss of a few elements (e.g., species or banks) could push a system into a regime of inherent instability. On the other hand, it may provide a way of diagnosing the risk of such a "tipping point".

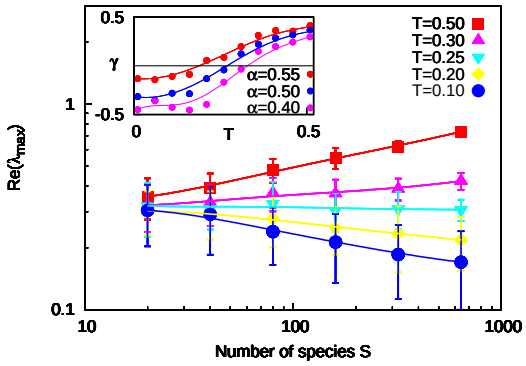

FIG. 2. Real part of the leading eigenvalue of the interaction matrix, $Re(\lambda_{max})$, against number of nodes, S, for networks generated with the PPM for different values of the parameter T. $Re(\lambda_{max})$ is the degree of self-regulation (e.g., intra-species competition in an ecosystem) required for the system to be (locally) stable; thus, the lower $Re(\lambda_{max})$, the more stable we consider the network. The density of links (complexity), K, is $K = S^{\alpha}$, with $\alpha = 0.5$ as recent estimates find for food webs. Inset: Slope of the stability-size curve, γ, against T for different exponents α.

* samuel.johnson@imperial.ac.uk
† Departamento de Electromagnetismo y Física de la Materia, and Instituto Carlos I de Física Teórica y Computacional, Universidad de Granada, 18071 Granada, Spain.

[1] R.M. May, "Will a large complex system be stable?" *Nature* **238**, 413–4 (1972)
[2] K.S. McCann, "The diversity-stability debate," *Nature* **405** 228–33 (2000).
[3] S. Johnson, V. Domínguez-García, and M.A. Muñoz, "The trophic coherence of food webs: Diversity and stability reconciled?," submitted to *Nature* (under review).

Burnett transport coefficients for inelastic Maxwell models

Nagi Khalil, Vicente Garzó, and Andrés Santos*
Departamento de Física, Universidad de Extremadura, E-06071 Badajoz, Spain

The inelastic Maxwell model (IMM) is used to describe a d-dimensional granular gas of particles of mass m. In the IMM, the one-particle distribution function obeys a Boltzmann-like equation with the usual hard-sphere collision rate replaced by a velocity-independent one. The effective frequency ν_0 is taken to be proportional to the density of particles n and the γ-power of the temperature T, i.e. $\nu_0 \propto nT^\gamma$. In that way, different values of γ can be chosen to mimic different interaction potentials in the elastic limit. In particular, $\gamma = 1/2$ represents hard spheres. The modification of the operator allows for explicit calculations[1] and, in general, leads to reasonable results[2].

In this work, the kinetic equation of the IMM is solved by means of the Chapman-Enskog method up to the second order in the spatial gradients of the hydrodynamic fields (density of particles n, macroscopic velocity $\mathbf{u}$, and temperature T). As a consequence, the constitutive equations for the pressure tensor and the heat flux are evaluated up to Burnett order, and hence a closed hydrodynamic description up to third order in the gradients is obtained.

In the Burnett order, the constitutive relations for the pressure tensor is

$$
\begin{aligned}
P_{ij}^{(2)} = {} & a_1 \frac{\kappa_0}{\nu_0}\left(\nabla_i\nabla_j T - \frac{1}{d}\delta_{ij}\nabla^2 T\right) \\
& + a_2 \frac{T\kappa_0}{p\nu_0}\left(\nabla_i\nabla_j p - \frac{1}{d}\delta_{ij}\nabla^2 p\right) \\
& + a_3 \frac{\kappa_0}{T\nu_0}\left[\nabla_i T\nabla_j T - \frac{1}{d}\delta_{ij}(\nabla T)^2\right] \\
& + a_4 \frac{T\kappa_0}{p^2\nu_0}\left[\nabla_i p\nabla_j p - \frac{1}{d}\delta_{ij}(\nabla p)^2\right] \\
& + a_5 \frac{\kappa_0}{p\nu_0}\left(\nabla_i T\nabla_j p + \nabla_i p\nabla_j T - \frac{2}{d}\delta_{ij}\nabla p\cdot\nabla T\right) \\
& + a_6 \frac{\eta_0}{\nu_0} D\left(D_{ij} - \frac{1}{d}\delta_{ij} D\right) \\
& + a_7 \frac{\eta_0}{\nu_0}\Bigg[D_{ik}D_{kj} - \omega_{ik}\omega_{kj} \\
& \quad - \frac{1}{d}\delta_{ij}\left(D_{lk}D_{kl} - \omega_{lk}\omega_{kl}\right) + \omega_{ij}D_{kj} - D_{ik}\omega_{kj}\Bigg],
\end{aligned}
$$

where $D = \nabla\cdot\mathbf{u}$, $D_{ij} = \frac{1}{2}(\nabla_i u_j + \nabla_j u_i)$, $\omega_{ij} = \frac{1}{2}(\nabla_j u_i - \nabla_i u_j)$, κ_0 is the elastic thermal conductivity, η_0 is the elastic viscosity, $p = nT$ is the pressure, and a_i are reduced transport coefficients that depend on d, the coefficient of normal restitution α, and γ, see Fig. 1. For the heat flux

$$
\begin{aligned}
q_i^{(2)} = {} & b_1 \frac{T\kappa_0}{\nu_0}\nabla^2 u_i + b_2 \frac{T\kappa_0}{\nu_0}\nabla_i D + b_3 \frac{\kappa_0}{\nu_0} D_{ij}\nabla_j T \\
& + b_4 \frac{\eta_0}{\rho\nu_0} D_{ij}\nabla_j p + b_5 \frac{\kappa_0}{\nu_0}\omega_{ij}\nabla_j T + b_6 \frac{\eta_0}{\rho\nu_0}\omega_{ij}\nabla_j p \\
& + b_7 \frac{\kappa_0}{\nu_0} D\nabla_i T + b_8 \frac{\eta_0}{\rho\nu_0} D\nabla_i p,
\end{aligned}
$$

where $\rho = nm$ is the mass density, and b_i are transport dimensionless coefficients. Figure 1 displays the α-dependence of the Burnett coefficients for $d = 3$ and $\gamma = 1/2$.

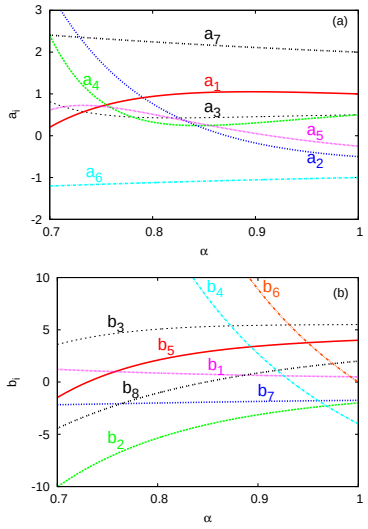

FIG. 1. Coefficients a_i (a) and b_i (b) for a three dimensional system ($d = 3$) and for $\gamma = 1/2$, as a function of the coefficient of normal restitution α.

For the elastic case ($\alpha = 1$), and for a three dimensional system, the expressions for the pressure tensor and the heat flux reduce, for any interaction potential between particles, to the classical ones in Ref.[3]. In addition, we provide a generalization of the elastic results to any dimension and any degree of dissipation. For inelastic situations, the structure of the constitutive equations is more complex than in the elastic case.

* nagi@us.es, vicenteg@unex.es, andres@unex.es

[1] V. Garzó and A. Santos, J. Phys. A: Math. Theor. 40, 14927 (2007).
[2] A. Santos and V. Garzó, J. Stat. Mech. p. P08021 (2007).
[3] S. Chapman and T. G. Cowling, Mathematical Theory of Non-Uniform Gases, Cambridge University Press (1952).

Evaluación de la importancia de las correcciones de largo alcance en el cálculo de la tensión superficial de fluidos simples mediante simulación en el colectivo gran canónico

J. Largo*
Departamento de Física Aplicada
Universidad de Cantabria 39005 Santander (España)

Una de las propiedades fundamentales asociadas a la interfase entre dos fluidos en coexistencia es la tensión superficial. El cálculo de la tensión superficial por simulación es considerablemente más complicado que la determinación de la coexistencia de fases. Por ejemplo, la simulación del equilibrio de fases mediante el método de Gibbs es factible precisamente porque evita la formación de las interfases, pero al mismo tiempo por ello no permite obtener propiedades de las mismas.

Diferentes métodos de simulación han sido formulados con el fin de obtener la tensión superficial. Así un procedimiento habitualmente utilizado para el cálculo por simulación de la tensión superficial se basa en la interpretación mecánica de la tensión superficial y requiere el cálculo de las componentes del tensor de presiones.

El método del Test-Area consiste por ejemplo en la determinación del cambio de energía libre producido por una variación en el área de la interfase[1]. Además con este método se soslaya, por ejemplo, el inconveniente en simulación por Monte Carlo de tener que realizar el cálculo de fuerzas de interacción. Y aunque mejora cuantitativamente la estimación de propiedades como: tensión superficial, densidades de coexistencia, perfil de densidad y anchura de la interfase, sin embargo, los resultados dependen en gran medida del tamaño del sistema y del tipo de correcciones de largo alcance utilizadas.

Un método que permite el cálculo de la tensión superficial y que no requiere la formación de interfases es el método de simulación de equilibrios de fase en el colectivo gran canónico[2]. El uso de técnicas como la de reponderación de los histogramas[3] en el colectivo grand canónico permite obtener no sólo las densidades de coexistencia, sino estimar la barrera de energía libre que debe sobrepasar el sistema al cambiar de fase[4]. Esta barrera está directamente relacionada con la tensión superficial, que de este modo puede ser determinada sin la formación de interfases.

Además con los datos obtenidos para diferentes tamaños de sistema es posible aplicar un análisis de tamaño finito[5] y calcular la tensión superficial para un rango de temperaturas cerca del punto crítico.

Para ampliar el rango de temperaturas en el que podemos sobrepasar la barrera de energía libre existente entre las dos fases, aplicaremos funciones de peso que faciliten el paso del sistema entre las fases en coexistencia (muestreo preferencial). Dicho peso se retira, evidentemente en el proceso de análisis.

En este trabajo queremos aprovechar la gran funcionalidad que posee el método gran canónico al aplicarse junto con técnicas de repesado de histograma y de muestreo preferencial y mostrar el amplio rango de aplicación de esta técnica de simulación.

En particular queremos presentar y analizar las diferencias observadas en el valor de la tensión superficial de un fluido de Lennard-Jones al introducir correcciones de largo alcance o no. En trabajos precedentes[6], hemos analizado la influencia que estas tienen en el equilibrio de fases. Sin embargo, es de particular interés el análisis sobre el valor de la tensión superficial, dada la gran influencia que tienen sobre esta propiedad dichas correcciones[7] de largo alcance.

Agradecimientos. Este trabajo ha sido financiado por el Ministerio de Ciencia e Innovación (MICINN), Proyecto No. FIS2009-09616.

---

* julio.largo@unican.es

[1] G. J. Gloor, G. Jackson, F. J. Blas y E. de Miguel, J. Chem. Phys. **123**, 134703 (2005)
[2] J. J. Potoff y A. Z. Panagiotopoulos, J. Chem. Phys. **112**, 6411 (2000).
[3] A. M. Ferrenberg y R.H. Swendsen, Phys. Rev. Lett. **63**, 1195 (1989).
[4] N. B. Wilding, Phys. Rev. E **52**, 602 (1995)
[5] K. Binder, Phys. Rev. A **25**, 1699 (1982).
[6] J. Largo, en preparación.
[7] G. A. Chapela, G. Saville, S. M. Thompson y J. S. Rowlinson, J. Chem. Soc. Faraday Trans. **73**, 1133 (1977).

Anomalous behaviour in a simple water/methanol model with two repulsive ranges

Enrique Lomba[a], Marcia Barbosa[b] and Alexandre Furlan[b]
[a] *IQFR-CSIC, Serrano 119, E-28006 Madrid, Spain*
[b] *Instituto de Física - UFRGS, CP15051 91501-970 - Porto Alegre - RS Brasil*

Water is well know for its thermodynamic, structural and dynamic anomalous behaviour[1], which can be interpreted as a result of the presence of two repulsive ranges of interaction stemming from a short range repulsion and a longer range contribution from the hydrogen network. In this connection the addition of small quantities of short chain alcohols alters the behaviour in a non monotonous fashion[4], due to the partial and progressive disruption of the hydrogen bond network. Since it is well known that the anomalies of water can be reproduced by simpler spherically shaped models with two ranges of repulsion[2], in this contribution, following the ideas of Su et al.[3], we construct a model for water/methanol mixtures in which water in modeled by means of an spherically shaped Lennard-Jones and two gaussian (LJ2G) potentials[5] and methanol using a dumbbell in which the methyl group is a simple Lennard-Jones and the hydroxil group is also represented by a LJ2G potential, thus accounting for the two repulsive ranges due to the hydogen bond network and the shorter range repulsion mostly induced by the oxygen atom. The cross interaction parameters of the model are adjusted so as to reproduce the experiemental excess properties of water-methanol mixtures. Calculations will be carried out using constant-pressure Molecular Dynamics simulations at various methanol concentrations in order to analyze the effect of the solute addition on the temperature of maximum density of water. The system will also be studied by means of the molecular Ornstein-Zernike approach[6] in particular in the low methanol concentration regime, for which water-water correlations can be modeled using a thermodynamic self-consistent approach that can reproduce the presence of thermodynamic anomalies.

---

* enrique.lomba@csic.es

[1] Poole, P. H.; Sciortino, F.; Essmann, U. and Stanley, H. E., Nature, **360**, 324 - 328 (1992).
[2] de Oliveira, A. B.; Netz, P. A.; Colla, T. and Barbosa, M. C., J. Chem. Phys., **125**, 084505 (2006).
[3] Su, Z.; Buldyrev, S. V.; Debenedetti, P. G.; Rossky, P. J. and Stanley, H. E., J. Chem. Phys., **136**, 044511 (2012)
[4] Wada, G. and Umeda, S., Bull. Chem. Soc. Jpn., **35**, 646 - 652 (1962)
[5] Bordin, J. R.; Diehl, A. and Barbosa, M. C., J. Phys. Chem. B, **117**, 7047 (2013)
[6] Anta, J.A.; Lomba, E.; Alvarez, M. ; Martin C., and Lombardero M., J. Chem. Phys., **106**, 2712 (1997)

Superuniversalidad y la distribución de Bramwell-Holdsworth-Pinton de magnitudes críticas

Juan M. López*
Instituto de Física de Cantabria (IFCA)
CSIC-Univ. de Cantabria, Santander

En 1998 Bramwell, Holdsworth y Pinton publicarón un sorprendente artículo en la revista Nature[1] donde mostraban una inesperada conexión entre la estadística de la disipación en un experimento con fluidos turbulentos y la distribución del parámetro de orden en el punto crítico de un modelo magnético en equilibrio. Esta misteriosa conexión entre ambos fenómenos, tan distantes a simple vista en términos físicos, fue poco después ampliada a otros sistemas críticos, tanto en equilibrio como disipativos, en otro artículo que apareció en Physical Review Letters[2] un año y medio después. Estos trabajos despertarón un gran interés[3] ya que apuntaban una conexión muy profunda de la estadística de propiedades macroscópicas en sistemas fuertemente correlacionados. Se vislumbraba la posibilidad de haber dado con una distribución universal, bautizada distribución BHP, para sistemas fuertemente correlacionados que jugaría el papel equivalente al que juega la distribución Gaussiana en el caso de los sistemas con correlación de corto alcance. Podríamos hablar del equivalente al Teorema Central del Límite de sistemas con correlación de largo alcance, de sistemas críticos. Se cuentan por cientos los artículos publicados sobre el problema desde entonces, incluyendo varios intentos más o menos infructuosos de explicar la existencia, hoy más que comprobada, de dicha superuniversalidad. El mayor obstáculo para la solución del problema ha sido sin duda la ausencia prácticamente total de resultados matemáticos rigurosos (o siquiera aproximados) acerca de la estadística de variables correlacionadas sobre los que poder construir la física correspondiente[4]. Después de más de 10 años de investigación y a la luz de resultados que presento en esta comunicación la solución al misterio se encuentre quizá ya muy cercana[5].

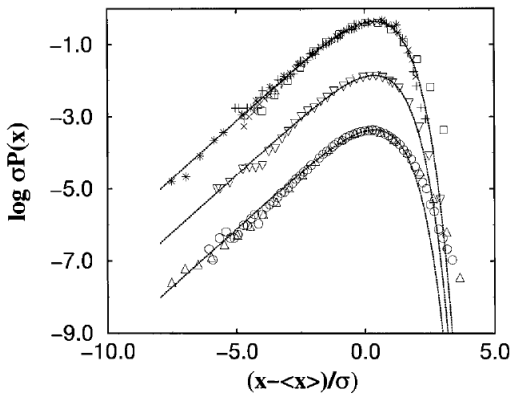

FIG. 2. Fluctuation spectra in equilibrium systems (lower curves): Ising (∘), percolation (△). The central curve (▽) corresponds to the fluctuation spectrum of the correlated extremal process — see text. The upper curves are the PDFs for the autoigniting forest fire model (×), the Sneppen depinning model (+), the granular media model (□), and the BTW sandpile model (∗). The lines are Eq. (6). For clarity, the sets of curves are shifted downwards by 1.5 in log units.

* lopez@ifca.unican.es

[1] S. T. Bramwell, P. C. W. Holdsworth, and J.-F. Pinton, Nature (London) **396**, 552 (1998).
[2] S. T. Bramwell, K. Christensen, J.-Y. Fortin, P. C.W. Holdsworth, H. J. Jensen, S. Lise, J. M. López, M. Nicodemi, J.-F. Pinton, and M. Sellitto, Phys. Rev. Lett. **84**, 3744 (2000).
[3] Según Google Scholar el artículo en PRL anterior se ha citado en casi 250 trabajos y proceedings de conferencias.
[4] S. T. Bramwell, Nat. Phys **5**, 444 (2009)
[5] J. M. López, unpublished (2013).

Vegetation patterns without facilitative mechanisms.

Ricardo Martínez-García, Justin M. Calabrese, Emilio Hernández-García, Cristóbal López
IFISC, Instituto de Física Interdisciplinar y Sistemas Complejos
CSIC-Universidad de las Islas Baleares 07122-Palma (Mallorca)

Regular patterns and spatial organization of vegetation have been observed in many arid and semiarid ecosystems worldwide, covering a diverse range of plant taxa and soil types. A key common ingredient in these systems is that plant growth is severely limited by water availability, and thus plants likely compete strongly for water. The study of such patterns is especially interesting because their features may reveal much about the underlying physical and biological processes that generated them in addition to giving information on the characteristics of the ecosystem. It is possible, for instance, to infer their resilience against anthropogenic disturbances or climatic changes that could cause abrupt shifts in the sys- tem and lead it to a desert state.

Therefore much research has focused on identifying the underlying mechanisms that can produce spatial patterning in water-limited systems[1]. They are believed to arise from the interplay between long-range competition and facilitation processes acting at smaller distances[2]. This combination of mechanisms is justified by arguing that water percolates more readily through the soil in vegetated areas (short range), and that plants compete for water resources over greater distances via long lateral roots (long range). However, recent studies have shown that even in the limit of local facilitation patterns may still appear[3].

In this work[4], we show that, under rather general conditions, long- range competition alone may be enough to shape gapped and stripped vegetation patterns patterns typical of models that also account for facilitation in addition to competition. To this end we propose a simple, general model for the dynamics of vegetation, which includes only long- range competition between plants. Competition is introduced through a nonlocal term, where the kernel function quantifies the intensity of the interaction. When the finite range of the competitive interaction is considered, and thus there is a kernel function whose Fourier transform may have negative values, patterns emerge in the system. This is a rather general condition if we consider the finite length of the roots, responsible of long-range competition for water. Therefore, our findings support the notion that, under fairly broad conditions, only competition is required for patterns to occur and suggest that the role of short-range facilitation mechanisms may not be as fundamental to pattern formation as has previously been thought.

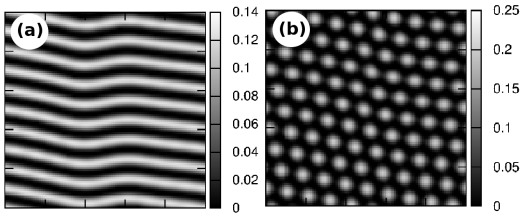

FIG. 1. Stripped (a) and gapped (b) patterns obtained with the model.

* ricardo@ifisc.uib-csic.es

[1] C.A. Klausmeier, Science, **284**, 1826-1828 (1999).
[2] F. Borgogno, P. D'Odorico, F. Laio and L. Ridolfi, Rev. Geophys., **47**, RG1005 (2009).
[3] R. Martínez-García, J.M. Calabrese, and C. López, Journal of Theoretical Biology, **333**, 156-165 (2013).
[4] R. Martínez-García, J. M. Calabrese, E. Hernández-García, and C. López, Geophys. Res. Lett., 40, doi:10.1002/2013GL058797 (2013).

Tuning the period of square-wave oscillations in delay-coupled opto-electronic systems

Jade Martínez-Llinàs[1]*, Pere Colet[1] and Thomas Erneux[2]
[1] *IFISC, Instituto de Física Interdisciplinar y Sistemas Complejos, CSIC-UIB, 07122-Palma, Mallorca*
[2] *Université Libre de Bruxelles, Optique Nonlinéaire Théorique, Campus Plaine, C.P. 231, 1050 Bruxelles, Belgium*

We examine the emergence of stable square-waves in a system of two delay-coupled opto-electronic oscillators. Each oscillator operates under its own delayed feedback and the presence of two delays allows a large number of stable square-wave time-periodic regimes. By using asymptotic methods based on the relatively large values of the two delays, we propose a systematic analytical study of the bifurcation mechanisms. The validity of all our results is tested by solving numerically the original evolution equations for the opto-electronic oscillators. Because of the two distinct delays, the bifurcation possibilities are rich but their derivations are relatively simple because the analysis essentially relies on the solutions of coupled equations for maps. In this sense, we expect that our analysis can be applied to other two-delayed coupled systems and lead to similar results.

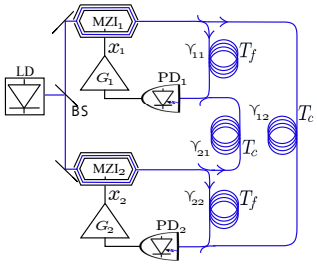

FIG. 1. Setup.

We consider two electro-optical delay systems[1] that are mutually coupled as shown in FIG.1. The light emitted by a cw semiconductor laser (LD) with intensity P is split into two beams, each beam feeding an electro-optical delay loop. Each loop consists of a Mach-Zehnder interferometer (MZI), an optical delay line, a photodiode (PD) and an amplifier. We use subindex i, $i = 1, 2$, to identify the variables associated to loop i. For loop i the optical output of MZI_i is split into two parts. A fraction γ_{ii} is delayed using a fibre loop by a time T_{ii}. A fraction γ_{ij} with $i, j = 1, 2$ and $j \neq i$ is injected from loop i into loop j after a delay T_{ij}. Self-feedback and cross-feedback optical signals are combined and the resulting intensity is detected by the PD. The electrical signal goes through a band-pass amplifier and is finally used to drive the Mach-Zehnder AC electrode. For each loop, the dynamics results from a combination of the nonlinear effect due to the MZI plus a linear filtering process associated to the electrical part of the loop. The dynamics of the electrical signal x_i is:

$$x_i(t) + \tau_i \frac{dx_i}{dt}(t) + \frac{1}{\theta_i}\int_{t_0}^{t} x_i(s)ds = PC_i,$$

$$C_i = \gamma_{ii}^2 \cos^2(z_{ii}) + \gamma_{ji}^2 \cos^2(z_{ji}) + \\ + 2\gamma_{ii}\gamma_{ji}\cos(z_{ii})\cos(z_{ji})\cos(z_{ii} - z_{ji}),$$

where $i, j = 1, 2$, $z_{ji} = x_j(t - T_{ji}) + \phi_j$, $T_{ii} = T_f$, $T_{ji,j\neq i} = T_c$, and ϕ_i is an offset phase.

We show that this system can display square-wave periodic solutions which can be synchronized in-phase or out-of-phase depending on the ratio $s_0 = T_f/T_c$; in particular, the synchronization is in-phase if the ratio involves two odd numbers while it is out-of-phase for ratios involving an odd and an even number. Furthermore, multiple periodic synchronized solutions can coexist for the same values of the fixed parameters, as it is illustrated in FIG.2. As a consequence, it is possible to generate square-wave oscillations with different periods by just changing the initial condition.

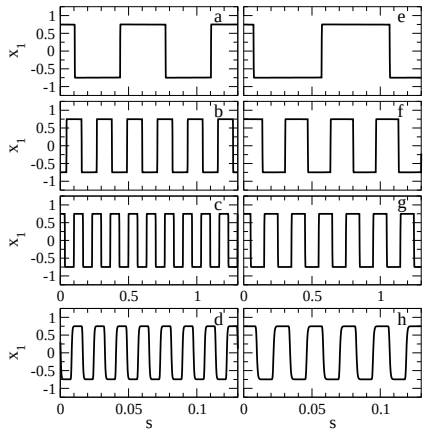

FIG. 2. Time trace of square-wave periodic solutions with $P = 1.5$, $\gamma_{ij} = 0.5$, $\phi = 0.25\pi$, and $T_f = 30ns$. The panels of the left column display coexisting in-phase solutions for $T_c = 90$ns ($s_0 = 1/3$). The panels of the right column display coexisting out-phase solutions for $T_c = 60$ns ($s_0 = 1/2$). In rows, fundamental solution (a, e), first harmonic (b, f), second harmonic (c, g), and twentieth harmonic (d, h). Notice that the time scale used in panels (d) and (h) is 10 times smaller than in the other panels. $s = t/T_c$ is the dimensionless time.

* jade@ifisc.uib-csic.es

[1] J. P. Goedgebuer, P. Levy, L. Larger, C.-C. Chen, and W.T. Rhodes, IEEE J. Quantum Electron. **38**, 1178 (2002)

Influencia de las correcciones de largo alcance dispersivas en el cálculo de propiedades interfaciales usando simulación de Monte Carlo

José Manuel Míguez[1], Manuel M. Piñeiro*[1], Felipe J. Blas[2]
[1] *Departamento de Física Aplicada, Facultade de Ciencias, Universidade de Vigo*
[1] *Departamento de Física Aplicada, Facultad de Ciencias Experimentales, Universidad de Huelva*

En este trabajo se ha analizado la influencia del tratamiento de las correcciones de largo alcance debidas al término dispersivo del potencial intermolecular en el cálculo de propiedades interfaciales de fluidos usando la técnica de simulación molecular de Monte Carlo mediante coexistencia directa de fases. Recientemente se han propuesto varias técnicas para determinar las propiedades interfaciales de fluidos mediante simulación molecular, y su uso está encontrando numerosas aplicaciones por su versatilidad.

Sin embargo, los resultados cuantitativos de estos métodos son muy sensibles a cuestiones como por ejemplo el tratamiento de las correcciones de largo alcance en el cálculo de las interacciones intermoleculares. En este trabajo se ha determinado la influencia de este tratamiento, en particular la contribución debida al término dispersivo del potencial intermolecular. Con este objetivo, se han realizado cálculos de tensión interfacial líquido-vapor por simulación de Monte Carlo en cajas inhomogéneas con interfase explícita para distintos modelos moleculares, comparando los resultados numéricos con valores experimentales. Se ha comparado el resultado de la determinación de la tensión interfacial utilizando distintos valores del radio de corte para truncar el potencial de interacción, comparados con el uso de correcciones de largo alcance analíticas, en particular con el método propuesto originalmente por Janeček[1], y refinado posteriormente por MacDowell y Blas[2].

Así, se han hecho cálculos para distintos modelos moleculares de átomos unidos, rígidos y no polarizables, representando a las moléculas de CH_4, H_2O y CO_2[3]. Para el caso del CH_4 se ha utilizado un modelo que considera la molécula como una única esfera Lennard-Jones (LJ). El modelo usado para el agua ha sido el TIP4P, en varias de sus versiones, que incluye un sitio LJ y tres cargas eléctricas puntuales, y para el CO_2 se han utilizado modelos que consideran tres sitios alineados, cada uno de ellos consistiendo de un centro LJ y una carga eléctrica (MSM, EPM2, TraPPE, y ZD). La tensión interfacial se ha calculado siguiendo la ruta mecánica, que implica la determinación de las componentes de tensor de presiones, y también la ruta termodinámica usando desplazamientos virtuales de volumen, según el método conocido como Test-Area[4].

Con esta configuración, se ha realizado un estudio sobre la evolución de las propiedades de coexistencia de fases (densidad), y tensión interfacial al variar el radio de corte del término dispersivo (LJ) del potencial intermolecular. Se ha comparado la evolución de estos valores con los resultados obtenidos aplicando el formalismo de corrección de efectos de largo alcance de MacDowell y Blas, y con otras técnicas de cálculo de las correcciones a posteriori. Al analizar diversos modelos moleculares, se ha podido evaluar la influencia del término dispersivo frente a las interacciones puramente electrostáticas.

Los resultados muestran claramente que un tratamiento poco riguroso de las correcciones de largo alcance dispersivas producen una subestimación sistemática de las propiedades interfaciales de los modelos estudiados. El uso de correcciones analíticas permite acceder al resultado exacto de estas propiedades para cada modelo, eliminando la dependencia de la elección arbitraria del radio de corte, y además produce una disminución muy notable del tiempo de cálculo, que es muy elevado para este tipo de simulaciones moleculares en cajas inhomogéneas con interfase explícita.

Agradecimientos: Los autores agradecen a CESGA (www.cesga.es, Santiago de Compostela), el acceso a recursos de computación.

---

* mmpineiro@uvigo.es

[1] J. Janeček, *J. Phys. Chem. B* 110, 6264 (2006).
[2] L. G. MacDowell y F. J. Blas, *J. Chem. Phys.* 131, 074705 (2009).
[3] J. M. Míguez, M.M. Piñeiro y F. J. Blas, *J. Chem. Phys.* 138, 034707 (2013).
[4] G. J. Gloor, G. Jackson, F. J. Blas, y E. de Miguel, *J. Chem. Phys.* 123, 134703 (2005).

Phase behavior of liquid-crystal monolayers of rod-like and plate-like particles

Yuri Martínez-Ratón[1], Sabolcsz Varga[2] and Enrique Velasco[3]
[1] *GISC, Departamento de Matemáticas, Universidad Carlos III de Madrid, Spain.* [2] *Institute of Physics and Mechatronics, University of Veszprem, Hungary.* [3] *Departamento de Física Teórica de la materia Condensada, Universidad Autónoma de Madrid, Spain.*

The structural and dynamical properties of 2D and even 1D complex fluids are experimentally accessible due to the recent development of nanofluidics and optical trapping methods. Liquid crystal monolayers can be prepared by confining colloidal particles between parallel walls[1,2] or by spreading colloidal nanoparticles or amphiphilic molecules at the air/liquid interface[3,4]. In the present work the orientational and positional ordering properties of liquid crystal monolayers are examined by means of Fundamental Measure Density Functional theory. The particles are modeled as hard boards, with their centers of mass restricted to move on a flat surface and their uniaxial axes allowed to rotate freely in three dimensions (within the restricted-orientation approximation). We find that the structure of the monolayer depends strongly on the shape of the constituting particles and the density. In the case of rod-like shapes, the particles align along the layer normal since that gives the lowest occupied area per particle, i.e. the phase is uniaxial nematic even at very low densities. In contrast, the lowest occupied area can be achieved by random in-plane ordering in the monolayer of plate-like particles, i.e. planar nematic ordering takes place even at vanishing densities. This random in-plane ordering is not favourable at higher densities and the system undergoes an in-plane ordering transition forming a biaxial nematic phase or a crystal. For certain values of the aspect ratio, the uniaxial-biaxial nematic phase transition is observed for both rod-like and plate-like particle shapes. The stability region of the biaxial nematic phase enhances with decreasing aspect ratios for plate-like particles, while the rod-like particles exhibit a reentrant phenomenon, with a uniaxial-biaxial-uniaxial nematic phase sequence with increasing density if the aspect ratio is larger than 21.34. In addition, packing fraction inversion is observed with increasing surface pressure due to alignment along the layer normal. At very high densities the nematic phase destabilizes to a nonuniform phase (columnar, smectic or crystalline phase) for both shapes.

[1] Y. Han, A. Alsayed, M. Nobili and A. G. Yodh, Phys. Rev. E 80, 011403 (2009).
[2] N. F. Bouxsein, C. Leal, C. S. McAllister, K. K. Ewert, Y. Li, C. E. Samuel and C. R. Safinya, J. Am. Chem. Soc., 133, 7585 (2011).
[3] T. E. Herod and R. S. Duran, Langmuir, 14, 6606 (1998).
[4] H. Razafindralambo, A. Richel, M. Paquot, L. Lins and C. Blecker, J. Phys. Chem. B, 116, 3998 (2012).

Formation of localized structures in bistable systems through nonlocal spatial coupling

Manuel A. Matías*, Pere Colet, and Damià Gomila
Instituto de Física Interdisciplinar y Sistemas Complejos, IFISC(CSIC-UIB), Campus Universitat de les Illes Balears, E-07122 Palma de Mallorca

Lendert Gelens
Applied Physics Research Group (APHY), Vrije Universiteit Brussel, Pleinlaan 2, 1050 Brussels, Belgium

In the recent years there has been a lot of interest in the study of extended systems with spatially nonlocal coupling, in the form of an integral over an spatial domain[1–3]. These systems are intermediate between classical evolution equations (e.g. the heat equation) described through Partial Differential Equations and systems of globally coupled constituents. Nonlocal interaction terms appear in chemical and biological systems after adiabatically eliminating a slowly diffusing reactant and also due to density-dependent effects in biological and ecological systems, and in physical systems when long-range interactions are considered.

In this work[4–6] we have studied the effect of nonlocal spatial coupling on the interaction of fronts connecting two equivalent homogeneous stable states. Leveraging spatial dynamics we provide a general framework to understand the effect of the nonlocality on the shape of the fronts connecting two stable states. In particular, for the 1-dimensional real Ginzburg-Landau equation, we show that while for local coupling the fronts are always monotonic and therefore the dynamical behavior leads to coarsening and the annihilation of pairs of fronts, nonlocal terms can induce spatial oscillations in the front tails. The interaction of these oscillatory tails allows for the creation of localized structures, that emerge from pinning between two fronts (a kink and and antikink). In parameter space the region where fronts are oscillatory is limited by three transitions: the modulational instability (MI) of the homogeneous state (a Hamiltonian Hopf (HH) bifurcation), the Belyakov-Devaney (BD) transition in which monotonic fronts acquire spatial oscillations with infinite wavelength, and a crossover in which monotonically decaying fronts develop spatial oscillations with a finite wavelength. We show how these transitions are organized by codimension 2 and 3 points and illustrate how by changing the parameters of the nonlocal coupling it is possible to bring the system into the region where localized structures can be formed.

We discuss the application of three different influence kernels. The first two, Gaussian and mod-exponential, are positive definite and decay exponentially or faster. Both of them exhibit a BD and a MI in the case of repulsive interactions, and LS are found in the region bounded by these two transitions. These transitions can be explained well from a codim-2 point with 4 null eigenvalues. The third kernel, a Mexican-hat kernel, is not positive-definite and exhibits a richer scenario. In particular, in some parameter range it exhibits a BD and a MI, and thus LS, but now for an interaction that overall is attractive, but in which short-range attraction coexists with long-range repulsion. In addition, it exhibits LS in the opposite case, i.e. an interaction is repulsive as a whole, but in which short-range repulsion coexists with long-range attraction. The range of parameter with LS is now bounded by a MI and a crossover line, in which the stability of a pair of real eigenvalues exchanges with a complex quartet, instead of a BD line in which a complex quartet emerges from the collision of two real doublets. This new transition can be also shown to unfold from a different codim-2 point, while the whole scenario results from the unfolding of a codim-3 point with 6 null eigenvalues.

In conclusion, we have studied the emergence of oscillatory tails and LS in a prototypical 1-dimensional model that only supports monotonic tails with a local interaction. We discuss a general theory[5] of the scenario and the application to three different interaction kernels[6]: Gaussian, mod-exponential and Mexican-hat.

---

* manuel@ifisc.uib-csic.es http://ifisc.uib-csic.es/

[1] J.D. Murray, *Mathematical Biology*, (Springer, 2002).
[2] G.B. Ermentrout, Rep. Prog. Phys. **61**, 353 (1998).
[3] S. Coombes, Biol. Cybern. **93**, 91 (2005).
[4] L. Gelens, D. Gomila, G. Van der Sande, M.A. Matías, and P. Colet, Phys. Rev. Lett. **104**, 154101 (2010).
[5] P. Colet, M.A. Matías, L. Gelens, and D. Gomila, *Formation of localized structures in bistable systems through nonlocal spatial coupling. I. General framework*, Phys. Rev. E (in press, 2013).
[6] L. Gelens, M.A. Matías, D. Gomila, and P. Colet, *Formation of localized structures in bistable systems through nonlocal spatial coupling. II. The nonlocal Ginzburg Landau Equation*, Phys. Rev. E (in press, 2013).

Estudio numérico experimental del flujo de partículas por estrechamientos

K. Asencio, M. Madrid♣, D. Maza
Dpto. de Física y Matemática Aplicada,
Universidad de Navarra, 31080 Pamplona, España
♣ *Dpt. Ing. Mecánica, UTN La Plata, La Plata, Argentina*

Cuando un grupo cualquiera de partículas son obligadas a pasar a través de un estrechamiento su flujo o caudal viene impuesto básicamente, por el campo de fuerzas que gobierna su dinámica de forma individual. Así, los fenómenos colectivos que pudieran afectar al sistema en su conjunto dentro de las regiones más densas, quedan fuertemente diluidos en la región donde las partículas atraviesan el estrechamiento, debido a los fuertes gradientes que introduce el campo externo sobre su campo de velocidades. Se asume en general que a partir de cierta región próxima al estrechamiento – denominada genéricamente como *free fall arch*– las partículas se mueven exclusivamente bajo la acción del campo impuesto externamente (como el gravitatorio en el caso de un silo) y no por la transferencia de energía proveniente de sus vecinos. Esta idealización implica –entre otras cosas– la independencia del flujo de salida del tamaño de las partículas más allá de un simple factor dimensional que relaciona su tamaño con el del orificio de salida. En este trabajo se presenta un análisis numérico y experimental de este fenómeno, introduciendo una valoración crítica de las expresiones comúnmente usadas para predecir el flujo de sistemas formados por agentes discretos que se ven obligados a pasar por un estrechamiento.

Estudio experimental de pilas granulares formadas por partículas con caras planas

D. Maza, JL Sanz-Bretón, K. Asencio, J. Montes, I. Zuriguel
Dpto. de Física y Matemática Aplicada,
Universidad de Navarra, 31080 Pamplona, España.

La propagación de esfuerzos en pilas granulares es uno de los ejemplos paradigmáticos del comportamiento colectivo de los sistemas formados por un gran número de partículas. Contrariamente a lo que la intuición dicta, la distribucion de cargas que sufre la base de una pila granular (que esperamos sea proporcional a la altura del material que tiene por encima), no tiene un máximo en el centro. Se ha demostrado además que este efecto resulta magnificado cuando las partículas no son esféricas.

En este trabajo se reportan resultados preliminares de este comportamiento para el caso en que las partículas tengan forma cuadrada. Este es un caso extremo donde la interacción partícula partícula es dificil de definir, y donde la presencia de caras planas induce orden de largo alcance, lo que puede influenciar de forma significativa la propagación de los esfueros dentro de la pila.

Eficiencia en la captura de energía del ruido con color mediante osciladores lineales

Vicenç Méndez*[1], Daniel Campos[1] and Werner Horsthemke[2]
[1] *Grup de Física Estadística. Universitat Autònoma de Barcelona. 08193 Cerdanyola (Bellaterra). Barcelona*
[2] *2Department of Chemistry, Southern Methodist University, Dallas, Texas 75275-0314, USA*

La idea de capturar energía del ambiente para hacer funcionar pequeños dispositivos ha atraído gran interés y ha generado cierto debate. Se han estudiado recientemente diversos sistemas de captura[1,2] pero los más representativos en la literatura han sido sin duda los capturadores basados en vibraciones mecánicas. Estos capturadores se pueden modelizar mediante simples osciladores harmónicos. Los primeros estudios se centraron en los osciladores harmónicos lineales que capturan la máxima energia cuando el oscilador entra en resonancia con la fuente externa. Como en el caso del oscilador harmónico la resonancia tiene lugar a lo largo de una banda estrecha de frecuencias y la energía procedente del ruido raramente se concentra entorno a una banda sino que más bien se distribuye a lo largo de una amplia banda de frecuencias, varios grupos han empezado ha estudiar los osciladores no-lineales y proponerlos como alternativa a los lineales[3].
En la presente contribución mostraremos un estudio[4] que se centra en el análisis de la potencia útil y la eficiencia de la captura realizada mediante osciladores lineales a partir de ruido con color. En particular, hemos obtenido expresiones exactas para ambas magnitudes en función de los parámetros característicos del oscilador y del transductor que convierte la energía mecÃ¡nica en eléctrica. Mostraremos como es posible optimizar tanto la potencia como la eficiencia en función del tiempo de correlación del ruido, para el caso de un ruido con correlación exponencial. Finalmente mostraremos una comparación entre los resultados teóricos y las simulaciones así como una comparación entre los valores de la potencia y la eficiencia entre el ruido blanco y el ruido con color.

---

* vicenc.mendez@uab.cat

[1] S. Priya and D. J. Inman (eds.), Energy Harvesting Technologies (Springer, New York, 2009).
[2] T. J. Kazmierski and S. Beeby (eds.), Energy Harvesting Systems: Principles, Modeling and Applications (Springer, New York, 2011).
[3] F. Cottone, H. Vocca, and L. Gammaitoni, Phys. Rev. Lett. **102**, 080601 (2009).
[4] V. Méndez, D. Campos, W. Horsthemke, Phys. Rev. E **88**, 022124 (2013)

Predicción de la línea de coexistencia trifásica en hidratos de CO_2 mediante Dinámica Molecular

José Manuel Míguez*[1], María M. Conde[2], Jean-Philippe Torré[1], Felipe J. Blas[3], Manuel M. Piñeiro[4], Carlos Vega[2]

[1] *Laboratoire des Fluides Complexes et leurs Réservoirs, Université de Pau et des Pays de l'Adour, Pau, France*
[2] *Departamento de Química Física, Universidad Complutense de Madrid*
[3] *Departamento de Física Aplicada, Facultad de Ciencias Experimentales, Universidad de Huelva*
[4] *Departamento de Física Aplicada, Facultade de Ciencias, Universidade de Vigo*

Los hidratos de gas son estructuras cristalinas compuestas por una red tridimensional de moléculas de agua que bajo ciertas condiciones de presión y temperatura pueden albergar moléculas de pequeño tamaño (d<10Å), como por ejemplo metano o CO_2. Estos compuestos tienen numerosas aplicaciones prácticas de considerable impacto económico, ya que son considerados como sistemas propicios para la captación/almacenamiento de CO_2 industrial, y la explotación de depósitos naturales de hidratos representaría una fuente alternativa de obtención de gas natural de importancia estratégica, ya que se estima que la cantidad de gas almacenada en este tipo de depósitos es superior a la encontrada en todos los depósitos convencionales conocidos[1].

En este trabajo se ha estimado la línea de coexistencia trifásica (hidrato - agua líquida - CO_2 líquido), que se puede diferenciar en el diagrama de fases de mezcla binaria agua - CO_2, mediante simulaciones de dinámica molecular, usando GROMACS como herramienta de cálculo. La temperatura y la presión a la cual las tres fases se encuentran en equilibrio fueron determinadas mediante simulaciones en el colectivo NPT usando el método de coexistencia directa de las tres fases involucradas. En estas simulaciones la molécula de CO_2 fue representada mediante un modelo molecular formado por tres átomos, cada uno de ellos representado por un centro Lennard-Jones y una carga eléctrica puntual. Dentro de las distintas versiones disponibles para esta estructura molecular, se ha seleccionado el modelo TraPPE[2], cuya eficacia en la descripción del equilibrio de fase sólido-líquido del CO_2 ha sido ya demostrada[3]. Para el caso del agua, se ha seleccionado también un modelo rígido no-polarizable, el denominado TIP4P-ICE[4] ya que este modelo proporciona una buena descripción de las fases sólidas del agua, y además predice correctamente los valores experimentales de la línea de tres fases para la mezcla agua-metano[5]. Las reglas de mezcla de Lorentz - Berthelot se aplicaron para la el cálculo de las interacciones cruzadas. Finalmente, la predicción de la línea trifásica mediante simulación molecular se comparó con los resultados experimentales.

---

* jose-manuel.miguez@univ-pau.fr

[1] G. J. MacDonald, *Annual Review of Energy* 15, 53 (1990).
[2] J. J. Potoff y J. I. Siepmann, *AIChE* 47, 1676 (2001).
[3] G. Pérez-Sánchez, D. González-Salgado, M. M. Piñeiro y C. Vega, *J. Chem. Phys.* 138, 084506 (2013).
[4] J. L. F. Abascal, E. Sanz, R. G. Fernández y C. Vega, *J. Chem. Phys.* 122, 234511, (2005).
[5] M. M. Conde y C. Vega, *J. Chem. Phys.* 133, 064507, (2010).

Stretched criticality and localization in hierarchical networks

Paolo Moretti* and Miguel Ángel Muñoz
Instituto Carlos I de Física Teórica y Computacional
Universidad de Granada, Fuentenueva s/n, 18071-Granada

The nature of the underlying contact pattern is known to play a crucial role in spreading and synchronization phenomena. The ability to access real data has recently revealed that several systems of biological and techno-social relevance can be described as hierarchical modular networks (social networks, brain networks, gene regulatory networks etc.). Hierarchical modular networks may exhibit fractal-like properties across several levels and consequently give rise to exotic dynamic behavior.

We study dynamical models of spreading, ordering and synchronization in hierarchical modular networks. We show that the traditional critical-point scenario, which characterizes spreading phenomena in generic complex networks, is replaced by an extended critical-like region, a Griffiths phase, which stems from the network structural multi-level heterogeneity [1]. Throughout the Griffiths phase, the system exhibits the attributes usually associated with critical points, such as enhanced response and huge dynamic range. More importantly, the Griffiths phase is characterized by persistent activity, lingering in rare regions that remain active for exponentially large times even below the dynamic threshold. Recent studies have shown how network heterogeneity or disorder may give rise to Griffiths phases in complex networks [2]. In analogy with the phenomenon of Anderson localization in disordered media, we prove that the emergence of the Griffiths phenomenon is related to the existence of localized states in the network contact pattern, resulting in exteded regions of persistent activity and slow synchronization. We provide a numerical method for fast sampling of the spectral hallmarks of localization in the adjacency matrix of large networks and propose a revised theoretical framework that adds localization to the traditional mean-field description.

Our methods prove effective in the study of activity in brain networks, where the extended regions of criticality observed in experiments arise from Griffiths phases induced by the hierarchical architecture of the brain neural network [3]. More importantly, we believe that our results on rare regions of localized and persistent activity are of great relevance to spreading processes occurring in low-dimensional disordered systems as well as hierarchical and localized contact patterns in social sciences and epidemiology, whether they are induced by social factors, non-trivial mobility constraints, geographical isolation or targeted border policies.

---

* moretti.paolo@gmail.com

[1] P. Moretti and M. A. Muñoz, *Nature Communn* **4**, 22521 (2013)
[2] Muñoz et al. (2010) *Phys. Rev. Lett.* **105**, 128701 (2010)
[3] A. Haimovici *et al.*, *Phys. Rev. Lett.* **110**, 178101 (2013)

New spreading law of thin film liquids controlled by gravity and vdW forces under thermal fluctuations

Svetozar Nesic*, Rodolfo Cuerno, Esteban Moro
Grupo Interdisciplinar de Sistemas Complejos(GISC) and Departamento de Matemáticas, Universidad Carlos III de Madrid, Avenida de la Universidad 30, E-28911 Leganés, Spain

The dynamics of a stochastic thin film is given by the equation

$$\frac{\partial h}{\partial t} = \nabla \cdot \left(h^3 \nabla\, p\right) + \sqrt{2\sigma}\,\nabla\left[h^{3/2}\epsilon(x,t)\right] \qquad (1)$$

where p is a generalized pressure term accounting for the effects of surface tension, gravity and van der Waals (vdW) attraction. The second term on the RHS represents thermal fluctuations where $\epsilon(x,t)$ is a Gaussian white noise, zero mean and delta correlated.[1,2] When surface tension is dominant force (no vdW, gravity nor noise) any perturbation of a film as well as the droplet spreading will lead to a flat film solution. In the case of droplet spreading, the droplet width ℓ, see the fig. 1, undergoes Tanner's law[3], $\ell \sim t^{1/7}$. If thermal fluctuations are accounted, it was shown[4] that the stochastic force will take over the dynamics of the system and introduce a new enhanced spreading low $\ell \sim t^{1/4}$.

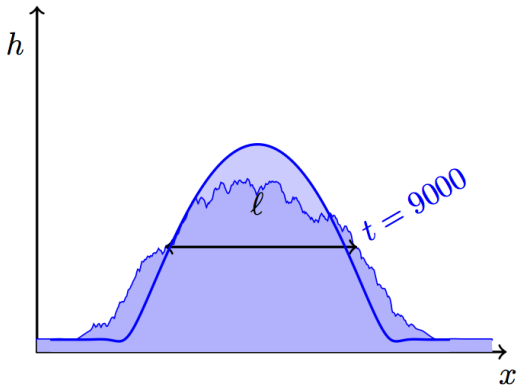

FIG. 1. Stochastic and Deterministic droplet surface. Droplet width ℓ describes dynamics of a droplet. Results from simulations.

On the other hand, when we have both surface tension and vdW force the stable solution will be a droplet with a contact angle formed[5] as a result of the interplay between these two forces. The contact angle can easily be calculated using Laplace-Young condition.[6]

Here we present results from simulations of the $1d$ stochastic thin film equation 1 using finite differences scheme,[7] in which noise competes with the effects of vdW and surface tension forces which introduce a fixed contact angle. On the fig. 2 we show that on average there is a small change in droplet width in the region where the width has saturated when the noise term is introduced. The noise term together with surface tension tends to spread the droplet which leads to a small correction in the Laplace-Young condition.

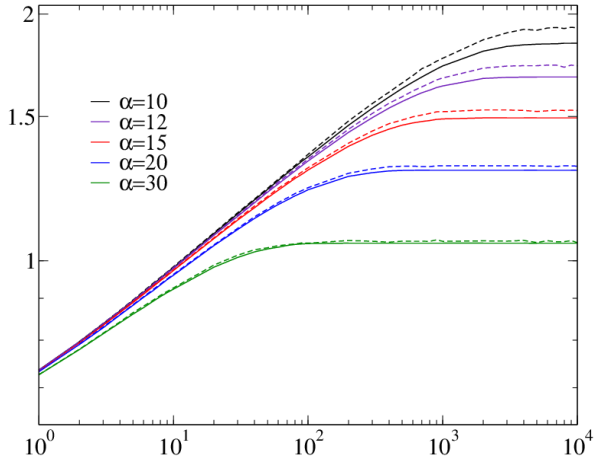

FIG. 2. Width of a droplet as a function of time for a given contact angle. Dashed lines represent stochastic films while continuous lines represent deterministic films.

Moreover, fluctuations accelerate breakup when a thin flat film is slightly perturbed[1,6] the final aim of the work being the study of the dynamics of such films in more realistic $3D$ setups.

* snesic@math.uc3m.es

[1] G. Grun, K. Mecke, M. Rauscher, J. of Stat. Phy. **122**, 1261 (2006)
[2] H. Bruus, *"Theoretical Microfluidics"*, Oxford University Press (2008).
[3] L. Tanner, J. Phys. D **95**, 1473 (1979)
[4] B. Davidovitch, E. Moro, and H. Stone, Phy. Rev. Lett. **95**, 244505 (2005).
[5] D. Bonn, J. Eggers, J. Indokeu, J. Meunier, E. Rolley, Rev. of Modern Phys. **81**, 0034-6861 (2009)
[6] J.A. Diez, L. Kondic, Phy. of Fluids **19**, 072107 (2007)
[7] J. A. Diez, L. Kondic, A. Bertozzi, Phys. Rev. E **63**, 011208 (2000).
[8] L. Bocquet and E. Charlaix, Chem. Society Rev. **39**, 1073 (2010).

Mapping dynamics to graphs. The visibility algorithm.

Bartolo Luque*, Lucas Lacasa, Ángel M. Núñez
EIAE, Universidad Politécnica de Madrid
Plaza del Cardenal Cisneros, 2 28040-Madrid

Disregarding any underlying process (and therefore any physical, chemical, economical or whichever meaning of its mere numeric values), we can consider a time series just as an ordered set of values and play the naive mathematical game of turning this set into a different mathematical object with the aids of an abstract mapping, and see what happens: which properties of the original set are conserved, which are transformed and how, what can we say about one of the mathematical representations just by looking at the other... This exercise is of mathematical interest by itself. In addition, it turns out that time series or signals is a universal method of extracting information from dynamical systems in any field of science. Therefore, the preceding mathematical game gains some unexpected practical interest as it opens the possibility of analyzing a time series (i.e. the outcome of a dynamical process) from an alternative angle. Of course, the information stored in the original time series should be somehow conserved in the mapping. The motivation is completed when the new representation belongs to a relatively mature mathematical field, where information encoded in such a representation can be effectively disentangled and processed. This is, in a nutshell, a first motivation to map time series into networks.

This motivation is increased by two interconnected factors: first, although a mature field, time series analysis has some limitations, when it refers to study the so called complex signals. Beyond the linear regime, there exist a wide range of phenomena (not exclusive to physics) which are usually embraced in the field of the so called Complex Systems. Under this vague definition lies a common feature: the relevant effect of nonlinearities in their mathematical representation. This feature can be reflected in the temporal evolution of (at least one of) the variables describing the system and necessitates the use of specific tools for nonlinear analysis. Dynamical phenomena such as chaos, long-range correlated stochastic processes, intermittency, multifractality, etc... are examples of complex phenomena where time series analysis is pushed to its own limits. Nonlinear time series analysis develops from techniques such as nonlinear correlation functions, embedding algorithms, multrifractal spectra, projection theorems... tools that increase in complexity parallel to the complexity of the process/series under study. New approaches, new paradigms to deal with complexity are not only welcome, but needed. Approaches that deal with the intrinsic nonlinearity by being intrinsically nonlinear, that deal with the possible multiscale character of the underlying process by being designed to naturally incorporate multiple scales. And such is the framework of networks, of graph theory. Second, the technological era brings us the possibility of digitally analyze myriads of data in a glimpse. Massive data sets can nowadays be parsed, and with the aid of well suited algorithms, we can have access and filter data from many processes, let it be of physical, technological or even social garment. It is now time to develop new approaches to filter such plethora of information.

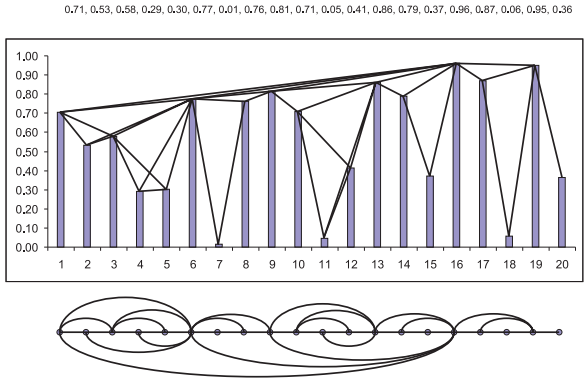

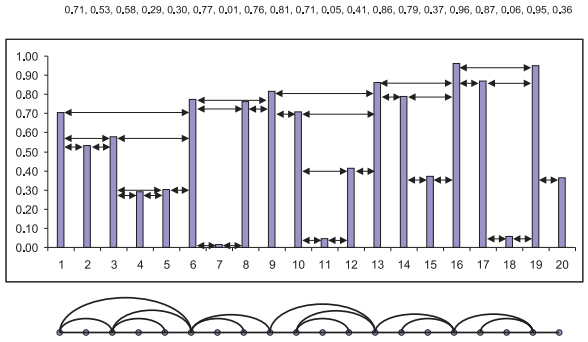

It is in this context that the network approach for time series analysis was born. The family of visibility algorithms (Va) constitute one of other possibilities to map a time series into a graph and subsequently analyze the structure of the series through the set of tools developed in the graph/complex networks theory.

The idea of mapping time series into graphs seems attractive because it lays a bridge between two prolific fields of modern science as Nonlinear Signal Analysis and Complex Networks Theory, so much so that it has attracted the attention of several research groups which have contributed to the topic with different strategies of mapping. Among all these methods of mapping, in this talk we will concentrate our attention on the one developed in[1] and

subsequent works. To cite some of its most relevant features, we will stress its intrinsic nonlocality, its low computational cost, its straightforward implementation and its quite 'simple' way of inherit the time series properties in the structure of the associated graphs. These features are going to make it easier to find connections between the underlying processes and the networks obtained from them by a direct analysis of the latter.

---

* bartolome.luque@upm.es

[1] Lacasa L., Luque B., Ballesteros F., Luque J. & Nuño J.C. (2008). From time series to complex networks: the visibility graph. *Proc. Natl. Acad. Sci. USA* **105**, 13, 4972-4975.

[2] Lacasa L., Luque B., Nuño J.C. & Luque J. (2009). The Visibility Graph: a new method for estimating the Hurst exponent of fractional Brownian motion. *EPL* **86**, 30001 (2009).

[3] Luque B., Lacasa L., Balleteros F., & Luque J. (2009). Horizontal visibility graphs: exact results for random time series. *Phys Rev E* **80**, 046103 (2009).

[4] Lacasa, L. & Toral, R. (2010). Description of stochastic and chaotic series using visibility graphs. *Phys. Rev. E* **82**, 036120 (2010).

[5] Núñez, A. M., Lacasa, L., Valero, E., Gómez, J.P. & Luque, B. (2010). Detecting series periodicity with horizontal visibility graphs. *International Journal of Bifurcation and Chaos*, **in press**, 2010.

[6] B. Luque, L. Lacasa, F.J. Ballesteros & A. Robledo (2011). Feigenbaum graphs: a complex network perspective of chaos *PLoS ONE* **6**, 9 (2011).

[7] Lacasa, L., Núñez, A. M., Roldan, E., Parrondo, J.M.R., & Luque, B. (2011).Time series irreversibility: a visibility graph approach. *European Physical Journal B* **85**, 217 (2012).

[8] Luque B., Lacasa L. & Robledo A., Feigenbaum graphs at the onset of chaos. *Physics Letters A* **376**, 3625-3629 (2012).

[9] Luque B., Lacasa L., Ballesteros F. & Robledo A., Analytical properties of horizontal visibility graphs in the Feigenbaum scenario. *Chaos* **22**, 013109 (2012).

[10] Luque B., Cordero-Gracia M., Gómez M. & Robledo A., Quasiperiodic graphs at the onset of chaos. arXiv:1312.3089.

[11] Núñez, Á. M., Luque, B., Lacasa L., Gómez J. P. & Robledo, A., *Phys. Rev. E* **87**, 5, 052801 (2013).

[12] Núñez, Á. M., Lacasa L., Gómez J. P., *Journal of Physics A* **in press** (2014).

Mapping dynamics to graphs. The case of intermittency.

Ángel M. Núñez*, Bartolo Luque, Lucas Lacasa, José Patricio Gómez
EIAE, Universidad Politécnica de Madrid
Plaza del Cardenal Cisneros, 2 28040-Madrid

The type-I and type-II intermittency routes to (or out of) chaos are investigated within the Horizontal Visibility (HV) graph theory. For that purpose, we address both trajectories generated by unimodal maps close to an inverse tangent bifurcation and trajectories generated by iterated maps close to a Neimark-Sacker bifurcation and we construct their associated HV graphs. We show how the alternation of laminar episodes and chaotic bursts imprints a fingerprint in the resulting graph structure. Accordingly, we derive a phenomenological theory with analytical results that predict quantitative values for several network parameters. In particular, we predict that the characteristic power-law scaling of the mean length of laminar trend sizes is fully inherited by the variance of the graphs degree distribution, in good agreement with the numerics. We also report numerical evidence on how the characteristic power-law scaling of the Lyapunov exponent as a function of the distance to the critical point is inherited in the graphs by an analogous scaling of block entropy functionals defined on the graphs. Furthermore, we are able to recast the full set of HV graphs generated by both types (I, II) of intermittent dynamics into renormalization group frameworks, where the fixed points of thier graph-theoretical Renormalization Group (RG) flows account for the different types of dynamics. We also establish that the nontrivial fixed points of these flows coincide with the critical condition in each case and that the corresponding invariant graphs exhibit extremal entropic properties.

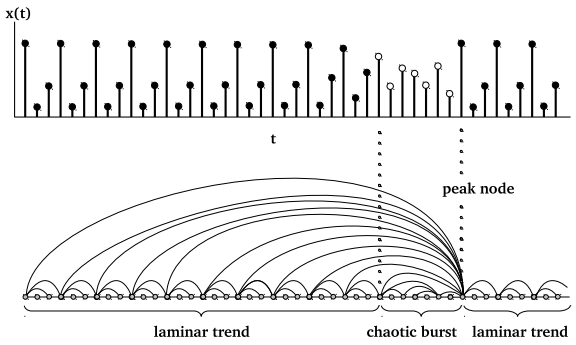

FIG. 1. Graphical illustration of how the Horizontal Visibility (HV) graph inherits in its structure the dynamics of the associated intermittent series. In the top of the figure we show a sample intermittent series generated by the logistic map close to μ_c ($\epsilon > 0$), producing laminar regions (black) mixed with chaotic bursts (white). In the bottom we plot the associated HV graph. Laminar regions are mapped into nodes with a periodic backbone, whereas the actual pseudoperiodicity of the series is inherited in the graph by the existence of so called peak or interfacial nodes. Chaotic bursts are mapped into chaotic nodes, with a characteristic degree distribution (see the text).

* angel.nunhez@gmail.com

[1] Núñez, Á. M., Luque, B., Lacasa L., Gómez J. P. & Robledo, A., *Phys. Rev. E* **87**, 5, 052801 (2013).
[2] Núñez, Á. M., Lacasa L., Gómez J. P., *Journal of Physics A* **in press** (2014).

Pattern selection by dynamical paths

David Palau-Ortin[1], Pau Formosa-Jordan, José María Sancho, Marta Ibañes
Departament d'Estructura i Constituents de la Matèria
Facultat de Física
Universitat de Barcelona
08028 Barcelona

During embryonic development isogenic cells acquire distinct traits, becoming differentiated into different cell types. Differentiation commonly involves spatial coupling through signaling gradients or cell-to-cell communication, and it is usually related to pattern formation. The selection of a specific pattern, with a characteristic number and location of each cell type, is crucial for tissue formation. Therefore, this selection is reliable done. Yet, the dynamics underlying developmental programs are highly complex, nonlinear and involve stochasticity. The stochasticity partially arises from the low copy number of the reactants involved in these genetic reactions. These dynamics can potentially drive multiple stable patterns. This raises the issue of how pattern selection can occur and how reliable selections can arise.

Herein we make use of a model[2] that mediates cell-to-cell communication through an intercellular mutual inhibition and includes a cell-autonomous negative feedback loop[3] to address these issues. drive several different stable pattern solutions[3]: homogeneous solutions – all cells are the same cell type (H in FIG. 1) –, *salt-and-pepper* patterns – periodic patterns composed of two cell types, one completely surrounding the other one (P and I in FIG. 1) –, and the stripped pattern – two cell types forming rows of cells (S in FIG. 1). This dynamics have been used to characterize the interaction between cells through the Notch pathway, which is one of the main signaling pathways acting during animal development. This pathway relies on a transmembrane receptor, Notch, that can bind to a ligand, Delta, anchored on an adjacent cell.

We consider the dynamical process of reaching a spatio–temporal pattern through the dynamical change of a control parameter (signal, Fig.1). Therefore, the pattern which is finally selected and the reliability of this selection depends on the dynamical evolution of this control parameter. Changes on parameters are translated into dynamical paths on the parameter space, where different regions are identified according to the pattern solutions that are stable. Hence, the characteristics of these dynamical paths are crucial for selecting a certain pattern under a scenario in which different solutions coexist.

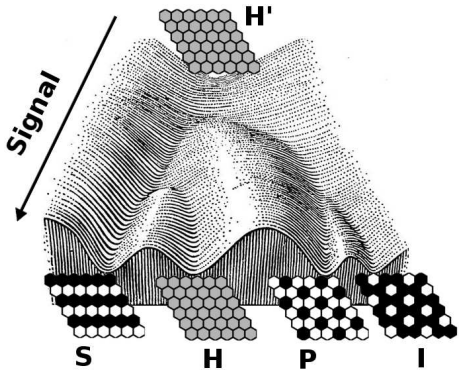

FIG. 1. Modification of the figure of Waddington's epigenetic landscape[5]. The system starts in a homogeneous solution (H) and, after a parameter modification (signal), it can select among four different patterns: S, H, P, I.

Our study shows the dependency of the pattern finally selected and the characteristics of the chosen dynamical path. These characteristics consist on (i) the existence of a pattern and its stability in the different regions crossed by the path, (ii) the velocity of the parameter changes, and (iii) whether the dynamical path simultaneously occurs in all cells or it sequentially occurs along the tissue through a propagating wave. Among others, we show that the pattern of stripes, which does not correspond to the fastest growing mode, can be selected if the parameter change propagates with an optimal velocity[5].

---

[1] palau@emc.ub.es

[2] Collier JR, Monk NA, Maini PK, and Lewis JH (1996) *Pattern formation by lateral inhibition with feedback: a mathematical model of Delta-Notch intercellular signalling.* J Theor Biol 183: 429–446.

[3] Formosa-Jordan P, Ibanes M (2013) Competition in Notch signaling with cis enriches cell fate decisions. Submitted.

[4] Waddington CH (1942) *Canalisation of development and the inheritance of acquired characters.* Nature 150: 563–564

[5] Palau–Ortin D, Formosa–Jordan P, Sancho JM, and Ibañes M (2014) *Pattern selection by dynamical paths.* Preprint

Sincronización de sistemas no idénticos con caos espacio-temporal

Diego Pazó*, Juan M. López y Miguel A. Rodríguez
IFCA, Instituto de Física de Cantabria
CSIC-Universidad de Cantabria 39005-Santander

La sincronización caótica entre sistemas *idénticos* con caos espacio-temporal demuestra una serie de propiedades universales. En particular, el error de sincronización —visto como un campo extendido en el espacio— tiene una dinámica que pertenece[1] a la clase de universalidad de la ecuación 'bounded' Kardar-Parisi-Zhang (bKPZ). Para la sincronización entre sistemas con retraso se encuentra[2] la misma universalidad, pues estos se comportan de forma efectiva como sistemas extendidos en el espacio.

El propósito de esta comunicación es describir como los resultados mencionados se trasladan a los sistemas *no* idénticos, situación inevitable en los experimentos. El problema tiene interés también debido a la relación entre la sincronización y la técnica de asimilación de datos conocida como 'nudging'.

En el caso de sistemas no idénticos acoplados unidireccionalmente, es decir la configuración maestro-esclavo o emisor-receptor, consideramos dos tipos de error:

1. Error entre el maestro y el esclavo.
2. Error entre el esclavo y un sistema auxiliar (o réplica), pues la convergencia de ambos es un criterio que se suele usar para determinar la 'sincronización generalizada'.

Si la diferencia entre el maestro y el esclavo está originada por una desintonía en los parámetros, encontramos[3] que:

1. El error entre el maestro y el esclavo puede describirse cualitativamente como una superficie gobernada por la ecuación de KPZ con dos muros (o 'doubly bounded').
2. El error entre el esclavo y un sistema auxiliar pertenece a la clase de universalidad de bKPZ.

---

* pazo@ifca.unican.es

[1] V. Ahlers y A. Pikovsky, Phys. Rev. Lett. **88**, 036202 (2002).
[2] I. G. Szendro y J. M. López, Phys. Rev. E **71**, 055203 (2005).
[3] D. Pazó, J. M. López y M. A. Rodríguez, J. Stat. Mech. (enviado).

Mixing and clustering in compressible chaotic stirred flows

Vicente Pérez-Muñuzuri*
Group of Nonlinear Physics, Faculty of Physics, University of Santiago de Compostela. E-15782 Santiago de Compostela, Spain

Transport of inertial (finite-size) particles in flows shows properties typical of compressible fluids, even in incompressible flows. The most unexpected behavior is the formation of clusters of particles out of an initially homogeneous distribution. In the limit the Stokes drag is very strong, inertial particles recover the motion of Lagrangian tracers and no clustering should be expected[1]. However, passive tracers moving on the surface of an incompressible flow may lead to the formation of cluster structures[2].

The effect of compressibility on the mixing of Lagrangian tracers is analyzed in chaotic stirred flows. Mixing is studied in terms of the Finite-Time Lyapunov Exponents (FTLE)[3]. Mixing and clustering of passive tracers surrounded by Lagrangian coherent structures is observed to increase with compressibility intensity. The role of the stirring rate and compressibility on mixing and clustering has been analyzed.

We investigate the effects of compressibility in the periodically varying double-gyre flow[4,5],

$$u = -\pi A \frac{\rho_0}{\rho} \sin(\pi f(x,t)) \cos(\pi y)$$
$$v = \pi A \frac{\rho_0}{\rho} \frac{\partial f}{\partial x} \cos(\pi f(x,t)) \sin(\pi y), \qquad (1)$$

where

$$f(x,t) = a(t)x^2 + b(t)x, \qquad (2)$$

over the domain $[0,2] \times [0,1]$. $a(t) = u_0 \sin \omega t$ and $b(t) = 1 - 2u_0 \sin \omega t$. $T = 2\pi/\omega$ and A are the period and amplitude of the flow, respectively. The periodic perturbation leads to mixing between the two gyres.

In order to satisfy the continuity equation, $\partial_i(\rho u_i) = 0$, the spatial dependence of the flow density can be written as,

$$\rho(x,y) = \rho_0 \left[1 + \epsilon \sin(2\pi x/\lambda) \sin(2\pi y/\lambda)\right], \qquad (3)$$

where ϵ and λ are the compressibility of the flow and wavelength, respectively.

We analyze the effects of ϵ and λ on the mixing of the double-gyre flow in terms of the FTLE fields. Compressibility perturbation wrinkles the LCS in the small-wavelength limit, whereas for the large wavelengths LCS are slightly distorted since the entire domain is embedded in nearly a wavelength (Fig. 1). The density profile favors some initial clustering of the particles that is broken by the periodically contracting and expanding of the gyres. Then particles move within the interstices between LCS.

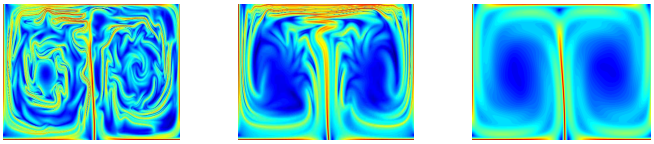

FIG. 1. Finite-Time Lyapunov Exponent σ for the double-gyre flow. $\lambda = 0.4$ (left panel) and $\lambda = 0.8$ (central panel). Right panel shows the FTLE for the incompressible flow model for comparison ($\epsilon = 0$).

Particles belonging to these clusters are characterized by a negative value of the FTLE, while for an incompressible flow ($\epsilon = 0$) the FTLE values are always positive. For any wavelength λ of the density field, as ϵ increases, mixing and clustering are enhanced. The mean FTLE and the variability of the FTLE increase with the compressibility. The increase of variability is due to an increase in the number of tracers with negative FTLE followed by an increase in the number of clusters or aggregates of these particles. Both, the mean and the variability of the FTLE, decrease with increasing λ. However, while the number of tracers with negative Lyapunov exponent hardly it changes with λ, the number of clusters and their size diminish with increasing λ. In other words, at fixed ϵ, clusters are smaller but more populated at large values of λ.

In the considered flow, mixing is strongly affected by compressibility, and the compressibility field forces a strong localization of density[7,2,6]. Formation of clusters separated by Lagrangian coherent structures has been analyzed in terms of ϵ. Cluster formation is enhanced as compressibility increases based on the combination of particles attracted to areas with large compression $\rho/\rho_0 > 1$, and detaching of patches of particles from these initial clusters that wander among the chaotic flow. For enough large stirring rate the flow is quenched and clusters survive forever for any wave length and compressibility intensity.

* vicente.perez@cesga.es

[1] J. Bec, Phys. Fluids **15**, L81–L84 (2003); G. Boffeta, F. de Lillo, and A. Gamba, Phys. Fluids **16**, L20–L23 (2004).
[2] V.I. Klyatskin and A.I. Saichev, J. Exp. Theor. Phys. **84**, 716–724 (1997).
[3] Z. Neufeld and E. Hernández-García, *Chemical and biological processes in fluid flows* (Imperial College Press, 2009).
[4] S.C. Shadden, F. Lekien, and J. Marsden, Physica D **212**, 271–304 (2005).
[5] V. Pérez-Muñuzuri and F. Huhn, Nonlin. Processes Geophys. **20**, 987–991 (2013).
[6] F. Bianco, S. Chibbaro, D. Vergni and A. Vulpiani, Phys. Rev. E. **87**, 042924 (2013).

Potencial de interacción en hidratos de gas tipo sI

Martín Pérez-Rodríguez*, Ángel Vidal Vidal, Manuel M. Piñeiro
Departamento de Física Aplicada, Universidade de Vigo

Introducción. Los clatratos de gas (o hidratos de gas[1]) son compuestos en los que el agua se ordena en celdas geométricas alrededor de moléculas pequeñas como CO_2 or CH_4, que se repiten en el espacio formando una red periódica, a temperaturas bajas o presiones moderadamente altas. Los hidratos de gas presentan un interés creciente debido principalmente a su capacidad para secuestrar y retener gases de efecto invernadero, y a su abundancia en ciertos estratos de la corteza oceánica, que los convierte en una potencial fuente de gas natural.

Los diagramas de fases de estos sistemas son accesibles experimentalmente pero la falta de una teoría microscópica completa hace muy difícil su adecuada predicción. Tradicionalmente, el cálculo de diagramas de fase se viene haciendo mediante ecuaciones de estado, como SAFT[2] (Statistical Associating Fluid Theory), aunque hoy en día se emplean también en gran medida técnicas de simulación molecular, bien sean de dinámica clásica o de Monte Carlo. En todas ellas, el potencial de interacción entre las celdas y la molécula atrapada juega un papel clave en la capacidad predictiva del modelo. En este trabajo se presenta un estudio en curso del potencial dispersivo con el que el metano interacciona con la red de agua en el interior de los hidratos de tipo sI, y cuando se aproxima y pasa a través de las caras poligonales de una celda a otra adyacente.

Resultados. La estructura del clatrato sI está constituída por celdas de dos tipos: una con forma de dodecahedro (D) y otra de trapezoedro hexagonal truncado (T). Esta última consta de 12 caras pentagonales y 2 hexagonales por lo que fue elegida como modelo para los cálculos, ya que la celda D consta solamente de 12 caras pentagonales idénticas a las de la celda T. Se investigó la densidad electrónica debida a las moléculas de la red de agua dentro de la celda T utilizando un análisis topológico de la densidad electrónica[3], y posteriormente, el potencial de interacción del metano a su paso través de las caras de la celda mediante DFT[4] (Density Functional Theory). El análisis topológico (figura 1.A) permite describir los caminos de mínima densidad a través de las caras, sobre los que se podría deslizar la molécula de metano. El potencial de interacción a lo largo de estos caminos se ilustra en la figura 1.B. Las barreras de potencial obtenidas para las caras pentagonales son aproximadamente el doble de las obtenidas para las caras hexagonales, implicando una probabilidad mucho mayor de paso a través de estas últimas, lo que, unido a que en la estructura sI las caras hexagonales se alinean paralelamente en canales, sugiere una contribución preferente al transporte de gas. Con respecto a la forma del potencial, se observa que el pozo cuadrado clásico puede mejorarse suavizando las paredes del mismo. Si bien el fondo del potencial calculado muesta una región plana, los bordes presentan una pendiente finita (incluso más suave que Lennard-Jones), y que debe ser considerada a la hora de definir un potencial efectivo. Finalmente, estos resultados sugieren la posibilidad de introducir potenciales asimétricos, dada la preferencia de paso a través de las caras alineadas.

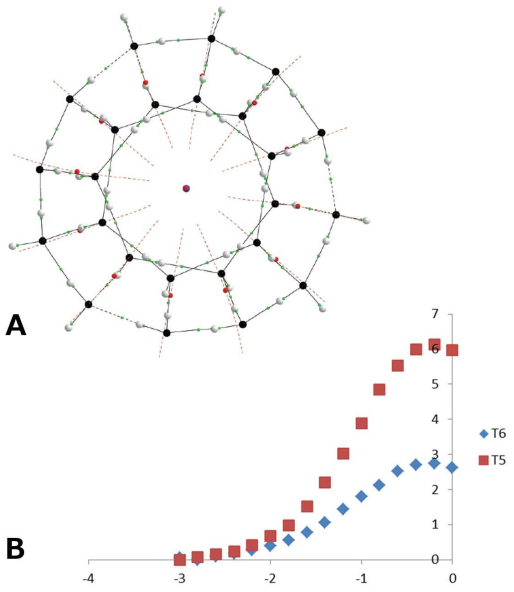

FIG. 1. A. Análisis de la densidad electrónica en una celda de tipo T en la estructura de hidrato sI. Las esferas negras correspoden a átomos de oxígeno y las grises a hidrógeno. Las esferas rojas representan el centro de las caras, por donde se deslizan los caminos de menor densidad electrónica representados con líneas de trazos. B. Potencial de interacción de una molécula de CH_4 aproximándose al centro de una cara pentagonal(T5) y hexagonal (T6).

Los autores agradecen al CESGA (Centro de Supercomputación de Galicia) los recursos computacionales.

* martinperez@uvigo.es.

[1] Sloan, E. D. *Clathrate Hydrates of Natural Gases*, 2nd ed.; Marcel Dekker: New York, 1998.
[2] Dufal, S., Galindo, A., Jackson, G., Haslam, A.J., Mol. Phys. (2012), 110, 1223.
[3] Bader, R. *A quantum theory of molecular structure and its applications*, Chemical Reviews (1991), 91, 893.
[4] W. Kohn and L. J. Sham, Phys. Rev. (1965), 140, A1133. En concreto, se ha utilizado el nivel de teoría B3LYP/6-311+g(d,p) en la aproximación del programa Gaussian 09 (www.gaussian.com).

On the selective advantage of diffusing faster

Simone Pigolotti*
Dept. de Fisica i Eng. Nuclear, Universitat Politecnica de Catalunya Edif. GAIA, Rambla Sant Nebridi 22, 08222 Terrassa, Barcelona, Spain.

We present a stochastic spatial model of biological competition in which two species have the same birth and death rates, but differ in their diffusion constants. We show that even a relative difference in diffusivity on the order of a few percent may lead to a strong bias in the coarsening process favoring the more agile species. We quantify this selective advantage theoretically and present analytical formulas for the average growth of the fastest species and its fixation probability. Finally, we show that advection by an incompressible flow does not alter our result, provided the turbulent scale is sufficiently large.

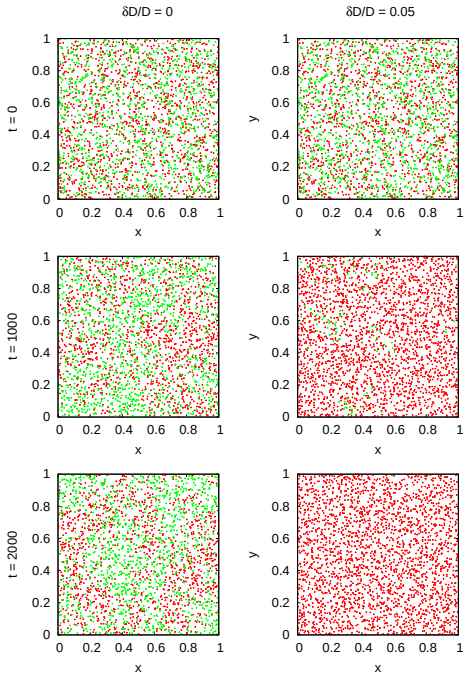

FIG. 1. Snapshots of $2d$ configurations of the particle model at different times. In all panels, parameters are $N = 10^4$ and $D = 10^{-4}$. In the simulation of the left column, the two species have the same diffusivity, while in the right column the red species has diffusivity $D + \delta D$ with $\delta D/D = 0.05$. To help the viewer, configurations has been downsampled (one every four particles, chosen at random, are shown).

* simone.pigolotti@upc.edu

[1] S. Pigolotti and R. Benzi, submitted (arXiv:1307.8252).

Fusión de datos en redes de sensores móviles

M. Rebollo*
Universitat Politècnica de València
Camino de Vera s/n 46021 Valencia

Las técnicas de fusión de datos permiten combinar la información recogida por un conjunto de sensores incluyendo información redundante. Los algoritmos de *gossip* y, en particular, los algoritmos de consenso[1] han sido ampliamente utilizados con este propósito, pues constituyen una forma eficiente de sincronizar la información de la red de sensores de forma descentralizada.

El presente trabajo estudia el efecto que distintos esquemas de movimiento en la velocidad de cubrimiento del área completa. En segundo lugar, se propone una modificación del algoritmo de consenso para que se cada nodo incorpore de forma local los valores leídos de las nuevas posiciones y lo incorpore al cómputo global del valor medio, de manera que el proceso converja de manera incremental al valor promedio exacto del campo.

Sea un campo escalar cuyo valor medio se desea medir. Sobre él se sitúa una red de n sensores, cada uno de los cuales determina el valor medio de los puntos del campo que ha recorrido hasta el momento (Fig. 1). Cada sensor tiene un alcance r e intercambia información con todos los sensores que se encuentren dentro de su radio siguiendo el algoritmo de consenso, cuya dinámica se rige por la ecuación:

$$x_i(t+1) = x_i(t) + \varepsilon \sum_{j \in N_i(t)} [x_j(t) - x_i(t)]$$

donde $N_i(t)$ son los vecinos del sensor i en el instante t. El algoritmo converge al valor medio de los valores iniciales $x_i(0)$.

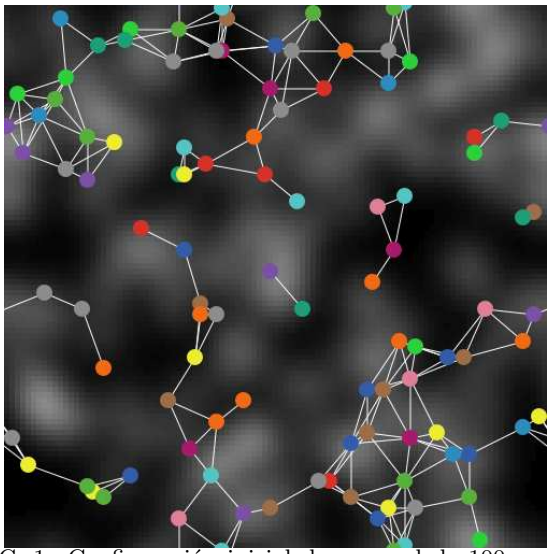

FIG. 1. Configuración inicial de una red de 100 sensores con enlaces a una distancia máxima de 12 uds. sobre un campo escalar.

Se han estudiado 4 tipos de movimientos: (i) rectilíneo (todos los sensores en la misma dirección), (ii) un modelo de partículas con choques elásticos, (iii) paseos aleatorios y (iv) vuelos de Lêvy (Fig. 2). Estos últimos cubren todo el área en el mismo orden de magnitud que el movimiento rectilíneo (que se puede considerar óptimo), pero la red converge al valor medio del campo al formar un único componente conexo. No ocurre así en general con el movimiento rectilíneo, pues los vecinos de cada sensor no varían al desplazarse en el mismo sentido y a la misma velocidad.)

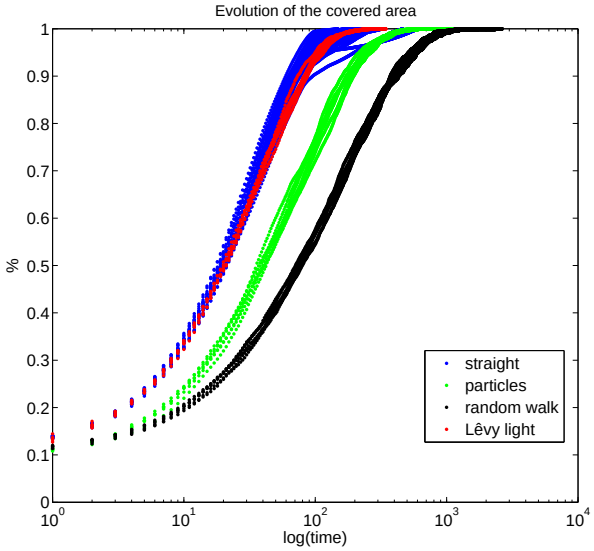

FIG. 2. Evolución del porcentaje del área cubierta con el tiempo usando caminos rectos, un modelo de dinámica de partículas, paseos aleatorios y vuelos de Lêvy

Por otro lado, para corregir la desviación de la media, hay que tener en cuenta que en el proceso de consenso se conserva la suma de los valores iniciales, $s = \sum_i x_i(0) = \sum_i x_i(t)\ \forall t$. Sea $z_i(0)$ el nuevo valor medio para el sensor i. La nueva suma debería ser $\hat{s} = z_i(0) + \sum_{j \neq i} x_j(0) = z_i(0) + \sum_i x_i(0) - x_i(0) = z_i(0) - x_i(0) + s$. Luego es suficiente con añadir al nodo i la variación que se ha producido en su valor medio para que converja al valor medio exacto del campo.

* mrebollo@dsic.upv.es

[1] R. Olfati-Saber and R.M. Murray, *IEEE T-AC*, **49**(9), 1520-1533, (2004).

Transición de rellenado tricrítica en el modelo de Ising 3D de doble cuña por simulación de Monte Carlo

Álvaro Rodríguez-Rivas*†, José Manuel Romero-Enrique†, Luis F. Rull† y Andrey Milchev‡ §

† *Universidad de Sevilla, Dept. de Física Atómica, Molecular y Nuclear, Avenida Reina mercedes s/n, 41012, Sevilla, España*

‡ *Institute for Physical Chemistry, Bulgarian Academy of Sciences, 1113 Sofia, Bulgaria*

§ *Institut für Physik, Johannes Gutenberg-Universität Mainz, Staudinger Weg 7, D-55099 Mainz, Germany*

En este trabajo se presentan simulaciones de Monte Carlo que muestran evidencias de una transición de rellenado tricrítica. Esta transición fue predicha en el marco del modelo de modos de respiración[3–5]. Las simulaciones se realizaron para el modelo de Ising tridimensional en una geometría de doble cuña, que era adecuada para el estudio de la transición de rellenado crítica[1,2,6]. Para nuestro estudio, hemos modificado dicho modelo, de manera que, adicionalmente a los campos superficiales H_S antisimétricos actuando en las paredes de la cuña superior e inferior, que favorecen diferentes fases de *bulk* en coexistencia, se introduce un nuevo campo magnético lineal h_l que actúa solamente sobre los nodos de las esquinas superiores e inferiores de la doble cuña. Esta contribución favorece la localización de la interfase en dichas esquinas, propiciando que la transición de rellenado se vuelva de primer orden.

Los resultados obtenidos para la curva de la función de distribución de probabilidades de la magnetización se han analizado para diferentes tamaños del sistema. Al aumentar el tamaño del sistema, las distribuciones de probabilidad tienden a la curva teórica analítica obtenida a partir de la teoría fenomenológica desarrollada por nuestro grupo (véase Fig. 1), que difiere de la correspondiente al caso crítico. Este hecho es una indicación clara de la existencia de una transición de rellenado tricrítica.

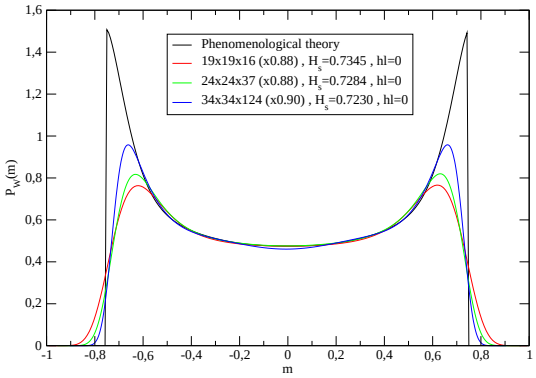

FIG. 1. Gráfica de las funciones de distribución de la probabilidad de la magnetización en las condiciones del punto tricrítico con $h_l = 0$, para: $H_s = 0.7345, 19 \times 19 \times 16$ (rojo), $H_s = 0.7284, 24 \times 24 \times 37$ (verde) y $H_s = 0.7230, 34 \times 34 \times 124$ (azul) Un ajuste óptimo con la predicción de la teoría fenomenológica para el punto tricrítico se obtine usando los factores de scala 0.88, 0.88, 0.90 y 0.94, respectivamente.

* arodriguezrivas@us.es

[1] A. Milchev, M Müller, K. Binder, and D.P. Landau, *Phy. Rev. Lett.*, **90**, 136101 (2003).

[2] A. Milchev, M Müller, K. Binder, and D.P. Landau, *Phy. Rev. E*, **68**, 031601 (2003).

[3] J.M. Romero-Enrique and A.O. Parry, *Europhys. Lett.*, **72**, 1004 (2005).

[4] J.M. Romero-Enrique and A.O. Parry, *J. Phys.: Condens. Matter*, **17**, S3487 (2005).

[5] J.M. Romero-Enrique and A.O. Parry, *New J. Phys.*, **9**, 167 (2007).

[6] J.M. Romero-Enrique, A. Rodriguez-Rivas, L.F. Rull and A.O. Parry, *Soft Matter*, **9**, 7069 (2013).

Análisis de las texturas de cristales líquidos nemáticos en presencia de sustratos sinusoidales y almenados.

O. A. Rojas-Gómez*† y J. M. Romero-Enrique**‡

†*Departamento de Sistemas Físicos, Químicos y Naturales, Universidad Pablo de Olavide, 41013 Sevilla, España*

‡*Departamento de Física Atómica, Molecular y Nuclear, Área de Física Teórica, Universidad de Sevilla, Apartado de Correos 1065, 41080 Sevilla, España*

En este trabajo se han estudiado las diferentes texturas que un cristal líquido puede mostrar en presencia de sustratos microestructrurados, en concreto sustratos sinusoidales y sustratos almenados, que favorecen un anclaje fuerte y homeotrópico del nemático a la superficie. Este estudio se ha realizado en el marco teórico del modelo de Berreman generalizado[1,2] para la caracterización de la contribución elástica a la densidad de energía libre superficial de sistemas de cristal líquido nemático en contacto con sustratos microestructurados arbitrarios. En ambos casos se consideran los sistemas sometidos a anclaje fuerte y homeotrópico. Esta aproximación permite explorar situaciones donde la longitud de onda asociada a la periodicidad del sustrato es mucho mayor que la longitud de correlación nemática, en contraste con estudios previos dentro del marco del modelo de Landau-de Gennes[3–5], que sólo permiten analizar sistemas con longitudes de onda de varias decenas de longitudes de correlación.

En el caso del sustrato almenado, se observan diferentes texturas metaestables. En particular, y dependiendo de la intensidad del anclaje y la rugosidad del sustrato, se observa una transición entre una textura simétrica (para rugosidades pequeñas) y otra antisimétrica (para rugosidades mayores), similar a la observada en el modelo de Landau-de Gennes[5]. Respecto al caso sinusoidal, se ha analizado la aparición de texturas con defectos nucleados en *bulk*, y las diferentes transiciones de fase entre dichas texturas.

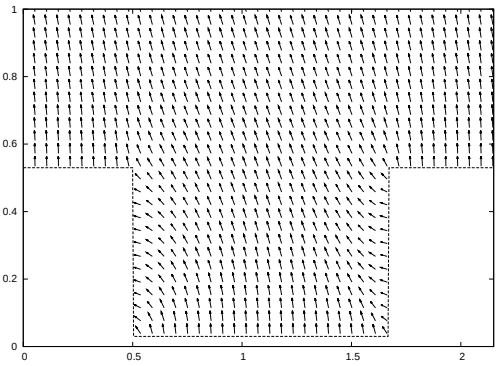

FIG. 1. Textura antisimétrica para un nemático en contacto con un sustrato almenado.

* oarojas@us.es

** enrome@us.es

[1] O. A. Rojas-Gómez y J. M. Romero-Enrique, Phys. Rev. E 86, 041706 (2012).

[2] J. M. Romero-Enrique, C.-T. Pham y P. Patrício, Phys. Rev. E 82, 011707 (2010).

[3] P. Patrício, J. M. Romero-Enrique, N. M. Silvestre, N. R. Bernardino y M. M. Telo da Gama, Molec. Phys. **109**, 1067 (2011).

[4] P. Patrício, N. M. Silvestre, Chi-Tuong Pham y J. M. Romero-Enrique, Physical Review E **84**, 021701 (2011).

[5] N. M. Silvestre, Z. Eskandari, P. Patricío, J. M. Romero-Enrique and M. M. Telo da Gama, Phys. Rev. E 86, 011703 (2012).

Molecular dynamics algorithm for simulating a system of ellipsoids on GPU architecture

S.M. Rubio-Largo*, Pedro G. Lind†, R.C. Hidalgo
*Departamento de Física y Matemática Aplicada. Facultad de Ciencias. Universidad de Navarra. Navarra. Spain.
†Institute of Physics. Carl Von Ossiatzky. University of Oldenburg.D-26111. Oldenburg. Germany.

General-purpose computation on Graphics Processing Units (GPU) has recently become an attractive alternative to parallel computing on clusters and supercomputers[1]. We present a hybrid GPU-CPU implementation of an accurate molecular dynamics algorithm for a system of ellipsoids (see Fig. 1).

Following our procedure, the ellipsoids has three translational degrees of freedom and its rotational movement is described by a quaternion formalism[1]. The contact interaction between two generalized ellipsoids (A and B) is described by a very accurate force law $\vec{F}_{AB} = F^N_{AB}\cdot\vec{n} + F^T_{AB}\cdot\vec{t}$, which accounts for the elastic and dissipative interactions. Following our approach, the contact plane $\vec{n}$ is analytically obtained by solving the characteristic equation $|A+\lambda B| = 0$ and deducing its corresponding eigenvectors. Based on some algebraic conditions[2–5], we have implemented an accurate algorithm to solve this problem. In our poster we will show several details about this implementation (see Fig. 2).

Finally, we show that the algorithm complies with the statistical mechanical laws by examining the homogeneous cooling of a granular gas of polydisperse generalized ellipsoids. The new algorithm dramatically reduces computational time, compared with a traditional CPU implementation.

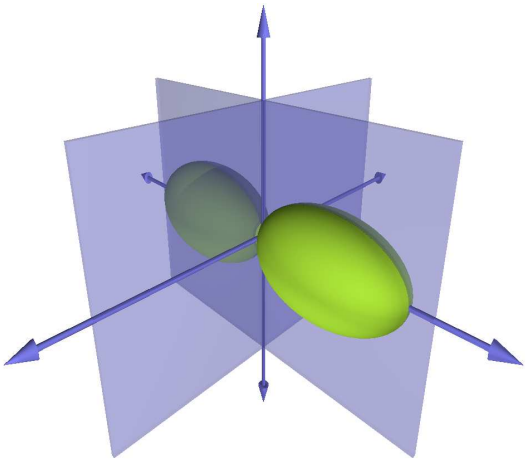

FIG. 1. Normal and tangential contact planes of two colliding ellipsoids.

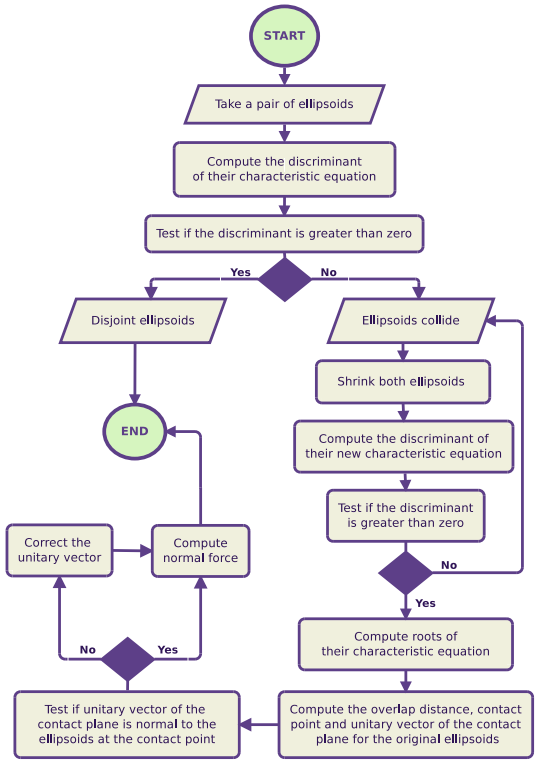

FIG. 2. Flow-chart of the algorithm for computation of normal contact force between two arbitrary ellipsoids.

* srubio.4@alumni.unav.es

[1] R. C. Hidalgo, T. Kanzaki, F. Alonso-Marroquin, and S. Luding. On the use of graphics processing units (GPUs) for molecular dynamics simulation of spherical particles. *AIP. Conference Proceedings* (2013).
[2] W. Wang, Y-K.Choi, B. Chand, Hong kong, M-S.Kim, Seoul, J.Wang, Jinan. Efficient collision detection for moving ellipsoids using seperating planes. *Computing. Springer.* (2004).
[3] Xiaohong Jia, Yi-King Choi, Bernard Mourrain, Wenping Wang. An algebraic approach to continuous collision detection for ellipsoids. *Computer Aided Geometric Design.* (2011).
[4] P. G. Lind. Sequential random packings of spheres and ellipsoids. *Powders and Grains 2009, Proc. 6. Int. Conf. on Micromechanics of Granular Media, pp. 219-222.* (2009).
[5] Reza M. Baram, and Pedro G. Lind. Deposition of general ellipsoidal particles. *Physical Review E 85 041301* (2012).

Are viral blips in HIV-1-infected patients clinically relevant?

D. Sánchez-Taltavull* and T. Alarcón†
Centre de Recerca Matemàtica

The initialization of Highly Active Antiretroviral Therapy (HAART) in HIV-1 patients is followed by an important decrease of the viral load below the detection limit (e.g. 50 copies/mL). However, this does not imply that the virus has been completely suppressed, supersensitive assays are able to detect the viral load below that limit. There have been observations of transient episodes of viremia above the detection limit ("blips")[1]. Different explanations have been suggested for explain the appearance of these viral blips, the first one was a drug failure, activation of latently infected cells when these cells encounter their relevant antigens[2,3], or simply that these blips represent biological fluctuations around the mean viral load or they are often the result of laboratory artifacts. Thus, there is a current discussion on the medical relevance of the viral blips. In this talk we try to throw some light on these two questions:

- Are they the product of random fluctuations or a different mechanism must be considered?
- Is their likelihood and frequency affected by laboratory procedures?

The previous models are homogeneous models in the blood stream. Latently cell activation has been studied by Perelson et al[2], they proposed a model that considers latently infected cell activation in response to stochastic antigenic stimulation and showed that programmed expansion and contraction of latently infected cells can generate intermittent viral blips. Conway and Coombs[3] formulated a stochastic model where cells and virions are supposed to be homogeneously distributed in the blood (well-stirred system assumption). Under this hypothesis, blips appear only under uncommonly high virion production.

Latent cells and virions are present in very low numbers. Thus, inhomogeneities in concentration are likely. We propose a compartmental model where the total volume of blood is divided in a number of compartments where a local stochastic population model (similar in its ingredients to the Conway-Coombs model), supplemented with random diffusion of cells and virions between compartments. We show two different compartmental models, just considering the healthy CD4+T cells, the latently infected cells, the productively infected cells and the viral load. One of the models taking into account just the dynamics in the body and the other one also taking into account the dynamics of the virus and cells in the blood sample after the extraction.

* dsanchez@crm.cat
† talarcon@crm.cat

[1] R. E. Nettles, T. L. Kieffer, P. Kwon et al. Intermittent HIV-1 viremia (blips) and drug resistance in patients receiving HAART. *JAMA*, 293(7): 817-829, 2005.
[2] L. Rong and A.S. Perelson. Modeling Latently Infected Cell Activation: Viral and Latent Reservoir Persistence, and Viral Blips in HIV-infected Patients on Potent Therapy. *PLoS Comput Biol* 5(10): e1000533, 2009.
[3] J.M. Conway and D.Coombs. A Stochastic Model of Latently Infected Cell Reactivation and Viral Blip Generation in Treated HIV Patients. *PLoS Comput Biol*, 7(4):e1002033, 2011.

Bolas en métricas aleatorias: la borrachera de Euclides.

Silvia N. Santalla[†,§*], Javier Rodríguez-Laguna[†,‡], Rodolfo Cuerno[†,‡]
[†] *Grupo Interdisciplinar de Sistemas Complejos (GISC), Universidad Carlos III de Madrid.*
[§] *Dpt. Física, Universidad Carlos III de Madrid.*
[‡] *Dpt. Matemáticas, Universidad Carlos III de Madrid.*

Ya en otras ocasiones hemos discutido sobre la dinámica del crecimiento de interfases, cuando la frontera se modeliza con la ecuación de Kadar-Parisi-Zhang (KPZ), particularmente en su versión covariante[1]. La dependencia de la rugosidad con el tiempo y con la escala se caracterizan por unos determinados exponentes críticos. Además, en crecimiento circular[2], las fluctuaciones de los radios siguen la distribución de probabilidad de Tracy-Widom para el autovalor maximal de matrices unitarias (colectividad GUE).

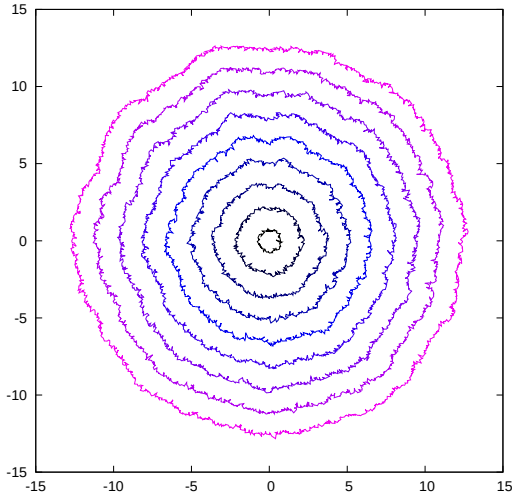

FIG. 1. Perfiles de las bolas en una métrica aleatoria para diferentes tiempos.

En esta ocasión, en lugar de estudiar crecimiento aleatorio sobre una métrica euclídea, vamos a mostrar las peculiaridades del crecimiento determinista sobre una métrica aleatoria. Estudiaremos la rugosidad de la frontera de la región del espacio que se puede alcanzar en un tiempo dado, las fluctuaciones de las geodésicas y en los tiempos de llegada, y relacionaremos esta dinámica con la de KPZ.

* silvia.santalla@uc3m.es

[1] J. Rodriguez-Laguna, S.N. Santalla, R. Cuerno, J. Stat. Mech. P05032 (2011).
[2] S.N. Santalla, J. Rodriguez-Laguna, R. Cuerno, Phys. Rev. E **89**, 010401(R) (2014)

Equation of state of sticky-hard-sphere fluids in the chemical-potential route

René D. Rohrmann*,† Andrés Santos‡
Departamento de Física, Universidad de Extremadura, E-06071 Badajoz, Spain

The chemical potential of a fluid can be evaluated as the change in the Helmholtz free energy when a new particle is added to the system through a coupling parameter (ξ) which determines the strength of the interaction of the added particle to the rest of the system. This method provides the equation of the state (EOS) of the fluid in the so-called chemical-potential route (or μ-route). This can be considered as the fourth route in addition to the better known routes based on the pressure (or virial), compressibility, and energy equations. All these ways to obtain the EOS are *formally* equivalent.

In practice, the various thermodynamics routes have been mostly developed (under the assumption of additive pair interactions) using the so-called radial distribution function $g(r)$. Since all well-known theoretical methods to obtain $g(r)$ give approximate solutions, with the exception of a few, simple fluid models (for example, one-dimensional systems whose particles interact only with their nearest neighbors), the EOS obtained from different routes differ in general from one another.

The μ-route has been largely unexplored, except in the scaled-particle theory.[1] Recently, this method has been used to obtain a hitherto unknown EOS for the hard-sphere (HS) model in the Percus–Yevick (PY) approximation.[2] This method was then extended to multicomponent fluids for arbitrary dimensionality, interaction potential, and coupling protocol.[3] Its application to HS mixtures allowed us to provide a new EOS of this classical model in the PY approximation. Evidently, the μ-route represents a helpful tool for the construction of new EOS and the analysis of thermodynamic properties of fluids. It is therefore of great interest to consider its application to non-HS models.

In this paper we use the μ-route to evaluate the EOS of Baxter's sticky-hard-sphere (SHS) model. In this fluid, impenetrable particles of diameter σ interact through a square-well potential of infinite depth and vanishing width, characterized by a "stickiness" parameter α. The μ-route yields[4]

$$\beta\mu^{\text{ex}} = -\ln(1-\eta) - 24\eta\int_{1/2}^{1} d\xi\, M(\eta,\xi), \qquad (1)$$

$$M(\eta,\xi) \equiv \frac{\partial\,(\alpha_\xi - 1)\,\xi}{\partial\xi}\xi^2 y_\xi(\xi\sigma) + \frac{\alpha_\xi\xi}{\sigma}\left.\frac{\partial[r^2 y_\xi(r)]}{\partial r}\right|_{r=\xi\sigma}.$$

Here, η is the packing fraction and $y_\xi(r)$ is the cavity function of the added particle, which interacts with the rest of the particles via an SHS interaction of diameter $\xi\sigma$ and stickiness α_ξ.

By exploiting the exact knowledge of $y_\xi(r)$ within the PY approximation,[5] we have obtained the compressibility factor $Z \equiv p/\rho k_B T$ stemming from Eq. (1) with three different *protocols*: (A) $\alpha_\xi = (2\xi-1)^2\alpha$, (B) $\alpha_\xi = (2\xi-1)\alpha$, and (C) $\alpha_\xi = (2\xi-1)^{1/2}\alpha$. Not surprisingly, the resulting EOS depends on the protocol and differs from the one obtained from the virial (v), compressibility (c), or energy (e) routes.

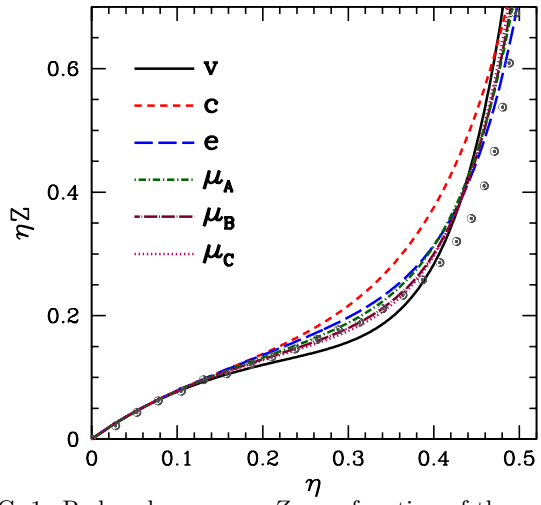

FIG. 1. Reduced pressure ηZ as a function of the packing fraction for and SHS fluid at $\alpha = \frac{5}{9} \simeq 0.556$. The curves correspond to PY results from various routes (as indicated on the plot), while open circles represent Monte Carlo calculations.[6]

As an illustration, Fig. 1 shows the density dependence of the reduced pressure ηZ at $\alpha = \frac{5}{9}$, as obtained from MC simulations and from the PY approximation via different routes. We can observe that the best performance in the region $0.15 \lesssim \eta \lesssim 0.4$ corresponds to the three versions of the μ-route, followed by the energy route. We have also obtained the vapor-liquid coexistence curve and observed that the best overall agreement with computer simulations[6] corresponds again to the μ-route.

* ICATE-CONICET, 5400 San Juan, Argentina
† rohr@icate-conicet.gob.ar
‡ andres@unex.es

[1] H. Reiss, H. L. Frisch, and J. L. Lebowitz, J. Chem. Phys. **31**, 369 (1959).
[2] A. Santos, Phys. Rev. Lett. **109**, 120601 (2012).
[3] A. Santos and R. D. Rohrmann, Phys. Rev. E **87**, 052138 (2013).
[4] R. D. Rohrmann and A. Santos, unpublished (2014).
[5] J. W. Perram and E. R. Smith, Chem. Phys. Lett. **35**, 138 (1975).
[6] M. A. Miller and D. Frenkel, J. Chem. Phys. **121**, 535 (2004).

Transport coefficients of a granular gas of inelastic rough hard spheres

Andrés Santos* and Gilberto M. Kremer†,‡
Departamento de Física, Universidad de Extremadura, E-06071 Badajoz, Spain

The dynamics of a dilute granular gas, modeled as a system of hard spheres colliding inelastically with constant coefficients of normal (α) and tangential (β) restitution, can be described at a mesoscopic level by the (inelastic) Boltzmann equation for the one-body velocity distribution function $f(\mathbf{r},\mathbf{v},\boldsymbol{\omega},t)$.[1,2] A granular gas is intrinsically out of equilibrium and thus, in contrast to the case of energy conservation (elastic collisions), breakdown of equipartition is present (i.e., $\theta \equiv T^{\rm rot}/T^{\rm tr} \neq 1$, where $T^{\rm tr}$ and $T^{\rm rot}$ are the translational and rotational *granular* temperatures, respectively), even in homogeneous and isotropic states.

There exists compelling evidence on the applicability of hydrodynamics to granular gases. On the other hand, while the Navier–Stokes–Fourier (NSF) transport coefficients have been obtained from the Boltzmann equation in the case of *smooth* spheres[3] (i.e., $\beta=-1$), the generalization to rough spheres ($-1<\beta\leq 1$) is yet unclear.[4]

The aim of this work is to present the NSF constitutive equations for arbitrary values of α and β, as derived from application of the Chapman–Enskog method to the Boltzmann equation. In order to obtain explicit expressions, the usual (first) Sonine approximation is used. In the case of zero mean spin, the structure of the constitutive equations is

$$P_{ij}=\left(\frac{2nT}{1+\theta^{(0)}}-\eta_b\nabla\cdot\mathbf{u}\right)\delta_{ij} -\eta\left(\nabla_i u_j+\nabla_j u_i-\frac{2}{3}\nabla\cdot\mathbf{u}\delta_{ij}\right),$$

$$\mathbf{q}=-\kappa\nabla T-\mu\nabla n,$$

$$\zeta=\zeta^{(0)}+\xi\nabla\cdot\mathbf{u}.$$

Here, n is the number density, $T=\frac{1}{2}\left(T^{\rm tr}+T^{\rm rot}\right)$ is the total temperature, $\mathbf{u}$ is the flow velocity, P_{ij} is the pressure tensor, $\mathbf{q}$ is the total energy flux, and ζ is the cooling rate. The superscript (0) denotes quantities in the homogeneous cooling state, while η_b (bulk viscosity), η (shear viscosity), κ (thermal conductivity), μ, and ξ are NSF transport coefficients. In the smooth case $\eta_b=\xi=0$. Moreover, $\mu=0$ for elastic and smooth spheres.

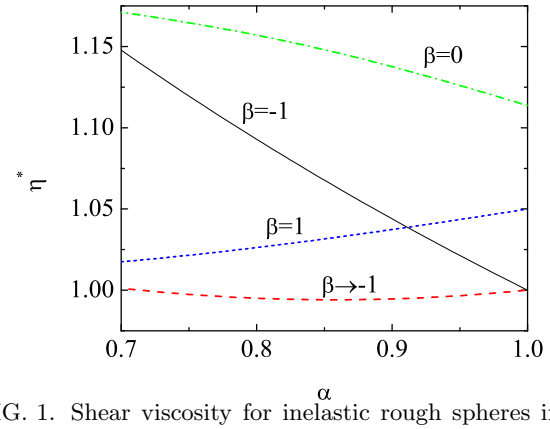

FIG. 1. Shear viscosity for inelastic rough spheres in the limit $\beta\to -1$, at $\beta=0$, and at $\beta=1$. The curve corresponding to smooth spheres ($\beta=-1$) is also included.

As an illustration, Fig. 1 shows the α-dependence of the shear viscosity (reduced with respect to that of elastic and smooth spheres) at several values of β. We observe that the limit $\beta\to -1$ widely differs from the result for pure smooth spheres ($\beta=1$). This is a consequence of the *singular* character of the limit $\beta\to -1$, in which case $\theta^{(0)}$ diverges and the influence of the internal degrees of freedom cannot be neglected.[2] In fact, the known results for smooth spheres[3] are recovered if, in addition to $\beta\to -1$, one *formally* makes $\theta^{(0)}\to 0$. In the special case of elastic and completely rough spheres ($\alpha=1$, $\beta=1$), Pidduck's expressions for the transport coefficients[5] are reobtained.

* andres@unex.es
http://www.unex.es/eweb/fisteor/andres
† Departamento de Física, Universidade Federal do Paraná, Curitiba, Brazil
‡ kremer@fisica.ufpr.br

[1] A. Santos, G. M. Kremer, and V. Garzó, *Prog. Theor. Phys. Suppl.* **184**, 31 (2010).
[2] A. Santos, G. M. Kremer, and M. dos Santos, *Phys. Fluids* **23**, 030604 (2011).
[3] J. J. Brey, J. W. Dufty, C. S. Kim, and A. Santos, Phys. Rev. E 58, 4638(1998).
[4] A. Goldshtein and M. Shapiro, J. Fluid Mech. 282, 75 (1995).
[5] G. M. Kremer, *An Introduction to the Boltzmann Equation and Transport Processes in Gases* (Springer, Berlin, 2010).

Ground state microstructures of magnetic filaments

P. A. Sánchez[1], J. J. Cerdà[2] and T. Sintes[2*]
[1] *Faculty of Physics, University of Vienna. Boltzmanngasse 5, 1090-Vienna.*
[2] *IFISC, Instituto de Física Interdisciplinar y Sistemas Complejos CSIC-Universidad de las Islas Baleares. 07122-Palma de Mallorca*

The synthesis of artificial magnetic filaments by mutually linking particles with magnetic properties has set the path towards the construction of supramolecular magnetic polymers at the scale of tenths of nanometers[1,2]. These novel structures, known as magnetic filaments, can hold a permanent dipolar moment at room temperature even in the absence of an external magnetic field. The potential use of magnetic filaments in technological applications, from magnetic memories to chemical and pressure nanosensors, has raised the interest in the study of their fundamental microstructure properties and to elucidate their ground state conformations.

In this work we investigate the ground state structures of stiff magnetic filaments in the bulk and in constrained 2D geometries via extensive Langevin dynamics simulations. The magnetic filament is represented by a coarse-grained bead-spring model where each bead bears a point dipole, free to rotate in 3 dimensions and located in its center. The excluded volume interaction is introduced via a soft-core repulsive potential[3].

We analyze the different topological structures that are likely to exist at low temperatures in terms of the competing dipole strength, soft-core repulsion, spring elasticity and chain stiffness interactions. In the range of parameters studied we find the majority of structures to fall in two categories: rod-like elongated chains and rings. This result reproduces the aggregates observed and predicted from density functional studies in quasi-2D ferrofluid monolayers[4,5]. Furthermore, we determine, in the limit of zero temperature and at a given dipole strength, the minimum filament length beyond which the transition from elongated towards a ring structure exists. As a difference with the ferrofluid monolayers, we find in the ring domain an optimal ring size value corresponding to configurations with a minimum energy per polymer bead. As a consequence, long filaments wish to form rings with its corresponding optimal size, leading to fascinating structures that strongly differ depending on the embedded system dimensionality (see Fig.1).

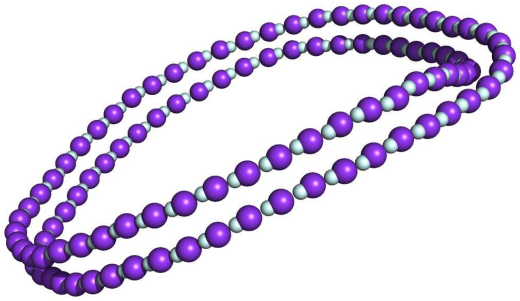

FIG. 1. Typical snapshot of an equilibrium configuration of a flexible magnetic filament in the bulk (3D)

* tomas@ifisc.uib-csic.es

[1] Singh H, Laibinis P E and Hatton T A. (2005) *Nano Lett.* **5** 2149.
[2] Evans B A, Shields A R, Carroll R L, Washburn S, Falvo M R and Superfine R. (2007) *Nano Lett.* **7** 1809.
[3] Sánchez P A, Cerdà J J, Sintes T, and Holm C. (2013) *J. of Chem. Phys.* **139** 044904. Cerdà J J, Sánchez P A, Holm C and Sintes T. (2013) *Soft Matter* **9** 7185.
[4] Kantorovich S, Cerdà J J and Holm C. (2008) *Phys. Chem. Chem. Physics* **10** 1883.
[5] Prokopieva T A, Danilov V A, Kantorovich S and Holm C. (2009) *Phys. Rev. E* **80** 031404.

Propiedades termodinámicas de un fluido de Lennard-Jones con núcleo duro mediante simulación Monte Carlo y teoría RHNC

J. Largo y J. R. Solana*
Departamento de Física Aplicada
Universidad de Cantabria 39005 Santander (España)

Entre las teorías más fructíferas para obtener las propiedades termodinámicas y estructurales de fluidos (y sólidos), se encuentran las teorías de perturbaciones,[1] en las cuales el potencial $u(r)$ de interacción entre dos partículas se divide en dos contribuciones: un potencial de referencia $u_0(r)$ y un potencial perturbativo $u_0(r)$, de modo que el potencial total es

$$u(r) = u_0(r) + u_1(r). \quad (1)$$

Si introducimos un parámetro de acoplamiento α, con $0 \leq \alpha \leq 1$, podemos construir una familia de potenciales de la forma

$$u(r, \alpha) = u_0(r) + \alpha u_1(r), \quad (2)$$

de manera que tomando $\alpha = 0$ el potencial se reduce al potencial de referencia $u_0(r)$ y para $\alpha = 1$ se recupera el potencial completo $u(r)$. La energía libre del fluido con potencial $u(r, \alpha)$ viene dada por la expresión

$$F(\alpha) = F_0 + 2\pi N\rho \int_0^\alpha d\alpha' \int_0^\infty u_1(r) g(r; \alpha') r^2 dr, \quad (3)$$

que puede desarrollarse en serie de Taylor con el resultado

$$\beta F(\alpha) = \beta F_0$$

$$+2\pi N\rho \sum_{n=1}^{\infty} \frac{\beta}{n!} \int_0^\infty u_1(r) \frac{\partial^{n-1} g(r;\alpha)}{\partial \alpha^{n-1}}\bigg|_{\alpha=0} r^2 dr, \quad (4)$$

expresión que en sí misma es exacta. El problema que se presenta es la determinación de las derivadas que aparecen en ella. Por ello, en general las teorías de perturbaciones se ven obligadas a recurrir a aproximaciones más o menos drásticas. Sin embargo, bastante recientemente se ha propuesto[2,3] un procedimiento consistente en determinar $g(r; \alpha)$ para diversos valores de α próximos a cero mediante la solución numérica de la ecuación de Ornstein-Zernike en la aproximación RHNC y realizar numéricamente las mencionadas derivadas. Los resultados obtenidos para fluidos con diversos modelos de potencial resultan ser superiores a los obtenidos con otras teorías de perturbaciones.[4–8]

Resulta pertinente realizar un análisis exhaustivo de las ventajas e inconvenientes de la citada teoría de perturbaciones. A este respecto, la primera cuestión que se plantea es si la teoría representa alguna ventaja sobre la RHNC en la que se basa. Al objeto de tratar de aclarar este aspecto, hemos elegido el modelo de potencial

$$\begin{aligned} u(r) &= \infty, & r \leq \sigma, \\ &= 4\varepsilon \left[\left(\frac{\sigma}{r}\right)^{12} - \left(\frac{\sigma}{r}\right)^{6} \right], & r > \sigma, \end{aligned} \quad (5)$$

es decir, se trata de un potencial de Lennard-Jones con núcleo duro. Esta última condición es requerida por la naturaleza de la propia teoría RHNC.

El primer paso a realizar con el objetivo propuesto consiste en analizar la precisión de la propia teoría RHNC. A tal fin, en primer lugar hemos obtenido las propiedades termodinámicas y estructurales de un fluido con el potencial (5) mediante Monte Carlo para diferentes temperaturas y densidades. A continuación hemos calculado dichas propiedades mediante la teoría RHNC, consistente en resolver la ecuación de Ornsein-Zernike con la condición de cierre

$$c(r) = h(r) - \ln y(r) + B_0(r), \quad (6)$$

donde $B_0(r)$ es la función puente del fluido de referencia, en nuestro caso el fluido de esferas duras. Para esta última hemos utilizado la parametrización de Malijevský y Labík.[9]

Los resultados así obtenidos para la ecuación de estado, la energía de exceso y la función de distribución radial, los cuales se presentan en este trabajo, se encuentran en excelente concordancia con los datos de simulación.

Agradecimientos. Este trabajo ha sido financiado por el Ministerio de Ciencia e Innovación (MICINN), Proyecto No. FIS2009-09616.

---

* ramon.solana@unican.es

[1] J. R. Solana, *Perturbation theories for the thermodynamic properties of fluids and solids*, CRC Press (2013).
[2] S. Zhou, Phys. Rev. E **74**, 031119 (2006).
[3] S. Zhou, J. Chem. Phys. **155**, 144518 (2006).
[4] S. Zhou and J. R. Solana, Phys. Rev. E **78**, 021503 (2008).
[5] J. R. Solana, J. Chem. Phys. **129**, 244502 (2008).
[6] S. Zhou and J. R. Solana, J. Chem. Phys. **131**, 134106 (2008).
[7] S. Zhou and J. R. Solana, J. Chem. Phys. **138**, 244115 (2013).
[8] S. Zhou and J. R. Solana, J. Phys. Chem. B **117** 9305 (2013).
[9] A. Malijevský and S. Labík, Mol. Phys. **60**, 663 (1987).

Weighted-ensemble Brownian dynamics simulation: Sampling of rare events in non-equilibrium systems

Raul Toral(1)*, Justus A. Kromer(2), Lutz Schimansky-Geier(2)
(1)IFISC, Instituto de Física Interdisciplinar y Sistemas Complejos, CSIC-Universidad de las Islas Baleares, 07122-Palma
(2)Department of Physics, Humboldt-Universität zu Berlin, Newtonstr. 15, 12489 Berlin, Germany

Rare events are ubiquitous in many biological, chemical and physical processes. Whereas the density of states is known in systems at thermal equilibrium, interesting phenomena often occur in non-equilibrium systems. Unfortunately, many such problems are inaccessible to analytic methods. Therefore computer simulations are a widely used tool to estimate the density of states or transition rates between them. Since standard Brownian dynamic simulation provides computational costs that are inversely proportional to the state's probability, specialized methods have to be used to adequately sample rare events, i.e. states with low probability or low transition rates.

We have developed an algorithm[1], based on the previously developed weighted-ensemble (WE) Brownian dynamics simulations that allows one to calculate the stationary probability density function (SPDF) as well as transition rates between particular states. Like in WE simulations the space of interest is divided into several subregions and the probability for finding the system in them is calculated by generating equally weighted walkers in each region. By moving to the underlying dynamics, the walkers transport probability between the subregions. Thus, WE methods are usually applied to systems of Brownian particles moving in a potential landscape[2,3]. Our algorithm is based on WE Brownian dynamic simulations, but uses a uniform distribution of walkers within each subregion. In general the algorithm can be applied to arbitrary dynamical systems of the form:

$$\dot{x}_n = f_n(\mathbf{x}) + g_n(\mathbf{x})\xi_n(t),\ n = 1, ..., d, \qquad (1)$$

where d is the number of stochastic time-dependent degrees of freedom. We are interested in high precision sampling of the stationary probability current $J_{st}(\mathbf{x})$ and the SPDF $p_{st}(\mathbf{x})$ of finding the system in the d-dimensional cube $[x_1, x_1 + dx_1], \ldots, [x_d, x_d + dx_d]$.

Our method outperforms Brownian dynamics simulation by several orders of magnitude and its efficiency is comparable to weighted-ensemble Brownian dynamic simulations in all studied systems and lead to impressive results in regions of low probability and small rates. As an example, we show in the first figure the pdf computed for the classic double well potential $U(x) = -\frac{1}{2}x^2 + \frac{1}{4}x^4$ as well as, in the second figure, the verification of Kramers law for the probability current. Note that the vertical scale in both cases shows the high efficiency of the method in sampling low-probability events, as we are able to sample correctly events with probability of the order of 10^{-300} and currents of the order of 10^{-300}.

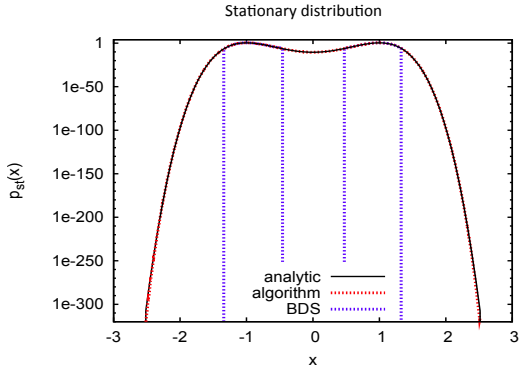

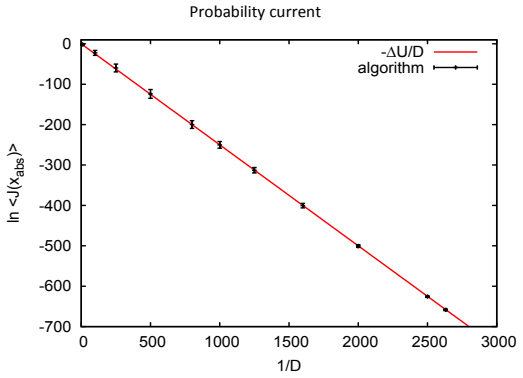

* raul@ifisc.uib-csic.es

[1] J . A. Kromer, L. Schimansky-Geier, R. Toral Physical Review **E87**, 063311 (2013).
[2] D. Bhatt, B. Zhang and D. Zuckerman, J. Chem. Phys **133**, 014110 (2010).
[3] D. Bhatt and D. Zuckerman, J. Chem. Theory Comput. **7**, 2520 (2011).

Interplay between columnar and smectic stability in suspensions of polydisperse colloidal platelets

Enrique Velasco[1] and Yuri Martínez-Ratón[2]
[1] *Departamento de Física Teórica de la materia Condensada, Universidad Autónoma de Madrid, Spain.*
[2] *GISC, Departamento de Matemáticas, Universidad Carlos III de Madrid, Spain.*

The phase behavior of a model suspension of colloidal polydisperse platelets is studied using density-functional theory[1]. Platelets are modelled as parallel rectangular prisms of square section l and height h, with length and height distributions given by different polydispersities δ_l and δ_h. The model is intended to qualitatively represent the experimental colloidal platelet suspensions at high densities with highly degree of orientational ordering. These colloidal platelets have been synthesised by different techniques, but they can never be produced with uniform size; therefore, they possess an intrinsic polydispersity both in thickness and lateral size. Size polydispersity is known to greatly modify the phase behaviour of colloidal suspensions, since phases with (partial or full) spatial order cannot easily form: particles cannot accommodate into regular periodic structures due to the disparity in size. When two polydispersities come into play, the final structure delicately depends on their values, and order will develop along the less-frustrated spatial dimension(s).

With our theory, we can obtain the phase behavior of the model colloidal suspension, including nematic (N), smectic (S) and columnar (C) phases and its dependence with the two polydispersities δ_l and δ_h. When $\delta_l > \delta_h$ we observe that the smectic phase stabilises first with respect to the columnar. If $\delta_h > \delta_l$ we observe the opposite behavior. Other more complicated cases occur, e.g. the smectic stabilises from the nematic first but then there exists a first-order transition to the columnar phase. Our model assumes plate-rod symmetry, but the regions of stability of smectic and columnar phases are non-symmetric in the $\delta_l - \delta_h$ plane due to the different dimensionality of ordering in the two phases. Microsegregation effects, i.e. different spatial distribution for different sizes within the periodic cell, take place in both phases. The theory confirms the stabilities of C and S phases as found in experiments on colloidal suspensions of mineral anisotropic particles (see figure)[2–4].

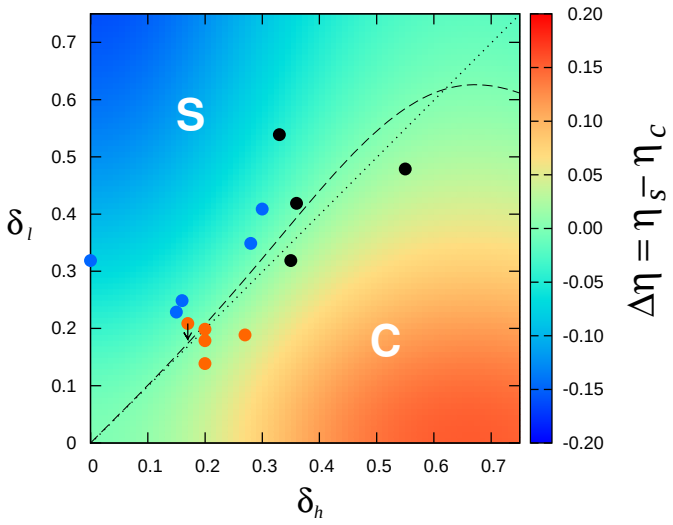

FIG. 1. Difference $\Delta\eta = \eta_s - \eta_c$ of packing fractions of bifurcated S and C phases as a function of polydispersities δ_l and δ_h, in false colour. Dashed line corresponds to the curve $\Delta\eta = 0$ (S and C phases bifurcate at the same packing fraction). The S (C) label indicates the region where the S (C) phase bifurcates from the N first. Dotted line is the bisectrice $\delta_l = \delta_h$. Orange, blue and black filled circles correspond to experiments where C, S and C+S are found. In the case of black circles and the orange circle with a down arrow, polydispersities correspond to those of the parent phase.

[1] E. Velasco and Y. Martínez-Ratón, Phys. Chem. Chem. Phys. **16**, 765 (2014).
[2] F. M. van der Kooij, K. Kassapidou, and H. N. W. Lekkerkerker, Nature **406**, 868 (2000).
[3] F. M. van der Kooij and H. N. W. Lekkerkerker, Phys. Rev. Lett. **84**, 781 (2000).
[4] J. G. Vroege, D. M. E. Thies-Weesie, A. V. Petukhov, B. J. Lemaire and P. Davidson, Advanced Materials **18**, 2565 (2006).

Malware spreading and critical nodes in multi-layered networks under computer viruses attack

Rafael Vida[†], Javier Galeano, Sara Cuenda[‡]
Complex System Group (GSC), Universidad Politécnica de Madrid

Computer viruses are evolving by developing spreading mechanisms based on the use of multiple vectors of propagation adapted to different kinds of vulnerabilities. The use of the social network as an extra vector of attack to penetrate the security measures in IP networks is improving the effectiveness of the malware, and have therefore been used by new and most aggressive viruses, like Conficker and Stuxnet[1]. These multi-vector viruses can be modeled in multi-layered networks in which each node belongs simultaneously to different layers, adapting the spreading vector to the properties of the layer.

In particular, we study the propagation of a SIS model on a multi-layer network where the state of each node is layer-independent and the dynamics in each network follows either a contact process or a reactive process, with different propagation rates. We show that the interplay between the layers leads to a non-trivial contagion matrix[2].

As an example, we apply this study to a multi-layered network formed by two layers: the social network of collaboration of the Spanish scientific community of Statistical Physics, FisEs, and the telecommunication network of each institution.

We also analyze the spreading of a virus in a multi-layered network formed by M layers for different network couplings. In the figure we show the density of infected nodes in the quasi stationary state, ρ, vs. the density of infected nodes in the initial seed, $\rho(0)$, in the FisEs network. The infection strategy is based on the strength of nodes in the contagion matrix. The contagion rates are $\beta_1 = 1.0$, $\beta_2 = 0.0$ (blue); $\beta_1 = 0.0$, $\beta_2 = 0.027$ (green) and $\beta_1 = 0.18$, $\beta_2 = 0.02$ (red).

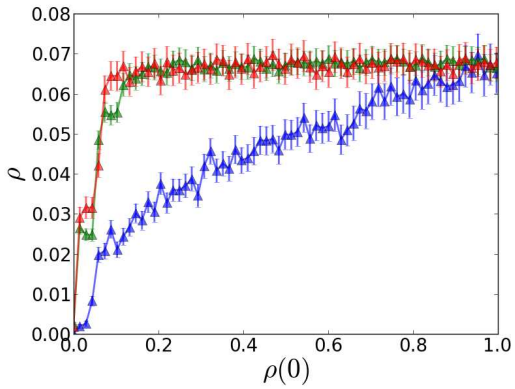

[†] Dept. de Sistemas Informáticos, E. T. S. de Ingeniería (ICAI), Univ. Pontificia de Comillas.
[‡] Dept. Economía Cuantitativa, Universidad Autónoma de Madrid.

[1] V. Antoine, R. Bongiorni, A. Borza, P. Bosmajian, D. Duesterhaus, M. Dransfield, B. Eppinger, K. Gallicchio, J. Houser, A. Kim, et al. Router security configuration guide, version 1.1 b. Technical Report C4-040R-02, System and Network Attack Center (SNAC), National Security Agency (NSA) (2003).
[2] R. Vida, J. Galeano and S. Cuenda. ArXiv:1310.0741 [physics.soc-ph].

Adsorption of Proteins onto Nanoparticles: Modelling the protein corona

O. Vilanova*, K. Dawson, G. Franzese*
Departament de Física Fonamental
Universitat de Barcelona

Cellular responses to materials in a biological medium reflect greatly the adsorbed biomolecular layer, rather than the material itself. Here, we study by molecular dynamic simulations the competitive protein adsorption on surfaces, i.e. the non-monotonic behavior of the amount of protein adsorbed on a surface in contact with plasma as a function of contact time and plasma concentration.

We try to understand the fundamental mechanisms of general competitive protein adsorption on surfaces. We make use of computational models to describe and analyze protein adsorption onto flat surfaces and curved surfaces such as Nanoparticles. This last case is specially interesting in many biological problems, for example NP uptake into cells, and a fully understanding of the dependence on surface curvature, size, or surface chemistry of how do proteins adsorb on NP is very important.

We implement Molecular Dynamics simulations in the NVT ensemble when the number of proteins is fixed or in a pseudo-μVT ensemble keeping constant the concentration of each kind of protein in the bulk when needed. We write high-performance GPGPU codes performing large-scale simulations. We use a coarse-grained model of protein interactions where each protein is described by two characteristic lenght-scales and its binding affinity with the surface. The solvent is also coarse-grained and it is implicit in the parametrization of the interaction forces. The protein-protein interactions are described with a CSW potential and the protein-NP interactions are described within the DLVO theory.

* ovilanova@ffn.ub.es
* gfranzese@ub.edu

Prohibition of discontinuous transitions in non-equilibrium disordered systems ($d \leq 2$)

Paula Villa Martin*[1], Juan A. Bonachela[2] and Miguel A. Muñoz[1]
[1] Departamento de Electromagnetismo y Física de la Materia, Facultad de Ciencias, Universidad de Granada, 18071, Spain
[2] Department of Ecology and Evolutionary Biology, Princeton University, Princeton, NJ, 08544-1003, USA

The effect of quenched disorder on both, the statics and the dynamics of many-particle systems, is drastic. An interesting example is the great influence it has on the order of phase transitions in low dimensional systems ($d \leq 2$). It is known that, in equilibrium systems, spontaneously broken symmetries cannot exist after the introduction of disorder. Indeed, discontinuos phase transitions are rounded by this disorder and become a continuous transition[2] that would probably exhibit critical exponents consistent with those of the corresponding pure model as it has been suggested by Kardar et al[3]. This effects has been verified in countless examples, both experimentally and numerically and has been discussed in many works. A time-honored argument by Imry and Ma[4] explains the first case based on the analysis of the energetics of the system. They conclude that there will always exist a large enough region of linear size L, with a majority of random fields opposing the broken-symmetry state, for which it will become energetically favorable to the system to align to the random field and thus preventing symmetries from being spontaneously broken and continuous phase transitions from existing. An extension of this argument explains the effect on discontinuos case.

Above studies have been done in equilibrium systems, but what happens in non-equilibrium cases? A recent work by Barghathi and Vojta[5] shows that, in a one-dimensional non-equilibrium system with spontaneously broken symmetry between two absorbing states, the continuous transition persist in spite of the introduction of quenched disorder. Therefore, *the Imry-Ma argument does not apply to these non-equilibrium systems owing to the presence of absorbing states.* Regarding these results, the question arises as to whether this shattering of a fundamental cornerstone of equilibrium Statistical Mechanics would happen in the case of discontinuous transitions too (see figure 1 for a synthetic summary).

Aimed at shedding some light on this issue, we study one of the simplest non-equilibrium model exhibiting a first-order/discontinuous transition, the quadratic contact process, in which two particles are needed to generate an offspring while isolated particles can spontaneously disappear. We employ a model which was numerically studied in two-dimensions and verified to exhibit a first-order phase transition separating an active from an absorbing phase[6]. As a first step, we study the behaviour of the pure version and verify that it exhibits first-order. Then we introduce disorder in the form of a site-dependent transition rates and investigate whether the discontinuous character of the transition survives.

In the disordered case we have found results as those reported for the standard contact process with quenched disorder[7], i.e. a second order phase transition with a Griffiths phase and an activated type of scaling fully compatible with the standard strong-disorder fixed point of the corresponding universality class (quenched directed percolation). In conclusion, we conjecture that the Imry-Ma-Aizenman-Wehr-Berker argument for equilibrium systems can be extended to non-equilibrium situations including absorbing states, i.e first-order phase transitions cannot appear in these low-dimensional disordered systems. The underlying reason for this is that, even if the absorbing phase is fluctuation-less and hence is free from the destabilizing effects the Imry-Ma argument relies on, the other phase is active and subject to fluctuation effects. Therefore, intrinsic fluctuations destabilize it as predicted by the Imry-Ma-Aizenman-Wehr-Berker argument, precluding phase coexistence.

System with Random Fields $d \leq 2$	2^{nd} order (spontaneous sym. breaking)	1^{st} order (phase coexistence)
Equilibrium	NO [3]	NO [1,2]
Non-equilibrium (abs. states)	YES [4]	NO

FIG. 1. **Summary of the effects of quenched random fields** on the existence of second and first order phase transitions in $d \leq 2$ systems. Both, the equilibrium and non-equilibrium cases are considered, the latter including the possibility of one or more absorbing states.

* pvilla@ugr.es

[1] P.Villa Martin, J.A. Bonachela and M.A. Muñoz, Under review in Phys. Rev. E (2013).
[2] M. Aizenman and J. Wehr, Phys. Rev. Lett. 62, 2503 (1989).
[3] G.S.M. Kardar, A.L. Stella and B. Derrida, Phys. Rev. E 52, R1269 (1995).
[4] Y. Imry and S.K. Ma, Phys. Rev. Lett. 35, 1399 (1975).
[5] H. Barghathi, T. Vojta, Phys. Rev. Lett. 109, 170603 (2012).
[6] A. Windus and H. Jensen, J. Phys. A: Math. Theor. 40, 22872297 (2007).
[7] T. Vojta and A. Farquhar, J. Mast, Phys. Rev. E 79, 11111 (2009).

Robustness of cooperative behaviours in reputation-based evolving populations

Daniele Vilone*, Francesca Giardini and Mario Paolucci
Laboratory of Agent Based Social Simulation, National Research Council (CNR) - Via Palestro 32, 00185 Rome, Italy.

The uprising and maintenance of cooperation in human societies, despite its inconvenience at the individual level, is a very important topic in game theory, complex systems physics, sociology and politics, debated not only for strictly scientific reasons, but also in order to have hints of how societies can enhance cooperation among its members.

Among others, one of the proposed mechanisms is the indirect reciprocity, originally suggested by Alexander[1], stating that individuals help recipients in order to receive help in their turn not necessarily by the same recipients they cooperated with in the past, but by someone else in their community. A somehow realistic way to implement indirect reciprocity in experiments and simulations is reputation. Nowak and Sigmund[2] conceived a smart model to simulate the effect of reputation on the evolution and enhancement of cooperation in a totally connected population playing a Prisoner's Dilemma Game. Here, each agent is characterized by a public reputation, which is a variable increasing each time she cooperates and decreasing when she defects. At the same time, an individual i chooses to cooperate only when opponent's reputation has at least a minumum value, k_i, which is in general different for each individual and depends on her past experience. Afterwards, Suzuki and Akiyama[3] generalized Nowak and Sigmund's results applying the same mechanism to a particular Public Goods Game, finding similar results: reputation can evolve and spread through the whole system; this effect is much stronger when agents play the PGG in samll groups; in medium-sized communities cooperative species can coexist in a stable manner with defecting species.

In this work, we have furtherly generalized the model, verifying its behaviour with different values of the parameters of the game (cost, synergy, total population size, *etc.*), and also testing it on networks, above all on bipartite graphs. We show that when the effects of reputation on cooperation are positive, they are enough stable if some parameters or topology of the model are changed, and we also have begun to think to possible experimental platforms in order to validate the simulative outcomes[4].

---

* daniele.vilone@gmail.com

[1] Alexander R. D., *Darwinism and human affairs*, University of Washington Press (1979).
[2] Nowak M. A. and Sigmund K., *Nature*, **393**, 573 (1998).
[3] Suzuki S. and Akiyama E., *Proceedings of the Royal Society*, **272**, 1373 (2005).
[4] Vilone D., Giardini F. and Paolucci M., in preparation (2014).

Strong anisotropy in two-dimensional surfaces with generic scale invariance: Non-linear effects

Edoardo Vivo*, Matteo Nicoli,† and Rodolfo Cuerno
Departamento de Matemáticas and Grupo Interdisciplinar de Sistemas Complejos (GISC)
Universidad Carlos III de Madrid
Avenida de la Universidad 30, E-28911 Leganés (Madrid)

Scale invariant, two-dimensional surfaces that are anisotropic in space abound in Science and Technology, for systems spanning many orders of magnitude in length scales. Examples range from epitaxial thin films in nanoscience[1] to micro and macroscopic crack formation in solids,[2] to geological systems, such as landscape evolution induced by rivers.[3] Mathematically, the surfaces that occur in these and many other systems are self-affine fractals,[4] whose fractal dimension (or, equivalently, roughness exponent) differs, depending on the direction along which it is measured. Due to the lack of characteristic distances, the scaling behavior just described is a form of anisotropic critical behavior,[5] which moreover often occurs without the need of parameter fine-tuning that adjusts the system to a critical point. These are thus examples of so-called generic scale invariance (GSI).[6] A context for this type of behavior, in which anisotropy has remained relatively little studied, is that of surface kinetic roughening.[4] In this work we pursue a continuum description of GSI systems through stochastic partial differential equations. Our cases of interest will be those conditions that lead to GSI while applying to the most important universality classes in surface kinetic roughening. Namely,[6] systems with non-conserved dynamics, like the celebrated Kardar-Parisi-Zhang (KPZ) equation,[7] or else systems with conserved dynamics and non-conserved noise, like e.g. the so-called conserved KPZ (cKPZ) equation.[8] Remarkably, the anisotropic generalizations of the two previous equations, namely, the so-called anisotropic KPZ (aKPZ)[9] and conserved anisotropic KPZ (caKPZ) equations,[10] do *not* lead asymptotically to anisotropic behavior (strong anisotropy, SA). Rather, in spite of being nominally anisotropic, they lead to isotropic asymptotics (weak anisotropy, WA), in universality classes that depend on parameter conditions. This fact contrasts strikingly with the unambiguous observation of SA in experiments on surface kinetic roughening for two-dimensional interfaces, see Ref. 11 and references therein.

In this work we focus on a number of representative equations, like the Hwa-Kardar equation, proposed in the context of self-organized criticality,[12] and both the conserved and non-conserved anisotropic KPZ equations.[9,10] All of them display GSI, and remained outside our previous analysis,[13] due to the unavailability of accurate approximations through linear equations for most of the cases. Thus, here we employ techniques that in principle can tackle strongly non-linear systems, such as the Dynamic Renormalization Group and direct numerical simulations. We show[14] that for non-conserved dynamics SA simply does not occur, even for special conditions under which only one of the nonlinearities is suppressed. On the other hand, for systems with conserved dynamics SA can be obtained, and even whole families of equations can be formulated which display this property. However, both in the presence and in the absence of the shift symmetry $h \to h + \text{const.}$, this seems only possible for "incomplete" equations in which one of the nonlinearities is suppressed. In general, conditions of this type depend critically on details of the dynamics that is being described, acting as special constraints, and are in this sense non-generic in parameter space. Hence, they cannot be obtained from simple-minded derivations of the equations of motion based on symmetries and conservation laws.

Partial support for this work has been provided by MICINN (Spain) Grant No. FIS2012-38866-C05-01. E. V. acknowledges support by Universidad Carlos III de Madrid.

* evivo@math.uc3m.es
† Center for Interdisciplinary Research on Complex Systems, Department of Physics, Northeastern University Boston, USA

[1] C. Misbah, O. Pierre-Louis, and Y. Saito, Rev. Mod. Phys. **82**, 981 (2010).
[2] D. Bonamy and E. Bouchaud, Phys. Rep. **498**, 1 (2011).
[3] R. Pastor-Satorras and D. H. Rothman, J. Stat. Phys. **93**, 477 (1998).
[4] A.-L. Barabási and H. E. Stanley, *Fractal Concepts in Surface Growth*, Cambridge University Press, Cambridge, UK (1995).
[5] U. C. Täuber, *Critical dynamics: a field theory approach to equilibrium and non-equilibrium scaling behavior*, unpublished. *http://www.phys.vt.edu/tauber.28*
[6] G. Grinstein, *Scale Invariance, Interfaces, and Non-Equilibrium Dynamics*, Plenum Press, New York (1995).
[7] M. Kardar, G. Parisi, and Y.-C. Zhang, Phys. Rev. Lett. **56**, 889 (1986).
[8] Z.-W. Lai and S. Das Sarma, Phys. Rev. Lett. **66**, 2348 (1991).
[9] D. E. Wolf, Phys. Rev. Lett. **67**, 1783 (1991).
[10] H. Kallabis, J. Phys. A: Math. Gen. **31**, L581 (1998).
[11] E. Vivo, M. Nicoli, M. Engler, T. Michely, L. Vázquez, and R. Cuerno, Phys. Rev. B **86**, 245427 (2012).
[12] T. Hwa and M. Kardar, Phys. Rev. Lett. **62**, 1813 (1989).
[13] E. Vivo, M. Nicoli, and R. Cuerno, Phys. Rev. E **86**, 051611 (2012).
[14] E. Vivo, M. Nicoli, and R. Cuerno, arXiv:1311.7638 (2013).

Interplay between internal time scales and network topology in coupled nonlinear oscillators

Jordi Zamora-Munt*, Manuel A. Matías, and Pere Colet
IFISC, Instituto de Física Interdisciplinar y Sistemas Complejos
CSIC-UIB, Universidad de las Islas Baleares 07122-Palma (Mallorca)

Interaction through a mediator is a robust mechanism to achieve a high degree of synchronization in large populations of oscillators. Some examples of this behavior include yeast cells in a common medium[1], pedestrians walking in a bridge[2] or star-coupled semiconductor lasers[3]. In this context a progressive transition from the incoherent state for active oscillators or a sudden transitions from the quiescent state for passive oscillators have been reported when the number of oscillators is above a critical value[4]. All those systems consider a very symmetric coupling, as all the oscillators see the same mean field as averaged by the hub. On the other hand, one expects that in real systems this mediated coupling through a common element coexists with direct interactions among the oscillators. However, in this context the interplay between these two types of interaction, mediated and direct, is an open problem.

Being our goal to consider the transitions induced by coupling in quiescent units to global oscillations, our model consists of N (synchronous) identical Landau-Stuart (LS) oscillators, z_j , coupled through a common linear damped oscillator or hub, F , and directly coupled by direct coupling:

$$\dot{z_j} = (\mu + i\omega)z_j - |z_j|^2 z_j + k_A^{(1)}(F - z_j) + k_B \sum_{k=1}^{N} B_{jk} z_k, \quad (1)$$

$$\dot{F} = (-\gamma + i\Omega)F + k_A^{(2)} \sum_{j=1}^{N} z_j. \quad (2)$$

where μ is the linear gain parameter, such that a supercritical Hopf bifurcation happens for $\mu = 0$ and ω is the oscillation frequency. We will consider the case $\mu < 0$, in which the oscillators are quiescent, case in which it has been shown that coupling through a common element, $k_B = 0$, induces a transition to a oscillatory synchronized state[2–4]. The hub acts as a bandpass filter where $\gamma > 0$ can be related to the filter bandwidth and Ω to the central frequency with maximum transfer function. The direct interactions can be attractive when B_{jk} is positive or respulsive when B_{jk} is negative. The entries B_{jk} defines the topology of the direct couplings, and k_A^i and k_B are positive coupling strengths.

Our goal is to analyze the combined effect of direct, i. e. $k_B \neq 0$, and hub mediated interactions among a set of identical LS oscillators. We have carried out this study using the Master Stability Function formalism for identical oscillators[5] recently generalized to consider synchronization between groups of oscillators[6]. The conditions for stable synchronization in the proposed system are obtained analytically with this formalism for any interaction topology.

Two different cases have been considered:

For a resonant hub ($\omega = \Omega$) we demonstrate that synchronization is stable for any direct coupling topology with $B_{jk} \geq 0$ for all j and k. In turn, if some B_{jk} are negative, i. e. for some repulsive interactions, a more complex scenario is observed. Synchronization is stable in a broad range of parameters. However, large repulsive coupling coefficients can destabilize the synchronized state. In this case, a rich variety of coexisting dynamics such as inhomogeneous amplitude synchronization or rotating waves of different orders become stable.

For a nonresonant hub ($\omega \neq \Omega$) and attractive direct coupling the scenario is similar to the resonant case. Stable synchronization is observed for any direct coupling topology while, a large enough frequency detuning leads to amplitude death of the oscillations. More interesting is the case when attractive and repulsive direct interactions coexist. We report the existence of stable synchronization in a narrow range of nonzero frequency detunings that can be interpreted as the resonance of the internal time scales of the dynamical units with the modes of the coupling topology.

Our study shows that the inclusion of a direct coupling topology in a system of oscillators initially coupled through a common passive medium has two substantially different cases depending on the sign of the interactions. When all the interactions are attractive, synchronization is reinforced by the direct coupling. However, when both attractive and repulsive couplings coexist, two opposite effects can be observed. Negative interactions can either destabilize the synchronous state or they can also have the opposite effect of stabilizing it. The latter being the result of a non-trivial interplay between the coupling topology and the dynamics of the oscillators.

* jordi@ifisc.uib-csic.es

[1] J. Aldridge and E. K. Pye, Nature **259**, 670 (1976).
[2] S. H. Strogatz, D. M. Abrams, A. McRobie, B. Eckhardt, and E. Ott, Nature **438**, 43 (2005).
[3] J. Zamora-Munt, C. Masoller, J. García-Ojalvo, and R. Roy, Phys. Rev. Lett. **105**, 264101 (2010).
[4] A. F. Taylor, M. R. Tinsley, F. Wang, Z. Huang, and K. Showalter, Science **323**, 614 (2009).
[5] L.M. Pecora, T. L. Carroll, Phys. Rev. Lett. **80**, 2109 (1998).
[6] T. Dahms, J. Lehnert, and E. Scholl, Phys. Rev. E **86**, 016202 (2012).

Análisis topológico de depósitos granulares usando homología persistente

Sergio Ardanza-Trevijano, Iker Zuriguel*, Diego Maza
Departamento de Física, Facultad de Ciencias, Universidad de Navarra, 31080 Pamplona, Spain.

Roberto Arévalo
CNR–SPIN, Dipartimento di Scienze Fisiche, Università di Napoli Federico II, I-80126, Napoli, Italy

Cuando una capa granular se somete a una sucesión de golpes verticales, la fracción de empaquetamiento (ϕ) alcanza un estado estacionario en el cual los valores de este parámetro oscilan entorno a una media bien definida (ϕ_S). El valor de ϕ_S depende de la intensidad de la perturbación (Γ). Aunque en principio se creía que esta dependencia era monótona decreciente (a mayor excitación, menor compactación), en los últimos años se ha descubierto que para excitaciones muy elevadas se invierte esta tendencia[1]. Una de las implicaciones mas importantes de este resultado es que con Γ muy diferentes se pueden alcanzar estados con el mismo empaquetamiento. En este mismo trabajo también se demostró que estos estados se diferencian en el tensor de esfuerzos.

En un trabajo posterior basado en simulaciones numéricas, se identificó (para cada depósito) cada uno de los contactos entre las partículas que lo conformaban[2]. A partir de estos datos se construyó la red de contactos que permitió identificar algunas diferencias topológicas entre estados con el mismo ϕ pero diferente tensor de esfuerzos. En concreto, se evidenció que los polígonos de la red, y en especial los de tercer orden (triángulos), son especialmente sensibles a las diferencias en los depósitos. Sin embargo, una limitación importante de este trabajo es que, para una correcta definición de estos polígonos, se requiere conocer con total exactitud la existencia de todos y cada uno de los contactos entre las partículas. Desde un punto de vista experimental esta tarea es, a día de hoy, inaccesible.

En los últimos años, el uso de la homología persistente está experimentando un gran auge como técnica de caracterización de redes complejas. En particular, Kondic y colaboradores la han implementado por primera vez para el caso de los medios granulares[3,4]. En este trabajo presentamos un estudio donde usamos homología persistente para tratar de distinguir estados con igual ϕ a partir, únicamente, de la posición de las partículas. En concreto se construyen complejos de Vietoris-Rips de depósitos generados tanto experimental como numéricamente. En primer lugar se usan los resultados numéricos donde se calcula el primer número de Betti del grafo resultante tras añadir diferentes niveles de ruido en la posición de las partículas y usando un rango de parámetros de filtrado δ (Fig. 1). Entre dos partículas (nodos) existe conexión cuando la distancia entre sus centros es menor que el valor de δ. Se observa que, incluso en los sistemas donde el nivel de ruido es importante, una elección apropiada del parámetro δ permite distinguir estados con el mismo ϕ.

Tras este resultado numérico, se procede al mismo análisis para los datos experimentales donde el nivel de ruido en la posición de las partículas se conoce solo aproximadamente. Los resultados obtenidos muestran que: 1) Mediante el uso de la homología persistente se puede diferenciar entre estados distintos pero con igual ϕ. 2) Los resultados experimentales muestran el mismo comportamiento cualitativo que los numéricos para un nivel de ruido de estos últimos de alrededor del 1%.

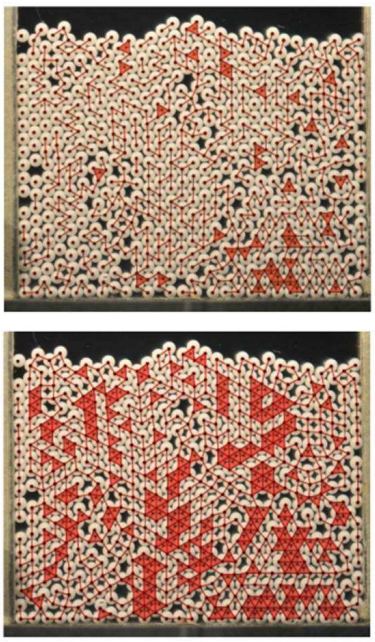

FIG. 1. Ejemplo de las redes obtenidas a partir de las posiciones de las partículas al usar $\delta = d$ (arriba) y $\delta = 1.01$ (abajo).

* iker@unav.es

[1] L. A. Pugnaloni et al. Phys. Rev. E **82** 050301R (2010).
[2] R. Arévalo et al. Phys. Rev. E **87**, 022203 (2013).
[3] L. Kondic et al., Europhys. Lett. **97**, 54001 (2012).
[4] L. Kondic et al., Phys. Rev. E. **85**, 011305 (2012).

Deformation and failure of curved nanocrystalline shells

M. Carmen Miguel*
Departament de Física Fonamental, Facultat de Física, Universitat de Barcelona
Diagonal 645, E-08028 Barcelona, Spain

We study the mechanical response of curved crystalline shells subject to load. These structures, mainly conceived for encapsulation purposes at small scales, show peculiar behavior due to their topological properties, i.e., the minimum energy configuration of any curved crystalline surface contains geometrically necessary topological defects in agreement with its Euler characteristic. The microstructure evolution is therefore influenced by the dynamics of those topological defects on the curved interface and exhibits a rather rich and non-trivial phenomenology. The quasi-static deformation of these structures is characterized by intermittent dynamics with collective particle reorganizations mediated by the proliferation of dislocation pairs and the dynamic delocalization of disclinations in the form of grain boundary scars. At large deformations, depending on bending rigidity, sample size, and geometry, one may observe buckling instabilities and structural failure phenomena such as the cavitation of the crystal shells.

* carmen.miguel@ub.edu

Phase and Interface behavior along three-phase line in type-III Lennard-Jones mixture. A comparative study between Gradient Theory and Molecular Dynamics

José Matías Garrido*[1], Héctor Quinteros-Lama[1], Andrés Mejía[1], Hugo Segura[1] and Manuel M. Piñeiro[2]
[1] *Departamento de Ingeniería Química, Universidad de Concepción, POB-160 C, Concepción, Chile*
[2] *Departamento de Física Aplicada, Facultade de Ciencias, Universidade de Vigo, Spain*

A rational guide able to qualitatively predict the effect of added components on the thermo-physical properties of fluid mixtures plays a relevant role in pursuing the purpose of screening adequate solvents. As part of a global approach where theory and Molecular Simulations (MS) collaborate in characterizing phase and interface behaviors, it has been well established the need of a unequivocal guidance for estimating initial guesses of conditions able to generate stable MS experiments devoted to predict specific phenomena. Theoretical Equation of State (EoS) models[1–3] and MS provide key pieces of such an approach since, on the one hand, they are closely related in terms of the underlying molecular model -i.e. the force potential field- and, on the other hand, they directly depend on the interactions exerted by unlike molecules. In addition, in previous contributions we have demonstrated[4,5] that the global phase diagram (GPD) calculated from theoretically based EoSs is effective for designing molecular simulation experiments involving different types of phase behavior[6].

In this contribution two complementary methods, namely Molecular Dynamics simulations (MD) and Square Gradient Theory (SGT) have been used for describing the interfacial region, thus allowing predicting both the macroscopic and molecular details of mixtures exhibiting three-phase equilibrium. SGT calculations rely on the predicition of the GLLE by means of the equation of state developed by Johnson *et al.*[1] (JZG-EoS). MD simulations are then performed in the canonical ensemble using a Lennard-Jones potential field in order to confirm the presence of the coexisting phases and their accompanying interface. In order to perform a consistent comparison between both methodologies, the molecular parameters of this type of mixture were defined from the GPD of equal size Lennard-Jones mixtures. For all conditions explored in this work, this type-III mixture shows a three-phase equilibrium composed by a bulk immiscible liquid phase (L_1) and a bulk gas phase (G) separated by a second immiscible liquid phase (L_2).

* josemagarrido@udec.cl

[1] J. K. Johnson, J. A. Zollweg and K. E. Gubbins, *Mol. Phys.* 78, 591 (1993).
[2] J. K. Johnson, E. A. Müller and K. E. Gubbins, *J. Phys. Chem.* 98, 6413 (1994).
[3] T. Lafitte, A. Apostolakou, C. Avendaño, A. Galindo, C. S. Adjiman, E. A. Müller and G. Jackson, *J. Phys. Chem.* 139, 154504 (2013).
[4] A. Mejía, J. C. Pàmies, D. Duque, H. Segura and L. F. Vega, *J. Phys. Chem.* 123, 034505 (2005).
[5] A. Mejía and L. F. Vega, *J. Phys. Chem.* 124, 244505 (2006).
[6] P. H. van Konynenburg and R. L. Scott, *Philos. Trans. R. Soc. London, Ser. A* 298, 495 (1980).

Índice Autores